

**Assessment of tsunami vulnerability and resilience of coastal ecosystems at the Andaman Sea coast of Thailand – potential and limitations of remote sensing and GIS techniques for a local scale approach**

Dissertation

zur Erlangung des Doktorgrades  
der Mathematisch-Naturwissenschaftlichen Fakultät  
der Christian-Albrechts-Universität  
zu Kiel

vorgelegt von  
**Hannes Römer**

Kiel, 2011



Referent: Prof. Dr. Horst Sterr

Korreferent: Prof. Dr. Ralf Ludwig

Tag der mündlichen Prüfung: 23.02.2011

Zum Druck genehmigt: Kiel, den 28.03.2011

Prof. Dr. Lutz Kipp (Der Dekan)





## Vorwort

Die vorliegende Dissertation entstand im Rahmen meiner dreijährigen Forschungstätigkeit am Lehrstuhl für Küstengeographie und Klimafolgenforschung an der Christian-Albrechts-Universität zu Kiel. Die Arbeit ist im Rahmen des DFG-Projektes TRAIT (Tsunami Risks, Vulnerability and Resilience at the Andaman Coast of Thailand) entstanden, das auf einer deutsch-thailändischen Forschungskoooperation zwischen den Universitäten in Kiel, Hannover und München (LMU) sowie in Bangkok (Chulalongkorn University) basiert. Der Projektbeginn war der 1. Oktober 2007. Daher gilt mein Dank vor allem denen, die für das Zustandekommen des Projektes verantwortlich waren und mir dadurch die Möglichkeit eröffneten, in diesem spannenden Projekt wissenschaftlich zu arbeiten. Hierzu zählt vor allem die Möglichkeit, vor Ort in der Untersuchungsregion mit thailändischen Kollegen zu arbeiten, was zweifelslos für mich den erfahrungsreichsten Teil meiner Arbeit, sowohl in wissenschaftlicher als auch in kultureller Hinsicht dargestellt hat. In diesem Sinne gilt mein besonderer Dank vor allem meinen beiden Betreuern Prof. Dr. Horst Sterr und Prof. Dr. Ralf Ludwig, die mich darüber hinaus im Rahmen meiner wissenschaftlichen Tätigkeit begleitet und unterstützt haben und mir den nötigen Freiraum aber auch die Zuversicht für die selbstständige Arbeit ermöglicht haben.

Weiterhin möchte ich mich für die enge und konstruktive Zusammenarbeit mit Dr. Gunilla Kaiser bedanken. Aufgrund ihres großen Erfahrungsschatzes auf dem Gebiet der Risiko- und Vulnerabilitätsanalyse erhielt ich nützliche Anregungen, die ich bei meiner Arbeit umsetzen konnte. Hierzu zählt auch die Bereitstellung von numerischen Modellierungsergebnissen aus dem Überflutungsmodell Mike 21 FM.

Für die Unterstützung bei den Geländearbeiten und insbesondere bei der Vegetationskartierung möchte ich mich beim thailändischen WWF-Team (C.J. Dunbar, S. Chaksuin, S. Buanium and J. Jeewarongkakul) bedanken. Hervorzuheben ist dabei die enge Zusammenarbeit mit Jirapong Jeewarongkakul, der durch seine umfassenden pflanzen-ökologischen sowie lokalen Kenntnisse eine wichtige Hilfestellung und Bereicherung für meine Arbeiten sowie das Projekt insgesamt darstellte.

Weiterhin gilt mein Dank all denen, die mich bei der sprachlichen Korrektur meiner Arbeit unterstützt haben. Hierzu zählen vor allem Prof. Dr. Athanasios Vafeidis, Dr. John Rapaglia und Dr. Barbara Neumann.

Für die moralische und finanzielle Unterstützung möchte ich mich besonders bei meinen Eltern aus Berlin sowie meinen Schwiegereltern aus Oldenburg in Niedersachsen bedanken. Ein besonderes Dankeschön gilt dabei meiner Schwiegermutter für die Unterstützung der Betreuung unserer Kinder.

Widmen möchte ich diese Arbeit meiner Frau Fee Sophie und meinen beiden Töchtern Maya Emilia und Lila Mathilda. Was hätte ich nur ohne meinen lieben Töchter gemacht, die mir durch ihre kindliche Sicht auf die Welt und ihre Lebensenergie immer wieder klar machten, dass das Leben auch aus anderen schönen und wichtigen Dingen außer der Arbeit besteht. Mein ganz besonderer Dank gilt natürlich meiner Frau, die mir einen großen Teil der täglichen familiären Aufgaben abgenommen hat und mir dadurch den Rücken für meine wissenschaftlichen Arbeiten weitestgehend freihalten konnte. Vielen, vielen Dank für dein Verständnis für den teilweise großen Zeitbedarf meiner Arbeit und für deine Kraft und deinen Rückhalt.



*„So eine Arbeit wird eigentlich nie fertig,  
man muß sie für fertig erklären,  
wenn man nach Zeit und Umständen  
das mögliche getan hat.“*

*Johann-Wolfgang von Goethe, Italienische Reise (1787)*

*Das Foto zeigt einen nahezu unberührten Strandabschnitt bei Ban Bang Sak an der Andamanküste Thailands.  
Im Hintergrund sind junge Bestände von Strandkasuarinen zu erkennen, die sich seit dem Tsunamieignis  
im Jahr 2004 neu entwickelten.*

**Contents – overview**

- 1 INTRODUCTION ..... 1**
- 2 THEORETICAL BACKGROUND: VULNERABILITY, ECOLOGICAL  
VULNERABILITY AND REMOTE SENSING APPLICATIONS..... 11**
- 3 TSUNAMI IMPACTS ON COASTAL ECOSYSTEMS AND NATURAL  
RESOURCES AT THE ANDAMAN SEA COAST OF THAILAND ..... 20**
- 4 METHODOLOGICAL APPROACH AND DATASETS..... 33**
- 5 RESULTS OF THE REMOTE SENSING APPLICATIONS:  
EXPOSURE, TSUNAMI IMPACTS AND RECOVERY PROCESSES ..... 56**
- 6 SYNTHESIS ..... 99**
- 7 CONCLUSIONS AND OUTLOOK ..... 127**
- 8 REFERENCES..... 129**
- 9 APPENDIX ..... 141**

## Contents

List of Figures.....	IV
List of Tables.....	VI
Abbreviations.....	VII
Summary.....	VIII
Kurzfassung.....	IX
<b>1 INTRODUCTION .....</b>	<b>1</b>
1.1 The TRAIT project - starting point and general conceptual framework of the thesis .....	1
1.2 Objectives .....	2
1.3 Structure of the thesis .....	4
1.4 The study area.....	5
1.4.1 Climate and geomorphology .....	5
1.4.2 The landscape and human influences.....	7
1.4.3 Ecological characteristics .....	9
<b>2 THEORETICAL BACKGROUND: VULNERABILITY, ECOLOGICAL VULNERABILITY AND REMOTE SENSING APPLICATIONS.....</b>	<b>11</b>
2.1 Vulnerability.....	11
2.2 Ecological vulnerability – definitions and concepts .....	14
2.3 Assessment of vulnerability and ecological vulnerability.....	15
2.4 The role of remote sensing in vulnerability assessments.....	17
<b>3 TSUNAMI IMPACTS ON COASTAL ECOSYSTEMS AND NATURAL RESOURCES AT THE ANDAMAN SEA COAST OF THAILAND .....</b>	<b>20</b>
3.1 Coral reefs.....	20
3.2 Seagrass beds.....	22
3.3 Mangrove forests.....	24
3.4 Marine endangered species.....	26
3.5 Coastal forests.....	27
3.6 Crops and soils .....	27
3.7 Water resources.....	29
3.7.1 Seawater quality .....	29
3.7.2 Groundwater and surface water quality.....	30

<b>4</b>	<b>METHODOLOGICAL APPROACH AND DATASETS.....</b>	<b>33</b>
4.1	IKONOS data and pre-processing.....	34
4.2	Exposure analysis.....	38
4.2.1	Creation of a LULC-map.....	39
4.2.2	Ground truth data.....	42
4.3	Analysis of tsunami induced impacts as a basis to assess sensitivity.....	44
4.4	Analysis of recovery processes as a basis to estimate tsunami resilience.....	46
4.4.1	General approach.....	46
4.4.2	Ground truth data collection.....	48
4.5	Additional data sets.....	53
4.5.1	Elevation data.....	53
4.5.2	Results from inundation modelling.....	54
4.5.3	Other geodata.....	54
<b>5</b>	<b>RESULTS OF THE REMOTE SENSING APPLICATIONS: EXPOSURE, TSUNAMI IMPACTS AND RECOVERY PROCESSES.....</b>	<b>56</b>
5.1	Results of the exposure analysis.....	56
5.2	The submitted articles.....	59
<b>6</b>	<b>SYNTHESIS.....</b>	<b>99</b>
6.1	Summary of key findings of the two articles.....	99
6.1.1	Methodological aspects.....	99
6.1.2	Ecological perspective.....	100
6.2	Assessment and analysis of the tsunami vulnerability.....	105
6.2.1	Retrospective analysis of tsunami vulnerability.....	105
6.2.2	Identification of factors determining the tsunami vulnerability.....	110
6.2.2.1	Dependent variables.....	111
6.2.2.2	Independent variables.....	111
6.2.2.3	Results of the statistical analysis.....	113
6.2.2.4	Evaluation of the statistical approach.....	117
6.3	Evaluation of the potential and limitations of remote sensing techniques in ecological vulnerability analysis.....	120
6.4	Evaluation of the ecological vulnerability of the study area.....	122
<b>7</b>	<b>CONCLUSIONS AND OUTLOOK.....</b>	<b>127</b>
<b>8</b>	<b>REFERENCES.....</b>	<b>129</b>
<b>9</b>	<b>APPENDIX.....</b>	<b>141</b>

## List of Figures

Figure 1-1. Risk framework of TRAIT (simplified).	2
Figure 1-2. Location of the study area including the three extents of the IKONOS images.	6
Figure 1-3. Climate data of Ranong. Modified from Mühr (2006).	7
Figure 1-4. Modified from DMR (2001).	8
Figure 1-5. A freshwater pond near Ban Nam Khem as a result of opencast mining.	8
Figure 1-6. Thailand total marine shrimp production during 1985-2004. BIOTEC (2005).	9
Figure 1-7. Ecological characteristics of the study area. GIS-data are provided by DMCR (n.d.).	10
Figure 2-1. The spheres of vulnerability. Birkmann (2005).	12
Figure 2-2. The vulnerability framework of Turner. Turner <i>et al.</i> (2003).	12
Figure 2-3. The vulnerability framework applied in TRAIT.	13
Figure 3-1. Damage patterns of coral reefs along the Phang-Nga coast. DMCR (2005).	22
Figure 3-2. Damage patterns of seagrass meadows around Yao Yai island. Modified from DMCR (2005).	23
Figure 3-3. Tsunami induced impacts on seagrass meadows. DMCR (2005).	24
Figure 3-4. Physical damage of mangrove stands in Thailand. Modified from FAO and MOAC (2005).	25
Figure 3-5. A male dugong was captured and returned to the sea on December 29, 2004. DMCR (2005).	26
Figure 3-6. Tsunami induced crop damage. Modified from FAO and MOAC (2005).	28
Figure 3-7. Coastal water quality along the coast of Ranong, Phang-Nga and northern Phuket. DMCR (2005).	30
Figure 4-1. Concept of analysing tsunami vulnerability of coastal ecosystems based on remote sensing.	34
Figure 4-2. Overview of IKONOS image data used in this study.	36
Figure 4-3. Selection of ground control points (GCPs).	37
Figure 4-4. Gram-Schmidt-Spectral-sharpening.	38
Figure 4-5. Concept of exposure analysis based on remote sensing applications.	39
Figure 4-6. Classification strategies applied in object-oriented image analysis.	41
Figure 4-7. LULC-map derived by object-oriented image analysis.	42
Figure 4-8. LULC-classes of the study area.	43
Figure 4-9. LULC-mapping carried out between October and December 2008.	44
Figure 4-10. Applying change detection techniques for tsunami damage assessments.	45
Figure 4-11. Concept of impact analysis based on remote sensing applications.	46
Figure 4-12. The principle of applying change detection techniques for vegetation recovery assessments.	47
Figure 4-13. Concept of the recovery analysis based on remote sensing application.	48
Figure 4-14. Configuration of study sites and plots.	49
Figure 4-15. Study sites collected between January and March 2009.	49
Figure 4-16. A typical location and scenery of a study site.	50
Figure 4-17. Estimation of percentage ground cover. Modified from Carpenter (1987).	51
Figure 5-1. Photos of the ecological exposure units considered in this study.	56
Figure 5-2. Map of the ecological tsunami exposure considered in this study.	57
Figure 5-3. Relation between the exposed area and the total area of the five examined ecosystems.	58
Figure 5-4. Distances to shoreline of the examined ecosystems.	102
Figure 6-2. Direct impacts on coconut plantations.	103
Figure 6-3. Defoliated and dead trees occurring in mixed beach forests.	103
Figure 6-4. Two approaches for assessing and analysing tsunami vulnerability.	105
Figure 6-5. Retrospective assessment of the vulnerability of mangrove forests.	106
Figure 6-6. Retrospective analysis of tsunami vulnerability of mangrove areas (patch level).	109
Figure 6-7. Concept of the statistical approach for the identification of factors determining tsunami sensitivity and recovery	111

Figure 6-8. Standardised beta values calculated for selected regression models, exemplified for mangrove forest.	117
Figure 6-9. Observed and modelled tsunami induced impacts, exemplified for a mangrove area near Ban Nam Khem.	119
Figure 6-10. Human pressure on the environment on tambon level.	125
Figure 6-11. Human induced impacts on mangroves in the study area (cp. red polygons).	126

## List of tables

Table 3-1. Number of affected stations categorised by impact levels. DMCR (2005).	21
Table 3-2. Classification scheme for the estimation of the damage intensity of coral reefs. DMCR (2005).	21
Table 3-3. Damaged cropping areas by Province. FAO and MOAC (2005).	28
Table 3-4. Assessment and classification of field damage. FAO and MOAC (2005).	29
Table 4-1. IKONOS sensor specifications. GeoEye (2006).	35
Table 4-2. IKONOS band dependent parameters. Taylor (2009), Geoeye (2006).	37
Table 4-3. Study sites and their main characteristics.	52
Table 4-4. Species inventory carried out on the plot level.	52
Table 4-5. Specification of MFC 1-3. Börner <i>et al.</i> (2008).	53
Table 4-6. Overview of geo-data used in this study.	55
Table 6-1. Calculation of tsunami sensitivity, resilience and vulnerability for mangroves (patch region).	108
Table 6-2. Results of the correlation and regression analysis.	116
Table 6-3. Comparison of human pressure indicators on tambon level.	124



## Abbreviations

ASTER	Advanced Spaceborne Thermal Emission and Reflection Radiometer
BIOTEC	National Centre for Genetic Engineering and Biotechnology
CCD	Charge-Coupled-Device
CHL <i>a</i>	Chlorophyll <i>a</i>
CRISP	Centre of Remote Sensing and Preprocessing
CVA	Change Vector Analysis
DFG	Deutsche Forschungsgemeinschaft
DGR	Department of Groundwater Resources
DHI	Danish Hydraulic Institute
DLSM	Digital Land Surface Model
DMC	Direct Multi-Date Classification
DMCR	Department of Marine and Coastal Resources
DMR	Department of Mineral Resources
DN	Digital Number
DNP	Department of National Parks, Wildlife and Plant Conservation
DO	Dissolved Oxygen
DOS	Dark Object Subtraction
DSM	Digital Surface Model
FAO	Food and Agriculture Organisation
GCP	Ground Control Point
GIS	Geographic Information System
GMT	Greenwich Mean Time
GPS	Global Positioning System
IAARD	Indonesian Agency for Agriculture Research and Development
LULC	Land Use-Land Cover
MFC	Multi Functional Camera
MOAC	Ministry of Agriculture & Cooperatives
MWQI	Marine Water Quality Index
NOAA/WDC	National Oceanic and Atmospheric Administration / Word Data Center
NRCT	National Research Council of Thailand
NSO	National Statistical Office
NSW-DPI	New South Wales Department of Primary Industries
OECD	Organisation for Economic Co-operation and Development
RMSE	Root Mean Square Error
SDS	Spatial Dimension Solutions
SRTM	Shuttle radar Topography Mission
TC	Tassel Cap
TDS	Total Dissolved Solids
TNDVI	Transformed Normalised Difference Vegetation Index
TRAIT	Tsunami Risks, Vulnerability and Resilience in the Phang-Nga Province, Thailand: Tsunami Risk and Information Tool
TRIAS	Tracing Tsunami Impacts onshore and offshore in the Andaman Sea Region
TSS	Total Suspended Solid
UNEP	United Nations Environment Programme
UTC	Coordinated Universal Time
UTM	Universal Transverse Mercator
VIF	Variance Inflation Factor
USGS	U.S. Geological Survey
WCMC	World Conservation Monitoring Centre
WGS	World Geodetic System
WWF	World Wide Fund for Nature
ZKI	Zentrum für satellitengestützte Kriseninformation

## Summary

The Indian Ocean tsunami of December 26, 2004 strongly impacted the Andaman Sea coast of Thailand. Besides the enormous number of fatalities and the massive destruction of settlements and infrastructure, valuable coastal ecosystems such as mangrove forests and coral reefs were deteriorated and destroyed. In order to reduce the severity of potential impacts in case of a future tsunami, it is essential to introduce an effective tsunami risk management for this region. This was the starting point of the Thai-German research project TRAIT (Tsunami Risks, Vulnerability and Resilience at the Andaman Coast of Thailand, started in October 1, 2007) aiming at supporting the local tsunami risk management for the two tsunami impacted provinces Phang-Nga and Phuket. A major component in TRAIT encompasses the holistic assessment of the tsunami vulnerability including the ecological, social and economic dimension. One of the central methodological questions to be examined in this context is to what extent remote sensing applications can be applied to assess vulnerability.

This thesis was conducted within the scope of the TRAIT project and focuses on the assessment of the ecological tsunami vulnerability and resilience by applying a remote sensing based approach based on high-resolution IKONOS imagery. In this study the vulnerability is analysed for five different coastal ecosystems by considering the three components of vulnerability: *exposure*, *sensitivity* and *resilience*. Ecological exposure is defined as “the degree to which an ecosystem [...] comes into contact with particular stresses or perturbations” (Clark *et al.* 2000, p. 9) and is assessed based on an object-oriented classification approach using pre-tsunami IKONOS images from the year 2003. *Mangrove forests*, *casuarina beach forests*, *coconut plantations*, *mixed beach forests* and *melaleuca forests* were defined as exposure units. The ecological sensitivity, “the degree to which an exposure unit is affected by exposure to any set of stresses” (Clark *et al.* 2000, p. 9), was assessed based on a tsunami impact analysis using digital change detection techniques based on pre- and post-tsunami imagery from January 2003 and January 2005. A *change vector analysis* (CVA) and a *direct multi-date classification* (DMC) were applied in this context. The resilience was assessed through the analysis of the recovery processes of the examined ecosystems three, respectively four years after the tsunami (cp. the definitions of Clark *et al.* 2000; Mittelbach *et al.* 1995; Pimm 1991). Here, multi-date IKONOS images from January 2003, January 2005 and February 2008 were applied in a change detection study using the CVA and a calculation of a *recovery rate based on the comparison of multi-date TNDVI-images*. Ground truth measurements conducted between January and March 2009 played an important role in validating and interpreting the change detection results.

The results provided by the impact and the recovery analysis were then examined in combination in order to estimate the tsunami vulnerability of the five coastal ecosystems. The results show that vulnerability varied in space and in ecosystem type: Although casuarina beach forests were the most impacted and sensitive of all examined forest ecosystems, its vulnerability was found to be relatively low, as it could recover very quickly after the tsunami. In contrast, mangroves had to a large extent not been affected by the tsunami. This is mainly due to its occurrence in sheltered coastal areas. However, some mangrove sites did show a high vulnerability; particularly small and isolated mangrove patches were impacted significantly by the tsunami. As the other examined forest ecosystems were either low or not directly impacted by the tsunami, tsunami vulnerability was found to be low for these.

Furthermore, the thesis makes clear that in general, the tsunami related impacts on the coastal ecosystems at the Andaman Sea coast are relatively small in comparison to the continuing impacts resulting from human activities, such as shrimp farming, the development of the tourism industry and tin activities from the last century.

Regarding the potential and limitations of the remote sensing based approach, it can be said that remote sensing applications can contribute to the spatial and retrospective analysis of tsunami vulnerability. Additionally, a detailed new geo-database on the spatial distribution of terrestrial ecosystems and their vulnerability was developed for this area. This information can serve as a flexible basis to regionalise other information on ecological vulnerability derived from other sources, such as field studies or expert interviews and thus can be used to further investigate ecological and socio-ecological vulnerability. However, the study reveals that some important causal relationships of vulnerability cannot be adequately analysed and interpreted only by the use of remotely sensed data. This applies particularly to the assessment of the intrinsic vulnerability and the resilience (cp. Villa and McLeod 2002) which requires a comprehensive understanding of the state and temporal changes of the internal structure and functionality of an ecosystem. For this purpose, more data from field measurements and laboratory analyses acquired from longer observation periods would have been necessary (cp. Paphavasit *et al.* 2009; Villa and McLeod 2002). Other limitations result from the low temporal resolution of the acquired imagery and from problems in acquiring cloud free imagery.

Furthermore, it can be concluded that not all aspects of ecological vulnerability can be directly observed by means of remote sensing. This applies for example to the monitoring of changes in soil and groundwater conditions or the estimation of the social consequences of the tsunami.

## Kurzfassung

Der Tsunami vom 26. 12. 2004 erschütterte große Areale der thailändischen Andamanküste. Neben der beträchtlich hohen Opferzahl und massiven Schäden an Gebäuden und Infrastruktur, kam es zu Schäden und Zerstörungen von wertvollen Küstenökosystemen wie Korallenriffen und Mangroven. Um jedoch die möglichen Konsequenzen eines zukünftigen Tsunamis in dieser Region zu reduzieren, bedarf es eines effektiven Tsunami-Risikomanagements in dieser Region. Aus dieser Problematik heraus entstand das deutsch-thailändischen Forschungsprojekt TRAIT (Tsunami Risks, Vulnerability and Resilience at the Andaman Coast of Thailand), das auf eine Unterstützung des lokalen Tsunami-Risikomanagements für die vom Tsunami schwer betroffenen thailändischen Provinzen Phang-Nga und Phuket abzielt. Eine wesentliche Komponente hierfür ist dabei die Abschätzung der Tsunamivulnerabilität der Küstenregion unter Berücksichtigung der ökologischen, sozialen und ökonomischen Vulnerabilität. Als ein wesentlicher methodischer Ansatz soll dabei untersucht werden, inwiefern sich Fernerkundungstechniken für die Vulnerabilitätsabschätzung anwenden lassen.

Die vorliegende Dissertation ist im Rahmen des Forschungsprojektes TRAIT entstanden und widmet sich der Thematik der Abschätzung der lokalen ökologischen Tsunamivulnerabilität und Resilienz, wobei ein fernerkundungsbasierter Ansatz mit IKONOS-Daten gewählt wurde. Die Vulnerabilität wird dabei für fünf Küstenökosysteme untersucht, unter Berücksichtigung der drei Vulnerabilitätskomponenten *Exposure*, *Sensitivität* und *Resilienz*.

Das ökologische Exposure, “the degree to which an ecosystem [...] comes into contact with particular stresses or perturbations” (Clark *et al.* 2000, p. 9) wurde mit Hilfe eines objektbasierten Klassifikationsansatzes basierend auf Pre-Tsunami IKONOS-Daten aus dem Jahr 2003 untersucht. Dabei konnten die fünf Küstenökosteme *Mangroven*, *Kasuarinen-Strandwälder*, *Strand-Mischwälder*, *Melaleuca-Savannen* sowie *Kokospflanzungen* als Exposure-Einheiten definiert werden. Die Analyse der ökologischen Tsunami-Sensitivität, „the degree to which an exposure unit is affected by exposure to any set of stresses“ (Clark *et al.* 2000, p. 9), basiert dagegen auf einer detaillierten Schadensanalyse unter Verwendung von Pre- und Post-Tsunami IKONOS Daten aus den beiden Jahren 2003 und 2005. Dabei wurden zwei Change-Detection-Verfahren, die *change vector analysis (CVA)* sowie die *direkte multitemporale Klassifikation (DMC)*, verwendet. Die Bewertung der Resilienz erfolgte vorwiegend indirekt durch die Analyse der Erholungsprozesse der untersuchten Ökosysteme drei beziehungsweise vier Jahre nach dem Tsunamieignis (vgl. Clark *et al.* 2000; Mittelbach *et al.* 1995; Pimm 1991). Dabei wurden die zwei Change-Detection-Verfahren *CVA* sowie die *Berechnung einer Erholungsrate aus multitemporalen TNDVI-Bilddaten* angewendet. Außerdem wurden durch den Autor Ground-Truth-Daten zu den Erholungsprozessen erhoben, die als wertvolle Informationsquelle für die Validierung und Interpretation der Fernerkundungsergebnisse dienten.

Für die Abschätzung der Tsunamivulnerabilität der untersuchten Ökosysteme wurden die Fernerkundungsergebnisse sowie die Ergebnisse aus den Felduntersuchungen kombiniert betrachtet. Dabei konnte festgestellt werden, dass die Vulnerabilität räumlich sehr variiert und sich außerdem je nach Ökoystemtyp unterscheidet: Obwohl die Kasuarinen-Strandwälder durch eine hohe Schadensanfälligkeit bzw. Sensitivität gekennzeichnet waren, sind sie aufgrund ihres hohen Regenerationsvermögens als insgesamt gering vulnerables Ökosystem anzusehen. Im Gegensatz dazu, auch wenn Mangroven aufgrund ihrer geschützten Lage meist kaum durch den Tsunami beeinflusst wurden, ergibt sich dennoch lokal eine hohe ökologische Vulnerabilität. Dies trifft vor allem auf kleine, isolierte und stark zerstörte Mangrovegebiete zu. Da die anderen untersuchten Wald-Ökosysteme meist nur gering durch den Tsunami geschädigt wurden, ergibt sich hier auch eine relativ geringe Tsunami- Vulnerabilität.

Diese Studie macht außerdem deutlich, dass die nachhaltigsten Schädigungen an Küstenökosystemen an der Andamanküste nicht durch den Tsunami, sondern primär durch den Menschen verursacht werden. Hierzu zählen etwa die Folgen des Zinnabbaus aus den 60er und 70er Jahren, die Expansion der Shrimp-Aquakultur, sowie die touristische Entwicklung in den Küstengebieten.

Hinsichtlich der Potentiale und Grenzen des verwendeten Fernerkundungsansatzes wurde deutlich, dass sich Fernerkundungsverfahren insbesondere für die räumliche und retrospektive Abschätzung von Tsunami-Vulnerabilitäten eignen. Außerdem konnte eine für die Region neuartige und wertvolle Datenbasis zur räumlichen Verteilung wichtiger Küstenökosysteme sowie zu ihrer Vulnerabilität geschaffen werden. Diese kann als eine flexible Basis für die Regionalisierung von Informationen zur ökologischen Vulnerabilität aus anderen Datenquellen (z.B. detaillierte Geländearbeiten, Expertenbefragungen) fungieren, was eine weiterführende Untersuchung zur ökologischen und sozio-ökologischen Vulnerabilität ermöglicht. Des Weiteren kann die Datenbasis im Rahmen einer GIS-basierten Vulnerabilitätsabschätzung in TRAIT Anwendung finden.

Darüber hinaus hat diese Studie deutlich gemacht, dass sich einige wichtige kausale Zusammenhänge der ökologischen Vulnerabilität nicht allein aus Fernerkundungsdaten erschließen lassen. Dies betrifft vor allem die systeminterne oder intrinsische Vulnerabilität sowie Fragestellungen zur ökologischen Resilienz, die ein genaueres Verständnis über den Zustand sowie die zeitliche Veränderung des internen Systemgefüges voraussetzt.

Hierzu wären vor allem umfassende Daten aus Feldmessungen oder Laboranalysen aus längeren Beobachtungszeiträumen erforderlich gewesen (Paphavasit *et al.* 2009; Villa and McLeod 2002).

Weitere Limitierungen ergaben sich zum einen aus der geringen zeitlichen Auflösung der verwendeten Bilddaten, sowie aus der Beschaffung von wolkenfreien Satellitendaten. Es muss außerdem berücksichtigt werden, dass nicht alle Aspekte zur der ökologischen Vulnerabilität direkt durch Fernerkundungsdaten untersucht werden können. Hierzu zählen Veränderungen in Böden oder Grundwasserressourcen, sowie die soziale Auswirkungen des Tsunamis.



## 1 Introduction

In comparison to hurricanes, floods, or earthquakes, tsunamis are relatively infrequent natural hazards and were outside public attention until the Indian Ocean tsunami event on December 26, 2004. Statistics from historical tsunami databases (e.g. NOAA/WDC tsunami database) as well as palaeo-tsunami records, however, reveal that tsunamis are widespread and abundant phenomena. Two famous examples are the Lisbon earthquake and tsunami of November 1, 1755 and the Krakatoa Tsunami of August 28, 1883 in the Pacific Ocean.

The 2004 Indian Ocean tsunami or Asian tsunami was caused by an undersea mega thrust earthquake which occurred at 00:58:53 UTC on December 26, 2004 off the west coast of northern Sumatra. The earthquake was the second largest ever recorded on a seismograph (surface wave magnitude 9.0). The tsunami severely damaged coastal communities in countries around the Indian Ocean including Indonesia, Sri Lanka, India, Thailand and the Maldives. According to Telford and Cosgrave (2006) 227.898 people were dead or missing, whereas UNEP (2005) lists approximately 250.000 casualties. This makes this earthquake one of the deadliest earthquakes in recorded history.

### 1.1 The TRAIT project - starting point and general conceptual framework of the thesis

The Phang-Nga province of Thailand - on the Andaman Sea coast - was one of the most severely affected regions from the Tsunami event. In addition to the enormous number of fatalities (5395) and the massive destruction of settlements and infrastructure, coastal ecosystems were also deteriorated and destroyed (e.g. Phongsuwan *et al.* 2006; Szczucinski *et al.* 2006). Variations in the mode and intensity of the tsunami impacts, resulting from the specific vulnerability of different communities were witnessed. The question remains as to which factors determine vulnerability and how can vulnerability be quantitatively assessed? These questions are the foci of the Thai-German research project TRAIT (Tsunami Risks, Vulnerability and Resilience at the Andaman Coast of Thailand), which form the conceptual framework for this thesis. TRAIT is conducted by the universities of Kiel (Prof. Dr. H. Sterr, Department of Department of Geography – Coastal Geography and Natural Hazards), Munich (Prof. Dr. R. Ludwig, Department of Geography – Physical Geography and Remote Sensing), Hannover (Prof. Dr. J. Revilla Diez, Department of Economic Geography) and by the Chulalongkorn University of Bangkok (Dr. S. (Meprasert) Jitpraphai, Marine Science Department). The project aims to determine a) the causes and mechanisms of tsunami-related impacts in the coastal zones (risk pathways), b) the vulnerability to the local natural, social and economic systems against these impacts and c) the factors and mechanisms determining the resilience (its strength or its lack thereof) of the coastal population, community structures, economic sector etc. Finally, these findings will be used for developing a generic methodology (TRAIT = Tsunami Risk and Information Tool) which is suitable for risk assessments at various levels of scale and also applicable for different types of coastal zones. Thus, TRAIT will contribute to a better risk management for extreme events in the region and beyond. Figure 1-1 illustrates the simplified framework focused in TRAIT encompassing the analysis of hazards, vulnerability and risk and finally the management of risk (Sterr 2007).

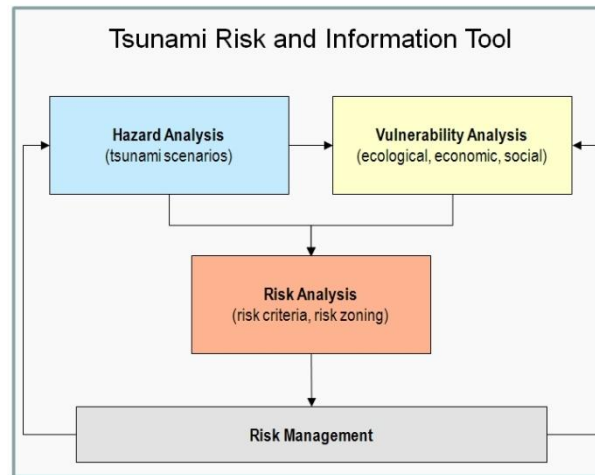


Figure 1-1. Risk framework of TRAIT (simplified).

Within the TRAIT project four coastal communities were selected as case study regions including Patong beach, Khao Lak, Ban Nam Khem and Thai Mueang. These regions are representative of different environmental and socio-economic characteristics of the coastal regions at the Thai Andaman coast. This makes the whole approach of TRAIT more transferrable to other coastal areas.

TRAIT is embedded in the larger project package of TRIAS (Tracing Tsunami Impacts onshore and offshore in the Andaman Sea Region) funded by the German Research Foundation (DFG) and the National Research Council of Thailand (NRCT). TRIAS focuses on tsunami related research by addressing various scientific questions dealing with tsunami impacts and risks in Thai national waters and on land. The overall aims of the project are to gain a better understanding of the physical impacts of tsunamis on both the seafloor and land; to generate knowledge for better coastal protection; and to develop risk management strategies for areas endangered by tsunamis.

## 1.2 Objectives

This thesis aims to assess the ecological vulnerability to tsunamis by applying remote sensing and GIS techniques and focuses on two major objectives:

### 1) The analysis of ecological vulnerability

The coastal area at the Andaman Sea of Thailand hosts a number of valuable coastal ecosystems, such as coral reefs, sea grass beds, mangrove forests and other coastal forests that were affected by the 2004 Indian Ocean tsunami. Although studies on the rapid impacts of the tsunami on coastal ecosystems and natural resources were carried out immediately after the tsunami in Thailand, the knowledge of the tsunami vulnerability, particularly at the local scale, is not well understood.

As these ecosystems provide essential services and functions to the social and environmental system, the knowledge of the ecological vulnerability is crucial for estimating the total vulnerability of the coastal region. This thesis aims to analyse the ecological vulnerability through the application of a bio-centric perspective (cp. Birkmann and Wisner 2006). Here, the vulnerability of five coastal ecosystems is investigated considering the following three components:



- a) the ecological exposure - “the degree to which an ecosystem [...] comes into contact with particular stresses or perturbations” (Clark *et al.* 2000, p. 9),
- b) the sensitivity – “the degree to which an exposure unit is affected by exposure to any set of stresses” (Clark *et al.* 2000, p. 9),
- c) the tsunami resilience – which was predominantly assessed by analysing the recovery processes of the examined ecosystems, and is defined as the rate and potential at which ecosystems reclaim its habitat by natural succession processes after being degraded or removed by the tsunami. Thus this definition is based on the resilience concepts of Mittelbach *et al.* (1995) and Pimm (1991).

With regard to the definitions of Clark *et al.* (2000), in this study the perturbations or stresses are represented by the tsunami impacts.

- II) Evaluation of the potential of remote sensing techniques for assessing ecological vulnerability:

This study also evolved from a main methodological challenge of the TRAIT project to implement and evaluate remote sensing data and technology in the context of vulnerability analysis. Remote sensing can be regarded as a time-saving and cost efficient alternative to conventional field measurements. There is, therefore a need to investigate if remote sensing techniques can support ecological vulnerability analysis. As vulnerability varies by location, it can be assumed that information provided by remotely sensed data can substantially contribute to a better understanding of the processes that causes the spatial variability of vulnerability. Thus, in this thesis a methodological concept based on multi-temporal high-resolution IKONOS imagery and GIS-techniques is developed and applied to assess the local tsunami vulnerability of coastal ecosystems for three case study regions at the Andaman Sea coast of Thailand. The ecological exposure is identified with an object-oriented classification approach based on IKONOS pre-tsunami images from January 2003. Due to a poor depth penetration of near infra-red electromagnetic radiation (< 1 m) into water and a small extent of shallow water reefs covered by the satellite images, a focus is given to valuable terrestrial and semi-terrestrial ecosystems, such as mangrove forests, casuarina beach forests, coconut plantations, mixed beach forests and melaleuca forests (cp. Green *et al.* 2000). The ecological sensitivity is assessed based on an impact or damage assessment using digital change detection techniques based on pre- and post-tsunami images of January 2003 and January 2005. Here, the *change vector analysis* (CVA) and the *direct multi-date classification* (DMC) were applied. The tsunami resilience was assessed by analyzing the recovery processes of the examined ecosystems using the multi-date IKONOS images from three acquisitions dates: January 2003, January 2005 and February 2008.

The applied change-detection-techniques were a) the CVA and b) the calculation of a recovery rate derived from multi-temporal TNDVI-images. Additionally, ground truth measurements conducted between January and March 2009 were used for validation and interpretation purposes.

Thus, the study provides methods and answers to the following questions:

- a) Which coastal ecosystems were affected by the tsunami?
- b) To which degree coastal ecosystems were impacted by the tsunami and whether they could recover?
- c) Which factors determine the tsunami sensitivity, resilience and the vulnerability?
- d) To what degree can remote sensing applications support the assessment of ecological vulnerability and resilience?

### 1.3 Structure of the thesis

Briefly, the thesis continues with a short introduction and description of the study area including a focus on environmental characteristics. Section 2 provides theoretical background on the underlying concepts of vulnerability particularly ecological vulnerability and summarises the current state of research on remote sensing applications for vulnerability analyses. The third section summarises the findings from the literature on the main tsunami induced ecological impacts which occurred in South Thailand and identifies still open questions regarding the local ecological vulnerability resulting from the literature review. The main methodological approach, as well as a detailed description on the used datasets is presented in section 4.

The core of this study is comprised of the two articles presented in section 5 and the synthesis chapter provided in section 6. The first article “Using remote sensing to assess tsunami-induced impacts on coastal forest ecosystems at the Andaman Sea coast of Thailand” (Roemer *et al.* 2010a) deals with the analysis of tsunami-induced damage on five different coastal forest ecosystems at the Phang-Nga province coast based on multi-date IKONOS imagery. The second article “Monitoring post-tsunami vegetation recovery in Phang-Nga province, Thailand – a remote sensing based approach” (Roemer *et al.* 2010b) concerns the assessment of recovery of coastal vegetation at the Phang-Nga province coast based on field measurements and multi-date IKONOS imagery.

In the synthesis section the key findings of both articles will be summarised with regard to a) the sensitivity and resilience of the examined ecosystems and b) the applied remote sensing techniques. Furthermore, it will be discussed and evaluated whether and to what extent remote sensing applications can be used to assess ecological vulnerability and thus whether they can be implemented in the risk framework of TRAIT. Here, two methodological approaches, a) a GIS-based retrospective vulnerability assessment concept and b) a statistical modelling approach are presented. Here, the results provided by the two articles are used to further analyse the local tsunami vulnerability. A general evaluation of the ecological tsunami vulnerability on a regional scale is provided in section 6.4.

## 1.4 The study area

The study area (Figure 1-2) covers a 50 km long coastal stripe in the Phang-Nga province of Thailand and includes the five Tambons Ban Mueang, Khuek Kak, Laem Kaen, Thung Maphrao and Thai Mueang. Tambons are the administrative subdivisions of the provinces in Thailand. The region is generally sparsely populated with a total population of 41 424 and a population density of 78 people per km<sup>2</sup> (NSO 2003). The extents of the IKONOS imagery (cp. three red rectangles on Figure 1-2) represent the actual dimension of the study area. The satellite images cover the intensively impacted coastal plains between Ban Nam Khem and Ban Bang Sak in the North (8° 52' 10'' N to 8° 46' 30'' N), the coastal lowlands around the three villages Khuk Kak, Bang Niang and Nang Thong (Khao Lak) in the centre (8° 44' 30'' N to 8° 37' 52'' N) and the coastal area between Tap Lamru and Thai Mueang city to the South (8° 35' 15'' N to 8° 28' 28'').

The three areas differ by their main socio-economic and environmental configuration: The northern part is dominated by the fishing village of Ban Nam Khem and agriculture, the central section, meanwhile represents a booming tourism resort with large hotel complexes scattered near the coast. The southern part, in contrast, hosts large areas of intact coastal ecosystems like mangrove forests and rain forests which are partial protected by national park status (Khao Lampi - Hat Thai Mueang National Park).

The coastal area was strongly impacted by the tsunami with run-up elevations mostly ranging between 5 to 10 m. Highest values were observed in the area of Khao Lak with 10 to 12 m and between 8 and 9 m near Ban Nam Khem. Lower run-up elevations were documented in the south, e.g. at Khao Lampi - Hat Thai Mueang National Park with values ranging between 3.5 to 6.5 m (Bell *et al.* 2004; Ioualalen 2007; Szczucinski *et al.* 2006). The inundation distance varied from a few hundred of meters around Ban Bang Sak and Thai Mueang to more than 1.5 km near Pakarang Cape (Szczucinski *et al.* 2006; ZKI 2005).

### 1.4.1 Climate and geomorphology

According to the Köppen classification system, the climate of the study area is within the tropical monsoon climate (cp. Figure 1-3). Ranong station is located at the west coast of Phang-Nga province in the northern section of the study area. Three seasons can be distinguished in South Thailand: a) the winter monsoon between October and February with relatively cool temperatures, cool northerly winds and little rainfall, b) the hot season between March and April with relatively high temperatures, little rainfall and increased humidity, and c) the summer monsoon with an average rainfall of 1000 mm and more than 3000 mm depending on the location (Weischet and Endlicher 2000).

The topography of the coastal area is mostly flat with elevations below 20 meters above sea level (asl.). The coastal plains are divided by the foothills of the Phuket mountain range east of the study area, e.g. between Ban Bang Sak and Pakarang Cape or between Nang Thong and Tap Lamru. Here, the coasts are predominantly rocky with cliff heights of about 50 meters (Hin Chang Cape or at Ao Kham Cape). However, most of the west-exposed coasts are built up by sand and are characterised by sequences of beach ridges. These are usually up to two meters high and aligned parallel to the beach. The ridges often alternate with linear swampy depressions known as swales (Pajimans 1976).

Coasts marked by silty substrates are located near river mouths, e.g. near Ban Nam Khem or south of Tap Lamru. The coastal lowland is well-drained by several smaller rivers which have their origin in the Phuket mountain range to the east and follow the main slope direction of the land from east to west (Eichenberg-Suvarnatisha 1991).

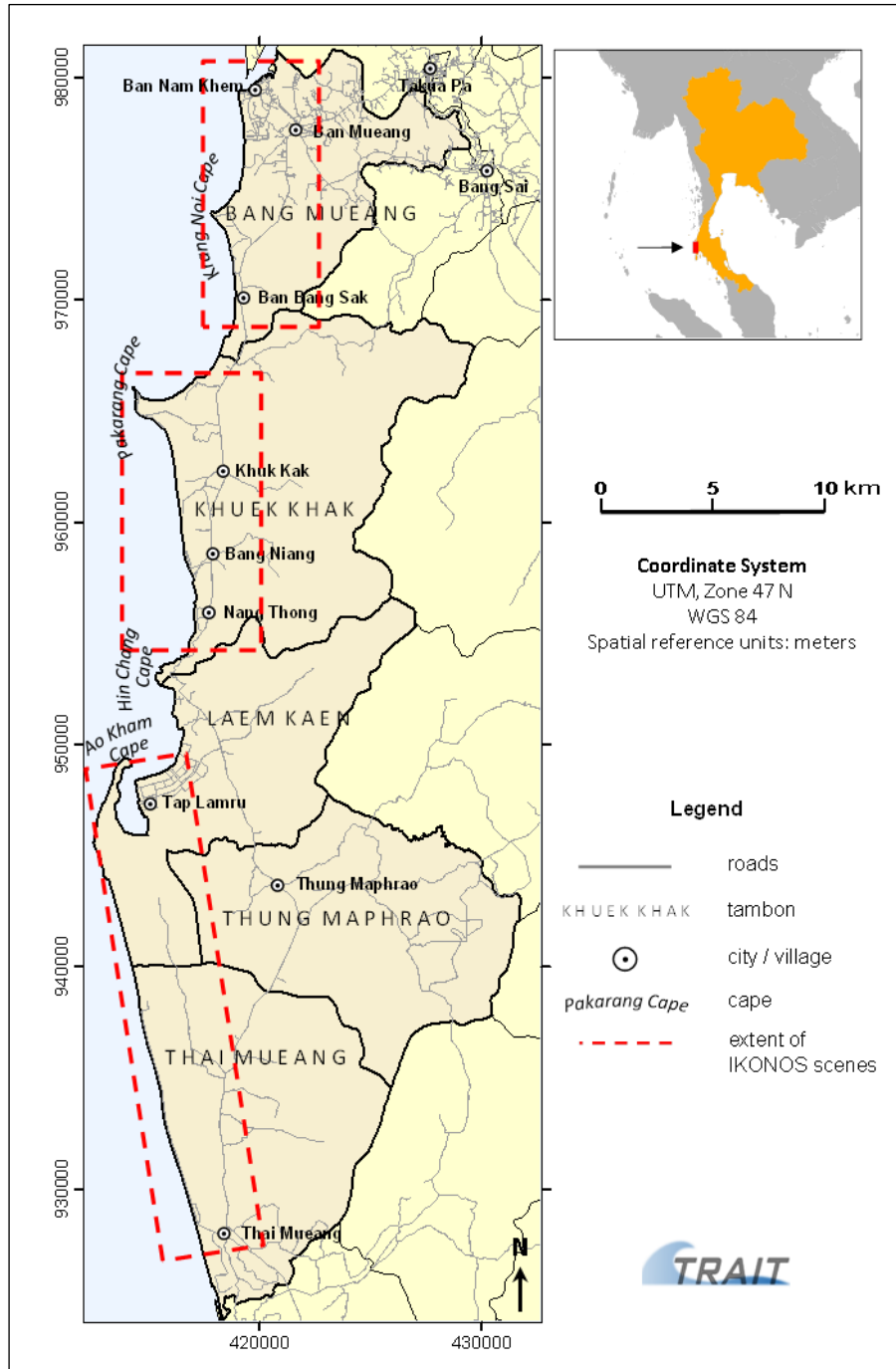


Figure 1-2. Location of the study area including the three extents of the IKONOS images.

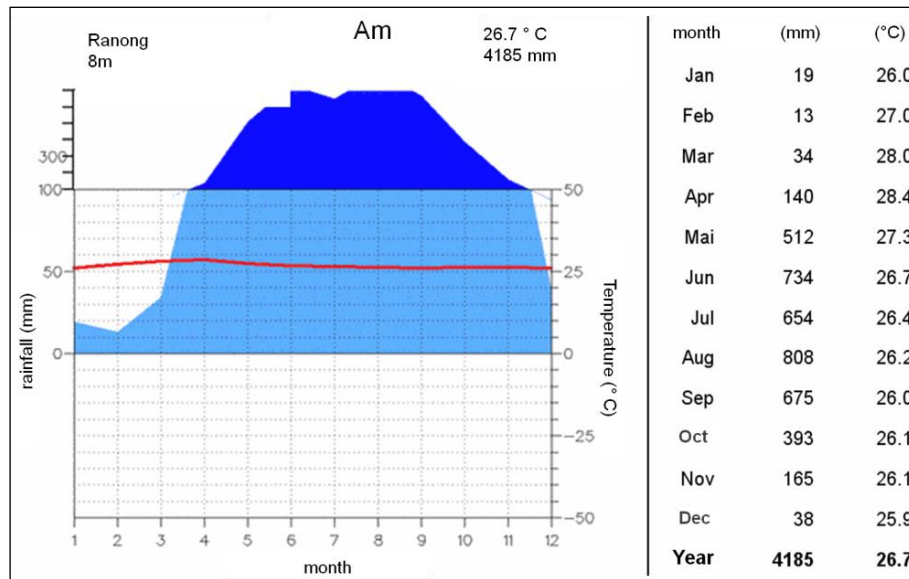
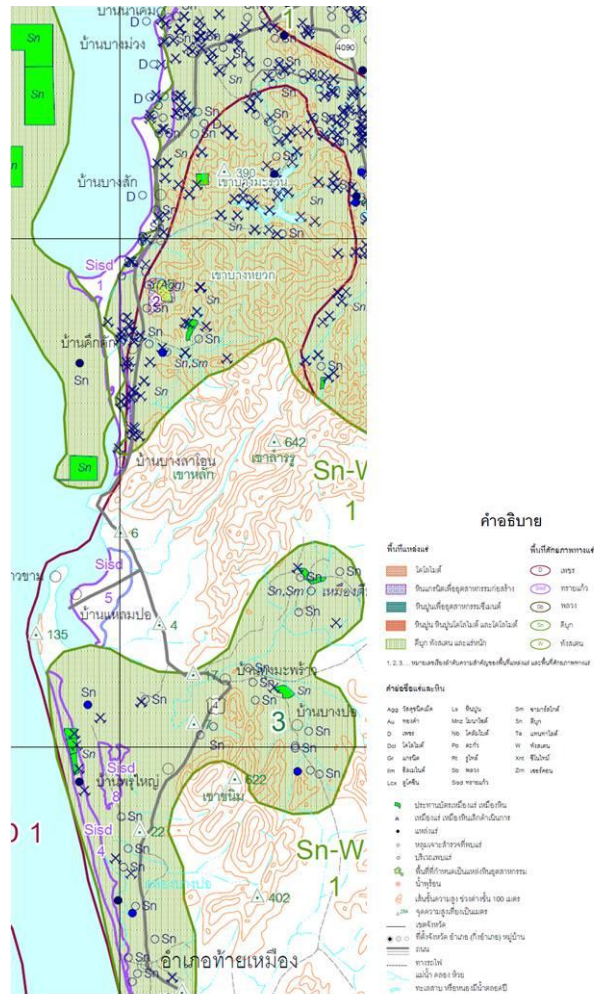


Figure 1-3. Climate data of Ranong. Modified from Mühr (2006).

#### 1.4.2 The landscape and human influences

The landscape of the coastal area is predominantly shaped by humans. Tin mining activities, shrimp aquaculture and intensive agriculture have strongly influenced the overall appearance of the landscape. With the exception of the hilly mountainous areas in the eastern part of the study area, most of the natural tropical forests disappeared and were replaced by agroforestry. Important crops include rubber, oil palm, coconut and cashew nut. According to FAO and MOAC (2005), about 69% of the total cropping area or 26% of the total land area of the Phang-Nga province was used for rubber (FAO and MOAC 2005). The occurrence of open landscapes and tropical grasslands (mainly *Poaceae* family) is due to human activities such as clearance for agriculture, logging for timber and tin mining. Mining activities predominantly took place in the northern part of the study area and finished in the seventies (cp. Figure 1-4). The effect on the environment include mainly the long-term degradation of soils (e.g. due to arsenic contaminations) limiting the growth and succession of woody vegetation. Furthermore, fresh water ponds and sand pits can be found in the landscape marking former opencast mining areas (Corlett 2008; Donner 1989; Szczucinski *et al.* 2006; Williams *et al.* 1996). In this regard, Figure 1-5 shows a freshwater pond near Ban Nam Khem.

Mangrove forests have been largely lost over the last few decades due to the process of several development activities. By the mid 1990s the total mangrove area was reduced by 33% (FAO and MOAC 2005). A main threat to the mangrove forests is related with the development of coastal aquaculture (which took place up to the late 1990s), particularly the shrimp farm industry with the black tiger prawn as its main export product (Adger *et al.* 2005; Plathong and Sitthirach 1997; UNEP 2005). Figure 1-6 illustrates that in 2004, 84% of the total marine shrimp production in Thailand resulted from aquaculture production. In the study area coastal aquaculture particularly occurs in the northern parts, such as in Ban Nam Khem at Krang Noi Cape.



**Figure 1-4.** Map of the mineral resources and mining activities in the study area. A full translation of the legend is included in Appendix A. The tin mining activities on this map are represented by the green shaded areas (resource area) and the mining symbols indicating former mining places. Modified from DMR (2001).



**Figure 1-5.** A freshwater pond near Ban Nam Khem as a result of opencast mining. The Photo was taken on 05.09.2008.



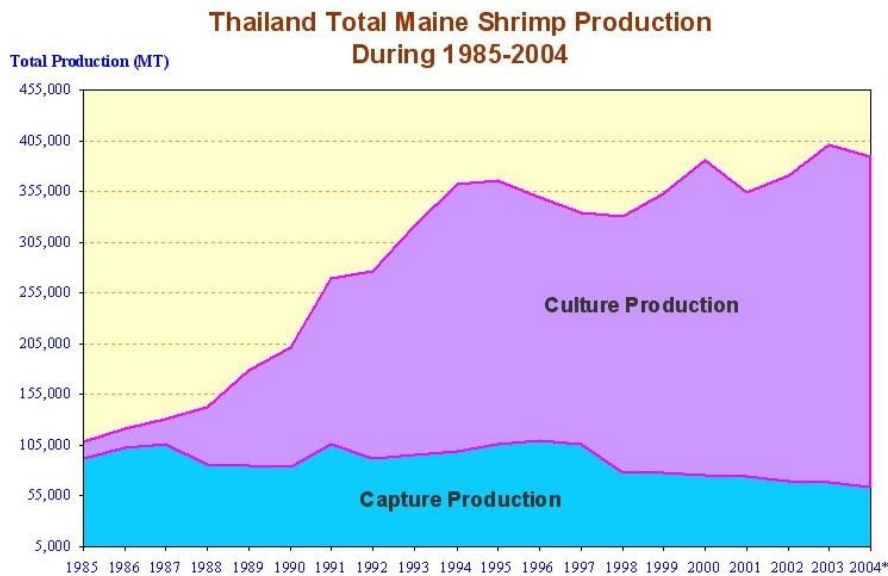


Figure 1-6. Thailand total marine shrimp production during 1985-2004. BIOTEC (2005).

### 1.4.3 Ecological characteristics

The following map on Figure 1-7 shows the distribution of major ecosystems and national parks within the study area. The GIS-data provided by the Ministry of Natural Resources and Environment, Department of Marine and Coastal Resources (DMCR n.d.) reveal that the majority of the coral reefs, seagrass beds and mangrove forests are located in the southern Tambons. Coral reefs are highly vulnerable to negative impacts from overuse and degradations of habitats including the degradation of interconnected ecosystems, i.e. mangroves (Phongsuwan *et al.* 2006; UNEP 2005). The northern reefs at Pakarang Cape and Krang Nui Cape are shallow water reefs which had been degraded prior to the tsunami event due to the effects of offshore mining in the 1970s (DMCR 2005). In contrast, the southern reefs which are located in water depths between six and ten meters are still intact and are characterised by high biodiversity of stony corals i.e. *Acropora* and *Porites* (DNP 2003). The total reef area is 889 hectares.

Seagrass beds are restricted to the intertidal zone between Tap Lamru and Ao Kham Cape. Even though the total area is relatively small (only 89 hectares), seagrass beds play an important role in marine ecosystems. They provide important nursery areas and habitats for coral reef fishes, endangered species, i.e. the dugong (*Dugong Dugon*) and dolphins (*Sousa chinensis* and *Tursiops aduncus*) and also ensure the sustainable abundance of commercial fish or crustaceans in near-shore fisheries (Adulyanukosol and Poovachiranon 2008; Millennium Ecosystem Assessment 2005a). Sickle seagrass (*Thalassia hemprichii*) is found to be the dominant seagrass species in the study area (DMCR n.d.).

There are two major mangrove areas: one mangrove area is located in the north, east of Ban Nam Khem; a second, larger area is located around a tidal inlet sheltered by a peninsular in the southern Tambons Lem Kaen, Thung Maphrao and Thai Mueang. Due to the massive degradation of mangrove forests in the last decades (cp. section 1.4.2) the majority of mangroves in south Thailand are secondary forests with trees that are less than 12 cm in diameter and 10 m in height (FAO and MOAC 2005). However, several parts of the mangrove forests in the South are still intact and partially protected by national park status (Khao Lampi - Hat Thai Mueang National Park).

According to Yanagisawa *et al.* (2009) and Phapavasit *et al.* (2009) the dominant mangrove species found in the study area are *Rhizophora apiculata*, *R. mucronata*, *Ceriops tagal* and *Bruguiera sp.*. From the GIS-data provided by the DMCR, one can assume that there are no mangrove forests occurring between Ban Nam Khem and Nan Thong. This could not be supported by the detailed analysis of high resolution imagery and will become apparent when discussed in section 5.1).

In addition to the ecosystems described above, there are other important natural resources and biotopes that should be taken into consideration including coastal forests and natural rain forests. Unfortunately detailed geographic information on these ecosystems were not available prior to this study and thus had to be created within this thesis (section 5.1). In general, natural rain forests are located in the mountainous terrain east of the study area and therefore were not affected by the tsunami (and not further considered in this study). They are protected by the two national parks, Khao Lampi - Hat Thai Mueang National Park in the South and the Khao Lak Lam Ru National Park south of Nang Thong. Regarding the beach forests, a widespread and important (for dune stabilisation and forestry) tree species is the *Casuarina equisetifolia*. It can form mono-specific stands and forms the landward edge of the *pes-caprae* formation (named after *Ipomoea pes-caprae*). They are common pioneers in beach ridges and flat environments (Whitten *et al.* 1997). *Casuarina equisetifolia* is often interspersed with other tree species such as *Pandanus odoratissimus*, *Cocos nucifera*, *Barringtonia asiatica* and *Terminalia catappa* (FAO and MOAC 2005; Whitten *et al.* 1997). Additionally further types of coastal forests can be distinguished, such as mixed littoral forests and melaleuca forests (cp. section 5.1).

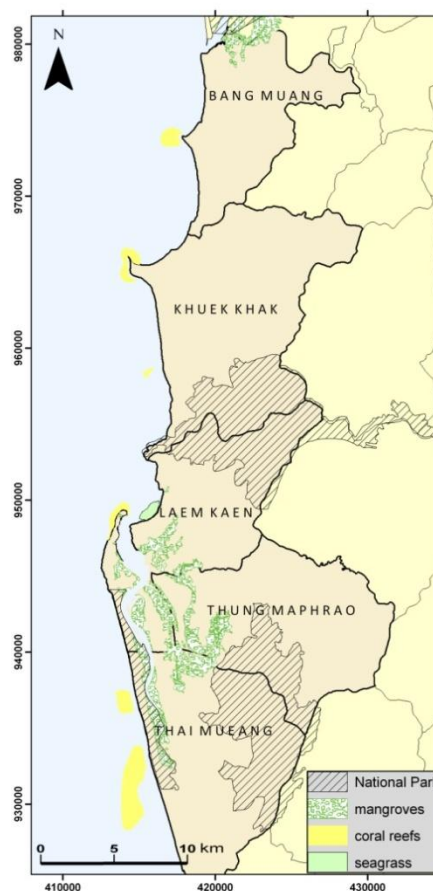


Figure 1-7. Ecological characteristics of the study area. GIS-data are provided by DMCR (n.d.).



## 2 Theoretical background: vulnerability, ecological vulnerability and remote sensing applications

Since this thesis addresses the broad topics of vulnerability research and remote sensing, this section is aimed at providing the reader a comprehensive overview of the following issues: *vulnerability, ecological vulnerability, risk and remote sensing and vulnerability assessment*. The methodological approach developed in this study is provided in section 4.

### 2.1 Vulnerability

A literature review regarding vulnerability reveals that there is a lack of a consistent definition of vulnerability (McLaughlin and Dietz 2008; Villagrán De León 2006). According to Villagrán De León (2006) different views on vulnerability stem from research groups and professionals in academia, disaster management agencies, the climate change community and development agencies. Academia for example focuses on the analysis of all aspects pertaining to the term including the anthropologic, social, economic, environmental and technical and engineering point of view with the purpose to promote awareness or to provide advice for policymakers and development agencies. In contrast, disaster reduction and development agencies simplify the term to practical level allowing them to assess vulnerability as an initial means to reduce it. Current efforts in vulnerability research are hampered by limiting theorizing, conflicting conceptual frameworks, unconsolidated data and inadequate models (Clark *et al.* 2000; Oliver-Smith 1996).

The lowest common denominator concerning vulnerability can be seen in the fact that vulnerability is mostly seen as an internal side of risk (intrinsic vulnerability) which is characterised by the conditions of the exposed element or community at risk (Cardona 2004; UN/ISDR 2004; Wisner 2002). These intrinsic conditions of the exposed element or system are often termed as its susceptibility. In this context Birkmann (2005) presents a concept of the spheres of vulnerability (Figure 2-1) which starts with the inner sphere, the intrinsic vulnerability or in the broader context the “exposure” and “susceptibility”. With each higher sphere the concept of vulnerability is extended depending on the scale, theme and disciplinary focus and purpose of the definition. According to the definition of Wisner (2002) and Wisner *et al.* (2004) vulnerability is determined by the likelihood of injury, death, loss and disruption of livelihood in a hazardous situation and/or unusual difficulties in recovering from negative impacts and extreme events (second sphere). A dualistic understanding of vulnerability encompassing both the *susceptibility*, defined as characteristics which describes the weakness of a system or element exposed, and the *coping capacity* which is the positive resource to deal with the negative impacts of a hazardous event and its impacts. This understanding underlies many vulnerability approaches and can be observed in Wisner (2002) and partly in Bohle (2001). Multi-structure-definitions widen the concept of vulnerability by encompassing susceptibility, coping capacity and also the adaptive capacity, exposure and the interactions with stresses and perturbations (fourth sphere). Here, Turner *et al.* (2003) provide a comprehensive framework (Figure 2-2) of a coupled scale-dependent system’s vulnerability to hazard, where the human-environmental system represents the vulnerability including the exposure, sensitivity and resilience (coping/response, impacts/response, adjustment and adaptation). A fifth sphere of vulnerability can be seen by broadening the thematic dimension of vulnerability encompassing physical, economic social, environmental and institutional aspects.

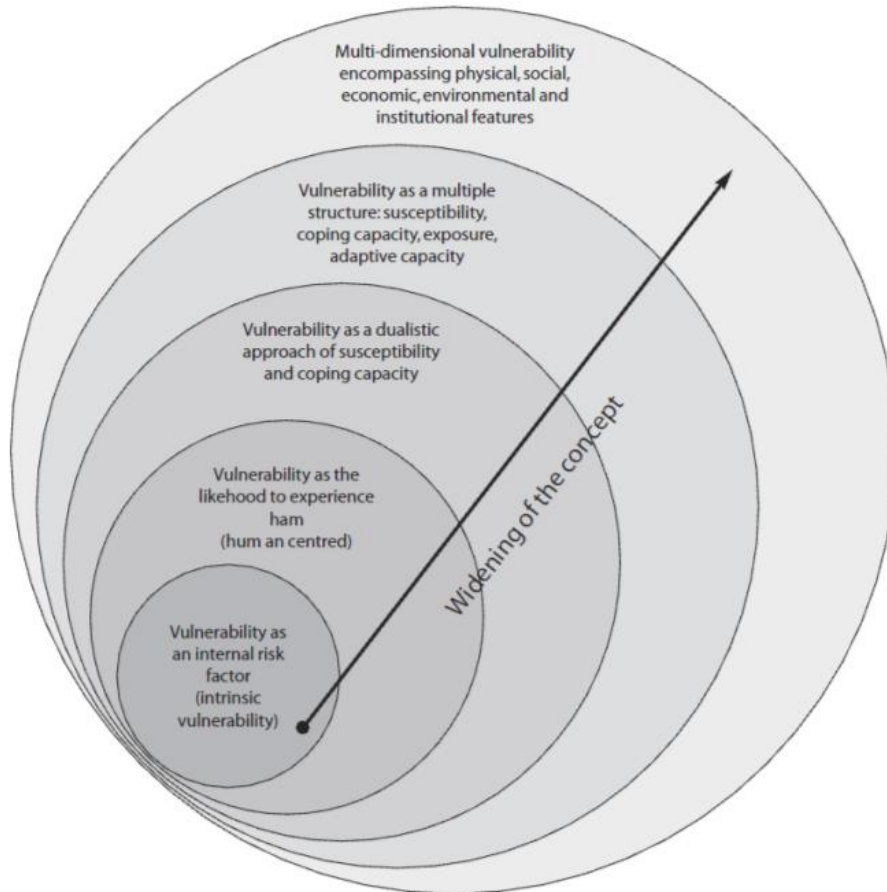


Figure 2-1. The spheres of vulnerability. Birkmann (2005).

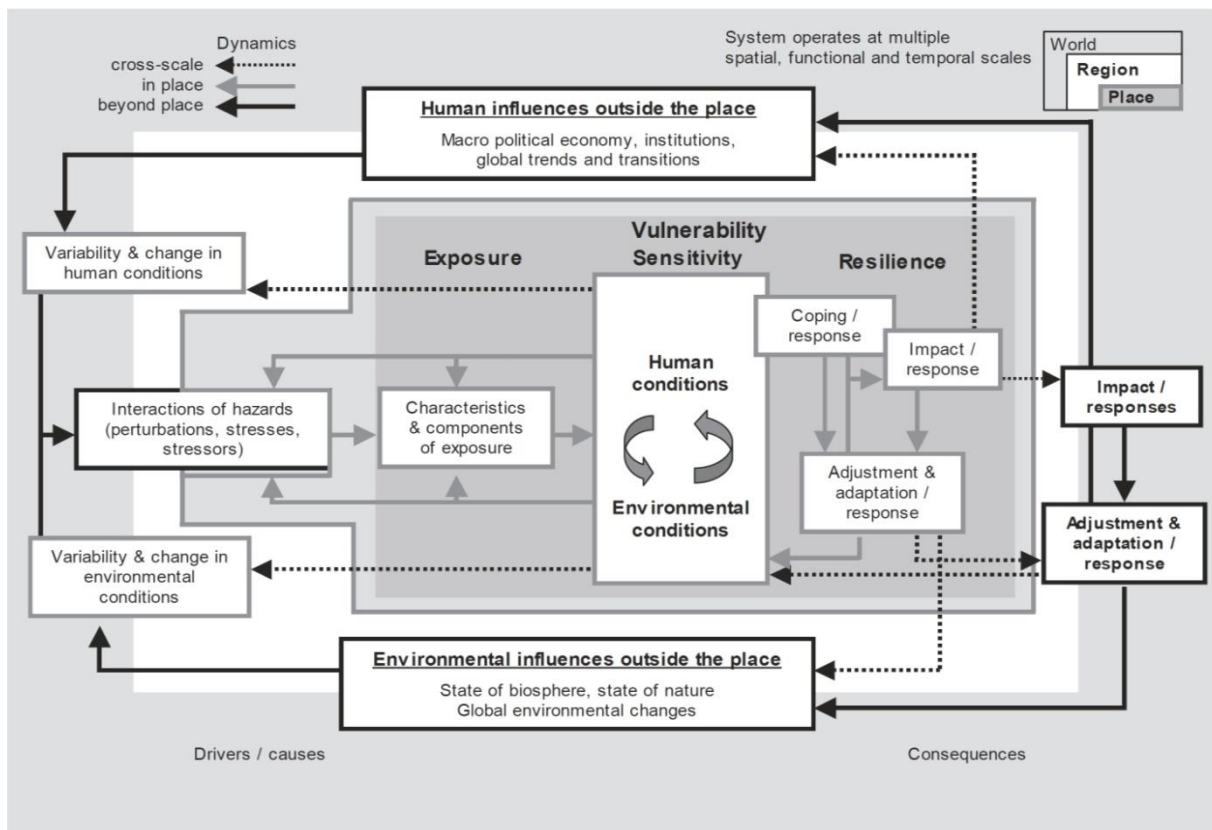


Figure 2-2. The vulnerability framework of Turner. Turner et al. (2003).

While a number of closely related definitions and frameworks of vulnerability can be found in the literature, e.g. Clark *et al.* (2000) or the BBC-conceptual framework of risk and vulnerability based on Bogardi and Birkmann (2004) and Cardona (1999, 2001), a further discussion of the nuances of each definitions is not focused. According to Adger (2006), the challenge for vulnerability research is to develop robust methods allowing the incorporation of diverse methods that include perceptions of risk and vulnerability, as well as the incorporate of governance research on the mechanisms that mediate vulnerability and promote adaptive action and resilience.

In TRAIT the vulnerability concepts of Turner *et al.* (2003) and partly the one of Clark *et al.* (2000) are adopted including the three components of exposure, sensitivity and resilience and broadened by explicitly distinguishing between the social, economic and ecological vulnerability (cp. Figure 2-3). The question how this framework is applied in this study and approached by remote sensing techniques will be described in section 4.

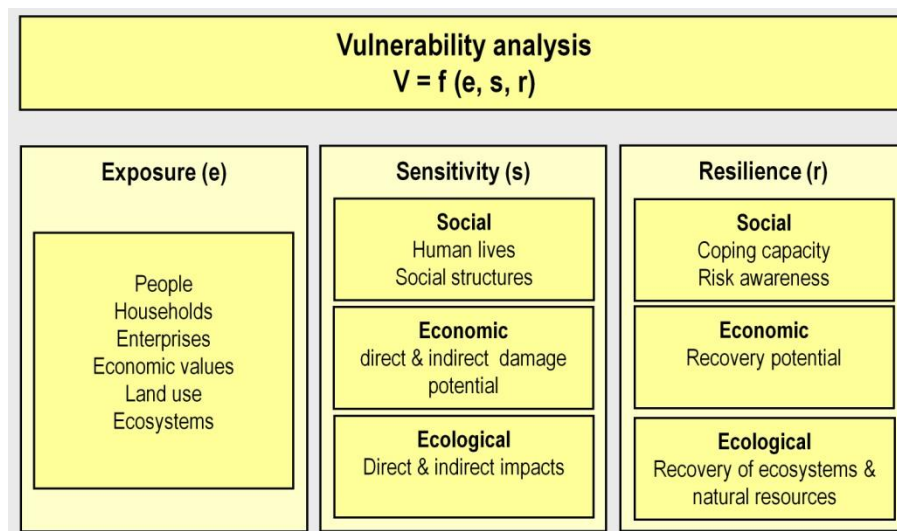


Figure 2-3. The vulnerability framework applied in TRAIT.

### The linkage between vulnerability and risk

Even though this thesis has its focus on the analysis of vulnerability, it should be clarified at this point how vulnerability is interlinked with risk and how the concept of vulnerability is implemented in the risk framework of TRAIT. According to Birkmann (2007), risk can be generally defined as a function of the hazard and the vulnerability of the element exposed. This explains the main framework of TRAIT which is composed of the analysis of hazard, vulnerability (including the exposure) and risk in order to perform risk management. The hazard in TRAIT is represented by the tsunami and can be will be assessed by the assessed by the relationship between likelihood of occurrence or probability and intensity (i.e. inundation height, flow velocity). The starting point here is the 2003 Indian Ocean tsunami, but also other possible tsunamis scenarios are considered. Thus, risk can be represented by the product of hazard potential and vulnerability (e.g. Kumpulainen 2006):

$$\text{Risk} = \text{Hazard} \times \text{Vulnerability} \quad (1)$$

Since in TRAIT vulnerability will be assessed in terms of exposure, sensitivity and resilience, the following mathematical expression of risk can be used (cp. Villagrán De León 2006):

$$\text{Risk} = \text{Hazard} \times \text{Exposure} \times \left( \frac{\text{Sensitivity}}{\text{Resilience}} \right) \quad (2)$$

## 2.2 Ecological vulnerability – definitions and concepts

Similar to the concept of vulnerability, a consistent definition of ecological vulnerability does not exist. Furthermore, the term is not consistently used. Common terms are *ecological vulnerability* (e.g. De Lange *et al.* 2006; Zhang *et al.* 2009), *ecosystem vulnerability* (e.g. Williams and Kaputcka 2000), *environmental vulnerability* (e.g. Birkmann and Wisner 2006; Villa and McLeod 2002) or *biophysical vulnerability* (Liverman 1990). Other scientists use the more general term of the *ecological dimension of vulnerability* (Kumpulainen 2006; Wilches-Chaux 1993) or extend the term by adding the social component such as *socio-ecological vulnerability* (Oliver-Smith 2009) or the *human ecological and political ecological perspective of vulnerability* (McLaughlin and Dietz 2008).

Despite of this inconsistency in terminology, two major views on ecological vulnerability can be differentiated (cp. Birkmann and Wisner 2006): a bio-centric and an anthropocentric perspective. The first point of view, which was also focused in this thesis, encompasses the analysis of the fragility and susceptibility of ecosystems and environmental components themselves. This definition implies that the impacts on human are a secondary consequence of ecological vulnerability. In this regard, Villa and McLeod (2002) use the term environmental vulnerability and distinguish between intrinsic and extrinsic vulnerability. Whereas intrinsic vulnerability refers to factors internal to the system (ecosystem health and resilience), extrinsic vulnerability involves factors external to the system, such as the present exposure and the external hazard. Thus, ecological vulnerability recognises both, the ecological damage potential and coping capacity (Kumpulainen 2006; Villa and McLeod 2002). Liverman (1990) uses the term of the biophysical perspective and focuses on the vulnerability or degradation of biophysical conditions and extrapolates from these estimates to the human environment of a landscape. According to De Lange *et al.* (2009) the term ecological vulnerability can be used at several hierarchical levels including organism, population, community, ecosystem and landscape. A species-specific approach was focused in De Lange *et al.* (2006), where ecological vulnerability of selected fauna wildlife species was assessed to soil and sediment contaminations. In contrast, ecosystem vulnerability (Williams and Kaputcka 2000) is defined as the inability of an ecosystem to tolerate stressors over time and space.

The second view on ecological vulnerability focuses on the disruption of environmental services which are essential for human well-being, such as clean drinking water, nontoxic soils for agriculture, food. The impacts of the hazard are analysed with regard to the interlinkages between human activities and their needs and ecosystem services and functions, the so-called socio-ecological system (Adger *et al.* 2005; Birkmann and Wisner 2006). This approach was adopted by the Millennium Ecosystem Assessment 2005 and also by the GEO-4 (UNEP 2002). In context of the tsunami event of 2004 the protective role of coastal vegetation – in particular mangroves – has become a main focus in ecological vulnerability assessments (e.g. Chang *et al.* 2006; Chatenoux and Peduzzi; Dahdouh-Guebas *et al.* 2005).

According to Oliver-Smith (2009) the socio-ecological vulnerability describes the degree to which a socio-ecological system is either susceptible or resilient to the impact of natural hazards and is the outcome of various factors: awareness of hazard, settlement and infrastructure patterns, public policy and administration, the level of social development and institutional capacities in disaster and risk management (Brooks *et al.* 2005; Nicholls and Hoozemans 2005).

It can be concluded that different approaches and definitions for ecological vulnerability exist leading to different ways of assessing ecological vulnerability including the definition of the exposure, sensitivity and resilience (compare the following section 2.3). In this study an ecosystem-specific or bio-centric approach of ecological vulnerability was adopted (cp. Williams and Kaputcka 2000). A detailed description of the main methodological approach including the definitions of the three components exposure, sensitivity and resilience is provided in section 4.

### 2.3 Assessment of vulnerability and ecological vulnerability

Vulnerability assessment traditionally began with the analysis of historical data on disaster, identifying and systemisation vulnerable conditions from damages and losses experienced by different communities. The need to identify indicators or proxies describing the characteristics or properties that bear a direct or indirect functional relationship to the hazard, exposure or the impacts of exposure make up the basic idea in vulnerability assessment (e.g. Birkmann and Wisner 2006; Polsky *et al.* 2003). The OECD (1993) defines an indicator generally as a “parameter or value that is derived from parameters characterizing the state of a phenomenon, environment or area with a significance extending beyond that directly associated with a parameter value.” In contrast, a parameter can be defined as the property that is measured or observed whereas an index comprises a set of aggregated or weighted parameters or indicators. According to Hahn (2003) disaster-risk indicators should have the following characteristics:

- Validity - Is the indicator appropriate for measuring the key element under consideration?
- Reliability – Is the indicator a consistent measure over time?
- Sensitivity – When the outcome changes – will the indicator be sensitive to those changes?
- Availability – Is it easy to measure the indicator or to collect the needed information?
- Objectivity – Can the data be reproduced if conditions change?

According to Villgran (2006) the use of indicators and indices has allowed the measurement of the status of community or a society, the comparison of various societies as well as the identification of important issues which need to be addressed in order to support the development of societies at certain paths. In the global change research, the OECD’s State of the Environment Group has adopted a framework comprising an indicator set targeting the environmental and its management and sustainability. In this frame work, known as Pressure-State-Respond-model (P-S-R), pressure indicators are related to the variables directly causing environmental problems (e.g. increased greenhouse gas emissions), whereas the State describes the current condition of the environment (e.g. current greenhouse gas concentrations). The response indicators are related to the efforts of the society to manage such issues (e.g. introduction of cars with catalytic converters).

According to Villgran (2006), this P-S-R model can be easily adapted to sectors, communities or societies in the context of vulnerability associated with natural hazards (e.g. earthquakes, landslides, etc.).

With regard to the assessment of ecological vulnerability several methods can be found in the literature. Referring to the more eco-centric approaches, De Lange *et al.* (2006) assess vulnerability of selected fauna wildlife species to soil and sediment contaminations. They used species traits and other auto-ecological characteristics to rank the wildlife species by vulnerability to a certain chemical. Some of the indicators used were habitat preference, lifespan or food web. Referring to a study of Penghua *et al.* (2007) at the landscape level, vulnerability was assessed by comparing seven types of land use for vulnerability to desertification and soil erosion. The land use types were classified by landscape pattern analysis and statistical models were applied for the vulnerability estimations. One of their main results was that the fragmentation and the sensitivity of land desertification had considerable effects on the vulnerability of landscape types and the whole area (they termed this as regional eco-environmental vulnerability). Regarding to a more anthropo-centric perspective on ecological vulnerability, indicators often relate to the potential capacity of an ecosystem or area to provide a certain service. This capacity can be expressed by the ecosystem health or the environmental quality (e.g. Rosenberg *et al.* 1996; Shen *et al.* 2004). In the context of the 2004 Indian Ocean tsunami, Renaud (2006), Adger (2006) and Dahdouh-Guebas *et al.* (2005) state that the pre-condition of mangrove stocks describe the buffering effect on the tsunami waves. Furthermore, chronic degradation of local environments has influenced both the short- and mid-term tsunami impacts and the long-term option for –rebuilding (Adger *et al.* 2005).

In a study on coastal vulnerability in India conducted by Noronha *et al.* (2001) pressure indicators were developed that have a potential effect on coastal ecosystems, such as mangroves, coastal water and ground water. The indicators used were population density, density of tourist rooms, area under intensive aquaculture (including land use change), number of potentially polluting industrial units located, etc. Another method developed by Coppolillo *et al.* (2004) was designed to select the appropriate species in a landscape for conservation purposes. Based on expert judgements, vertebrate species were scored on area requirement, heterogeneity, ecological functions, vulnerability and socio-economic function, etc. Vulnerability was assessed for each threat (= major land uses) by applying a formula incorporating exposure, severity of effect and probability of occurrence. Further studies focusing on socio-ecological vulnerability can be mentioned at this point such as De Chazal *et al.* (2008); Alessa *et al.* (2008) and Metzger and Schröter (2006).

In this section a theoretical background on the concepts of vulnerability, ecological vulnerability as well as a short literature review on ecological vulnerability assessments was provided. Since in this thesis a remote sensing based approach is intended, it needs to be emphasized how remote sensing techniques can be in principle applied in the natural hazard context and in the context of vulnerability assessments.



## 2.4 The role of remote sensing in vulnerability assessments

Remote sensing, as a technology for the monitoring of coastal environments and the mapping of natural hazards in particular, has advanced at an unprecedented rate during recent decades (Huh *et al.* 1991). Since the year 2000, several international space agencies have signed the International Charter “Space and Major Disasters” to develop a unified system of space data acquisition and delivery for authorities and decision makers in disaster affected areas. According to Oesch (2001) remote sensing is an established methodology that can be applied for different types of natural hazards. A main field of application encompasses the mapping and monitoring of natural hazards or hazardous situations and processes in order to provide advanced warning or to improve management of emergency situations following a disaster (Altan *et al.* 2001; Oesch 2001; San Miguel Ayanz *et al.* 2000). In this context, the German Aerospace Centre (DLR) has established the Centre for Satellite Based Crisis Information (ZKI) aiming at the coordinated use of the growing capabilities of multi-sensoral earth observations from space in order to provide near-real-time information for emergency mapping and crisis management. Other fields of applications in the natural hazard context involve the estimation of a region’s susceptibility to potential threats, e.g. earthquakes and volcano (e.g. Theilen-Willige 2006, 2010), the analysis of the duration and intensity of natural disasters (e.g. damage assessments) or the prediction and forecasting of natural hazards, e.g. extreme weather, tropical storm tracking (e.g. Miura *et al.* 2005). Furthermore remote sensing can be used to provide basic input data, such as land use, topography or snow cover that is required for modelling of natural hazards like river floods or slope stability analyses (Oesch 2001; Schultz 1993).

With regard to the assessment of vulnerability remote sensing can still be considered as a new tool (Nassel and Voigt 2006). However, although many remote sensing studies do not explicitly focus on the holistic assessment of vulnerability, they can provide valuable information which are required to assess vulnerability: e.g. those studies dealing with the extraction and characterisation of exposure units (e.g. houses, ecosystems) and damage and recovery assessments (e.g. Chang *et al.* 2006; Koshimura *et al.* 2010; Lu *et al.* 2003; Miura *et al.* 2005).

Due to the development of high-resolution satellite sensors (IKONOS, Quickbird) in the last few years, recent studies on vulnerability focus on buildings and infrastructure. According to Nassel and Voigt (2006) the basic idea is that vulnerability is linked to people who mostly live in houses and use certain infrastructure which can be assessed with satellite imagery. In the study of Nassel and Voigt (2006) object-oriented image analysis based on IKONOS-data was used to extract single houses and to derive proxy indicators referring to the construction quality of buildings and the economic wealth of people. Indicators representing the physical vulnerability of the built-environment, including the shape and size of single houses, the density of the built-environment as well as the possible risk area could be successfully derived by remote sensing (Nassel and Voigt 2006). Similar findings on the capabilities of high resolution imagery were produced by Taubenböck *et al.* (2008a) and Taubenböck (2008) in the context of earthquakes in Istanbul (Turkey) and by Taubenböck *et al.* (2008b) focusing on vulnerability towards tsunamis in Padang, Indonesia. Here, object-oriented classification approaches, GIS-analyses as well as ground truth observations were used to characterise physical vulnerability (e.g. urban structures, built-up densities, functions, building sizes), demographic vulnerability (population density and population distribution) and structural vulnerability of buildings. However, these studies showed that there are still limitations in assessing social, economic or political aspects of vulnerability (cp. McLaughlin and Dietz 2008).

In this context, Ebert *et al.* (2007) and Taubenböck *et al.* (2009) demonstrated that some broad social and social-economic indicators can be indirectly derived by remote sensing, such as socio-economic status, value of property, income or commercial and industrial development which can be used for social vulnerability assessments.

Regarding the assessment ecological vulnerability in the natural hazard context, there are only few studies which use remote sensing techniques. However, according to Dahdouh-Guebas (2001) remote sensing is an appropriate tool to assess the ecological impacts, resilience or recovery and thus provide valuable information for assessing ecological vulnerability. Several studies deal with the assessment of ecosystem damage or impacts or recovery following perturbation. With regard to the 2004 Indian Ocean tsunami, there are studies dealing with tsunami impacts on mangrove forests (e.g. Sirikulchayanon *et al.* 2008; Sridhar *et al.* 2006), coral reefs (e.g. Bahugana *et al.* 2008) or sandy beaches (Choowong *et al.* 2009; Vosberg 2010). Several studies in the tsunami context deal with the evaluation of the role of mangrove forests in mitigating tsunami impacts and thus have their focus on the anthropo-centric or socio-ecological vulnerability, such as Chang *et al.* (2006) and Olwig *et al.* (2007). Wang and Xu (, ) demonstrated in a more complex way how multi-date remotely sensed data can be used to estimate forest vulnerability to hurricane disturbances, caused by the Hurricane Katrina. First they tested several change detection techniques to assess forest damages; secondly proxy indicators which were mainly derived from Landsat data, such as vegetation indices, land cover, landscape metrics, were used to identify factors determining the probability of hurricane disturbances.

Several studies on ecological vulnerability do not refer to natural hazards, but to human pressures or ecosystem health respectively environmental quality. Dahdouh-Guebas (2001) examines how future mangrove vegetation structure and degradation can be predicted based on vegetation history and current vegetation structure in the field. He used sequential high resolution remote sensing imagery to assess whether a mangrove forest is dynamic or static and whether or not it has degraded. Studies that deal with the assessment of ecological vulnerability are often applied on a broader spatial scale such as landscapes or river-basins (e.g. Jones *et al.* 2003; Li *et al.* 2006; Penghua *et al.* 2007; Zhang *et al.* 2009). Here, the basic function of remote sensing techniques is to provide land use information which are evaluated in terms of composition, patterns and landscape metrics.

### Conclusion

From the literature review presented in this section it can be concluded that remote sensing can be employed in a wide range of applications in the natural hazard and vulnerability context. However regarding the assessment of ecological vulnerability, a lack of studies exists in those cases where:

- ecological vulnerability is comprehensively assessed by remote sensing techniques including the three components of vulnerability, exposure, sensitivity and resilience;
- the capabilities of remote sensing techniques in supporting the assessment of ecological vulnerability are critically discussed
- ecological vulnerability is assessed on the local level based on high resolution imagery and the automatic and thus transferrable procedures of digital image analysis (such as change detection studies or object-oriented image analysis)



Thus, one major motivation of this thesis results from the described gaps in the methodological concepts. Furthermore, another motivation results from a major gap of knowledge on the local ecological exposure, sensitivity and resilience in this study area which becomes apparent when reviewing the existing literature on tsunami impacts on coastal ecosystems and natural resources, presented in the following section.

### 3 Tsunami impacts on coastal ecosystems and natural resources at the Andaman Sea coast of Thailand

Soon after the tsunami event, government agencies initiated rapid assessments of the impacts on most of the natural resources in the affected regions in Thailand. In this section these reports and other scientific papers are summarised in order to provide a general overview of the tsunami induced impacts on the environment for the Andaman Sea coast of Thailand. A focus is given on the following coastal ecosystems and natural resources: coral reefs, seagrass beds, mangroves, crops and soils, endangered species and water resources.

#### 3.1 Coral reefs

Coral reefs represent valuable marine ecosystems and are found along the entire coast of Thailand. According to the Worldbank (2007) they are of major importance for fisheries, tourism, coastal protection, natural product industry and research and education. At the Andaman Sea coasts of Thailand the tsunami impacted coral reefs in various ways and intensities. A main damage pattern includes the physical destruction of the corals, either of the whole colonies or only the breaking of parts or branches of corals. These effects were either amplified by debris swept away from land by backwash (e.g. Bueno 2005; Phongsuwan *et al.* 2006) or by coral mining which caused a funneling of water through the gaps formed by mining (e.g. Fernando *et al.* 2005; Marris 2005). A second damage characteristic involved the smothering or burying of corals by sand and silt (siltation) resulting from intensive erosions of shallow sandy seabeds (DMCR 2005). An earthquake induced uplift of coral reefs above the high water mark was observed in Indonesia (UNEP 2005). Regarding the damage intensity, from a total of 174 study sites located in the Andaman Sea, 40% of the sites were not affected, 20% suffered very low damages, 17% and 9% suffered low and medium damages and only 13% of the sites were highly impacted (Table 3-1). Most damages occurred in the upper part of the peninsula, specifically in Ranong, the west coast of Phang-Nga, Surin and Similan Islands. The two provinces Satun and Phuket were almost unaffected. According to FAO and MOAC (2005), the total area of damaged coral reefs in Thailand was 3696 rai (591 ha).

The rapid damage assessments were carried out by the visual estimation of damage patterns found on the reefs in terms of percentage of damage areas related to the coral cover. The results were ranked according the following classification scheme, as described in Table 3-2.

**Table 3-1.** Number of affected stations categorised by impact levels. DMCR (2005).

Province	No impact (0 %)	Very low (1-10 %)	Low (11-30 %)	Medium (31-50 %)	High (>50 %)	Total
Ranong	0	2	2	1	7	12
Phangnga	21	12	16	10	13	72
- Surin Island	0	5	7	5	4	21
- Similan Is	11	7	8	5	7	38
Phuket	12	5	3	1	0	21
Krabi	12	8	4	4	2	30
- Phi Phi Island	5	4	2	3	1	15
Trang	2	4	2	0	0	8
Satun	22	5	3	0	1	31
Total	69	36	30	16	23	174

**Table 3-2.** Classification scheme for the estimation of the damage intensity of coral reefs. DMCR (2005).

Level of damage	% coral damage	Impact level
0	0%	No impact
1	1-10%	Very low impact
2	11-30%	Low impact
3	31-50%	Medium impact
4.	>50%	High impact

Figure 3-1 shows the impacts on coral reefs in Phang-Nga province that were observed during the rapid assessments. Reefs in shallow waters along the west coast had been affected severely by tsunami (80% of reefs were destroyed) including the Ka Island, Krang Noi Cape and Krang Yai Cape. The damage causes were mainly impacts from waves, which turned over coral heads, or corals being smothered or buried by sand. But according to DMCR (2005) these small reefs had been degraded before the tsunami due to the effect of sediment loaded from offshore mining activities in 1970s.

Referring to the factors determining the impact intensity DMCR (2005) concluded that coral damage was greatest on a) shallow water reefs occurring in highly exposed coasts (e.g. Ranong, west coast of Phang-Nga, Phi Phi island group), b) on reefs located in channels between two islands (e.g. between North Surin and South Surin) and c) near highly populated coast where debris caused major damages. Other possible factors included the pre-tsunami degradation of corals due to off-shore tin-mining, the coral type/material and the direction of striking waves (DMCR 2005; Phongsuwan *et al.* 2006).

Coral reefs are important marine ecosystems providing many ecosystem services. Thus, a major damage of this type of ecosystem can have serious consequences on humans, such as a potential loss of food security and malnutrition due to a lack of protein, reduced fish catches and tourism revenue, increase coastal erosion and increased risk of destruction from storms (e.g. UNEP 2005; UNEP-WCMC 2006; Worldbank 2007). But with 60% of sites showing little or no damage, the total damage of corals in Thailand can be considered as low (Phongsuwan and Brown 2007). Natural recovery of coral reefs depends on the severity of damage (UNEP 2005) and will take three to five years for reefs that suffered light damage and up to ten years for those that received greater damage.

Furthermore, recovery processes also depends on the degree of disturbances resulting from human activities, such as pollution, overfishing, climate changes, mangrove degradation (Phongsuwan *et al.* 2006; UNEP 2005).

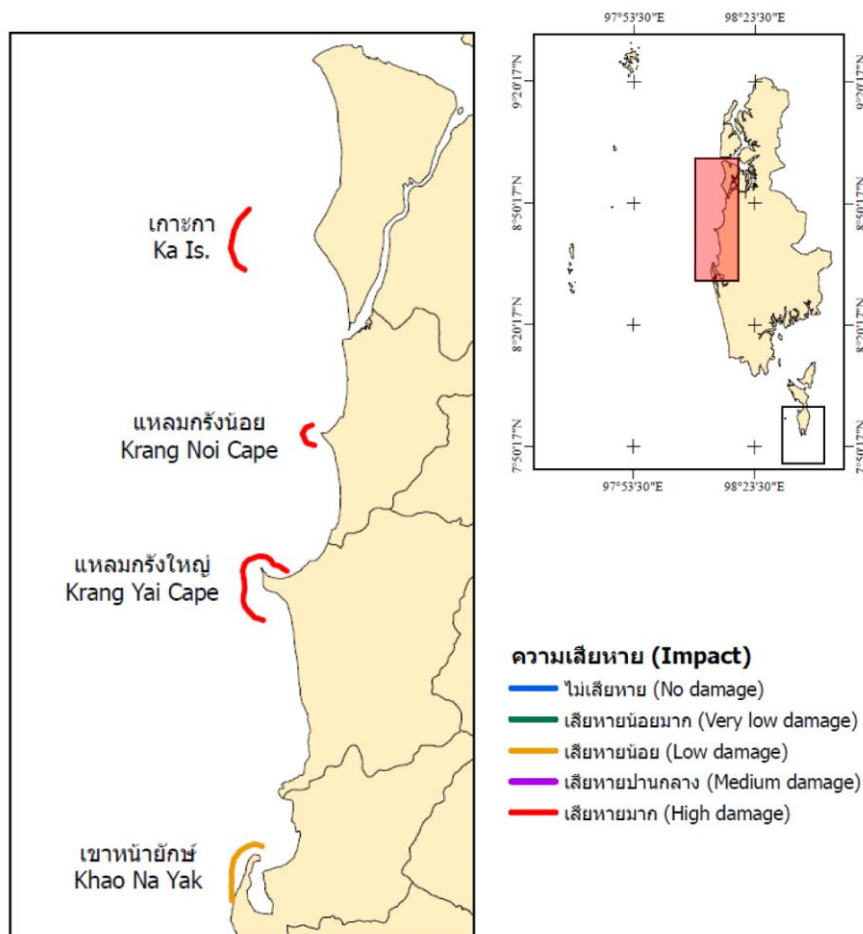


Figure 3-1. Damage patterns of coral reefs along the Phang-Nga coast. DMCR (2005).

### 3.2 Seagrass beds

Of a total of 104 square kilometers of sea grass habitats in Thailand, about 79 square kilometers are located in the Andaman Sea. They represent important ecosystems serving as feeding, breeding and nursery ground (habitats) for commercial fish and crustaceans and marine endangered species (Adulyanukosol and Poovachiranon 2008). Furthermore sea grasses improve water quality and can stabilise the sea bottom by their roots (Worldbank 2007).

In comparison to the coral reefs sea-meadows were less affected. A rapid assessment conducted by the DMCR covering 70% of the total seagrass area occurring in the Andaman Sea revealed that only 3.5% of the inspected area was impacted by sedimentation of silt and sand and 1.5% suffered a total habitat loss. The sites that experienced the highest degree of erosion and sand deposition were Thung Nagdam, the northern part of Phratong Island and near Yao Yai island (Figure 3-2) in Phang-Nga province (Bueno 2005; DMCR 2005). The quick assessment was carried out from 30. 12. 2004 to 13. 01. 2005 based on visual estimation of the damage type and percentage of damaged area.

The damage characteristics include both direct and indirect effects. Direct damages include effects like the detachment of seagrass leaves, the erosion of sand along the outer edges of the seagrass patches or on wave-exposed sites. Indirect effects include the deposition of sediments and the browning-off or rotting of seagrass leaves resulting from increased abrasion where bottom sediments had been disturbed and dispersed. The following Figure 3-3 illustrates the different damage patterns caused by the tsunami impact.



**Figure 3-2.** Damage patterns of seagrass meadows around Yao Yai island. Modified from DMCR (2005).

Although the total area of impacted seagrass meadows was relatively small, a loss of whole patches implies a loss of habitat functions and nursery ground of both commercial fish and crustaceans and marine endangered species (Adulyanukosol and Poovachiranon 2008). Recovery processes of seagrass are relatively fast, depending on the type and intensity of impact: Whereas new leaves can recover very fast (few months), recovery can take more than one year for seagrass beds that were buried by sandy sediments, e.g. from sand ridge erosion (DMCR 2005). The status and coverage of seagrass in Thailand in 2006 suggest that seagrass beds have nearly fully recovered in most areas of the Andaman Sea coast. Furthermore the main degradation of seagrass beds was found to be human related, for example due to sedimentation resulting from coastal construction, fisheries and illegal fishing (Adulyanukosol and Poovachiranon 2008).

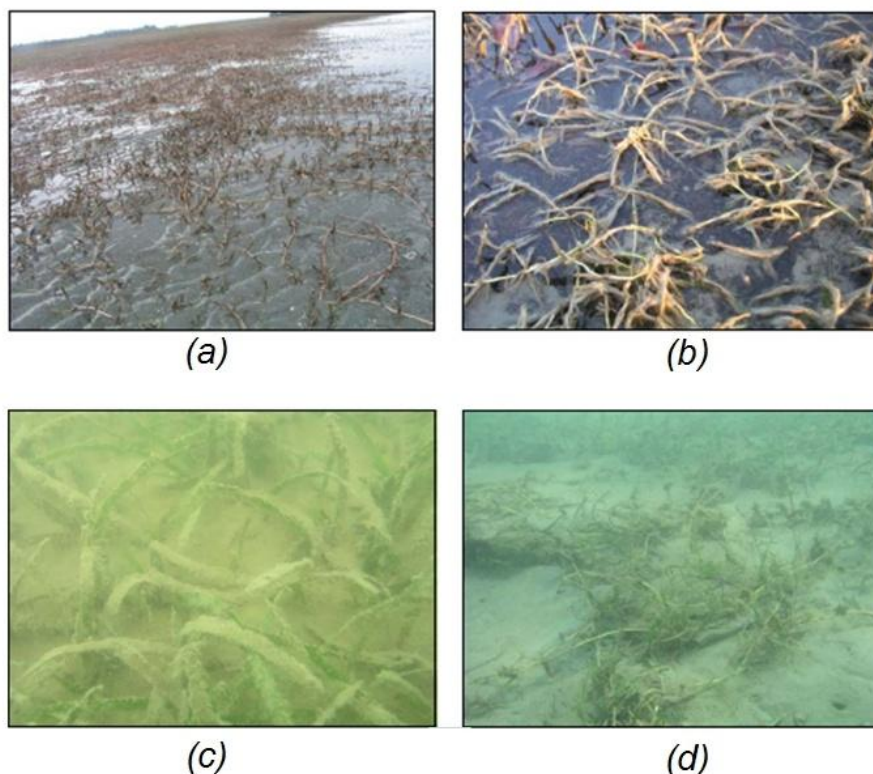


**Figure 3-3.** Tsunami induced impacts on seagrass meadows. (a) exposed rhizomes and roots caused by substrate erosions, (b) damages seagrass leaves, (c) siltation of seagrass and (d) detachments of rhizomes and roots caused by erosion. DMCR (2005).

### 3.3 Mangrove forests

Mangrove forests represent one of the most valuable coastal ecosystems on earth and many studies have been carried out on these ecosystems emphasizing their great value for the natural system (e.g. to serve as habitats, nursery and feeding ground) as well as for the human or socio-environmental system (serving as natural buffers against tsunami impacts, providing food and other products such as charcoal, timber, food), compare and Drude de Lacerda (2002) and UNEP-WCMC (2006). Detailed studies on the traditional and current uses of mangrove forests in South Thailand are provided in Plathong and Sitthirach (1997) and Paphavasit *et al.* (2009).

The Office of Mangrove Conservation, Department of Marine and Coastal Resources, Ministry of Natural Resources and Environment conducted a rapid assessment on mangrove impacts in Thailand, but unfortunately a detailed English documentation on these assessments is not available. According to UNEP and DMCR (2007) 585 ha of mangrove forests at the Andaman Sea coast were reported to have been impacted by the tsunami, amounting to 0.33% of the total mangrove area. The relatively small area of impacted forests results from the fact that mangrove communities tend to be located within sheltered coastal areas (e.g. Chatenoux and Peduzzi 2007). This finding will also be confirmed by the local scale approach conducted in this study (cp. section 6). The Phang-Nga province was the most affected region with 304 ha of impacted mangrove forests (FAO and MOAC 2005). Furthermore, damage to national parks was also reported, i.e. at Laem Son in Ranong, Sirinad in Phuket and Surin in Phang-Nga. Referring to the damage characteristics mangrove forests were mainly directly affected in three different ways: windthrow with uplifted or uprooted trees lying in the area, bole damage or broken stem with stems remaining in the area or standing death (Paphavasit *et al.* 2009).



Other physical impacts include an increase in sedimentation and soil erosion which was observed in mangroves near Pakarang Cape and in Ban Nam Khem (Paphavasit *et al.* 2009; Yanagisawa *et al.* 2009). Furthermore, impacts also include alterations in mangrove fauna and flora, changes in water and sediment quality as well as socio-economic aspects (particular on fishing communities). The following Figure 3-4 illustrates typical damage patterns of mangroves.

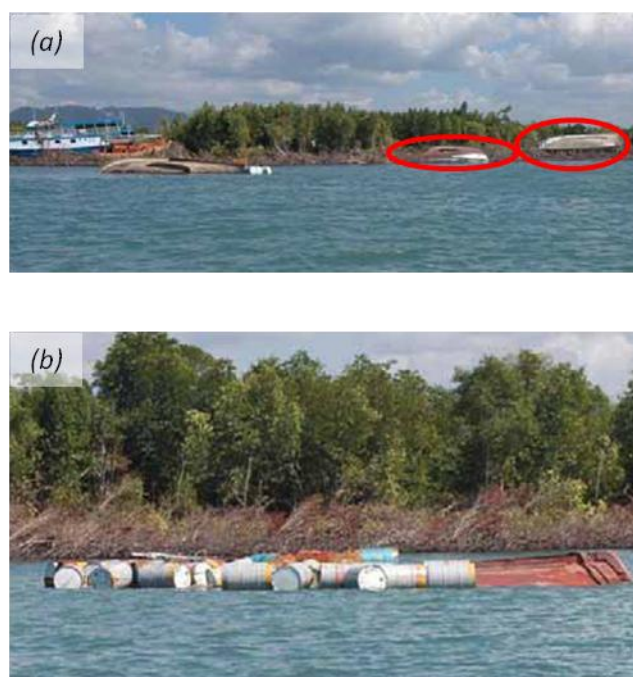


**Figure 3-4.** Physical damage of mangrove stands in Thailand: (a) caused by boats swept onshore by the tsunami and (b) broken mangrove trees along the sea front. Modified from FAO and MOAC (2005).

With regard to the factors determining the intensity of damage, preliminary data in study plots at Prapas Beach showed that smaller mangrove trees were more affected than larger trees (FAO 2005a). Since mangrove forests in South Thailand are usually secondary growth with average diameters less than 12 cm and 10 m in height, they are comparatively less resistant against tsunami impacts. Referring to tree species, the tsunami mostly destroyed the stilt root mangroves, e.g. *R. apiculata*, while larger trees of the slow-growing species (i.e. hard-wood) *Avicennia marina* or *Sonneratia alba* usually survived (FAO 2005b ; Tanaka *et al.* 2007). Contrary findings from in-depth analyses conducted in Phang-Nga province were observed by Paphavasit *et al.* (2009). They concluded that *Rhizophora* species have a higher ability to withstand the tsunami impacts than *Avicennia* species. However, it is broadly agreed that the tree's susceptibility to tsunami impacts refers to species characteristics such as root characteristics, wood density, flexibility of stems and branches, and the volume of tree crowns and density of foliage (Cochard *et al.* 2008). Referring to the site conditions, damage mainly occurred in the sea front areas where mangrove trees were broken or knocked down in a landward direction. In many areas the tsunami impacts were confined to ten meters inland, though in some places they extended to 450 m (FAO and MOAC 2005; Tanaka *et al.* 2007). Yanagisawa *et al.* (2009) and Paphavasit *et al.* (2009) concluded that mangrove trees were destroyed particularly around the river mouths and channels where the flow was concentrated.

Considering the long-term effects of the tsunami on mangrove ecosystems, field observations conducted in October and November 2005 at mangrove patches near Ban Nam Khem village (Phang-Nga province) and Bang Rong village (Phuket Province) revealed that mangrove forests were found to be resilient to the tsunami since they have continued to serve as habitats, nursery and feeding grounds for numerous mangrove inhabitants (Paphavasit *et al.* 2009). Additionally a high recovery rate of mangroves was predicted for this specific area. However, other studies on mangroves such as FAO 2005a/b from Thailand and Wibisono and Suryadiputra (2006) from Indonesia reveal that regeneration rates are relatively slow, especially where the tsunami have changed the main habitat characteristics (e.g. sand accumulations on forest floors). Fujioka *et al.* (2008) analysed stands and macrobenthic communities in mangrove swamps in Ranong province (Thailand) between September 26, 2003 and November 23, 2006 and concluded that population density and biomass of macrobenthic organism were not affected, but changes in community structure were observed. With an average growth rate of only less than one meter per year for *Rhizophora apiculata*, it can be assumed that the full restoration of a mangrove forest will take about 10 to 15 years (Duke 2006).

### 3.4 Marine endangered species

The Thailand Andaman Sea hosts a number of threatened fauna species including dolphins, sea turtles and dugongs. The most notable impact occurred to sea turtles. According to UNEP and DMCR (2007), 37 turtles were found stranded on land, whereas six of them were dead. Furthermore the tsunami affected four sea turtles conservation projects. At Tap Lamru Naval base in Phang-Nga province about 2 000 turtles are reported to have been lost (DMCR 2005). Indirect effects of the tsunami on sea turtles were caused by the erosion of nesting beaches along the coastline. In this context the study of Choowong *et al.* (2009) on the assessment of beach recovery at the Andaman Sea coast of Thailand based on remote sensing imagery revealed that beaches almost have recovered to their equilibrium stage within two years after the tsunami. Other indirect impacts on sea turtles resulted from debris which acted as obstacles for nesting animals (UNEP and DMCR 2007).

Additionally three dolphins and two dugongs were carried inland by the tsunami. One of the dugong and two of the dolphins (one was a bottlenose dolphin) died. The Figure 3-5 show rescue operations of a dugong stranded in a freshwater pond.



Figure 3-5. A male dugong was captured and returned to the sea on December 29, 2004. DMCR (2005).



### 3.5 Coastal forests

Coastal forests, such as casuarina beach forests form typical coastal ecosystems in Southeast Asia. These forests act as natural soil and sand dune stabilisers, as windbreakers and provide products such as timber, fuelwood and medicine. Furthermore, these forests are nitrogen fixers allowing them to tolerate poor soil conditions. In some areas casuarina trees are planted in order to prepare soils for cultivation purposes (cp. Whistler and Elevitch 2006; Jirapong Jeewarongkakul, personal communication). In contrast to coral reefs, seagrass and mangroves, no quick assessments on coastal forests and vegetation were carried out in early 2005 (FAO and MOAC 2005). Some first field observations from January 2005 reveal that beach forests sustained more serious damage than mangroves. These observations can be confirmed by the fact, that in Thailand 14 415 ha (90 093 rai) of beach forests were affected UNISDR (2005).

A more systematic impact assessment where forest structure, species composition, impact and recovery patterns were taken into account was carried out between April and October 2005 at some sites at the Andaman Sea coast (cp. FAO 2005a/b). The following damage patterns were distinguished during the assessments: no effect, up root, standing dead, declination or broken. It was observed that smaller casuarina trees were much more affected than larger trees. Bigger casuarina trees were uprooted in areas that were affected by intensive sand erosion (Cochard *et al.* 2008; Tanaka *et al.* 2007). Referring to the different tree species occurring in beach forests environments *Casuarina equisetifolia*, *Cocos nucifera*, *Terminalia catappa* and *Tamarindus indica* appear to have been relatively more resistant to the tsunami than other species such as Kapok trees (*Ceiba pentandra*), *Leucaena leucocephala* (ipil-ipil) and *Pandanus odoratissimus* (FAO and MOAC 2005; Tanaka *et al.* 2007). According to Cochard (2007) coconut palms appeared to be the most resistant coastline trees, reflecting their monopodial growth form and highly flexible trunks and foliage.

According FAO (2005a/b) regeneration rates of beach forests were reported to be slow, but even faster than for mangrove forest). In addition it can be concluded that *Casuarina equisetifolia* and *Derris indica* did well in competition with other tree species (Wibisono and Suryadiputra 2006).

### 3.6 Crops and soils

Since most of the agricultural land (including tree plantations, horticultural and other crops) is not located at close proximity to the coast line, direct impacts of the tsunami was reported to be low. However, some impacts were observed for coconut trees which are usually closer located to the coastline than other crops. According to FAO and MOAC (2005) significant damage to agricultural land resulted from the intrusion of seawater. About 20 300 ha of the mainland was flooded by seawater and 1 560 ha of the cropping area was damaged by salinity (Bueno 2005; FAO and MOAC 2005). Fruit and plantation trees show toxicity symptoms such as yellowing, browning and dying leaves (Figure 3-6). Fruit trees (e.g. rambutan, cashew or mango) and young oil palms were most vulnerable to salinity than other crops, such as rubber and coconut. However, Massmann (2010) concluded that yield losses in most agricultural areas in the study area were less than one year. Furthermore, the tsunami also changed physical soil properties including the increase in soil moisture content, decreases in drainage due to dispersion of organic matter and a loss of soil structure (puddling).

In summary, the total value of economic loss regarding the agricultural sector was estimated at 8.5 Mio. Baht (Israngkura 2005). A detailed summary on damage to the crop sector is presented on Table 3-3. The Phang-Nga province and particularly the district of Takua-Pah was the most severely affected region in Thailand (FAO and MOAC 2005). According to IAARD and NSW DPI (2008) the main factors determining the intensity of salinity of soils are *a*) the length of time the soil was inundated, *b*) the soil texture, specifically the level of clay, *c*) the amount of rainfall or availability of freshwater for leaching and *d*) the drainage and circulation of water. Referring to the first factor, if a soil was inundated for more than three days it was usually too saline for most crops to yield in the first year. Due to the humid climate in Thailand, most of the salt was already leached out within the first year (FAO 2005a/b; Massmann 2010; Szczucinski *et al.* 2006, 2007). Similar findings from Indonesia could be observed by Rachman *et al.* (2008). The local topography of an area influences both, the duration of inundation (factor *a*) and the characteristics of water circulation (factor *d*). In this context Szczucinski *et al.* (2006) concluded from their finding on tsunami deposits and water resources in the Phang-Nga and Phuket provinces that due to the open cast mining (cp. section 1.4.2) many depressions were left in the landscape acting as basins where salt water could stay for a long time and create potential long-term threats for contaminations. Furthermore, they found out that that arsenic and heavy metal concentrations were elevated in man-made land depressions, left after mining activities.



**Figure 3-6.** Tsunami induced crop damage. (a) Indirect damage to oil palms and (b) erosion and direct impacts to rubber trees. Modified from FAO and MOAC (2005).

**Table 3-3.** Damaged cropping areas by Province. FAO and MOAC (2005).

Province	Number of affected districts	Number of affected farmers	Affected area * (rai)	Damaged cropping area (rai)			Total (rai)
				Rice	Other field crops	Horticulture, coconut, oil palm	
Krabi	3	13	60	15	5	40	60
Trang	2	76	1 222	100	167	21	288
Phang-Nga	5	675	8 406	37	---	8 369	8 406
Phuket	1	10	68	---	10	80	90
Ranong	3	241	2 313	44	12	314	370
Satun	2	142	577	122	387	3	512
<b>Total</b>	<b>16</b>	<b>1 157</b>	<b>12 646</b>	<b>318</b>	<b>581</b>	<b>8 827</b>	<b>9 726</b>

\* Affected area: The agricultural land that was flooded by sea water

With the aim at a quick rehabilitation of agricultural lands in order to restore the production capacity of farmers and to ensure food security in rural areas, the FAO proposed a framework for a reclamation action plan for salt-affected soils. This plan includes first a comprehensive assessment of severity and extent of the salinity damage, second an identification of the capacities of farmers and local communities in restoring progressively their production capabilities, and third the identification of appropriate reclamation measures (FAO 2005d). The proposed ranking scheme for assessing damages to soils is illustrated in Table 3-4. Further technical instructions on the measurements of soil salinity are provided in FAO (1999).

**Table 3-4.** Assessment and classification of field damage. FAO and MOAC (2005).

Field damages	Low	Medium	High	Suggested ranking
Trash and debris	1	2	3	1 low or nil 2 medium scattered 3 massive impeding restart of field works
Erosion	1	4	6	1 small erosion here and there 2 medium erosion that needs some resurfacing light works 3 major erosion problems such as erased bunds, land levelling disturbances and/or soil top layer washed out that requires intervention for restoring capacity/fertility
Sedimentation	1	4	6	1 several centimetres 4 more than 10 centimetres 6 more than 20 centimetres
Flood duration	1	4	6	1 limited to several hours 4 flood lasted more than one day 6 flood lasted more than one week
Infiltration(*)	1	2	3	(**) 1 clay soil 2 medium 3 high vertical hydraulic characteristic (well drained soil)
Total	Between 5 and 24			Below 8 = Low damaged area Between 8 and 16 = Medium damage Above 16 = High damaged area

\* Infiltration rate of the upper soil layer influences the quantity of salt that contaminates the soil profile. Of course this aspect also influences the ability for remediation, highly infiltrating soil such as the sandy soils in Maldives are likely to be quickly leached and cleaned with fresh water.

\*\* The ranking given here is considering the damages resulting from a small duration flood which makes sandy soils more damaged than clay soils and more impacting the shallow fresh water aquifers.

### 3.7 Water resources

In this section the tsunami impacts on the water resources including seawater, surface water and groundwater will be summarised.

#### 3.7.1 Seawater quality

An assessment on sea water quality was carried out at various routine monitoring sites along the Andaman coast of Thailand. There were fifteen parameters monitored including temperature, salinity, pH, dissolved oxygen (DO), total suspended solid (TSS), chlorophyll *a* concentration (CHL *a*), dissolved nutrients and bacteria. The assessment was carried within one week after the tsunami starting from Phuket island and expanding throughout the Andaman coast (DMCR 2005). The assessment of the water quality was carried out using the Marine Water Quality Index (MWQI). This index is composed of eight parameters including pH, DO, temperature, salinity, TSS, nitrate, phosphate and total coliform bacteria (Ott 1978).

The results reveal that in comparison to the pre-tsunami data, no negative effect of the tsunami on the coastal water quality could be observed, although some parameters such as total suspended solids were higher than normal at few sites in the southern part of the Andaman coastline, e.g. Laem Sak (Krabi), Pak Meng (Trang) and Pak Bara (Satun). Water quality at most sampling sites was good to excellent. In the northern part of the peninsula such as Ranong, Phang-Nga and Phuket seawater quality even improved after the tsunami (cp. Figure 3-7). Prior to the tsunami, contamination of bacteria (faecal coliform and total coliform) was over the standard limit at several sites, but after the tsunami high contaminations were observed only at a single site at Laem Sak. However, the main causes of polluted sea water, particularly untreated effluent and garbage from highly populated areas, still needs close attention (DMCR 2005).

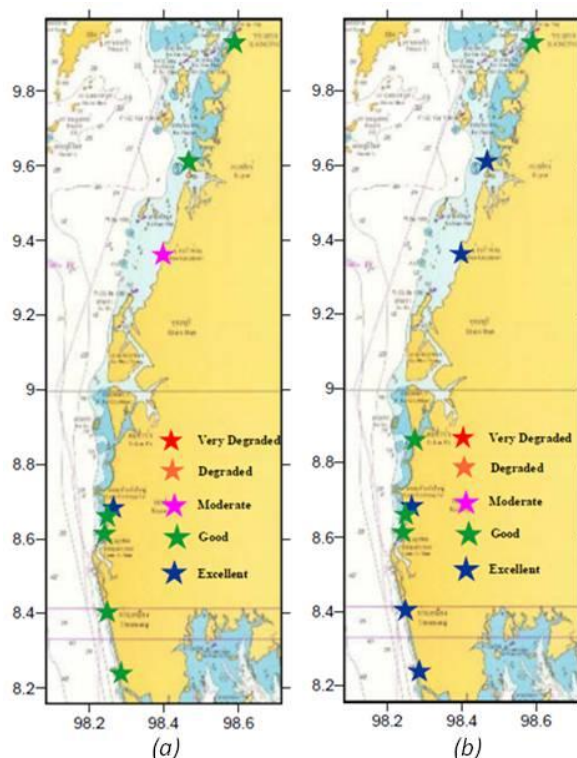


**Figure 3-7.** Coastal water quality along the coast of Ranong, Phang-Nga and northern Phuket. (a) December 2004 (before tsunami) and (b) January 2005 (after tsunami). DMCR (2005).

### 3.7.2 Groundwater and surface water quality

The availability of clean groundwater and surface water is an important factor for public health and wellness. According to the Department of Groundwater Resources (DGR 2006) groundwater and surface water is used in the study area (Ban Nam Khem and Bang Niang) mainly for household consumption and the tourism industry.

The Department of Groundwater Resources, Ministry of Natural Resources and Environment (MONRE) evaluated the damage of groundwater resources six months and two years after the tsunami. It was found that six months after the tsunami chloride levels in the six affected provinces were still increased in comparison to pre-tsunami conditions (with maximum chloride levels of almost 6 000 mg/l observed in Phang-Nga province). In December 2006 chloride levels had recovered in all provinces with values lower than the drinking water standard of 250 mg l<sup>-1</sup>.

However, Massmann (2010) concluded from focus group discussions and in-depth-interviews with local farmers, that salinity in ground water was locally still increased, even two to three years after the tsunami.

The Department of Health, Ministry of Public Health assessed the quality of well water in the six tsunami affected provinces for coliform bacteria, chlorine and suspended matter. A high contamination of well water in Phang-Nga Province could be observed: The water in 187 out of 530 wells is unsafe due to coliform bacteria contamination and in 32 out of 534 wells it is unsafe due to sea water intrusion. However, pre-tsunami water quality of these wells is not well documented. In Phuket, coliform bacteria contamination affected 55 wells severely and 44 slightly. In February 2005 the quality of the water in twelve of these wells has already been restored with the addition of chlorine (UNEP 2005). Similar findings were observed from measurements in Phang-Nga and Phuket carried out 50 days after the tsunami (cp. Szczucinski *et al.* 2005, 2006). They concluded that water conductivity of wells was much higher in areas which were located inside the tsunami inundation zone in comparison to a reference site located outside of the inundation area.

With regard to the factors determining the intensity of salt water intrusion into the ground water, the same factors used for soil salinity (section 3.6, cp. IAARD and NSW DPI 2008) can be adopted including the length of time the soil was inundated, the soil texture respectively the level of clay (here: the higher the permeability the faster salt water can reach the groundwater layer), c) the amount rainfall or availability of freshwater for leaching and d) the drainage and circulation of water.

Surface water quality was assessed on February 1<sup>st</sup>, 2005 by the department of Mineral Resources of MONRE. The conductivity measurements revealed that of the thirty water bodies sampled only one natural pond was not contaminated significantly; its waters could still be used as before the tsunami (UNEP 2005). Tharnpoophasiam *et al.* (2006) assessed the water quality of well, surface and drinking water two months after the tsunami in Phang-Nga and found out that the water samples taken from tsunami impacted areas were more contaminated than the samples taken from unaffected areas. Water quality was analysed considering microbiological (contamination of enteric bacteria) and physical-chemical properties (salinity, pH, conductivity, TDS). They concluded that surface and well water were still brackish and contaminated by seawater and thus could not be used for consumption.

#### Conclusion – from the ecological impacts towards ecological vulnerability

Even though it seems that the ecological impacts in Thailand were manageable, there is little knowledge about the long-term consequences of these impacts, resulting from both, the interrelations between ecosystems and social systems as well as from interrelations between different ecosystems (e.g. UNEP and DMCR 2007). Furthermore the literature review reveals that there is a lack of post-tsunami studies that either focus on a comprehensive assessment of vulnerability (an exception here is the study of Paphavasit *et al.* 2009) or that provide spatially accurate information on it.



Moreover, many studies simply do not cover the study area of TRAIT or do not refer to each coastal ecosystem (in particular coastal forests). According to UNEP and DMCR (2007) there is also little knowledge on the pre-tsunami condition of ecosystems and natural resources, i.e. on biodiversity. This has to be regarded as a general limiting factor for the assessment of ecological vulnerabilities, particularly the characterisation of the tsunami exposure and the intrinsic vulnerability (e.g. Birkmann and Wisner 2006; Dahdouh-Guebas *et al.* 2005).

In order to address this lack of information, TRAIT aims to apply remote sensing techniques based on high resolution imagery. This allows a retrospective analysis of ecological processes such as damage processes and recovery processes in order to provide valuable information on the local ecological vulnerability. This opportunity constitutes a second motivation for this thesis. The following section describes the methodological approach used for this thesis.

## 4 Methodological approach and datasets

This section aims to present the methodological approach used in this thesis to analyse the tsunami vulnerability of coastal ecosystems. Furthermore a detailed description of the applied datasets is given. Since all change detection techniques are detailed in both articles (Roemer *et al.* 2010a/b), they are only briefly presented within this section.

In this study, the vulnerability of coastal ecosystems is investigated by considering the three components of exposure, sensitivity and resilience. Thus, a bio-centric perspective of ecological vulnerability is focused (cp. Williams and Kaputcka 2000). The methodological concept (Figure 4-1) shows how the vulnerability concept is approached by remote sensing applications.

Here, the *exposure* definition of Clark *et al.* (2000) is applied. They define exposure as “the degree to which an ecosystem [...] comes into contact with particular stresses or perturbations” (Clark *et al.* 2000, p. 9). The definition is adopted and applied to the tsunami hazard context. Thus, in the narrower sense, *exposure* can be defined as the **degree to which an ecosystem comes into contact with a tsunami**. Major components of the exposure analysis include the definition and regionalisation of the exposed units (cp. section 4.2).

*Sensitivity* is defined as “**the degree to which an exposure unit is affected by exposure to any set of stresses**” (Clark *et al.* 2000, p. 9) or more simple as the **dose-response of an exposed entity to a hazard** (Turner *et al.* 2003). Therefore, sensitivity is indirectly assessed by remote sensing applications by focussing on tsunami induced impacts (cp. section 4.3).

The way, how the different concepts of ecological resilience can be approached by remote sensing techniques is more complicated: The term was introduced to the ecological literature by Holling (1973) who describes resilience as the amount of disturbance that an ecosystem could withstand without changing self-organised processes and structures. Other definitions are more pragmatic and focus on the time required for a system to return to an equilibrium or steady-state following a perturbation. Holling called this definition as engineering resilience (e.g. Mittelbach *et al.* 1995; Pimm 1991). Clark *et al.* (2000) defines resilience as the ability of an exposure unit to resist or recover from the damage associated with the convergence of multiple stresses. Particularly in the natural hazard context the term is often broadened to include a social component of resilience as well. In this regard, Adger *et al.* (2005) defines social-ecological resilience as the capacity of linked social-ecological systems to absorb recurrent disturbances such as hurricanes or floods so as to retain essential structures, processes, and feedbacks. The capacity encompasses both, the regenerative ability of ecosystems and their capability in the face of change to continue to deliver resources and ecosystem services that are essential for human livelihoods and societal development. For this study, the concept of the ecosystem recovery based on the definitions of Clark *et al.* (2000), Pimm (1991) and Mittelbach *et al.* (1995) is adopted to estimate the resilience (cp. section 4.4): **Recovery is defined as the rate and potential at which ecosystems reclaim its habitat by natural succession processes after being degraded or removed by the tsunami**. One advantage of focussing on the ecosystem recovery is that this definition allows a good starting point for implementing multi-temporal remote sensing techniques (cp. section 4.4).

The question of how the results provided by the remote sensing applications can be used for the analysis of ecological vulnerability is discussed in the synthesis section (section 6). Here two methods, a retrospective assessment of vulnerability and a statistical approach for the identification of the causes and factors determining the vulnerability, are presented.

As the pre-processed IKONOS-data make up the starting point of the methodological approach (Figure 4-1), this section continues with a short description of the acquired IKONOS imagery including image-pre-processing.

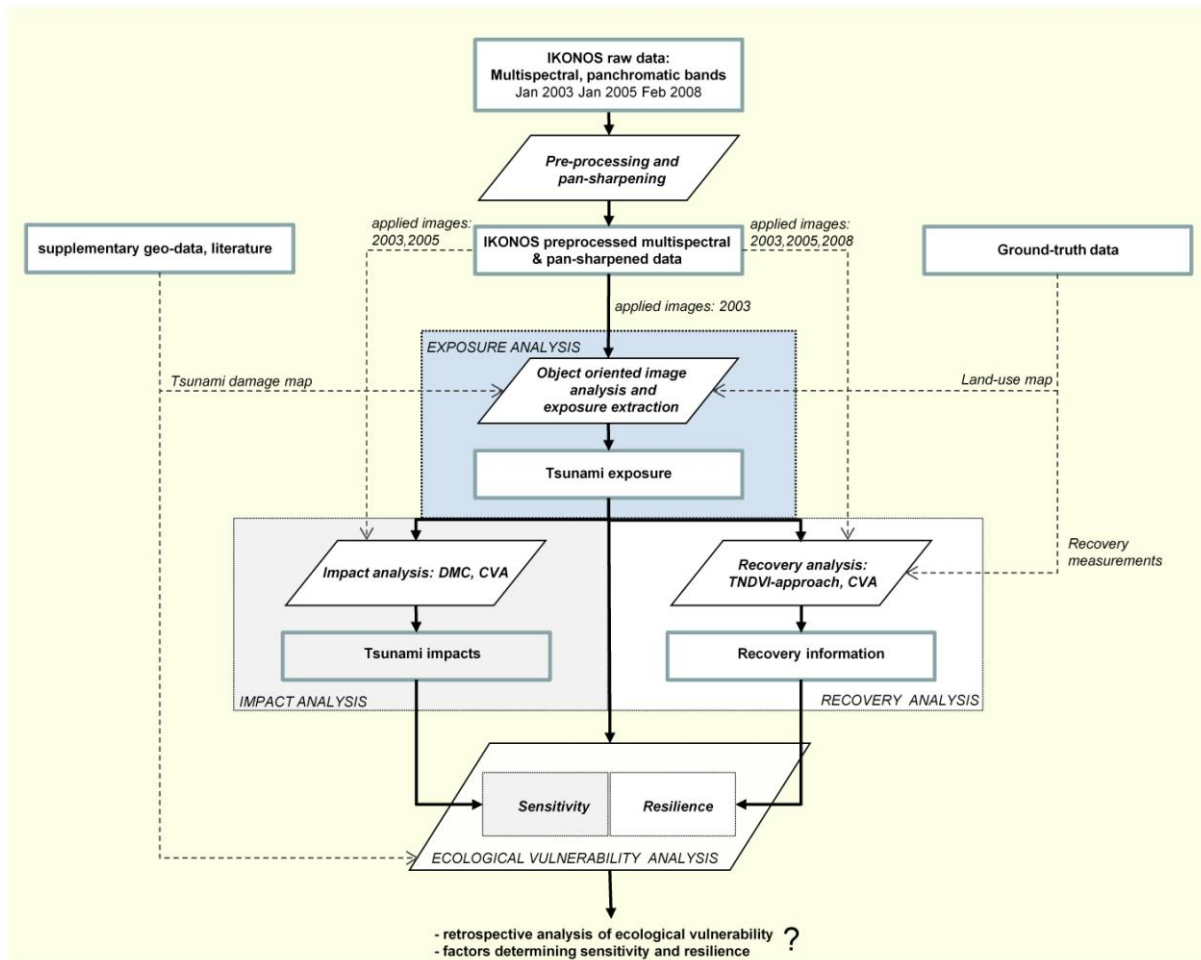


Figure 4-1. Concept of analysing tsunami vulnerability of coastal ecosystems based on remote sensing.

#### 4.1 IKONOS data and pre-processing

IKONOS (the word “icon” means “image” in Greek) is the world’s first commercial satellite able to collect panchromatic imagery of 0.82 m and multi-spectral imagery of 4.0 m resolution. IKONOS is owned by GeoEye and has a polar, circular and sun-synchronous 681 km orbit and a swath width of 11 km. The satellite was launched on September 24, 1999 and provides imagery beginning January 1, 2000. Further technical details on the sensor are provided in Table 4-1. IKONOS sensor specifications. GeoEye (2006).



Pre- and post-tsunami IKONOS data (Figure 4-2) were acquired from the image archives of the Centre of Remote Sensing and Processing (CRISP) at the National University of Singapore (<http://www.crisp.nus.edu.sg/>) in Singapore and Spatial Dimension Solutions (SDS) in Bangkok (<http://www.sd-solution.com/>). In order to avoid changes in phenology which would complicate the capabilities of change detection techniques, images were acquired from the same season (winter monsoon). The pre-tsunami state is represented by the image from January 13, 2003, the post-tsunami state by the images from January 15, 2005 and February 20, 2008. As already described in section 1.4, the IKONOS images cover three separate areas along the Andaman sea coast: a northern part (51.55 km<sup>2</sup>), a central part (60.71 km<sup>2</sup>) and a southern part (84.47 km<sup>2</sup>). Due to a limited availability of appropriate cloud free images for the third acquisition date, no imagery was acquired for the southern area between Tap Lamru and Thai Mueang. Clouds cover is usually lower than 3% on the acquired imagery scenes (cp. Figure 4-2).

**Table 4-1.** IKONOS sensor specifications. GeoEye (2006).

<b>Launch Date</b>	24 September 1999 Vandenberg Air Force Base, California
<b>Operational Life</b>	Over 7 Years
<b>Orbit</b>	98.1 degree, sun synchronous
<b>Speed on Orbit</b>	7.5 kilometers (4.7 miles) per second
<b>Speed Over the Ground</b>	6.8 kilometers (4.2 miles) per second
<b>Number of Revolutions Around the Earth</b>	14.7 every 24 hours
<b>Orbit Time Around the Earth</b>	98 minutes
<b>Altitude</b>	681 kilometers (423 miles)
<b>Resolution</b>	<b>Nadir:</b> 0.82 meters (2.7 feet) panchromatic 3.2 meters (10.5 feet) multispectral <b>26° Off-Nadir</b> 1.0 meter (3.3 feet) panchromatic 4.0 meters (13.1 feet) multispectral
<b>Image Swath</b>	11.3 kilometers (7.0 miles) at nadir 13.8 kilometers (8.6 miles) at 26° off-nadir
<b>Equator Crossing Time</b>	Nominally 10:30 a.m. solar time
<b>Revisit Time</b>	Approximately 3 days at 1-meter resolution, 40° latitude
<b>Dynamic Range</b>	11-bits per pixel
<b>Image Bands</b>	Panchromatic, blue, green, red, near infrared

All data were acquired as a bundle product including both the multispectral and the panchromatic channels and were standard geometrically corrected. At this processing level, radiometric correction is made to compensate the distortions due to the differences in viewing conditions. In addition the images are fitted to the standard cartographic projection (UTM WGS 84) without using ground control points at ground receiving stations. Therefore, a preliminary step in image analysis and particularly in change detection techniques includes the geometric and radiometric correction of the image data. A further step in image pre-processing includes the image pan-sharpening.

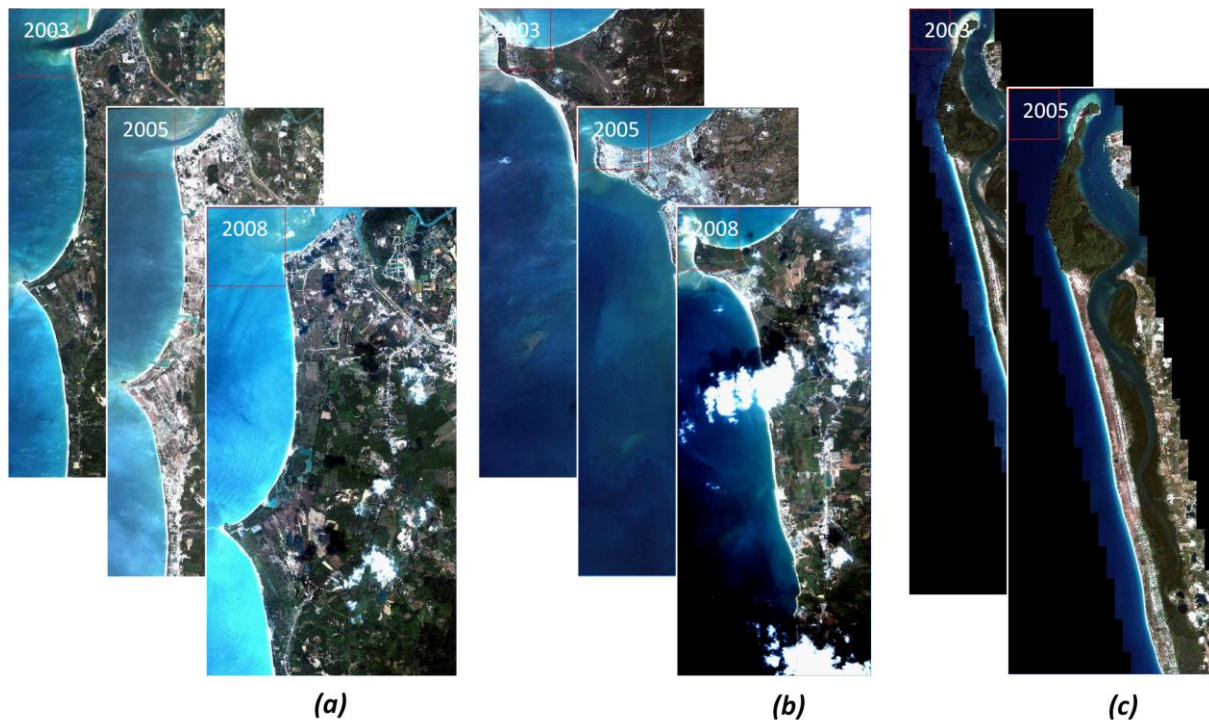


**Figure 4-2.** Overview of IKONOS image data used in this study. (a), (b) and (c) represent the three areas: (a) between Ban Nam Khem and Ban Bang Sak, (b) the coastal area between Pakarang Cape and Nang Thong (Khao Lak) and (c) between Tap Lamru and Thai Mueang city. The three acquisition dates are January 13, 2003 (04:11 GMT), January 15, 2005 (04:12 GMT) and February 20, 2008 (04:10 GMT), respectively.

#### Image pre-processing and pan-sharpening

A relative geometric correction of the IKONOS imagery was carried out by applying co-registration. Here, a set of 352 ground control points (GCPs) were selected from the pre-tsunami image, which was considered as the base image. The post-tsunami images were warped to this image using the selected GCPs. Building corners, crossroads and other noticeable landscape objects were chosen for GCP selection. The Figure 4-3 shows the GCPs selected for the northern segment of the study area between Ban Nam Khem and Ban Bang Sak. The co-registration RMSE of the post-tsunami images was reduced to less than one pixel (between 0.70 and 0.84).

Radiometric correction was performed in two steps. First, digital numbers from the IKONOS images (DN) were converted into at sensor's aperture radiance values ( $L_{\lambda}$ ,  $nm$ ) in order to create spectral information with meaningful units (cp. equation 3 and Table 4-2). Second, the image-based dark object subtraction technique (DOS) was applied for the atmospheric correction of the IKONOS images. The technique reduces the effects of scattering, which is an additive component in the original data values. Dark water surfaces like freshwater ponds were first identified from the images and considered as dark objects. Band minimum values derived from these objects were subtracted from all band values. However, in comparison to other absolute corrections methods using radiative transfer models, these techniques cannot reduce the effects resulting from atmospheric absorption (cp. Chavez 1988; Ekstrand 1994; Spanner *et al.* 1990).

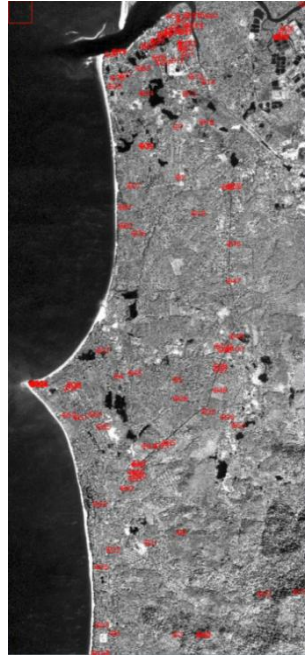


**Figure 4-3.** Selection of ground control points (GCPs). The Figure illustrates GCP selection for the panchromatic channel of the pre-tsunami image.

$$L_{\gamma} = \frac{10^4 \times DN_{\gamma}}{\text{CalCoef}_{\gamma} \times \text{Bandwidth}_{\gamma}} \quad (3)$$

where,

$DN_{\lambda}$  = digital value for spectral band  $\lambda$ ,

$\text{CalCoef}_{\lambda}$  = Radiometric calibration coefficient (DN/(mW/cm<sup>2</sup>-sr))

$\text{Bandwidth}_{\lambda}$  = Bandwidth of spectral band  $\lambda$  (nm).

Both  $\text{CalCoef}_{\lambda}$  and  $\text{Bandwidth}_{\lambda}$  are given in Table 4-2 (Taylor 2009).

**Table 4-2.** IKONOS band dependent parameters. Taylor (2009), Geoeye (2006).

IKONOS Band ( $\lambda$ )	spectral range (nm)	Bandwidth (nm)	resolution (m) nadir/26° off nadir	$\text{CalCoef}_{\lambda}$ * (DN/mW/cm <sup>2</sup> -sr)
Pan	526-929	403	0.82/1.0	161
Blue	445-516	71.3	3.2/4.0	728
Green	506-595	88.6	3.2/4.0	727
Red	632-698	65.8	3.2/4.0	949
NIR	757-853	95.4	3.2/4.0	843

\*Only for image production date Post 2/22/01 (Coefficients are for the 11-bit products)

A multi-resolution image fusion technique (pan-sharpening) was applied by which the spatial structure of the high resolution panchromatic image (1 m) could be combined with the spectral information of the lower resolution multispectral images (4 m). This technique allows the production of a high resolution multispectral image. Several pan-sharpening techniques including HSV-, Colour Normalised (Brovey)- and Gram-Schmidt Spectral-Sharpener were tested and evaluated in terms of spatial accuracy and colour quality in the pan-sharpened images (Laben and Brower 2000; Vrabel 1996). The Gram-Schmidt-Spectral-Sharpener technique turned out to be most appropriate technique (cp. Figure 4-4) and thus was used in this study. The pan-sharpened images were mainly used for visual image interpretation purposes, which was useful to a) locate appropriate study sites for the field campaign and b) to select test and training areas for the application change detection techniques and image classification.

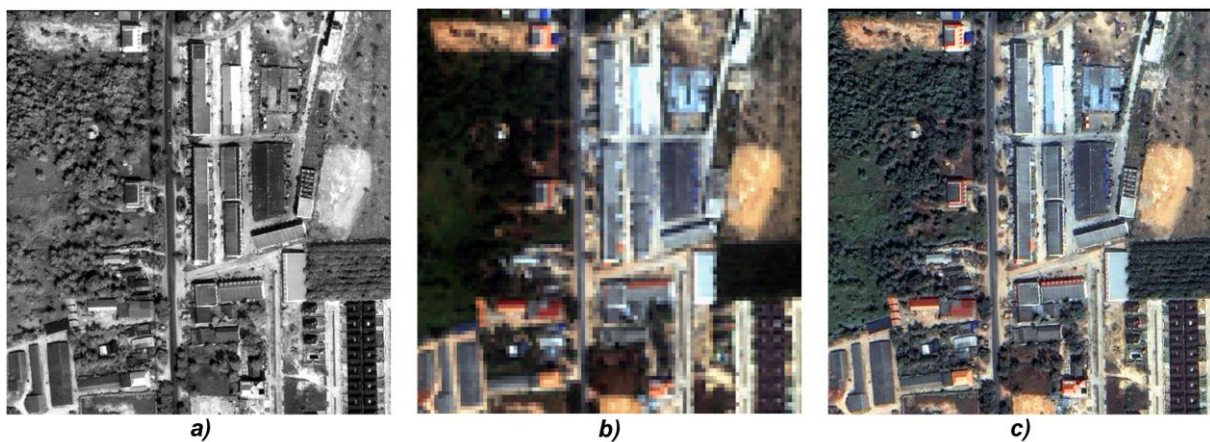


**Figure 4-4.** Gram-Schmidt-Spectral-sharpening. (a) the pan-chromatic band with 1-m pixel resolution, (b) multispectral bands (RGB) with 4-m resolution and (c) the pan-sharpened images with 1-m resolution.

## 4.2 Exposure analysis

The definition of the exposure units, here the exposed ecosystems, is a preliminary step in ecological vulnerability analysis (cp. Clark *et al.* 2000 and Figure 4-5). According to the Millennium Ecosystem Assessment (2005b) an ecosystem can be understood as a functional unit in which a dynamic complex of plant, animal and micro organism communities and the abiotic environment interacts. In this study relevant ecosystems are identified and regionalised based on a detailed land use and land cover (LULC) classification and based on expert judgments during field visits in September 2007 and March 2008. For classification, an object-oriented rule-based classification approach is applied on the pre-tsunami image of January 2003 in order to provide a very accurate database on the LULC of the area (cp. section 4.2.1; Römer 2007; Römer *et al.* 2009). The final classification is validated by:

- a) field data which were derived from LULC-mappings carried out between October and December 2008 by WWF-Thailand (section 4.2.2)
- b) geo-coded photos which were taken during field trips in August/September 2008 and January/February 2009 and by
- c) the visual interpretation of the higher resolution pan-sharpened imagery.



Due to poor depth penetration of near infra-red electromagnetic radiation (< 1 m) into water and due to the small extent of shallow water reefs in the study area, the focus of the classification and thus the vulnerability analysis lies on the terrestrial ecosystems such as coastal forests and mangroves (cp. section 5.1; Green *et al.* 2000). In order to distinguish between exposed and non exposed areas, a modified damage or inundation map of the 2004 Indian Ocean tsunami provided by ZKI (2005) is used. Although a real inundation zone derived from inundation modelling would have been more adequate for this concern, there was no better alternative dataset available at the time of investigation. The workflow of the exposure analysis is illustrated in Figure 4-5. This section continues with the description of the applied datasets including the LULC-map based on object-oriented image analysis as well as the applied field data. The results of the exposure analysis including the definition and regionalisation of the exposed units are presented in the result section (section 5.1).

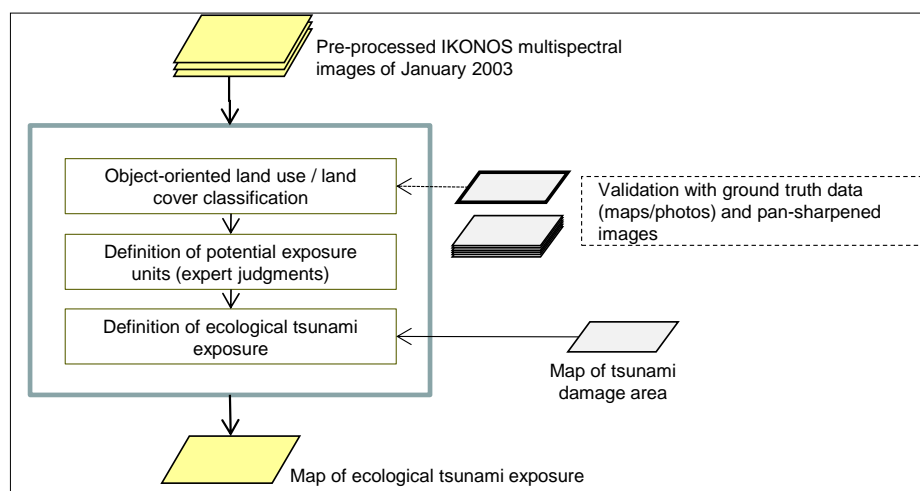


**Figure 4-5.** Concept of exposure analysis based on remote sensing applications.

#### 4.2.1 Creation of a LULC-map

An accurate LULC-map is created from the pre-tsunami IKONOS imagery from January 2003. Here, a rule-based object-oriented classification approach using the Definiens Developer 7.0 software is applied. A thorough knowledge on LULC-characteristics of the study area is an essential premise for the image-based classifications, particularly the rule-set development, and could be acquired during the field trips conducted in August/September 2008 and January/February 2009. Due to the huge amount of data in the IKONOS imagery ( $1.97 \times 10^8$  pixels in the panchromatic channel and  $1.23 \times 10^7$  in the multispectral channels) the classification is done for each of the three areas separately starting with the northern area between Ban Nam Khem and Ban Bang Sak. The rule set was then transferred and adjusted to the other two areas and is listed in Appendices B and C.

The entire rule set which comprises 21 different segmentation steps (16 multi-resolution segmentations and 5 chessboard segmentations) and 59 classes is not described in further detail in this thesis. For more technical details on image segmentations and membership functions please see Baatz and Schäpe (2000); Definiens (2007) and Weidner and Lemp (2005).

In general, the classification was carried out by using two hierarchical levels (Figure 4-6c). Whereas the lower level was created to classify landscape objects, such as single trees, shadows or single houses, the higher level was used to classify land uses and land cover. The reason for using two hierarchical levels is that some land use classes cannot be spectrally identified on the pixel or segment level as they are composed of several small scaled land cover types or landscape objects having different spectral properties. This problem applies particularly to urban areas or palm plantations (cp. Römer 2007). Thus, in order to derive meaningful land use information, the spatial patterns of the spectral information or the texture information have to be accounted for the classification process. This was realised in the upper segmentation level by using sub-level information: In the case of coconut plantation, a typical sub-level feature was the “Number of sub objects classified as medium round shadow/ Number of subobjects”.

Image segmentations (predominantly multi-resolution segmentations) in the upper level were flexibly used and adjusted according to the respective classes to be extracted. This means that several single segmentation processes were performed within only one hierarchical level. Thus, a typical sequence of process steps in the upper level includes a) image segmentation, b) rule-based classification of one or more LULC-classes, c) a classification and merging of the unclassified segments and d) a new segmentation based on the merged polygons (using the same hierarchical level), cp. Figure 4-6a.

Classification rules are mostly composed of a set of few core rules capturing most of the segments to be classified, and some additional rules to classify the segments which could not be assigned by the core rules. In some cases these additional rules refer to class neighbours. The underlying assumption is that segments that directly border to an image object very likely belong to the same class if its spectral, textural or shape-specific characteristics are comparable. This rule-based region growing approach worked well for huge or connected land use areas such as water or forest classes (e.g. rainforest\_raw1, ocean) and is illustrated in Figure 4-6b. However, some manual editing was still required in order to achieve a high accuracy and cartographic quality of the resulting LULC-map.

The rule set transfer to the two other areas required some adjustment in the parameterisation of the rules, particularly in the additionally rules. However, the general structure of the process tree and the segmentation strategy could be maintained and successfully transferred. Three additional classes were added for the southern image (between Tap Lamru and Thai Mueang) including the melaleuca forest, mixed beach forest and peat swamp forest (cp. rule set expansions listed in Appendices D and E).

The resulting LULC-map is illustrated on Figure 4-7 for the northern part of the study area and enlarged for the entire study area in Appendices F-I. The maps provide detailed information on land cover and in particular on land uses and forest types. The maps form the basis for the exposure analysis (cp. section 5.1), the impact and recovery analysis. Furthermore they played an important role within the TRAIT project, e.g. for the regionalisation of Manning roughness coefficients and thus to provide essential input data for tsunami inundation modelling (cp. Arp 2009; Kaiser *et al.* 2010a).

In comparison to the available GIS-data provided by the governmental organisations, the created LULC-maps could significantly improve the accuracy of thematic geo-data on terrestrial ecosystems and land uses in this area. In total 38 different LULC-classes could be distinguished on the final map. An accuracy assessment was carried by using ground truth data (cp. section 4.2.2) as well as the pan-sharpened images of 2003 for test area selection. With an overall accuracy of 93.60% and a Kappa of 0.90 the classification result can be considered as very accurate (Appendix J).

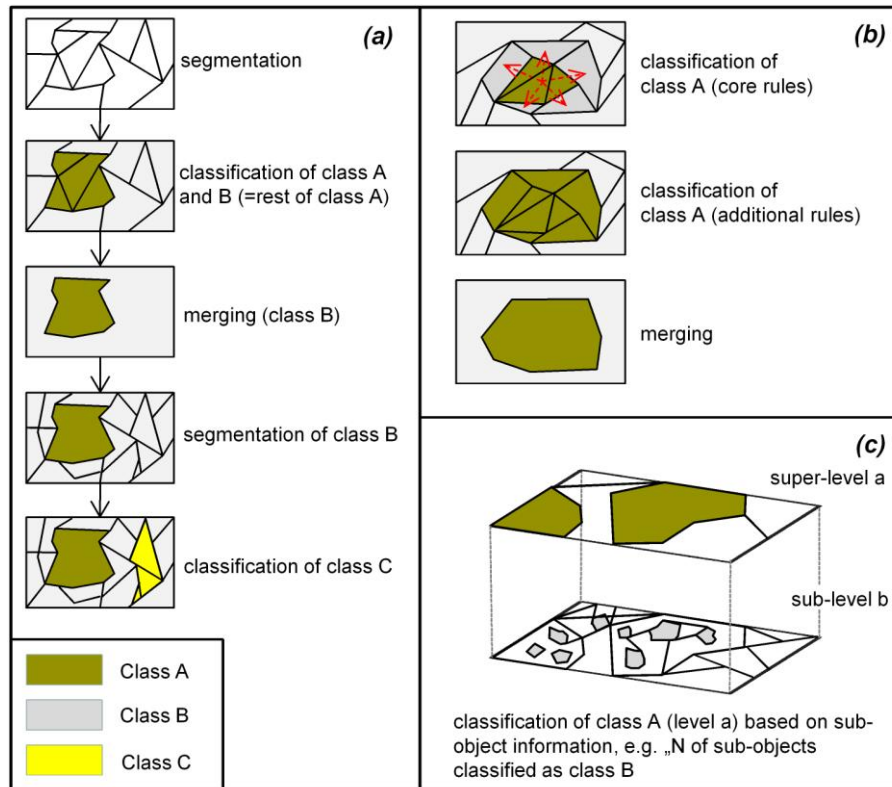


**Figure 4-6.** Classification strategies applied in object-oriented image analysis. (a) flexible use of image segmentations, (b) using similarities between similarities between neighbouring segments and (c) using sub-level information to derive texture information.

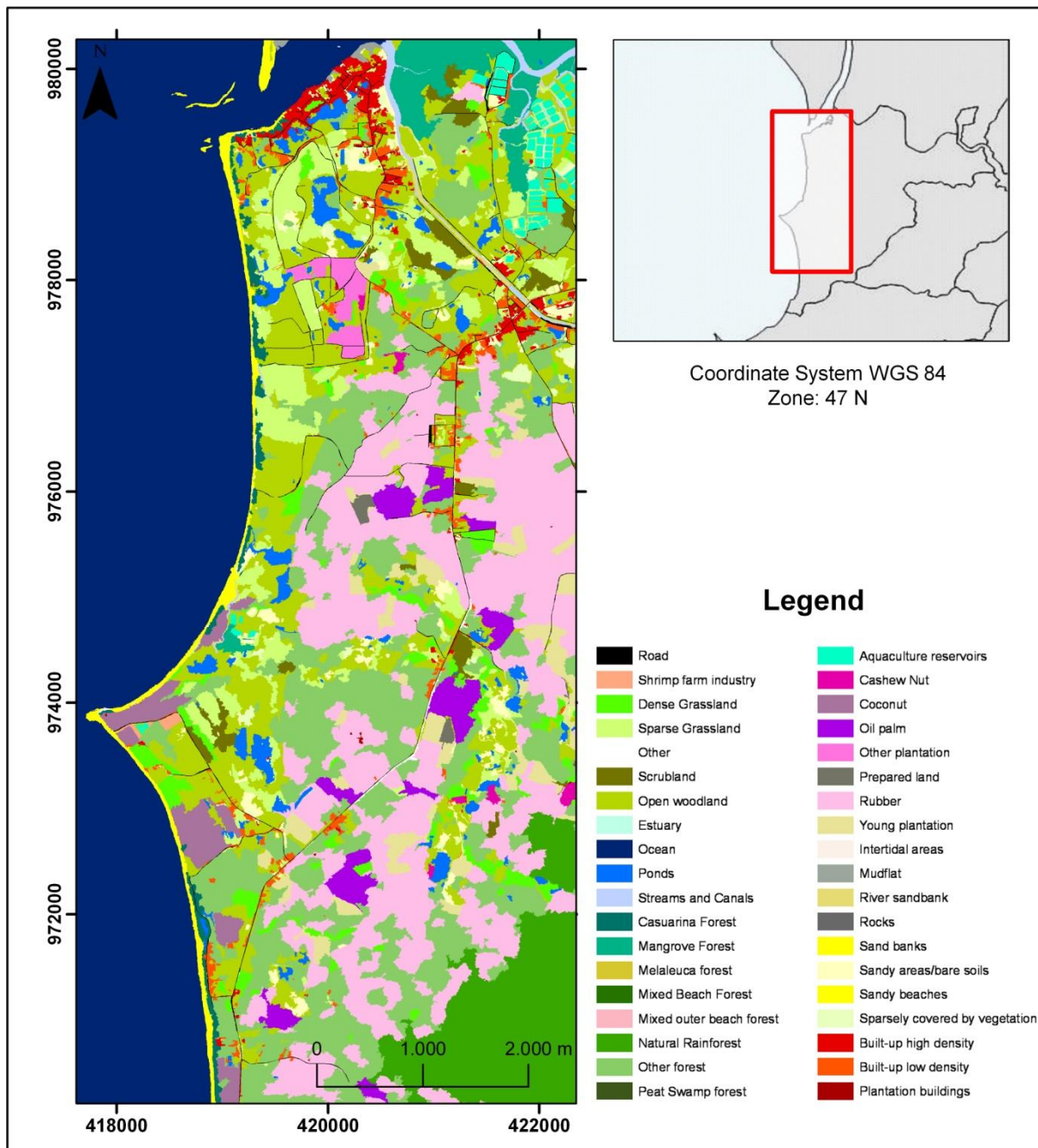


**Figure 4-7.** LULC-map derived by object-oriented image analysis. The figure shows the northern area between Ban Nam Khem and Ban Bang Sak. Spatial reference units are provided in meters.

#### 4.2.2 Ground truth data

Ground truth data play a fundamental role in any remote sensing based study. Since information derived from satellite imagery are indirectly related with the processes and phenomena on the earth surface, in-situ measurements can be used to compare, validate and parameterise these information. Referring to the ground truth information on LULC-information, many geo-coded photos were collected during the first two field trips in August/September 2008 and January/February 2009. In this regard Figure 4-8 provides an overview of the main LULC-types occurring in the study area, distinguished between human-shaped and more natural environments.



In addition, a land use mapping campaign was carried out between October and December 2008 by the WWF-team and coordinated by the author, in order to provide a reference source for the land use map derived from the satellite images. Due to a time lack between the pre-tsunami image (January 2003) and the time of ground truth observations, land-use mappings could only serve as a rough source of validation. However, in total 33 classes organised in eight super classes could be distinguished (cp. Appendix K). The total mapped area was 131 km<sup>2</sup> and is illustrated in Figure 4-9 for the aggregated LULC-classes.

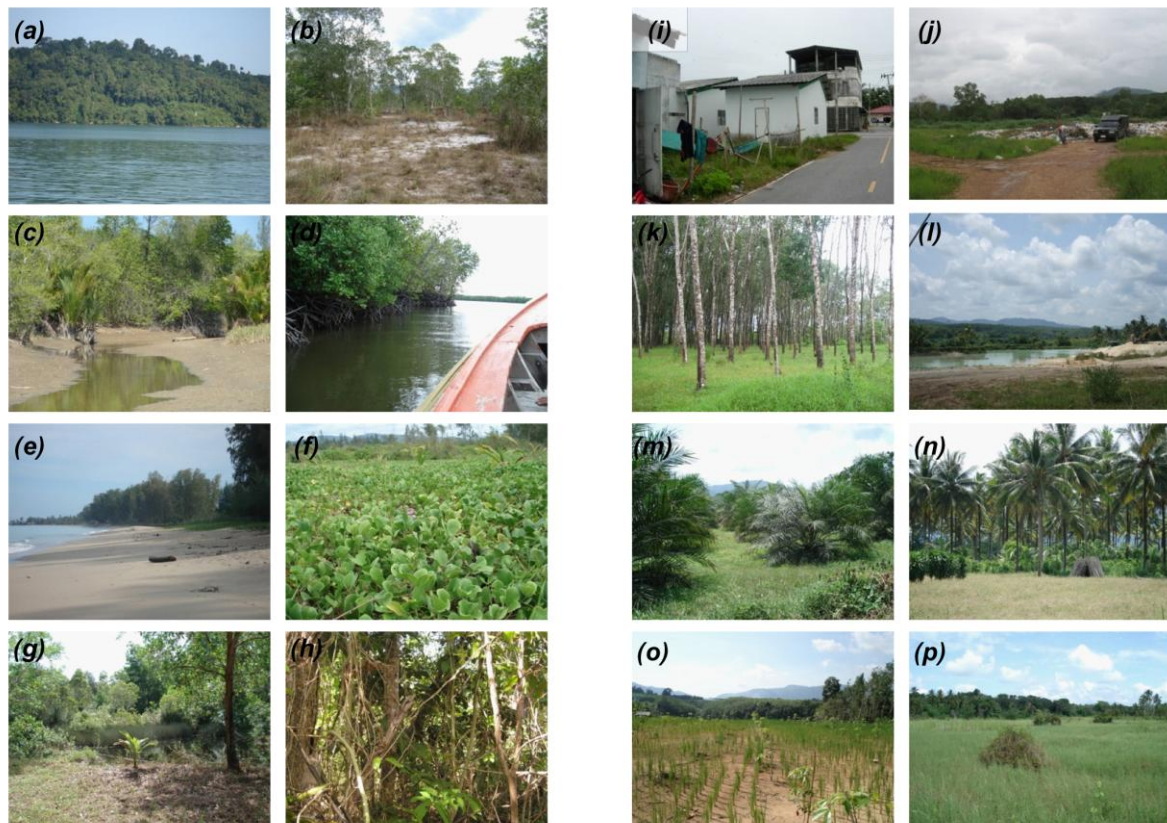


**Figure 4-8.** LULC-classes of the study area. Arp (2009) and own photos collected between September 2007 and March 2009. (a)-(h) show natural environments with limited human influences: (a) natural rainforest near Tap Lamru, (b) melaleuca fields in Khao Lampi - Hat Thai Mueang National Park, (c) Nipa palms (*Nipa fruticans*) occurring in a small mangrove patch near Khuk Kak, (d) intact mangrove stands near Ban Nam Khem, (e) casuarina beach forest near Ban Bang Sak beach, (f) large areas of *Pes-caprae* formations near Krang-Noi Cape, (g) peat swamp forest near Thai Mueang, (h) a stand of mixed beach forest at Khao Lampi - Hat Thai Mueang National Park. (i)-(p) show strongly human influenced areas: (i) village area of Ban Nam Khem, (j) a waste disposal place near Ban Bang Mueang. (k) rubber plantations near Bang Niang, (l) a sand pit and freshwater pond as a result of tin mining activities from the last century, (m) an oil palm plantation near Thai Mueang, (n) coconut plantations near Pakarang Cape, (o) a rice plantation near Tap Lamru and (p) open landscapes and grasslands near Ban Bang Sak.

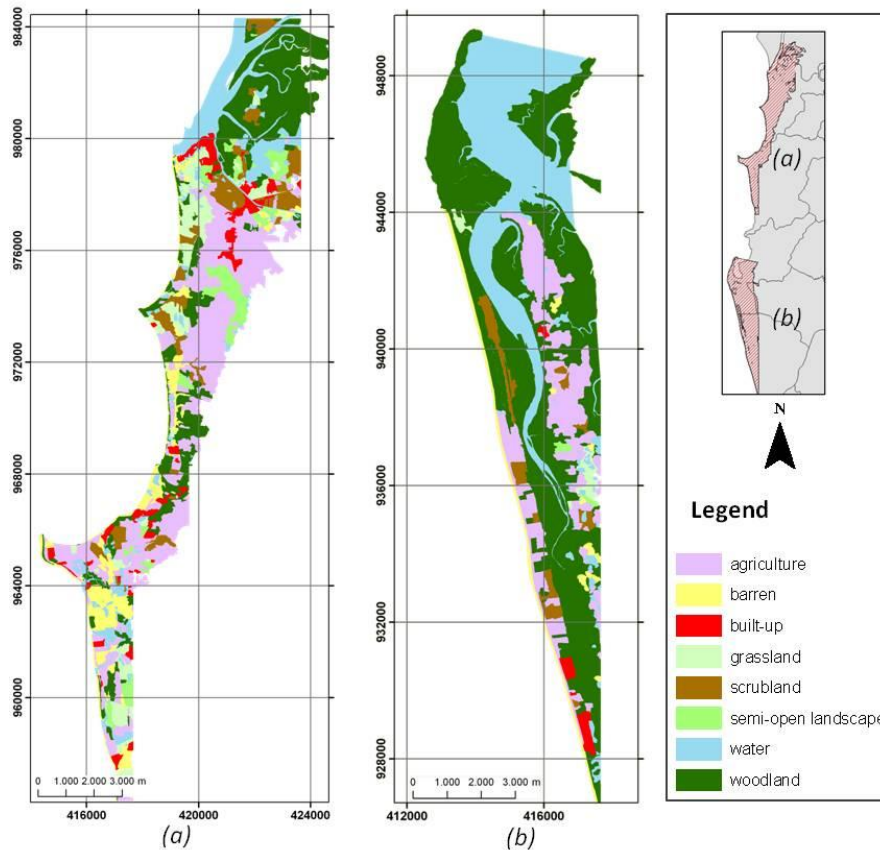


**Figure 4-9.** LULC-mapping carried out between October and December 2008. (a) the northern part between Ban Nam Khem and Khao Lak, (b) the southern part between Tap Lamru and Thai Mueang city. Spatial reference: UTM zone 47N, WGS 84.

### 4.3 Analysis of tsunami induced impacts as a basis to assess sensitivity

The basic idea for implementing remote sensing techniques was that tsunami-induced impacts (e.g. uprooting of a forest or the yellowing of leaves due to water stress symptoms) caused a change in the spectral signals of an exposed element. Furthermore, when comparing pre- and post-tsunami multispectral images, these changes need to be distinguishable from other signals such as those resulting from changes in atmospheric conditions, phenology state or in view geometry (Green *et al.* 1994). This principle of identifying changes in multi-date remotely sensed images makes up the fundamental basis of a big method family in remote sensing called change detection (cp. Coppin and Bauer 1996; Singh 1989). The principle of applying change detection for tsunami impact assessment is illustrated on Figure 4-10. Here a fictive impact scenario on a coastal forest is assumed (Figure 4-10a) including the corresponding changes in LULC-patterns (Figure 4-10b) and in spectral characteristics (Figure 4-10c). Thus, a first step of the sensitivity analysis includes the identification of an adequate change detection technique, which is capable to produce accurate information as to how and how intense coastal ecosystems were impacted by the tsunami.

Two change detection algorithms are applied on the IKONOS images of January 2003 (pre-tsunami) and January 2005 (post-tsunami): the change vector analysis (CVA), based on the first two tasselled cap components greenness and brightness (Horne 2003; Johnson 1994; Malila 1980), and the direct multi-date classification (DMC), based on the red, green and near-infrared channels in the multi-date dataset (cp. Mas 1999; Weissmiller *et al.* 1977).

In contrast to other common techniques such as band algebra, (e.g. vegetation index differencing, image regression) the two methods can provide a detailed change matrix (Coppin and Bauer 1996; Lu *et al.* 2004a, Weissmiller *et al.* 1977). In order to improve the quality of the change detection results, the polygon borders derived from the LULC-classification of 2003 served as a spatial reference i.e. as zones for the change detection application. The results of the impact analysis and a detailed description of the methodology are presented in Roemer *et al.* (2010a), respectively in section 5.2.

A major limitation of the sensitivity analysis results from a lack of accurate field data on tsunami related impacts on biotopes. Since this work started in January 2008 most of the evidence on the landscape of the tsunami effects were gone due to recovery processes of vegetation, beach erosions or beach accretions, leaching processes in soils or simply human related impacts in the landscape. Thus, the higher resolution pan-sharpened images of 2003 and 2005 as well as information taken from literature were used as proxy data for the missing ground truth information. Furthermore, there was a lack of available data for the time before the tsunami which was already described in section 3). This would have been necessary to better understand the mechanism of damage processes. The utility of the results provided by the impact analysis for the analysis of the sensitivity and vulnerability will be further discussed in the synthesis section (section 6.2). The concept of the impact analysis is illustrated on Figure 4-11.

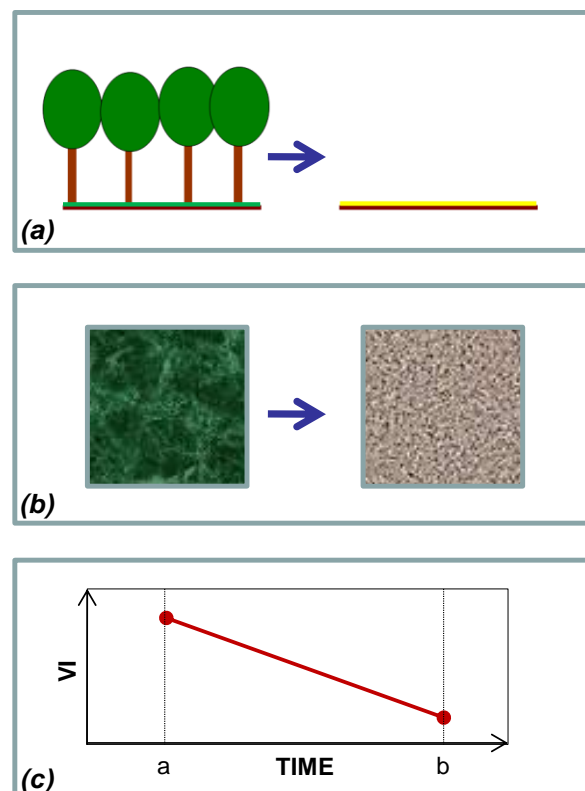


**Figure 4-10.** Applying change detection techniques for tsunami damage assessments. (a) a typical tsunami impact scenario on a forest: uprooting of forests and accumulation of marine sandy sediments on forest floors, (b) the corresponding land cover change which involves a transition of forest cover to sand / barren and (c) the corresponding spectral changes represented by the change of a fictive vegetation index.

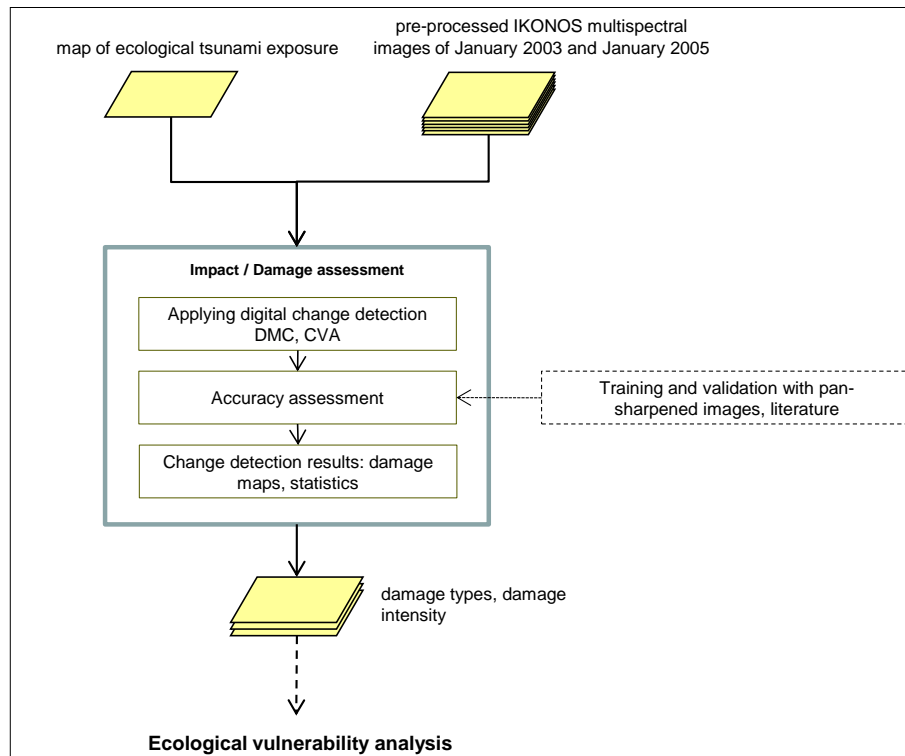
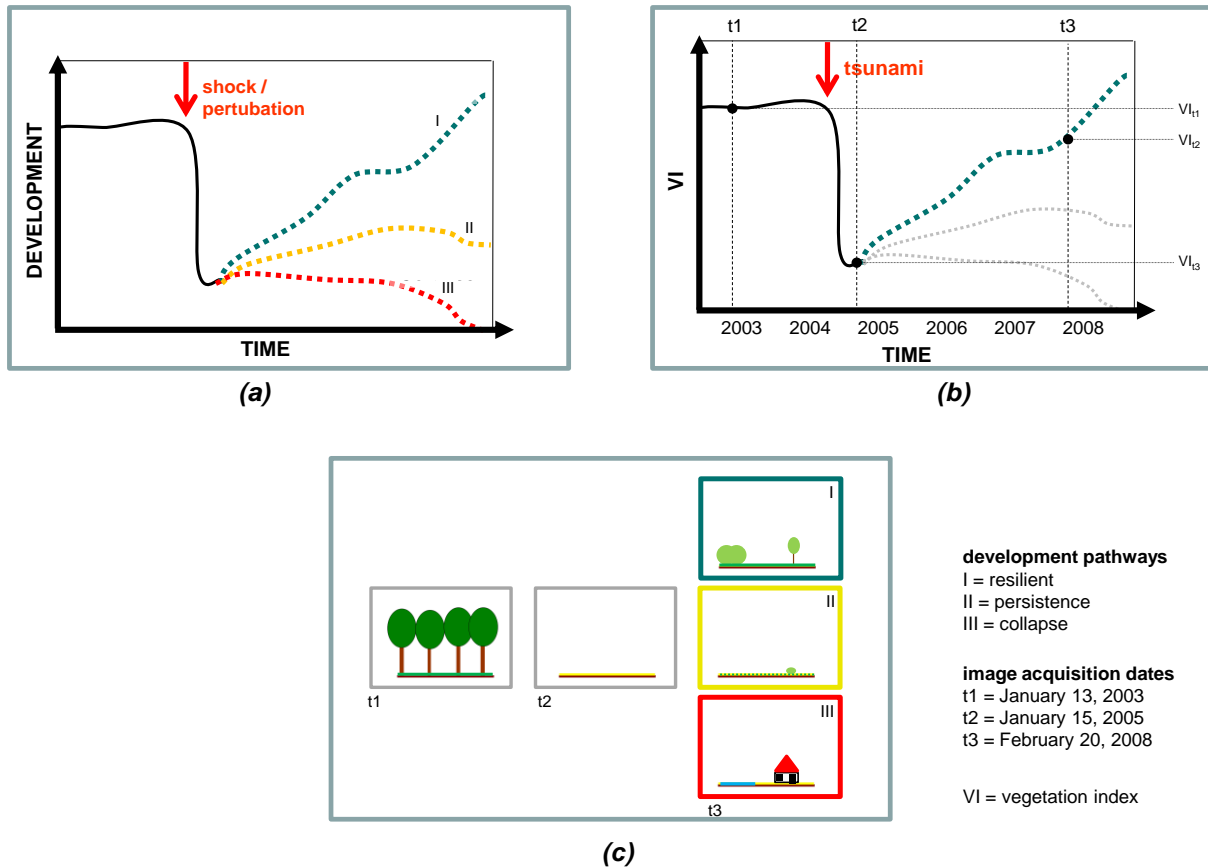


Figure 4-11. Concept of impact analysis based on remote sensing applications.

## 4.4 Analysis of recovery processes as a basis to estimate tsunami resilience

### 4.4.1 General approach

Just as with the analysis of tsunami induced impacts, change detection techniques played an important role for the recovery analysis. Figure 4-12 illustrates a theoretical and simplified example of how remote sensing applications can be used for the analysis of ecosystem recovery. Here, three fictive development pathways of an ecosystem following a perturbation are illustrated (Figure 4-12a). These pathways can be indirectly observed when comparing the vegetation indices (Figure 4-12b) of at least three satellite scenes from acquisition dates before and after the tsunami. Furthermore, the development pathways can also indirectly be analysed by evaluating the changes or transitions of LULC occurred between the acquisition dates (Figure 4-12c). In this study recovery processes were assessed based on two change detection techniques: The first technique involves the calculation of a recovery rate (%) from multiple TNDVI images (Washington-Allen *et al.* 2008) and thus adopts the idea of analysing the change of a vegetation index. The second technique, a modified version of the CVA, focuses more on the idea of analysing the transitions of land cover patterns. Both methods are applied on the multispectral IKONOS images from January 2003, January 2005 and February 2008 and are detailed in the second article (cp. section 5.2; Roemer *et al.* 2010b). As with the assessment of tsunami-induced impacts, a zone-based change detection approach is applied.



**Figure 4-12.** The principle of applying change detection techniques for vegetation recovery assessments. (a) the return time definition of engineering resilience, exemplified by three different development pathways of a fictive forest ecosystem following a shock event, (b) the adjusted resilience concept using the change of a vegetation index between the three image acquisition dates, illustrated for the development pathway (I) and (c) the possible transitions of land cover types that occur between the three acquisition dates, illustrated for all three scenarios.

In contrast to the study on tsunami induced impacts, recovery processes of terrestrial coastal ecosystems (e.g. forest ecosystems) were still present for the time of investigation, and thus could be observed in the field. The field work was conducted during January and March 2009 one year after the satellite images of February 20, 2008. The applied methods during field works are detailed in the following section. In contrast, the results of the field work are described in section 5.2. An overview of the workflow of the recovery analysis is illustrated on Figure 4-13.

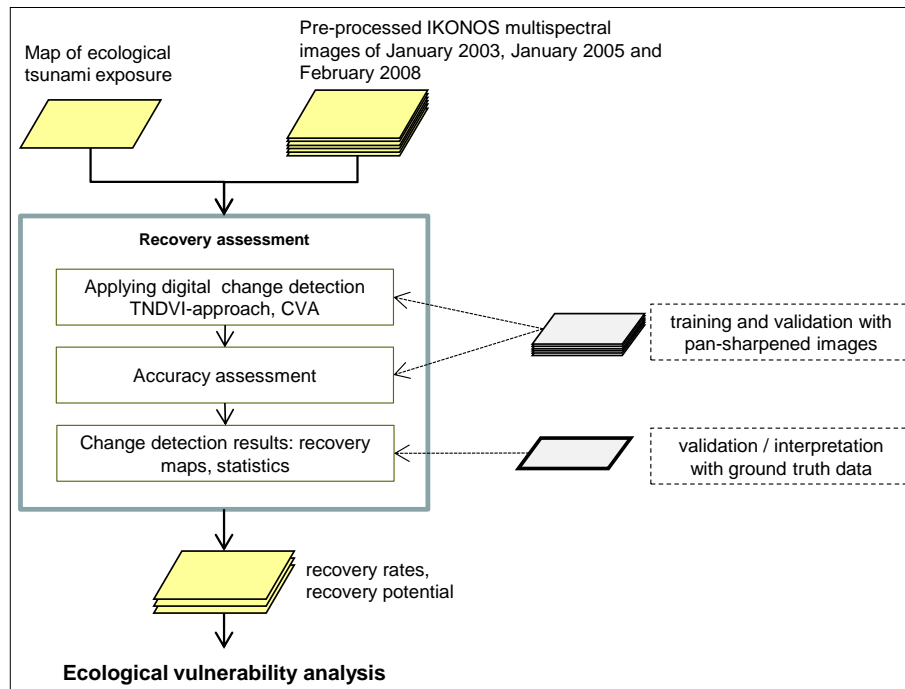


Figure 4-13. Concept of the recovery analysis based on remote sensing application.

#### 4.4.2 Ground truth data collection

Ground truth data played an important role for the recovery and resilience analysis. Unfortunately, due to difficulties in finding adequate (cloud free) satellite images for the year 2009, a time gap of one year between the third image acquisition date (IKONOS image of February 20, 2008) and the time of the field data collection (January – March 2009) had to be accepted. A challenge of the field campaign was to define and locate appropriate study sites. A major problem was that not all young forests occurring near the coasts could be automatically regarded as potential study sites. Forest renewal can be caused by different natural and human induced disturbances including heavy winds, wave impacts, storm surges, coastal erosions, burning and cutting. Furthermore, natural rejuvenation can also occur without any triggering disturbance. Because of this, pan-sharpened IKONOS images of 2003, 2005 and 2008 as well as hand-GPS devices were used in the field to identify areas which were intensively impacted by the tsunami. Thus, there was a high certainty that the observed recovery processes could be traced back to the tsunami event and secondly, mature trees shading the young vegetation by their dense canopies were usually absent. This allows a reasonable application of change detection for these areas.

According to Roemer *et al.* (2010b) a nested sampling strategy was selected in this study by which each study site (15 x 15 m / 225 m<sup>2</sup>) was divided into smaller plots (5 x 5 m / 25 m<sup>2</sup>). The quadratic sites were first polar-aligned and then staked out by using four plastic poles at each corner. Measuring lines were used to split the study sites into nine equal sized squares (5 x 5 m) whereas only five of these, the centre-plot and the four corner-plots were considered for the measurements (cp. Figure 4-14). This pattern was applied in order to a) reduce the total area needed for the quantitative measurements and b) to allow a representative and even distribution of plots within the sites.



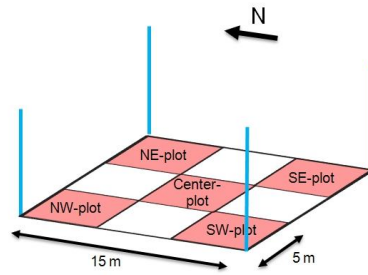


Figure 4-14. Configuration of study sites and plots.

Since no adequate IKONOS image for 2008 or 2009 could be acquired for the southern area between Tap Lamru and Thai Mueang city, only 27 of the 45 collected study sites were considered in this study (Figure 4-15). From the 27 sites, eleven were observed in former casuarina beach forests (termed as casuarina sites), ten in mangrove forests (mangrove sites) and six in coconut plantations (coconut sites). Except for the two sites 10 and 25, forest biotopes were intensively (directly) damaged by the tsunami. The following Figure 4-16 illustrates a typical location and scenery of a study site near Krang-Noi Cape. The photo shows a young stand of *Casuarina equisetifolia* which recovered after the tsunami.

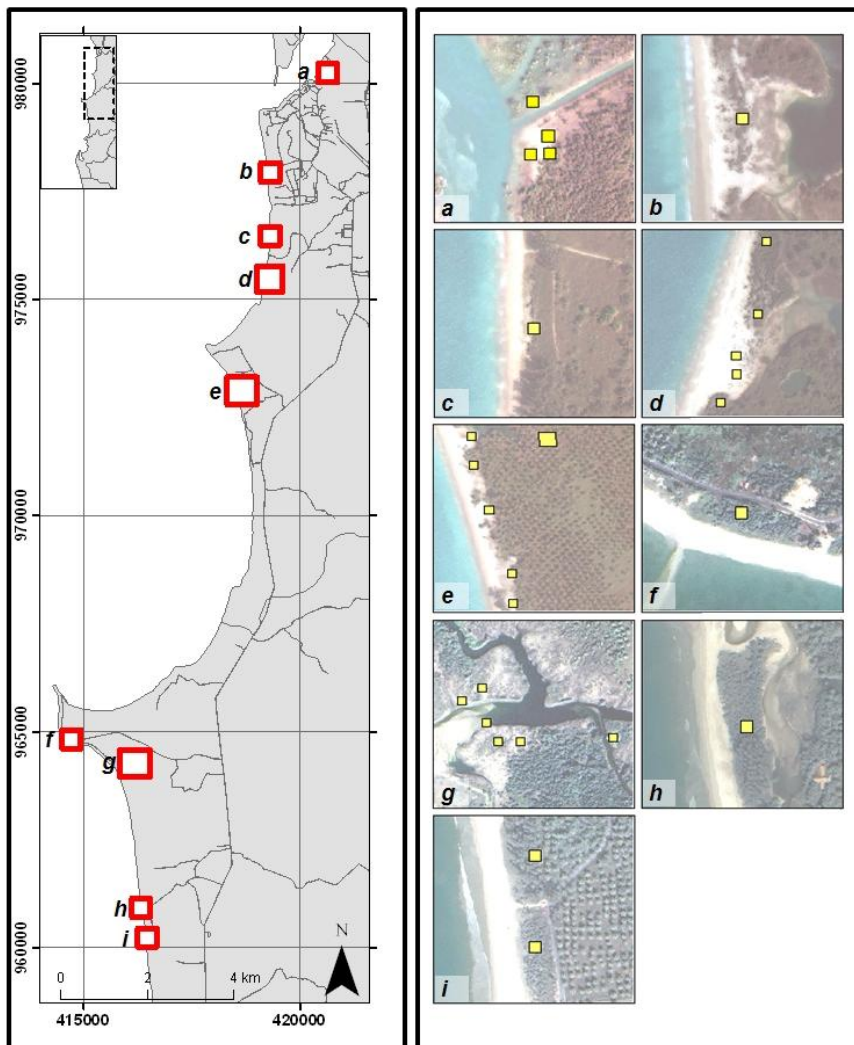
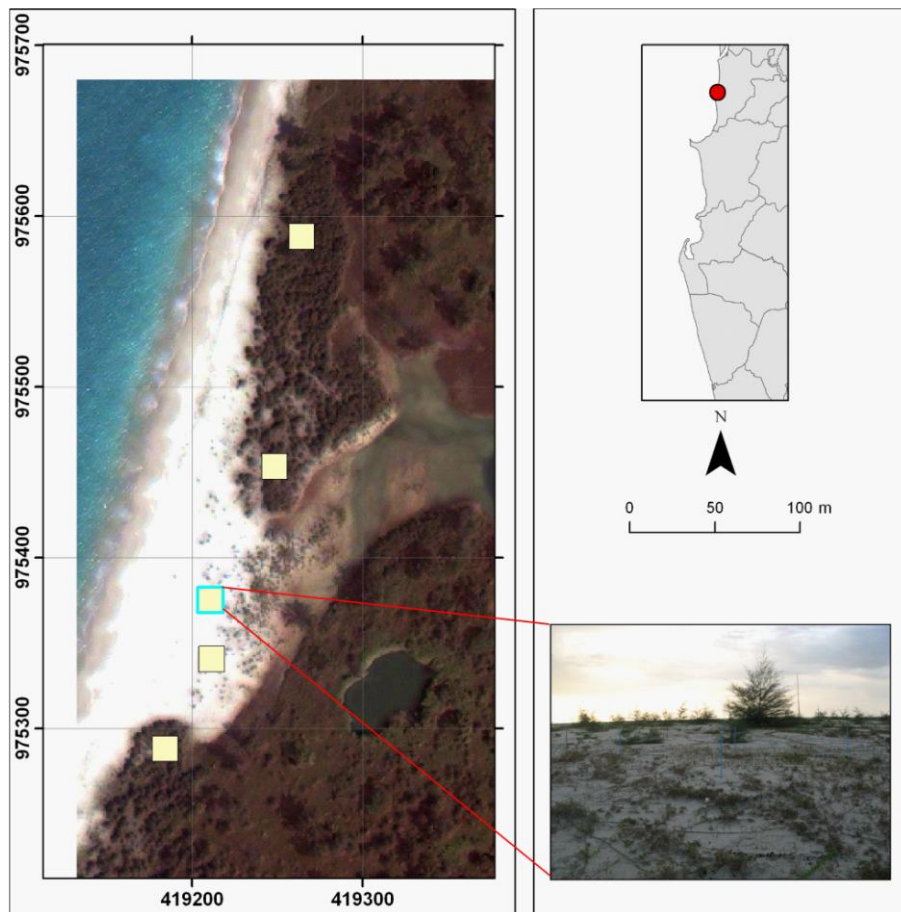


Figure 4-15. Study sites collected between January and March 2009. The study sites are highlighted by yellow squares.



**Figure 4-16.** A typical location and scenery of a study site. The example shows slow succession processes of *Casuarina equisetifolia* near Krang-Noi Cape.

Information on vegetation recovery was collected in two ways. An inventory of seedlings and saplings (here called as seedlings/saplings) was carried on the plot level out, in order to derive quantitative information on the recovery rate and the species community. Recovery rates were assessed based on the five vegetations stand parameters which were calculated for the seedlings/saplings: *average stand diameter (ADKH, cm)*, *Average stand height (AH, m)*, *Stand density (D, ha<sup>-2</sup>)*, *Basal area (BA, m<sup>2</sup> ha<sup>-1</sup>)* and *Stand volume (V, m<sup>3</sup> ha<sup>-1</sup>)*. These measures were derived from the three measures *number of seedlings/saplings in a plot (N)*, *diameter at knee height (DKH, cm)* and *total height (H, m)*, which were collected in the field for each seedling/sapling individual. Here, a diameter tape was used to measure trunk diameters, whereas a measuring staff was used to measure sapling heights (Lu *et al.* 2003; Otieno *et al.* 1991; Theron *et al.* 2004). Furthermore, recovery rates were also estimated by analysing the *ground cover of herbaceous vegetation (CH, %)* and the *ground cover of each seedlings/saplings species (CS, %)*. Here two methods were applied: a) the visual interpretation of percentage cover based on the Braun-Blanquet cover classes and b) the digital analysis of hemispherical photos which were taken at viewing angles approaching to 180° vertical up and 0° vertical down in each plot (Rich 1990; Schroeder *et al.* 2007). Figure 4-17 illustrates the two mentioned techniques. Additionally, the canopy closure (CT, %) of mature trees that have survived the tsunami was observed.



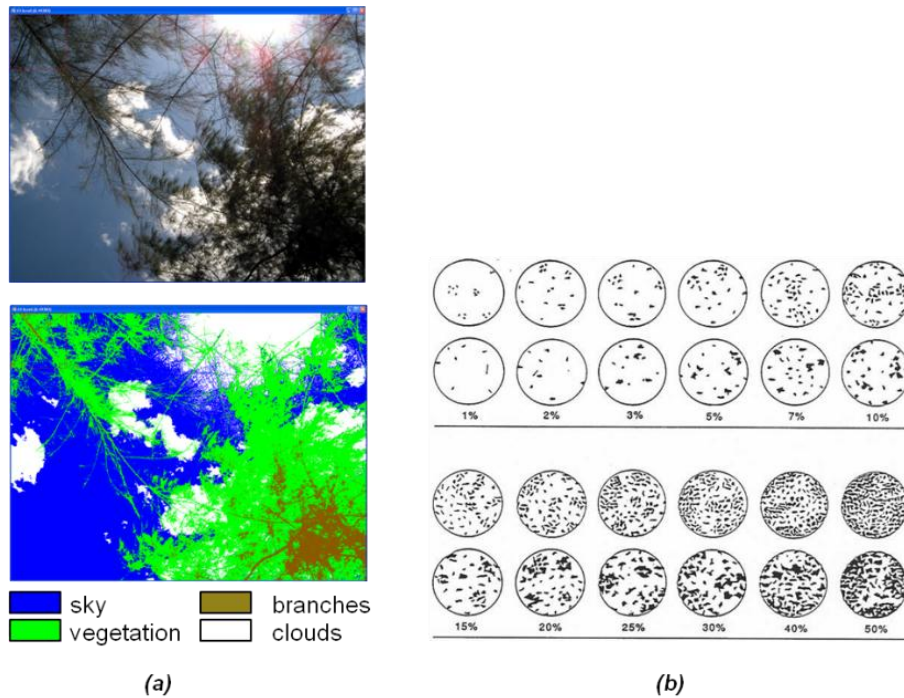


**Figure 4-17.** Estimation of percentage ground cover. (a) based on hemispherical photos and digital image analysis (supervised classification), (b) based on a cover table and visual estimations in the field. Modified from Carpenter (1987).

Qualitative measures were observed on the site level including a characterisation of the local topography, the soil texture of the first 20 cm of top soil (observed in the centre plot), the initial or pre-tsunami species community, a general classification the tsunami induced impact and additionally the land-use history. Furthermore, an identification of the species was done during the seedlings/saplings inventory in order to identify changes in habitats or species compositions. With regard to species structure of the inventoried seedlings/saplings, two major groups were distinguished in this study a) mangrove species such as *Avicennia sp.*, *Bruguiera gymnorrhiza*, *Ceriops tagal*, *Excocaria agallocha*, *Rhizophora apiculata* and *Xylocarpus granatum* and species usually occurring in sandy beach environments either belonging to the *Barringtonia* or *pes-caprae* formation including *Barringtonia sp.*, *Calophyllum inophyllum*, *Casuarina equisetifolia*, *Cocos nucifera*, *Milettia pinnata*, *Scaecola taccada*, *Terminalia catappa* and *Thespesia populina* (cp. Sukardjo 2006 and Whitten *et al.* 1997). Table 4-3 provides a short overview of the main characteristics of the 27 study sites; Table 4-4 illustrates the results of the species inventory carried out on the plot level.

Beside the ten hemispherical photos that were taken for each site, four more photos were taken from each corner of the site toward the plot centre. Elevation measurements based on hand GPS-devices turned out to be very erroneous and therefore are not further investigated in this study. The latest version of the field protocol from January 16, 2009 is provided in Appendix L.

**Table 4-3.** Study sites and their main characteristics.

Site number	X	Y	local topography	distance to shore (m)	biotope* (2003)	soil texture**
1	0419181	0975291	hill top (dune)	50-75	cas	sand (m)
2	0419242	0975460	depression	50-75	cas	sand (m)
3	0419206	0975383	hillside	50-75	cas	sand (m)
4	0419264	0975573	hillside	25-50	cas	sand (m)
5	0419204	0975344	hillside	50-75	cas	sand (m)
6	0419329	0976432	hilltop	25-50	cas	sand (m)
7	0419345	0976425	hillside	25-50	cas	sand (m/c)
8	0414717	0964808	plain	25-50	cas	sand (m)
9	0416466	0960282	hillside	25-50	cas	sand (m)
10	0416470	0960408	plain	25-50	cas	sand (m)
11	0416375	0960813	hillside	0-25	cas	sand (m)
12	0416158	0964190	plain	300-400	man	sand (f)
13	0416196	0964180	hill top	400-500	man	mud
14	0416178	0964218	plain	300-400	man	mud
15	0416097	0964267	plain	300-400	man	mud
16	0420695	0980194	plain	25-50	man	sand (f)
17	0420659	0980163	plain	25-50	man	sand (f)
18	0416128	0964292	plain	400-500	man	sand (m)
19	0420660	0980236	plain	0-25	man	mud
20	0420694	0980170	plain	25-50	man	sand (f)
21	0416334	0964188	plain	500-600	man	sand (f)
22	0418648	0972600	plain	25-50	coc	sand (m)
23	0418636	0972655	plain	25-50	coc	sand (m/c)
24	0418568	0972912	plain	25-50	coc	sand (m)
25	0418691	0972911	plain	100-200	coc	sand (m)
26	0418571	0972858	plain	25-50	coc	sand (m)
27	0418598	0972776	plain	25-50	coc	sand (m)

\* cas = casuarina sites, man = mangrove sites, coc = coconut sites

\*\*soil textures (sand fraction): f = fine, m = medium, m, c = medium to coarse

**Table 4-4.** Species inventory carried out on the plot level.

species name (community*)	casuarina sites											mangrove sites											coconut sites						Σ
	1	2	3	4	5	6	7	8	9	10	11	12	13	14	15	16	17	18	19	20	21	22	23	24	25	26	27		
<i>Avicennia sp. (M)</i>	0	0	0	0	0	0	0	0	0	0	0	0	0	0	5	10	71	0	20	16	0	0	0	0	0	0	122		
<i>Buguiera gymnorrhiza (M)</i>	0	0	0	0	0	0	0	0	0	0	0	0	0	0	1	0	0	35	12	0	9	0	5	2	0	0	0	64	
<i>Ceriops tagal (M)</i>	0	0	0	0	0	0	0	0	0	0	0	0	0	0	0	0	14	10	2	0	0	3	0	0	0	0	29		
<i>Excocaria agallocha (M)</i>	0	0	0	0	0	0	0	0	0	0	0	0	0	0	2	4	0	0	0	0	12	0	1	3	0	0	22		
<i>Rhizophora apiculata (M)</i>	0	0	0	0	0	0	0	0	0	0	0	0	0	0	0	0	7	26	0	5	16	59	0	0	0	0	113		
<i>Xylocarpus granatum (M)</i>	0	0	0	0	0	0	0	0	0	0	0	0	0	0	0	0	5	5	5	0	0	4	0	0	0	0	19		
<i>Barringtonia sp. (B)</i>	0	0	0	0	0	0	0	0	0	7	0	0	0	0	0	0	0	0	0	0	0	0	0	0	1	0	9		
<i>Calophyllum inophyllum (B)</i>	0	0	0	0	0	0	0	0	0	0	0	0	0	0	1	0	0	0	0	0	0	0	0	0	0	0	1		
<i>Casuarina equisetifolia (B)</i>	40	34	8	49	13	96	103	40	41	2	42	0	0	0	0	0	0	2	0	1	0	2	11	0	0	3	497		
<i>Cocos nucifera (B)</i>	1	0	0	0	0	4	0	2	2	0	0	1	0	0	0	0	0	2	0	0	0	0	0	0	0	3	18		
<i>Milettia pinnata (B)</i>	0	0	0	0	0	0	0	0	0	0	0	2	0	0	0	0	0	0	0	0	0	0	0	0	0	0	2		
<i>Scaevola taccada (B)</i>	1	0	0	0	0	0	0	0	0	0	6	0	0	0	0	0	0	0	0	0	0	0	0	0	0	0	7		
<i>Terminalia cattapa (B)</i>	2	0	0	1	0	1	0	0	1	0	0	0	0	0	0	0	0	0	0	0	0	0	0	0	0	0	5		
<i>Thespesia populnia (B)</i>	0	0	0	0	0	0	0	0	0	0	1	3	0	0	0	0	0	0	0	0	0	0	0	0	0	0	4		
Σ B	44	34	8	50	13	101	103	42	44	9	49	7	0	0	0	0	0	4	0	1	0	2	12	0	0	6	543		
Σ M	0	0	0	0	0	0	0	0	0	0	0	3	4	0	59	44	104	21	25	45	64	0	0	0	0	0	369		
Σ all	44	34	8	50	13	101	103	42	44	9	49	10	4	0	59	44	104	25	25	46	64	2	12	0	0	6	912		

\* species community: M = mangrove community, B = Barringtonia community (beach environment)

## 4.5 Additional data sets

### 4.5.1 Elevation data

Two elevation data sets were used: a higher resolution digital land surface model (DLSM) based on MFC-data for the area between Ban Nam Khem and Tap Lamru and lower resolution DLSM based on SRTM-data covering the southern area, south of Tap Lamru. The MFC-DLSM has a (x-y) pixel resolution of one meter (X-Y-direction) and was derived from a digital surface model (DSM) acquired by the MFC-3 multi-functional camera. The MFC was developed by the German Aerospace Centre and was used in an airborne campaign conducted within the TRAIT project between 18.11 and 25.11 2008. The core of the MFC is an array of three RGB-Charge-Coupled-Device (CCD)-lines-modules allowing the derivation of high-resolution colour images and digital surface models with a X-Y-Z-resolution of 15-35 cm and a geometrical accuracy of 8 cm (cp. Börner *et al.* 2008). Further technical details to the MFC-camera are provided in the Table 4-5.

**Table 4-5.** Specification of MFC 1-3. Börner *et al.* (2008).

Parameter	MFC-1	MFC-3	MFC-5
Number of modules	1	3	5
Number of pixels	2k, 6k, 8k	6k, 8k	8k, 10k, 14k*
Focal length	35mm, 80mm	80mm	100mm
Stereo angle	0	$\pm 12,6^\circ$	$\pm 10,2^\circ$ , $\pm 19,8^\circ$
Radiometric resolution	12bit	12bit	12bit, 10bit(optional)*
Mass	1.5kg	15kg	20kg
Interface	USB 2.0	Ethernet (1Gb/s)	Ethernet (1Gb/s)
Size (W×H×D (without optic and grips)	$4 \times 20 \times 15\text{cm}^3$	$20 \times 30 \times 30\text{cm}^3$	$20 \times 30 \times 30\text{cm}^3$
Application	Terrestrial, Airborne	Airborne	Airborne

Elevation data based on the Shuttle Radar Topography Mission (USGS 2004) was acquired from the University of Maryland, Global Land Cover Facility (<http://www.glcf.umd.edu/data/srtm/>) with a resolution of 3 arc seconds (90 m).

As both elevation datasets were provided as surface models, they had to be corrected in order to create elevation datasets that represents the real land surface elevation. The correction procedures were carried out within the TRAIT project and are only briefly described here. In general, the MFC-DLSM model was created based on two steps: First, a manual selection of ground control points (GCPs) carried out based on the visual interpretation of the MFC-DSM and the corresponding MFC-RGB-imagery. Only pixels that represent the terrain surface (e.g. barren areas) were considered as GCPs. The second step included the interpolation between the selected GCPs in order to create a DLSM. In contrast, the SRTM-DLSM was created by subtracting mean class heights of overlapping LULC-classes from the corresponding pixel value in the SRTM-DSM. Here, the LULC-classification which was derived within this study (cp. section 4.2.1) was used for this procedure.

#### 4.5.2 Results from inundation modelling

Two model outputs derived from tsunami inundation modelling are used: the maximum total water depth above ground ( $W$ ,  $m$ ) and the maximum current speed ( $CS$ ,  $ms^{-1}$ ). Both parameters were derived by applying the hydrodynamic model Mike 21 FM (DHI 2009). Inundation modelling was carried out by using the M 9.3 earthquake scenario from Løvholt *et al.* (2006), adding the tidal level from 26 December 2004, according to the Thailand Group (2005). As the high resolution MFC-DLSM do not cover the entire study region, model outputs calculated for the northern parts are more accurate than those calculated for the southern area (based on SRTM-DLSM): The interpolated mesh, that represents the topography used in the inundation model was 40 m (interpolated from 90 m) for the southern area and only seven meters for the northern area. Further details on model setups and model validation issues are provided in Soltysik (2009), Scheele (2010) and Kaiser *et al.* (2010b).

#### 4.5.3 Other geodata

Basic geo-data from Thailand are provided by Thai governmental institutions and were delivered through our Thai project partners. These data include the administrative units of Thailand, the coastline, the road and river network, the boundaries of seagrass beds, coral reefs, seagrass beds and national parks. Furthermore, a digitised and adjusted version of the tsunami damage area provided by the ZKI (2005) was used particularly for identifying the tsunami exposure. Building polygons of January 2003 and November 2009 were available as vector files. Whereas the polygons of the earlier date were manually digitised from the pre-tsunami pan-sharpened IKONOS image of January 2003, building polygons from the later date were created based on an automatic extraction approach using the MFC-data (cp. Tegtmeier 2009). Furthermore, land use data covering the coastal areas of the five Tambons Bang Mueang, Khuek Kak, Laem Kaen, Thung Maphrao and Thai Mueang for the years 2003 and 2006 were used. The LULC-data were derived within the TRAIT project from ASTER multispectral data using a supervised classification approach as described in Tiffert (2010). These data play an important role in the last section (section 6.4). The following Table 4-6 shows all geo-datasets used within this thesis.

**Table 4-6.** Overview of geo-data used in this study.

Data	Format*	Providers / References
Administrative boundaries: tambons, provinces	V (pg)	Ministry of Interior, Department of Provincial administration
Bathymetric map	R (175m)	Ministry of Defence, Royal Thai Navy
Building polygons	V (pg)	IKONOS imagery 2003 and MFC-data (Tegtmeier 2009)
Coral reefs, seagrass beds, mangroves	V (pg)	Ministry of Natural Resources and Environment, Department of Marine and Coastal Resources
MFC-DLSM, MFC RGB	R (1m)	acquired in November 2008; DLSM is based on MFC-DSM
SRTM-DLSM	R (90m)	Based on SRTM-DSM (open source)
IKONOS imagery	R (4/1m)	Centre of Remote Sensing and Processing (CRISP), Singapore; Spatial Dimension Solutions (SDS), Bangkok
Land use (ground truth)	V (pg)	Field campaign conducted in 2008 by the WWF-team
Land use (ASTER 2003, 2006)	R (15m)	derived within the TRAIT-project, based on ASTER-multispectral imagery, using the approach of Tiffert (2010)
Land use (IKONOS)	R (4m)	Rule based object-oriented classification provided by the author
national parks	V (pg)	Ministry of Natural Resources and Environment, National Park, Wildlife and Plant Conservation Department
Recovery information (ground truth)	V (pg)	Field campaign conducted in 2009 by the author
River network	V (pl)	Ministry of Natural Resources and Environment, Department of Water Resources
Road network	V (pl)	Ministry of Transport and Communications, Department of Highways
Shoreline	V (pl)	Ministry of Natural Resources and Environment, Department of Marine and Coastal Resources
Tsunami damage area	V (pg)	Digitised from ZKI (2005)
Tsunami modelling results:	R:	
- Based on MFC-DLSM	7m**	Kaiser <i>et al.</i> (2010b); Scheele 2010
- Based on SRTM-DLSM	90m**	Soltysik (2010)

\* Format: V = vector data with *pg* = polygon file, *pl* =polyline file; R = raster data, with the pixel resolution in meter

\*\* mesh resolution used in the model

## 5 Results of the remote sensing applications: exposure, tsunami impacts and recovery processes

In this section the two articles of the author are presented (Roemer *et al.* 2010a/b). The two papers are provided in their original form including all journal specific formats. As the results of the exposure analysis, as the preliminary step of the assessment of tsunami impacts and recovery, are only briefly mentioned in both articles, they will be presented in the following section.

### 5.1 Results of the exposure analysis

On the basis of the LULC-classification and expert judgements, the following coastal forest ecosystems were considered as exposure units and are further examined in this study: mangrove forests, casuarina beach forests, coconut plantations mixed beach forest and melaleuca forests (cp. Figure 5-2 and the exposure map on Figure 5-1 and enlarged Appendices M-P). The five ecosystems were considered as relevant for this study because they represent the most typical forest biotopes occurring throughout the coastal areas of Thailand and Southeast Asia (cp. Cochard *et al.* 2008; Donner 1989; Pajimans 1976). In addition, these ecosystems provide many important ecological functions and services to the human and natural system (Chatenoux and Peduzzi 2007; Millennium Ecosystem Assessment 2005a; Paphavasit *et al.* 2009; Plathong and Sitthirach 1997) making this study also relevant for further investigations on the social dimension of tsunami vulnerability (cp. section 6.3). It should be mentioned at this point, that sandy beaches are also important coastal ecosystems which can be assessed by the remote sensing. Here, the study of Vosberg (2010) focuses on the degradation and recovery processes of the beach area based on multi-temporal IKONOS imagery (cp. section 6.3).

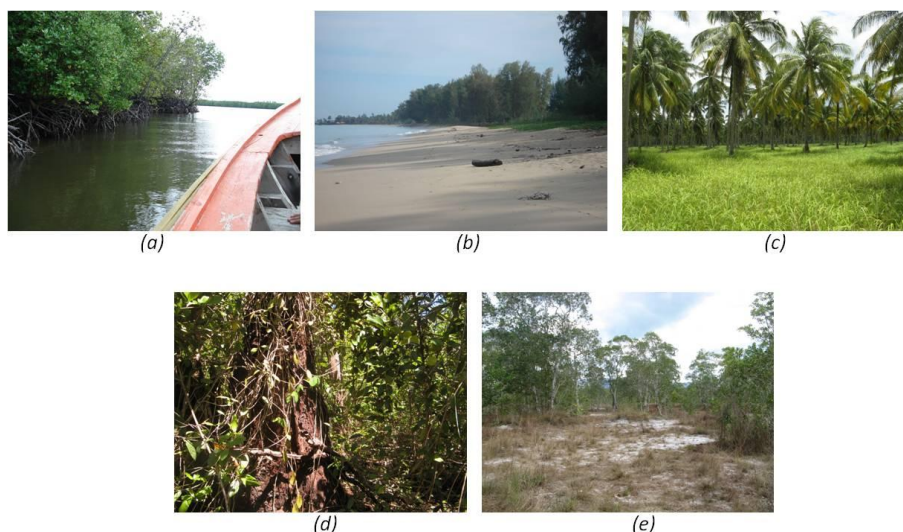


**Figure 5-1.** Photos of the ecological exposure units considered in this study. (a) mangrove forest, (b) casuarina beach forest, (c) coconut plantation, (d) mixed beach forest and (e) melaleuca forest. Photos were taken between January and March 2009.



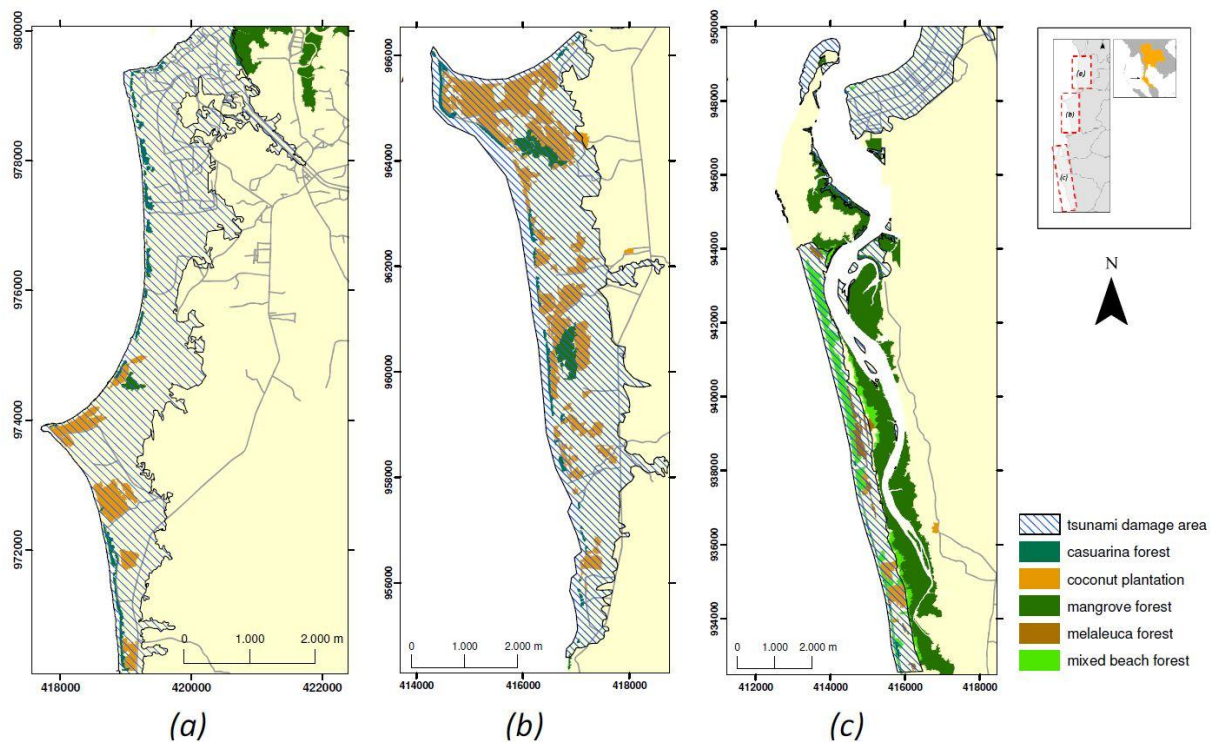


**Figure 5-2.** Map of the ecological tsunami exposure considered in this study. (a) the northern area between Ban Nam Khem and Ban Bang Sak, (b) the central part between Pakarang Cape and Bang Niang and (c) the southern area between Tap Lamru and Thai Mueang city.

The total mangrove area that was identified by the classification is 980 hectares, whereas only 111 hectares (11.30%) are directly exposed towards the tsunami (cp. Figure 5-3). This low exposition results from the fact, that large mangrove areas, particularly in the southern parts of the study area are located in sheltered areas (cp. Chatenoux and Peduzzi 2005). The mean distance to the wave-dominated west coast is 891 m (cp. Figure 5-4). In addition to the GIS-data provided by the DMCR (n.d.), three smaller isolated mangrove areas which are located at smaller creeks near Krang Nui Cape, Pakarang Cape and the village of Khuk Khak could be extracted from the images. The field measurements carried out by the author and by Arp (2009) reveal that the dominating mangrove species of the study areas are *Rhizophora apiculata*, *R. mucronata*, *Ceriops tagal*, *Bruguiera*, *Avicennia sp.*, *Bruguiera gymnorrhiza*, *Ceriops tagal*, *Excocaria agallocha*, *Xylocarpus granatum* and *Nypa fruticans*.

Casuarina beach forests occur throughout the study area and are located on beach ridges. As this forest type is located close to the shoreline (cp. Figure 5-4) it is the most exposed ecosystems, with 100% of the total forest area being located within the tsunami damage area (98 hectares), cp. Figure 5-3. Coconut plantations (*Cocos nucifera*) cover large mono-specific stands in the coastal plains. Generally, they occur directly behind the forest stripe of the casuarina beach forests with an average distance to the shoreline of 391 m. The total area is 494 hectares, whereas 451 hectares (91.1%) are exposed to the tsunami. Being strongly influenced by human induced processes, this biotope cannot be considered as a natural forest. A main problem of the cultivation of coconut plantations involves the clearing of unwanted vegetation, such as casuarina seedlings. Coconut plantations are of great economic importance since they serve as a major source of food and income for local communities.



Mixed littoral forests (here simply termed as mixed beach forests) and Melaleuca forests occur only in the southern part of the study area in the Khao Lampi - Hat Thai Mueang National Park covering a total area of 193 and 49 hectares, respectively. The majority of these forest biotopes are located within the tsunami damage area, with 137 hectares (71%) for mixed beach forests and 46 hectares (93.9%) for melaleuca forests (cp. Figure 5-3). Mixed beach forests occur mainly in swaley depression between beach ridges: Whereas a main part is located directly behind the stripe of casuarina beach forests, another part is located behind a second beach ridge and directly borders to swamp and mangrove forests. This spatial characteristic explains the bimodal frequency distribution of distance values for this forest type (cp. Figure 5-4). The forest type shows a great biodiversity and has to be considered as a valuable ecosystem. Typical canopy trees are *Syzigium grande*, *Diospyros sp.*, *Shorea sp.*, *Lepisanthes rubiginosa*, *Eugenia sp.* The melaleuca forest or melaleuca savannah directly borders to the mixed beach forest in the south and is also located inside of the national park. Its main species, the *Melaleuca leucadendron* is characterised by its bright fire-resistant paperbark and forms a widely spaced forest. Furthermore the melaleuca tree is characterised by its tolerance to salt spray and forest fires and can be used to obtain pharmaceutical products (cp. Budicadi *et al.* 2005; Wolter *et al.* 2001). The forest occurs either in coastal plains or temporary swampy depressions with a mean distance to shoreline of 343 m (cp. Figure 5-4).

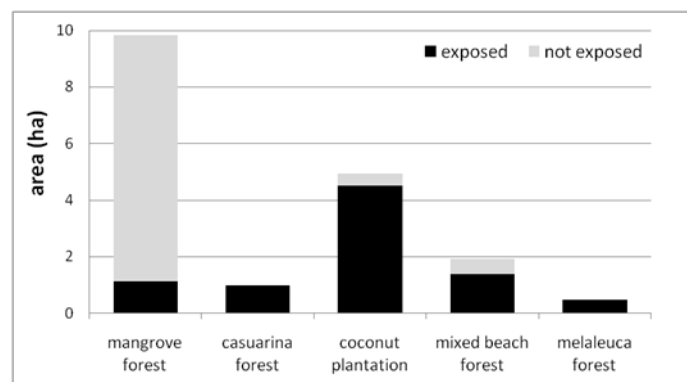


Figure 5-3. Relation between the exposed area and the total area of the five examined ecosystems.

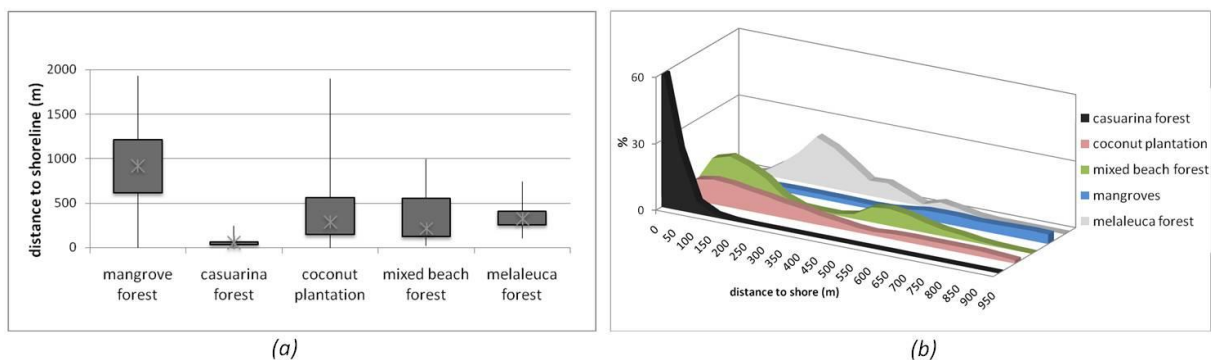


Figure 5-4. Distances to shoreline of the examined ecosystems. (a) box plots, (b) frequency distribution.

## 5.2 The submitted articles

Both articles were written by the author. Whereas Roemer *et al.* (2010a) was published on April 13, 2010, Roemer *et al.* 2010b is a preprint of a manuscript submitted for consideration in the International Journal of Remote Sensing [copyright Taylor & Francis]. The manuscript was submitted in revised form (following 'minor revision' requested by two anonymous reviewers) on November 11, 2010.

Roemer, H., Kaiser, G., Sterr, H. and Ludwig, R. (2010a): Using remote sensing to assess tsunami-induced impacts on coastal forest ecosystems at the Andaman Sea coast of Thailand. *Nat Hazard Earth Sys*, **10**, 729-746.

Roemer, H., Jeewarongkakul, J., Kaiser, G., Ludwig, R., Sterr, H. (2010b): Monitoring post-tsunami vegetation recovery in Phang-Nga, Thailand – a remote sensing based approach. *Int J Remote Sens*, submitted manuscript.

## Using remote sensing to assess tsunami-induced impacts on coastal forest ecosystems at the Andaman Sea coast of Thailand

H. Roemer<sup>1</sup>, G. Kaiser<sup>1</sup>, H. Sterr<sup>1</sup>, and R. Ludwig<sup>2</sup>

<sup>1</sup>Department of Geography, Christian-Albrechts-Universität zu Kiel, Kiel, Germany

<sup>2</sup>Department of Geography, Ludwig-Maximilians-Universität München, Munich, Germany

Received: 22 December 2009 – Revised: 16 March 2010 – Accepted: 20 March 2010 – Published: 13 April 2010

**Abstract.** The December 2004 tsunami strongly impacted coastal ecosystems along the Andaman Sea coast of Thailand. In this paper tsunami-induced damage of five different coastal forest ecosystems at the Phang-Nga province coast is analysed with a remote sensing driven approach based on multi-date IKONOS imagery. Two change detection algorithms, change vector analysis (CVA) and direct multi-date classification (DMC), are applied and compared regarding their applicability to assess tsunami impacts. The analysis shows that DMC outperforms CVA in terms of accuracy (Kappa values for DMC ranging between 0.947 and 0.950 and between 0.610–0.730 for CVA respectively) and the degree of detail of the created change classes. Results from DMC show that mangroves were the worst damaged among the five forests, with a 55% of directly damaged forest in the study area, followed by casuarina forest and coconut plantation. Additionally this study points out the uncertainties in both methods which are mainly due to a lack of ground truth information for the time between the two acquisition dates of satellite images. The created damage maps help to better understand the way the tsunami impacted coastal forests and give basic information for estimating tsunami sensitivity of coastal forests.

### 1 Introduction

The Indian Ocean Tsunami in 2004 was one of the most devastating natural disasters ever. Besides the enormous number of fatalities and the massive destruction of settlements and infrastructure, coastal ecosystems were deteriorated or

destroyed (e.g. Szczucinski et al., 2006; Phongsuwan et al., 2006). At the Andaman Sea coast of Thailand, the Phang-Nga province was one of the most severely affected regions. For instance, in total 386 ha of mangrove forests were impacted directly by the tsunami (Paphavasit et al., 2009), other coastal forests were uprooted or washed away, coral reefs were affected in various ways, and beaches as well as tidal inlets were eroded (e.g. Paphavasit et al., 2009; DMCR, 2005). There are some studies from Thailand referring to the assessment of tsunami impacts on coastal forests. Most of them are based on field work, e.g. measurements conducted by the Department of Marine and Coastal Resources (e.g. DMCR, 2005, 2006; DMCR and Thammasat University, 2005) or by UNEP (UNEP, 2005) or the Office of Natural Resources and Environmental Policy and Planning (ONEP) (ONEP, 2005). Some studies focus on the impacts on mangrove forests (Yanagisawa et al., 2009a, b; Paphavasit et al., 2009) and on the role of mangroves acting as natural buffers in mitigating tsunami impacts (Danielsen et al., 2005; Chang et al., 2006; Chatenoux and Peduzzi, 2007; Tanaka et al., 2006).

On a larger spatial scale, remote sensing based studies were conducted in Thailand in order to provide a quick damage assessment: Vu et al. (2007) used a dual-scale approach based on ASTER and IKONOS imagery, while Kouchi and Yamazaki (2007) used a digital elevation model and spectral indices (NDVI, NDWI, NDSI) developed from ASTER pre- and post-tsunami data. Other remote sensing studies refer to specific ecosystems like mangroves: Bahugana et al. (2008) analyse tsunami impacts on coral reefs and mangroves at the Andaman and Nicobar Islands using an unsupervised post-classification approach based on multi-temporal RESOURCESAT and AWiFS data. Damage assessment of mangroves based on SPOT pansharpened imagery has been conducted for Phang-Nga by Deedumchan



Correspondence to: H. Roemer  
(roemer@geographie.uni-kiel.de)

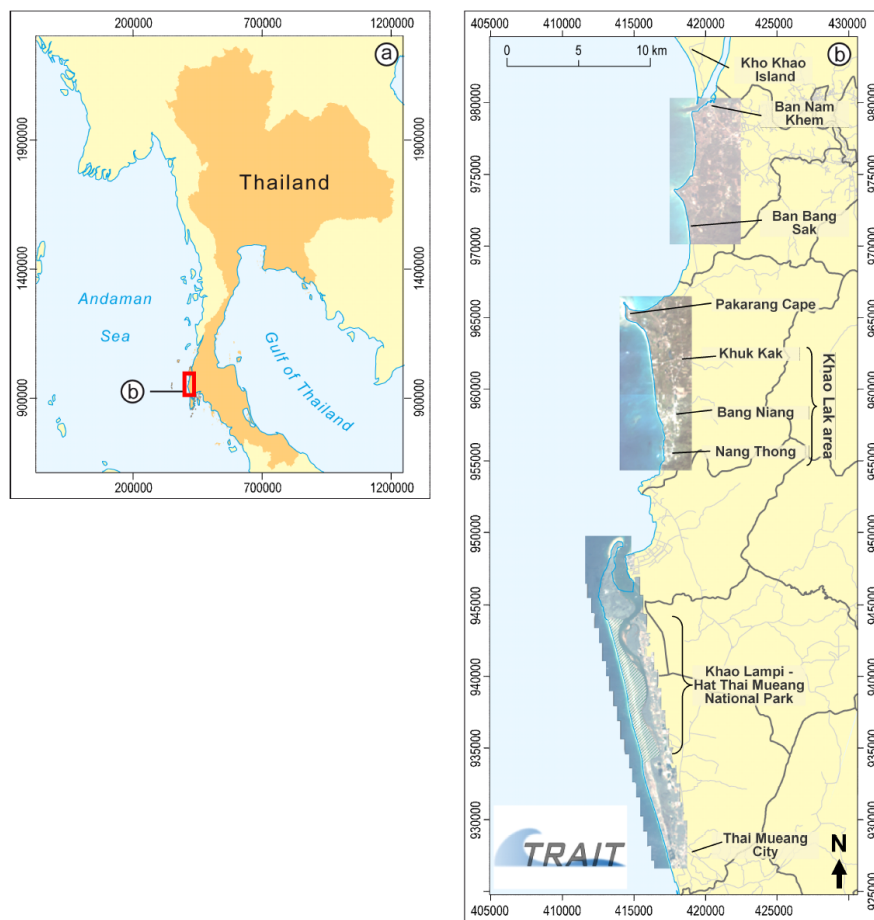


**Fig. 1.** Study area. Satellite images are based on IKONOS multispectral data from 13 January 2003. The administrative units are at the community level (muban).

et al. (2006). It was found that mangroves along the shores were impacted more strongly than those in the inner areas. A combined approach based on change detection techniques (Landsat TM) and GIS proximity analysis was presented by Sirikulchayanon et al. (2008).

In this study, tsunami-related impacts are determined from satellite image analyses for five different coastal forest ecosystems (including mangrove forests, casuarina beach forests, mixed beach forests, melaleuca forest and coconut plantation). Two different change detection techniques (change vector analysis, CVA, and direct multi-date classification, DMC) are compared. Thus, this study contributes to the general need for studies focussing on comparative evaluations of change detection studies (Mas, 1999). DMC (Weissmiller et al., 1977; Mas, 1999) was applied respectively for the red, green and near-infrared bands in the multi-date dataset; the CVA (e.g. Malila, 1980; Johnson, 1994) was

applied for the first two tasseled cap components brightness and greenness, which were calculated from all four multi-spectral bands (Horne, 2003).

The results of this study help to better understand the way coastal forests have been impacted by the tsunami and thus provide a further step for in-depth-assessments of ecological and socio-ecological tsunami sensitivity of the coastal area.

## 2 Study area

The study area (Fig. 1) covers a 50 km long coastal strip in the Phang-Nga province in Thailand from Ban Nam Khem in the north to Thai Mueang city in the south. The area was strongly impacted by the 2004 tsunami: Along the coast between Khao Lak and the northern tip of Kho Khao Island, runup heights were in the range of 5.0 to 10.0 m and the





**Fig. 2.** Coastal forest ecosystems examined in the study (photos taken in January 2009).

inundation varied from 200 m around Ban Bang Sak beach to more than 1.5 km at Pakarang Cape. Run up at Khao Lampi – Hat Thai Mueang National Park (here called as Thai Mueang National Park) was slightly lower, ranging from 3.5 to 6.5 m (Szcucinski et al., 2006; Ioualalen et al., 2007).

The sparsely populated northern part of the study area (8°52'10" N to 8°46'30" N) is dominated by agriculture (rubber, oil palm and coconut plantation, orchards). Further to the south, Khao Lak (the area between 8°44'30" and 8°37'52") represents a young booming tourism community with large hotel complexes scattered near the coast around the touristic villages Khuk Kak, Bang Niang and Nang Thong. The southern part (8°35'15" N to 8°28'28") is located on a peninsula around a tidal inlet and hosts large areas of intact coastal ecosystems like mangroves, beach forests and primary rain forest on the mountainous northern tip of the peninsula. The Thai Mueang National Park covers a main part of this peninsula. The whole study area is interspersed with smaller freshwater ponds resulting from tin mining activities during the last century (Williams et al., 1996; Szcucinski et al., 2006).

The topography of the coastal area is relatively flat, with elevations mostly below 20 m a.s.l. Coasts are predominantly built-up by sand. A sequence of beach ridges occurs in many coastal areas. They are usually up to 2 m high and aligned in parallel to the beach. These ridges often alternate with linear swampy depressions termed swales. Rocky coasts occur

north of Thai Mueang National Park at the northern tip of the peninsula and south of the Khao Lak area (Pajimans, 1976).

Regarding the vegetation characteristics, five coastal forests can be distinguished (Fig. 2): mangrove forests, casuarina beach forests, coconut plantation, mixed beach forest and melaleuca forests. Mangrove forests can be found in different places in the study area, mostly along the river mouths near Thai Mueang National Park. Other river mangroves occur near Ban Nam Khem and Pakarang Cape. The total area of mangrove forests within the tsunami inundation zone was about 108 ha. *Rhizophora apiculata*, *R. mucronata*, *Ceriops tagal*, *Bruguiera* sp. are the dominant species (Yanagisawa et al., 2009a; Phapavasit et al., 2009).

*Casuarina equisetifolia* is a common pioneer (*Ipomoea pes-caprae* formation) in beach ridges and flat environments and forms 20–30 m wide mono-specific stands above the high water-mark on sandy coasts, river mouths and offshore bars (Cochard et al., 2008; Pajimans, 1976; Wong, 2005). The total forest area is 76 ha.

Coconut plantations (*Cocos nucifera*), with a total area of 451 ha, can be found in many places along the coast, especially in the Khao Lak area and near Ban Nam Khem. Being strongly influenced by human interventions, it is not to be considered a natural forest (Kashio, 2005).

Mixed littoral forest (termed mixed beach forest in the following) is located in Thai Mueang National Park covering a total area of 130 ha. The forest is very dense at uniform

**Table 1.** IKONOS band dependent parameters of the scenes acquired on 13 January 2003, 04:11 GMT (pre-tsunami) and 15 January 2005 04:12 GMT (post-tsunami), after Taylor (2009), Geoeye (2006).

IKONOS band ( $\lambda$ )	spectral range (nm)	bandwidth (nm)	resolution (m) nadir/26° off nadir	CalCoef $_{\lambda}^*$ (DN/(mW/cm <sup>2</sup> -sr))
Pan	526–929	403	0.82/1.0	161
Blue	445–516	71.3	3.2/4.0	728
Green	506–595	88.6	3.2/4.0	727
Red	632–698	65.8	3.2/4.0	949
NIR	757–853	95.4	3.2/4.0	843

\* Only for image production date Post 22 February 2001 (coefficients are for the 11-bit products).

canopy height. Typical canopy trees are *Syzigium grande*, *Diospyros* sp., *Shorea* sp., *Lepisanthes rubiginosa*, *Eugenia* sp. The mixed beach forest directly borders to the melaleuca savannah (here called melaleuca forest), which is dominated by *Melaleuca leucadendron*. This widely spaced forest type covers a small area of 42 ha in Thai Mueang National Park.

### 3 Data and methods

The study used multi-date IKONOS images (Table 1) acquired on 13 January 2003 (pre-tsunami) and on 15 January 2005 (post-tsunami). All change detection techniques in this paper were carried out on the multispectral bands with a resolution of about four meters, whereas the higher resolution pan-sharpened data (1 m horizontal resolution) were used for validation purposes.

In order to distinguish between different types of coastal forest, a land use map was created from the pre-tsunami IKONOS image by object oriented image analysis (using Definiens Developer 7.0 software). With a total number of 42 different land use classes, the map provides information on the spatial distribution of mangrove forests, casuarina beach forests, mixed beach forests, melaleuca forest and coconut plantation. The forest polygons were used to reduce the classified pixel quantity from  $2.76 \times 10^7$  to  $5.04 \times 10^5$ .

## 4 Image processing

### 4.1 Pre-processing

Before applying change detection analyses, the digital numbers from IKONOS imagery ( $DN_{\lambda}$ ) were converted into at sensor's aperture radiance values ( $L_{\lambda}$ ), according to the equation (Taylor, 2009):

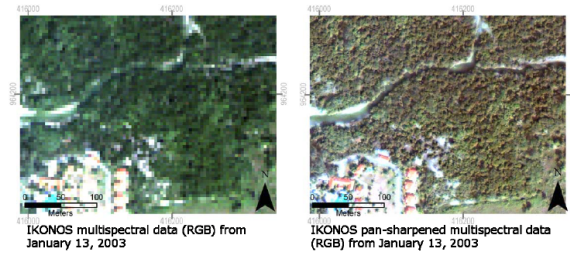


**Fig. 3.** IKONOS pan-sharpening based on the Gram-Schmidt-spectral sharpening technique (northern Khao Lak).

$$L_{\lambda} = \frac{10^4 \cdot DN_{\lambda}}{\text{CalCoef}_{\lambda} \cdot \text{Bandwidth}_{\lambda}}, \quad (1)$$

where,

$DN_{\lambda}$  = digital value for spectral band  $\lambda$ ,

$\text{CalCoef}_{\lambda}$  = Radiometric calibration coefficient (DN/(mW/cm<sup>2</sup>-sr))

$\text{Bandwidth}_{\lambda}$  = Bandwidth of spectral band  $\lambda$  (nm).

Both  $\text{CalCoef}_{\lambda}$  and  $\text{Bandwidth}_{\lambda}$  are given in Table 1.

Geometric correction (co-registration) was carried out by using a set of ground control points from the pre-tsunami scene. The post-tsunami scene was then warped to the base image. The dark object subtraction, one of the simplest and most widely used image-based absolute atmospheric correction approaches, was applied for radiometric correction (Spanner et al., 1990; Ekstrand, 1994).

Image pan-sharpening was applied using the Gram-Schmidt Spectral Sharpening approach (Laben and Brower, 2000). Therewith, the low resolution multispectral data (4 m) were sharpened using the high spatial resolution panchromatic band (1 m). The resulting high-resolution multispectral dataset (Fig. 3) was used to visually select training areas and for identifying appropriate test sites for the accuracy assessment of change classifications.

## 4.2 Change detection

### 4.2.1 Direct multi-date classification

The direct multi-date classification is performed according to the scheme in Fig. 4, starting with the definition of appropriate change classes and training areas.

Pan-sharpened IKONOS imagery as well as several studies on tsunami driven impacts on coastal ecosystems (Yanagisawa et al., 2009a; Phapavasit et al., 2009; Bechteler et al., 2006) revealed that coastal forests were damaged in different ways and intensities. As illustrated in Fig. 5, forest damage patterns were categorized in four major damage classes including (1) no/low damage, (2) direct forest damage, (3) indirect forest damage, and (4) degradation of understory



**Table 2.** Training and test area for DMC.

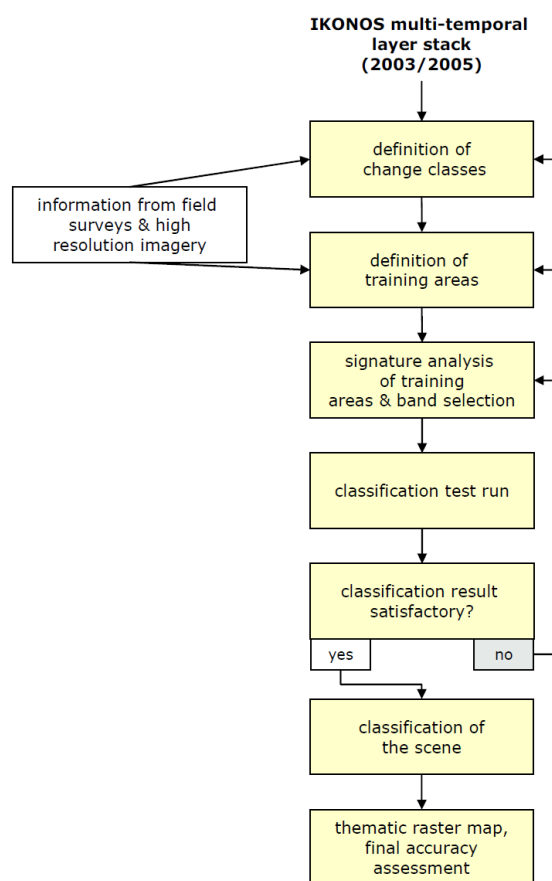
Change classes (ID/name)	Training area N*	Aggregated change classes	Test area N*
1 persistence vegetation	460	no damage	988
2 persistence sand	109		
3 understory vegetation → soil	29	degradation of soils/understory vegetation	59
4 understory → sand/sandy soils	18		
5 understory → water	163		
6 sand → water	97		
7 mud → water	123		
8 soil → sand	97		
9 forest → mud	295	direct forest damage	143
10 forest → sand	330		148
11 forest → water	314		187
12 forest → inclined/roots rem.	80		145
13 yellowing/standing leafless	248	indirect forest damage: yellowing/standing leafless	261

\* = number of pixels (total number of image pixels  $5.04 \times 10^5$  pixels).

vegetation and soils. Direct forest damage is closely related to the kinetic energy of massive water flows caused by the tsunami. Additionally it can be distinguished between a) a total removal of trees (termed as “forest to sand/water/mud”) or b) uprooting or inclination of trees without removal. Indirect tree damage, not affecting the physical structure of stem and branches (Bechteler et al., 2006; Obura and Abdulla, 2005), is understood for trees showing symptoms of toxic and water stress, such as yellowing, drying leaves or defoliation (due to sediment deposition or salt water intrusion). For those areas which are not covered by tree canopies, damage information obtained from satellite images are directly related to changes of soils and understory vegetation. Thus, a new class “degradation of soils/understory” was created. Of course this does not imply that understory vegetation or soils were unaffected in damage classes 2 and 3.

The definition of training and test areas was carried out based on the high resolution pan-sharpened imagery. As illustrated in Table 2, a total of 13 different training classes (6360 pixels) were selected, organized in eight super classes. Test areas (1931 pixel) were selected independently and only for the aggregated super-classes. Since the five forest types have different stand densities (low density in melaleuca forests and coconut plantations) and were impacted in different ways (e.g. direct impacts were rare in mixed beach forests), not all change classes could be selected as training areas in each of the five forest ecosystems. Figure 6 exemplifies the selection of seven different change sub-classes.

Pre- and post-tsunami IKONOS data capture four multi-spectral bands (Table 1). Since not all multispectral bands contain the same information, while adjacent bands in the visual domain are closely correlated (and therefore partly redundant), a preliminary step in image classification involves the definition of optimum multi-spectral band composition.

**Fig. 4.** Flowchart of direct multi-date supervised classification.

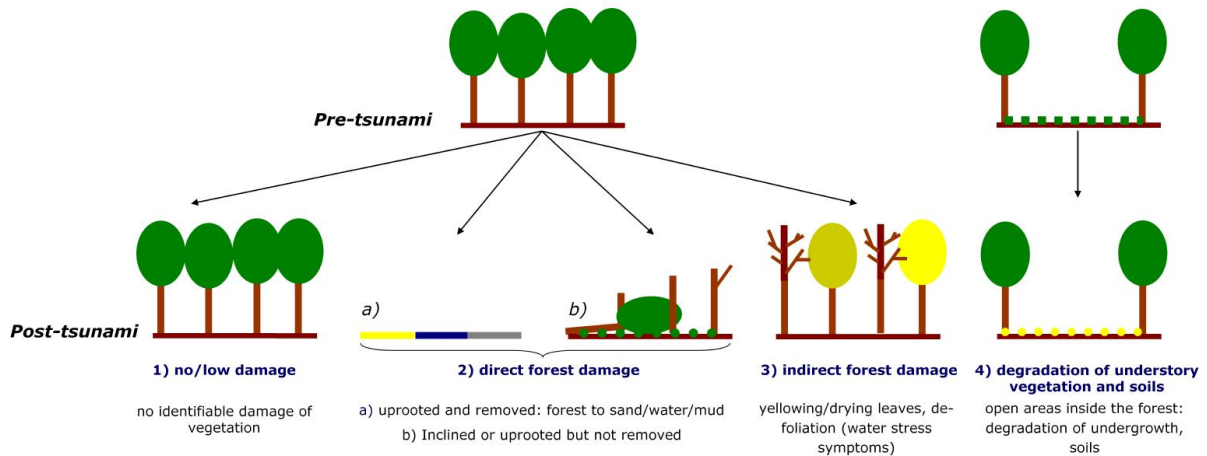


Fig. 5. Categorization of forest damage patterns.

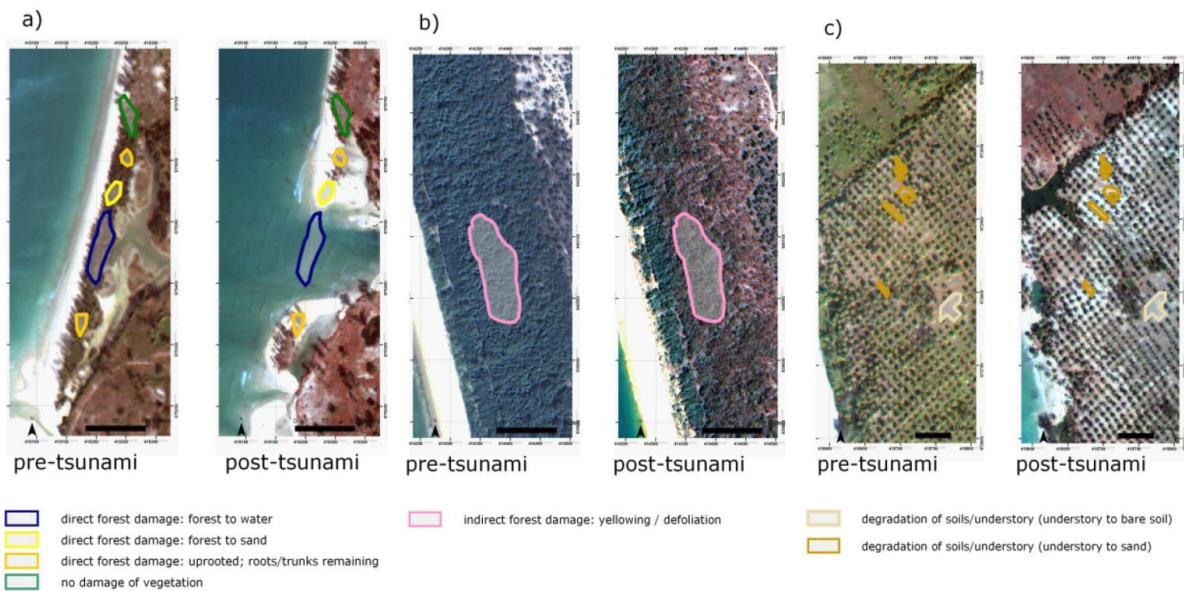


Fig. 6. Selection of training areas exemplified for seven different change classes. (a) casuarina beach forest near Ban Bang Sak, (b) mixed beach forest in Thai Mueang, and (c) coconut plantation near Ban Bang Sak.

Table 3. OIF calculation for multi-date IKONOS imagery.

band composites*	OIF 2003	OIF 2005	mean OIF
1/2/3	16.08	21.66	18.87
1/2/4	43.98	43.74	43.86
1/3/4	44.59	47.64	46.12
2/3/4	49.16	43.57	46.37

\* bands 1–4: 1 = blue, 2 = green, 3 = red, 4 = near infrared.

The Optimum Index Factor (OIF), determined as the ratio of band contrast and band correlation (Chavez et al., 1982) was calculated for both multispectral datasets. High OIF values indicate band combinations with high information content. According to Table 3, the highest values correspond to the composite containing the green, red and near infrared band for the pre-tsunami scene and the blue, red and near infrared band for the post-tsunami scene. In order to avoid using two different three-band combinations for multi-date classification, we used the combination with the highest mean OIF in

**Table 4.** Change class definition based on CVA.

change classes (ID/name)	aggregated change classes	direction (°)/ magnitude	test area n*
1 no damage	no damage	$-\leq 31.49$	988
2 regrowth		$0-90/>31.49$	
3 other	other	$270-360/>31.49$	–
4 sand → water	understory/soils to water	$250-270/>31.49$	150
5 mud → water		$225-250/31.49-46.06$	
6 understory → water		$225-250/>46.06$	
7 forest → water	direct forest damage (forest to water/mud)	$180-225/>46.06$	187
8 forest → mud		$180-225/31.49-46.06$	143
9 degradation	degradation	$90-180/>31.49$	613

= number of pixels (total number of image pixels  $5.04 \times 10^5$  pixels).

both scenes (compare to Table 2). The final band composite for multi-data classification contains the green, red and near-infrared bands in both scenes.

#### 4.2.2 Change Vector Analysis (CVA)

A first step of CVA involves the calculation of the tasseled cap components brightness (TC 1) and greenness (TC 2), in order to reduce the amount of redundant information of digital images to be analyzed (Kauth and Thomas, 1976). This process can be compared to defining a new two-dimensional feature space, in which the multispectral data occupy two new axes associated with biophysical properties in the areas of interest. According to Lorena et al. (2002), the brightness axis is correlated to variations of soil reflectance whereas the greenness axis is associated with amount and vitality of vegetation. Tasseled cap components were calculated for IKONOS multispectral data according to the equations (Horne, 2003):

$$TC\ 1 = 0.326 \cdot x_{blue} + 0.509 \cdot x_{green} + 0.560 \cdot x_{red} + 0.567 \cdot x_{nir},$$

$$TC\ 2 = -0.311 \cdot x_{blue} - 0.356 \cdot x_{green} - 0.325 \cdot x_{red} + 0.819 \cdot x_{nir}, \quad (2)$$

where TC 1 and TC 2 are the tasseled cap components brightness and greenness and  $x$  represents the value of the respective multispectral band. The position variation of the same pixel during different data acquisitions within the two-dimensional space can be determined by the magnitude and direction of the spectral change vectors. The vector's magnitude was calculated using the Euclidean distance between the positions of a pixel within the feature space of different data acquisitions, using the equation:

$$R = \sqrt{(ya - yb)^2 + (xa - xb)^2} \quad (3)$$

where  $R$  is the Euclidean distance,  $ya$  and  $yb$  are the greenness values from January 2005 and January 2003 respec-

tively, and  $xa$  and  $xb$  the brightness values from January 2005 and January 2003, respectively.

The direction or angle of the change vector is determined by the type of occurring change. Due to the fact that only two components are used for CVA, only four major change directions are possible:

- 0–90°: increase in both components,
- 90–180°: increase in brightness, decrease in greenness,
- 180–270°: decrease in both components,
- 270–360°: decrease in brightness and increase in greenness.

Similar to a decision tree classification, the final definition of change classes (Table 4) was carried out by user defined thresholds of direction and magnitude values. Spectral statistics of training areas, computed for the multi-date classification (Sect. 4.2.1), were used for decision support (Fig. 7). The threshold distinguishing between change- and no-change-information (31.49) was defined based on the first standard deviation from the mean magnitude calculated for training class IDs 1 and 2 (Table 2). Another threshold of 46.06 was defined based on 1.5 times the standard deviation of the vector's magnitude.

A differentiation between damage of understory vegetation and damage of forests was restricted to the third quadrant between 180 and 270° of the feature space. Thus, the change class defined in the second quadrant “degradation” contains multiple types of land cover changes as defined in DMC including the class IDs 3, 4, 8, 10, 12, and 13 from Table 2.

Except for the change classes 4–6 (understory/soils to water), the same test areas from DMC could be used again. The test area for the class “degradation” is composed of four different test areas resulting from the change class IDs 3, 4, 8, 10, 12, and 13.

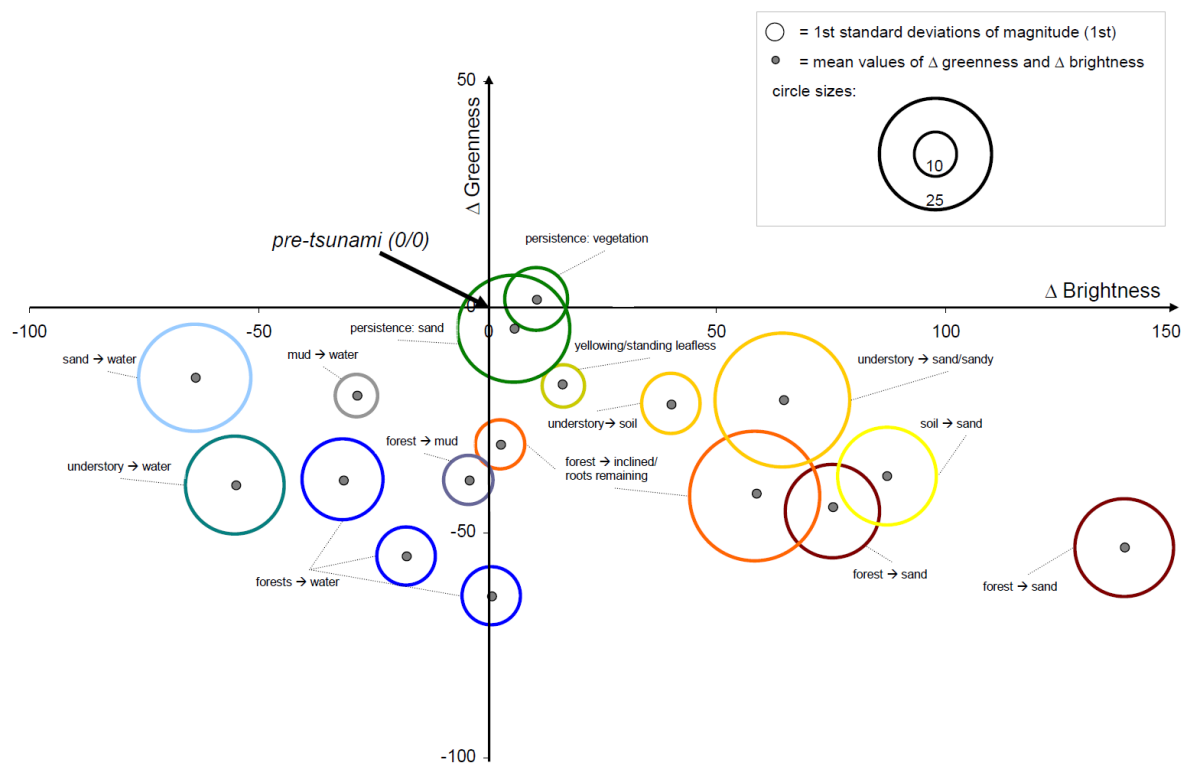


Fig. 7. Training classes from DMC displayed in a two dimensional feature space.

Table 5. Damage statistics (area in %) based on DMC.

damage type	mangrove forests	casuarina beach forest	coconut plantation	mixed beach forest	melaleuca forest
forest → sand	22.67	27.10	21.04	0.35	0.73
forest → water	3.42	4.94	0.88	0.13	0.47
forest → mud	23.37	0.27	0.12	0.48	0.00
forest inclined/roots remaining	4.17	5.67	5.59	0.29	0.02
indirect damage	7.52	1.69	3.52	52.90	21.36
degradation of soils/understory	4.97	13.72	34.24	1.10	15.85
no damage	32.05	45.52	34.58	44.76	61.68
other	0.31	1.08	0.03	0.00	0.00
total area (ha)	107.90	75.90	451.00	130.10	42.20

## 5 Results

### 5.1 Direct multi-date classification

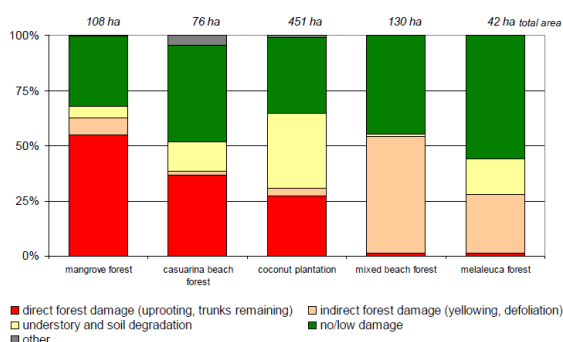
Damage statistics for all the five forest types are illustrated in Table 5 (aggregated, except for direct forest damage) and Fig. 8 (aggregated). It can be concluded that damage patterns vary among the five coastal forest ecosys-

tems: mangroves were the most damaged forest type with a total of 60 ha of forest area directly damaged (change classes 9–12, see Table 2). This relates to 55% of the initial mangrove area located within the inundation zone. Indirect damage, such as drying and yellowing of leaves or defoliation occurred mainly in mixed beach forests and melaleuca forests. These forests types are exclusively located in Thai Mueang National park where wave energy



**Table 6.** Damage statistics based on CVA.

damage type (area in %)	mangrove forests	casuarina beach forest	coconut plantation	mixed beach forest	melaleuca forest
understory/soils → water	0.32	0.35	0.59	0.04	0.33
forest → mud	4.80	0.86	1.0	3.93	0.03
forest → water	23.37	3.13	1.43	3.54	0.03
degradation	33.48	42.7	61.70	7.69	7.01
no damage	38.03	52.71	35.12	84.78	91.61
other	0	0.30	0.16	0.02	1.76
total area (ha)	107.90	75.90	451.00	130.10	42.20

**Fig. 8.** Damage patterns based on direct-multi-date classification.

was relatively low (Ioualalen et al., 2007). Casuarina beach forests were also severely damaged by the tsunami, with 38% of direct damage. Tsunami induced direct damage to coconut plantation is very likely overestimated, due to man made changes which have taken place between image acquisition dates. Damage of understory and soils is maximal in coconut plantation and melaleuca forest, where forest stand densities are usually low. Melaleuca forest was least damaged with approximately 62% of the area classified as “no/low damage” and about 16% as “understory or soil degradation”.

Spatial patterns of forest damage are shown in Fig. 9 for selected subsets. As illustrated in maps (a) and (d), severe damage occurred particularly near the rivers (blue areas). This is very likely related to the higher intensity of the tsunami backwash which was channelled and accelerated in river valleys. In example (e) a sand dune was completely breached. As a consequence, the tin mining pond in the back side of the dune has evolved to a small bay. Indirect tsunami impact on mixed beach forests are concentrated more in the hinterland than near the coast, probably a consequence of the present swales in this area. Another reason could be a change in species composition towards a higher abundance

of salt-intolerant species. The figure also illustrates (c) that melaleuca forests were only slightly affected by the tsunami.

The quality of change detection results was examined based on test areas (N=1931) as described in Table 2. An overall accuracy of 96.4% and a Kappa value of 0.947 indicate very good results. Confusion matrices are shown in Appendix A.

## 5.2 Change vector analysis

Because CVA is based on the combined examination of vector’s magnitude and direction, the isolated examination of both measures, as illustrated in Fig. 10, provide low information on the kind and intensity of forest damage.

Damage statistics derived from CVA are given in Table 6 and Fig. 11 for the aggregated classes. As already pointed out in DMC, 91.61% of the melaleuca forest area has been classified as “no damage”, closely followed by mixed beach forest with 84.5%. From the statistics it can be assumed that coconut plantations are the most damaged and thus most sensitive forest type in this study. Only 35% of the coconut area is classified as “no damage”, followed by mangroves with 38%. But without knowing the relation between understory or soil damage and direct tree damage, any assumptions concerning the actual forest damage are uncertain. Direct forest damage including “forest to water” and “forest to mud” occurred mainly in mangroves (28.17%), followed by mixed beach forest (7.5%) which is neither consistent with visual interpretation of pan-sharpened IKONOS imagery nor with findings from literature.

Spatial patterns of forest damage are shown in Fig. 12 for selected subsets. As pointed out in Fig. 9, severe direct damage to forest trees such as the class “forest to water” particularly occurred near the river mouths (Fig. 12a and e) or near the shore (Fig. 12d). In CVA the class “degradation” includes both, damage to understory vegetation or soils and damage to trees, which complicates the estimation of the damaged forest area. An accuracy assessment was carried out based on five test areas (2081 pixels) as described in Table 4. With

**Damage pattern analysis based on DMC**

- forest->sand
- inclined/trunks remaining
- no/low damage
- understory and soil degradation
- forest->water
- forest->mud
- yellowing, defoliation

- a) mangrove forest
- b) mixed beach forest
- c) melaleuca forest
- d) coconut plantation
- e) casuarina beach forest

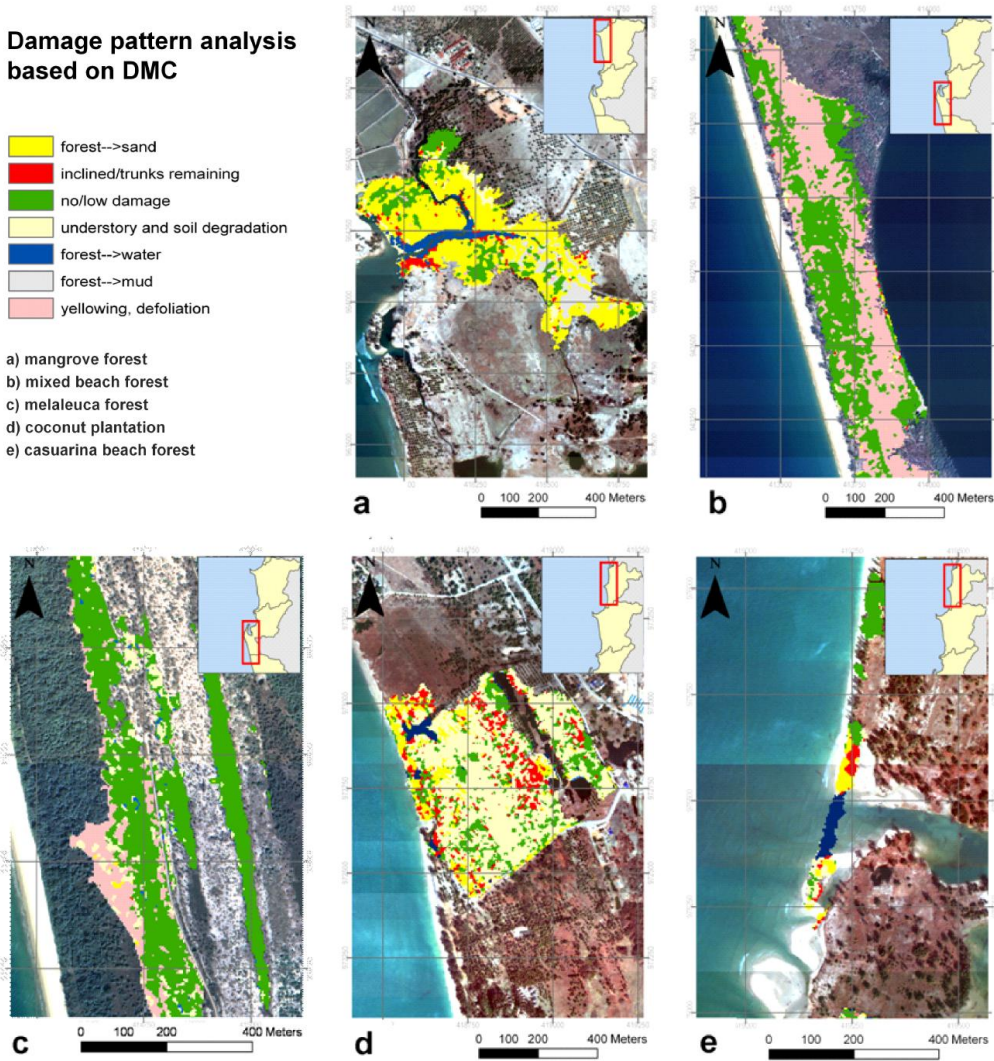


Fig. 9. Change maps based on DMC, illustrated for the five coastal forests in the Phang-Nga province.

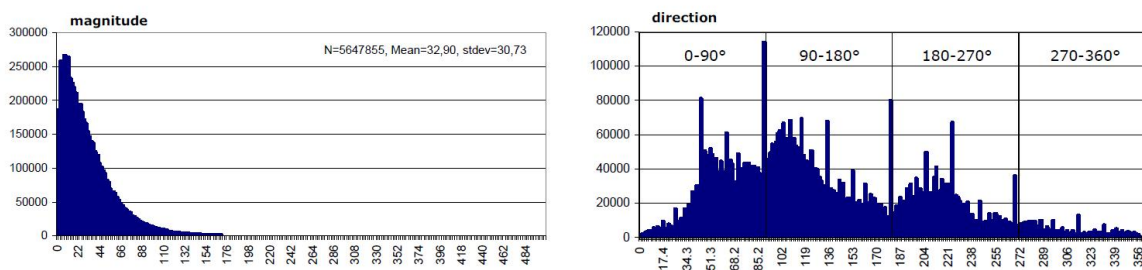


Fig. 10. Frequency distributions of change vector's magnitude and direction.



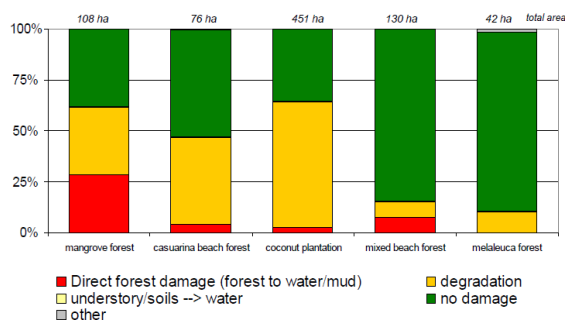


Fig. 11. Damage patterns based on CVA.

an overall accuracy of 68.62% and a Kappa value of 0.61, CVA led to satisfactory to sufficient results. Inaccuracies mainly appear for the class “degradation” (producer accuracy of 43%) where 39% of pixels were incorrectly classified as “no damage”. This becomes clear in Fig. 12b, where large areas which were damaged indirectly by the tsunami (see Fig. 9b) are now classified as “no damage”. Confusion matrices for CVA are listed in Appendix B.

## 6 Discussion

Assessing ecological vulnerability of coastal forests requires a good understanding of the damage caused by the tsunami. Since damage patterns vary in space and are determined by different influencing factors, such as distance to shoreline and rivers, elevation or coast inclination, detailed spatial damage information was derived for the whole coastal area between Ban Nam Khem in the North and Thai Mueang in the South. The two methods applied here showed different results, varying according to accuracy, expenditure of work and usefulness for vulnerability assessment.

### 6.1 Accuracy

As pointed out in Sect. 5, DMC provides much more accurate results than CVA in terms of information content and clearness of the created change classes and the calculated accuracy for the change maps (96.4% for DMC and 68.6% for CVA, respectively). Thus, damage assessment based on DMC is much more precise, especially for low density forests such as coconut plantations. The accuracy of the change detection results was also audited by aggregating change classes in one no-damage class and one damage class (cp. Table 7 and Appendices C and D). Although accuracy measures are closer than in the disaggregated approach in Sect. 5, DMC still provides more accurate results than CVA. It becomes clear that the total damage area is underestimated in CVA. This problem resulted from the difficulty of select-

ing an adequate threshold distinguishing between change- and no-change information, as described in Sect. 4.2.2.

Figure 13 shows that an underestimation of damage particularly occurs for melaleuca forests and mixed beach forest. These forest types have been predominantly damaged only slightly and indirectly.

### 6.2 Expenditure of time and work

Although technical implementation of CVA is easier than DMC, both methods require producer’s expertise in order to correctly interpret change detection results. Disadvantages in DMC involve the problem of considering many different types of change classes during the classification process and the fact that the degree of automation is relatively low. Performing CVA is quicker in the beginning phase, since rough change information can be automatically extracted from the change vector’s magnitude and direction. The challenge here lies in the selection of appropriate change thresholds and further differentiations of change classes (interpretation). Thus, expenditure of time and work is almost the same for both methods with some advantages for CVA.

### 6.3 Transferability and implementation

While being slightly more complex than CVA regarding expenditure of time and work, DMC provides more accurate results and is thus preferable for image based damage analysis. From this work it can be concluded that digital change detection techniques like CVA and DMC allow the estimation of ecological damages and are suited for ecological vulnerability assessment. Moreover it becomes clear that the selection of an adequate change detection technique is a crucial step when using remote sensing techniques to analyse forest damage. The usage of the high resolution IKONOS imagery is appropriate, because accurate spatial information of forest damage can be provided. Especially for the small patches of casuarina forests, it must be expected that the application of medium resolution imagery like ASTER (15 m) or Landsat ETM+ (30 m) would not have led to satisfactory results.

The application of remote sensing and digital change detection induces uncertainties which have to be taken into account when interpreting the results: Due to a lack of in-situ information on land use changes occurring between the first image acquisition date and the tsunami, land cover changes cannot be automatically related to tsunami induced impacts. Especially in the case of coconut plantations, human interventions may have occurred in this period. This problem may lead to an overestimation of the calculated damage area for coconut plantation, as illustrated in Fig. 14. Furthermore, there is a lack of more detailed spatial damage information, which cannot be sufficiently derived from satellite data, such as information on changes in soil conditions or damage information for specific plant species.

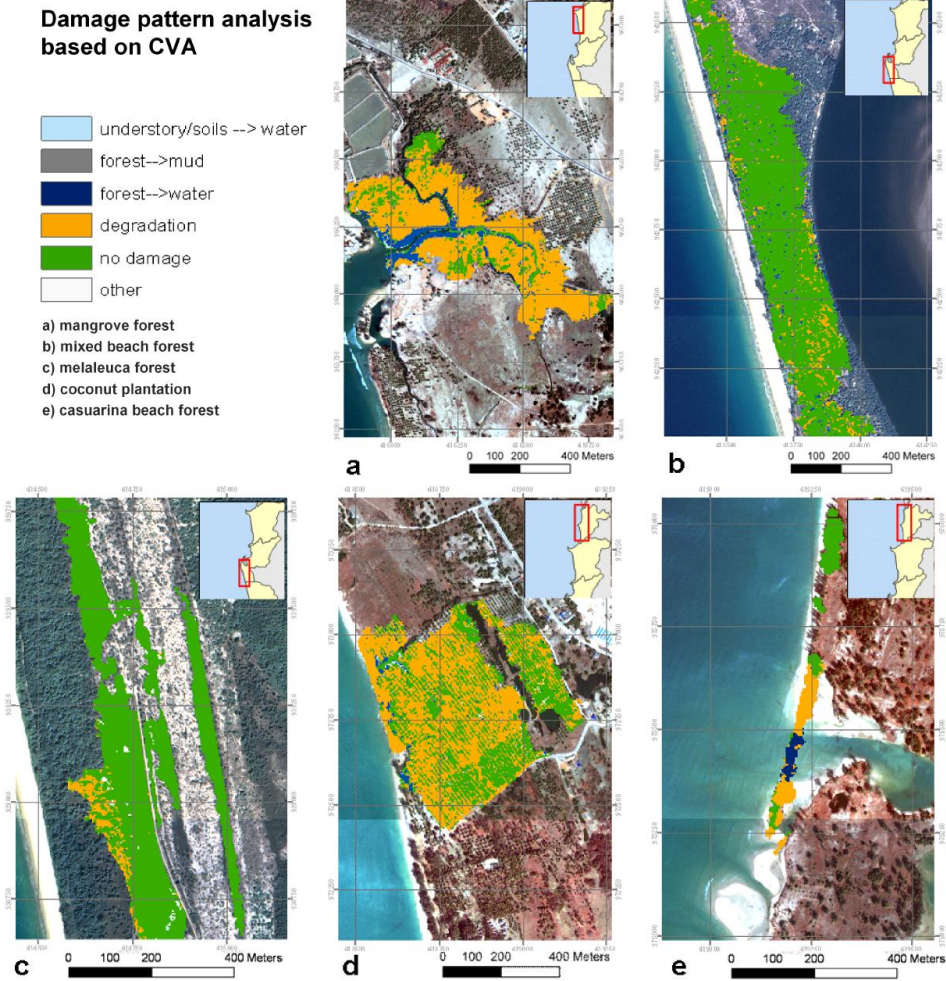


Fig. 12. Change maps based on CVA, illustrated for the five coastal forests in the Phang-Nga province.

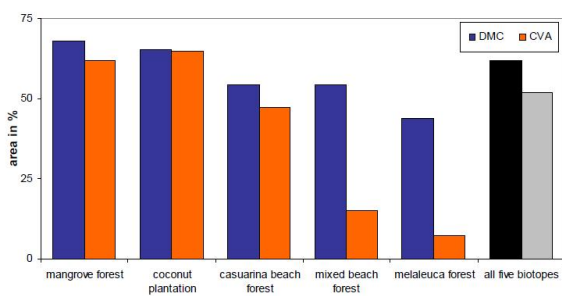
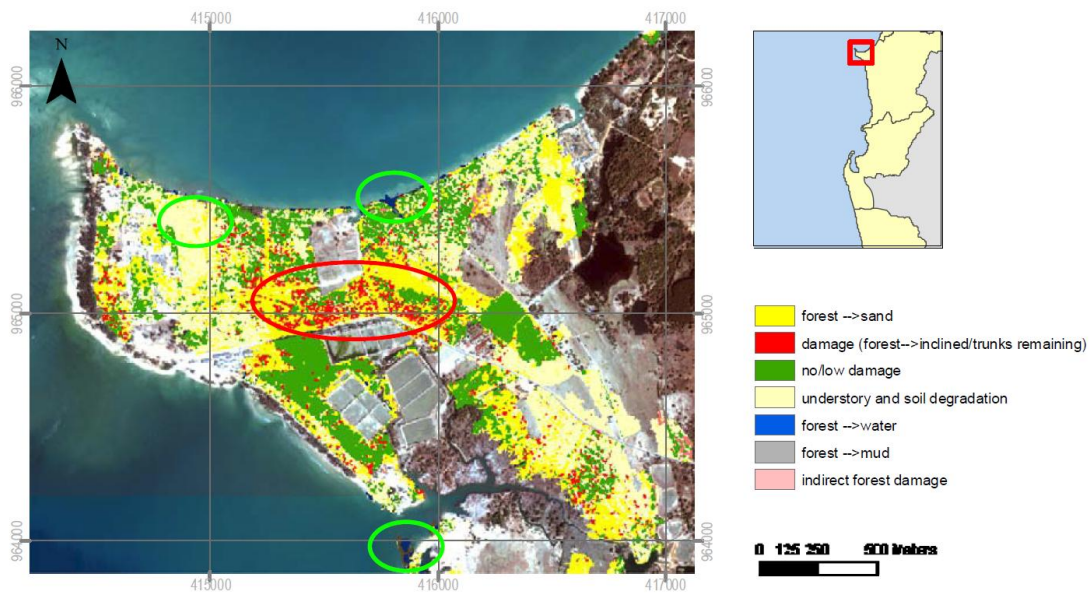


Fig. 13. Estimated damaged area for different forest types based on DMC and CVA.

### 7 Concluding remarks

This paper presents a remote sensing based approach for estimating tsunami induced impacts on coastal forests. The damage maps help to better understand the tsunami impact on coastal forest ecosystems. Additionally they provide valuable information to estimate tsunami sensitivity of coastal forests. It was emphasized that the accuracy of the results provided by digital change detection strongly depends on the respective technique. DMC clearly is the more effective and accurate change detection method, since a complex matrix of change information, so called from-to information, can be provided. For CVA, change information depends heavily on the selection of suitable thresholds (cp. Lu et al., 2004). This analysis showed that there are limitations in both methods, resulting from poor image data availability for the year 2004,





**Fig. 14.** Human induced land use changes versus tsunami induced changes illustrated for coconut plantation near Pakarang Cape (Khao Lak). Change detection results are based on DMC. Human induced land use changes in the hinterland are highlighted in red, whereas tsunami induced changes near the coast are highlighted in green.

**Table 7.** Aggregation of change classes for CVA and DMC.

Method	CVA	DMC
Class ID's*:	4–9/1–2	3–13/1–2
Damage/No damage		
Test area N (pixel):	1093/988	943/988
Damage/No damage		
Area (ha):	417/390	500/307
Damage/No damage		
Area (%):	51.96/48.04	61.96/38.04
Damage/No damage		
Accuracy	86.50/0.73	97.58/0.95
Overall accuracies (%)/ Kappa coefficient		

\* class ID's are taken from Table 2 from DMC and Table 4 for CVA, respectively.

and from the problem that not all of the damage information seen during field observations can easily be detected by digital image analysis. Hence, change detection cannot fully substitute field surveys. The advantages of remote sensing techniques include the possibility of (a) providing spatial information which is particularly necessary for areas difficult to access, (b) analysing processes that already have taken

place, such as the estimation of tsunami impacts on coastal forests, and (c) developing automated, transferable methods. These criteria make remote sensing an effective tool for hazard analysis. Regarding transferability, the change detection techniques from this study can also be applied for the assessment of ecological impacts from other natural or anthropogenic disasters, e.g. earthquakes, volcanic eruptions, hurricanes or tornados. Additionally, if more image data from the following periods are available, the techniques could also be applied for the estimation of long-term tsunami impacts on coastal forests as well as forest recovery.

## Appendix A

## Accuracy assessment DMC.

	Ground truth (Pixels)							total degradation
	forest → sand	forest inclined	forest → water	indirect	forest → mud	no damage	soil/understory degradation	
forest → sand	147	3	1	0	0	0	9	160
forest inclined	1	132	5	0	0	0	0	138
forest → water	0	0	180	0	0	0	0	180
indirect	0	0	0	225	0	0	0	225
forest → mud	0	0	0	0	143	0	0	143
no damage	0	7	0	36	0	984	0	1027
soil/understory degradation	0	3	1	0	0	4	50	58
total	148	145	187	261	143	988	59	1931

	Ground truth (Percent)							total degradation
	forest → sand	forest inclined	forest → water	indirect	forest → mud	no damage	soil/understory degradation	
forest → sand	99.32	2.07	0.53	0.00	0.00	0.00	15.25	13.45
forest inclined	0.68	91.03	2.67	0.00	0.00	0.00	0.00	11.60
forest → water	0.00	0.00	96.26	0.00	0.00	0.00	0.00	15.13
indirect	0.00	0.00	0.00	86.21	0.00	0.00	0.00	18.91
forest → mud	0.00	0.00	0.00	0.00	100.00	0.00	0.00	12.02
no damage	0.00	4.83	0.00	13.79	0.00	99.60	0.00	86.30
soil/understory degradation	0.00	2.07	0.53	0.00	0.00	0.40	84.75	4.87
total	100.00	100.00	100.00	100.00	100.00	100.00	100.00	100.00

Class	Commission (Percent)	Omission (Percent)	Commission (Pixels)	Omission (Pixels)
forest → sand	8.13	0.68	13/160	1/148
forest inclined	4.35	8.97	6/138	13/145
forest → water	0.00	3.74	0/180	7/187
forest → yellowing	0.00	13.79	0/225	36/261
forest → mud	0.00	0.00	0/143	0/143
no damage	4.19	0.40	43/1027	4/988
soil/understory degradation	13.79	15.25	8/58	9/59

Class	Prod. Acc. (Percent)	User Acc. (Percent)	Prod. Acc. (Pixels)	User Acc. (Pixels)
forest → sand	99.32	91.88	147/148	147/160
forest inclined	91.03	95.65	132/145	132/138
forest → water	96.26	100.00	180/187	180/180
forest → yellowing	86.21	100.00	225/261	225/225
forest → mud	100.00	100.00	143/143	143/143
no damage	99.60	95.81	984/988	984/1027
soil/understory degradation	84.75	86.21	50/59	50/58

**Appendix B****Accuracy assessment CVA.**

	Ground truth (Pixels)					
	understory → water/mud	forest → mud	degradation	no/low damage	forest → water	total
understory → water/mud	80	0	0	0	9	89
forest → mud	6	105	74	0	4	189
degradation	15	5	263	8	25	316
no/low damage	8	8	236	980	20	1252
forest → water	41	25	40	0	129	235
total	150	143	613	988	187	2081

	Ground truth (Percent)					
	understory → water/mud	forest → mud	degradation	no/low damage	forest → water	total
understory → water/mud	53.33	0.00	0.00	0.00	4.81	4.28
forest → mud	4.00	73.43	12.07	0.00	2.14	9.08
degradation	10.00	3.50	42.90	0.81	13.37	15.19
no/low damage	5.33	5.59	38.50	99.19	10.70	60.16
forest → water	27.33	17.48	6.53	0.00	68.98	11.29
total	100.00	100.00	100.00	100.00	100.00	100.00

Class	Commission	Omission	Commission	Omission
	(Percent)	(Percent)	(Pixels)	(Pixels)
understory → water/mud	10.11	46.67	9/89	70/150
forest → mud	44.44	26.57	84/189	38/143
degradation	16.77	57.10	53/316	350/613
no/low damage	21.73	0.81	272/1252	8/988
forest → water	45.11	31.02	0/143	58/187

Class	Prod. Acc.	User Acc.	Prod. Acc.	User Acc.
	(Percent)	(Percent)	(Pixels)	(Pixels)
understory → water/mud	53.33	89.89	147/148	147/160
forest → mud	73.43	55.56	132/145	132/138
degradation	42.90	83.23	180/187	180/180
no/low damage	99.19	78.27	225/261	225/225
forest → water	68.98	54.89	143/143	143/143

### Appendix C

#### Confusion matrices DMC (aggregated change classes).

	Ground truth (Pixels)		
	damage	no damage	total
damage	900	4	904
no damage	43	984	1027
total	943	988	1931

	Ground truth (Percent)		
	damage	no damage	total
damage	95.44	0.40	75.71
no damage	4.56	99.59	24.29
total	100.00	100.00	100.00

### Appendix D

#### Confusion matrices CVA (aggregated change classes).

	Ground truth (Pixels)		
	damage	no damage	total
damage	821	8	829
no damage	272	980	1252
total	1093	988	2081

	Ground truth (Percent)		
	damage	no damage	total
damage	75.11	0.81	39.84
no damage	24.89	99.19	60.16
total	100.00	100.00	100.00

*Acknowledgements.* The research presented in this paper builds upon the project “Tsunami Risks, Vulnerability and Resilience in the Phang-Nga Province, Thailand” funded by the German Research Foundation.

Edited by: K.-T. Chang

Reviewed by: two anonymous referees

### References

- Bahugana, A., Nayak, S., and Dam, R.: Impact of the tsunami and earthquake of 26th December 2004 on the vital coastal ecosystems of the Andaman and Nicobar Islands assessed using RESOURCESAT AWiFS data, *Int. J. Appl. Earth Obs.*, 10, 229–237, 2008.
- Bechteler, A., Pilkama, A., Permana, E., Poellath, J., Prasanai, K., Rahaju, S., Pessala, S., and Alam, S. A.: Coastal Zone Management in Southeast Asia. Case: Mangroves and Tsunami effects in Thailand. Report for ME 451: Tropical Forest Landscape Restoration in Southeast Asia, Fifth International Course on Tropical Forest Ecology and Silviculture, Thailand, 30 pp., 2006.
- Chang, S. E., Eeri, M., Adamas, B. J., Alder, J., Berke, P. R., Chuenpagdee, R., Ghosh, S., and Wabnitz, C.: Coastal ecosystems and tsunami protection after the December 2004 Indian Ocean Tsunami, *Earthq. Spectra*, 22, 863–887, 2006.
- Chatenoux, B. and Peduzzi, P.: Impacts from the 2004 Indian Ocean Tsunami: analyzing the potential protecting role of environmental features, *Nat. Hazards*, 40, 209–304, 2007.
- Chavez, P. S. J., Berlin, G. L., and Sowers, L. B.: Statistical methods for selecting Landsat MSS ratios, *J. Appl. Photogr. Eng.*, 8, 23–30, 1982.
- Cochard, R., Ranamukhaarachchi, S. L., Shivakoti, G. P., Shipin, O. V., Edwards, P. J., and Seeland, K. T.: The 2004 tsunami in Aceh and Southern Thailand: A review on coastal ecosystems, wave hazards and vulnerability, *Perspect. Plant. Ecol.*, 10, 3–40, 2008.
- Danielsen, F., Sorensen, M. K., Olwig, M. F., Selvam, V., Parish, F., Burgess, N. D., Hiraishi, T., Karunakaran, V. M., Rasmussen, M. S., Hansen, L. B., Quarto, A., and Suryadiputra, N.: The Asian tsunami: a protective role for vegetation, *Science*, 310, 643 pp., 2005.
- Deeudomchan, K., Potiracha, Y., and Anan, T.: Mangrove change after tsunami in Phang-Nga, Thailand, in: *Proceedings of the 27th Asian Conference on Remote Sensing (ACRS 2006)*, Ulaanbaatar, Mongolia, 1009–1013, 2006.
- Department of Marine and Coastal Resources (DMCR) and Thammasat University: Post tsunami impact on mangrove community and status quo of surrounding community: The case study in the area of Mangrove Resource Development Center, Phang Nga, Department of Marine and Coastal Resources, Ministry of natural Resources and Environment, Bangkok, Thailand, 100 pp., 2005.
- Department of Marine and Coastal Resources (DMCR): Rapid Assessment of the Tsunami Impact on Marine Resources in the Andaman Sea, Thailand, Phuket Marine Biological Center (PMBC), Phuket, Thailand, 76 pp., 2005.
- Department of Marine and Coastal Resources (DMCR): The study on ecosystems and changes of coastal forests affected by the 2004 tsunami, Department of Marine and Coastal Resources, Ministry of natural Resources and Environment, Bangkok, Thailand, 86 pp., 2006.
- Ekstrand, S.: Assessment of forest damage with Landsat TM: Correction for varying forest stand characteristics, *Remote Sens. Environ.*, 47, 291–302, 1994.
- GeoEye: IKONOS Imagery Products Guide Version 1.5, 21 pp., 2006.
- Horne, J. H.: A tasseled cap transformation for IKONOS images, in *Proceedings of the ASPRS Annual Conference*, Anchorage,



- USA, 5–9 May 2003.
- Ioualalen, M., Asavanant, J., Kaewbanjak, N., Grilli, S. T., Kirby, J. T., and Watts, P.: Modelling the 26 December 2004 Indian Ocean tsunami: Case study of impact in Thailand, *J. Geophys. Res.*, 112, C07024, doi:10.1029/2006JC003850, 2007.
- Johnson, R. D.: Change Vector Analysis for disaster assessment: a case study of Hurricane Andrew, *Geocarto International*, 9, 41–45, 1994.
- Kashio, M.: Tsunami impact assessment in mangroves and other coastal forests in the southern Thailand, *FAO Regional Office for Asia and the Pacific, Bangkok, Thailand*, 8 pp., 2005.
- Kauth, R. J. and Thomas, G. S.: Tasseled Cap – a graphic description of the spectral-temporal development of agricultural crops as seen by Landsat, in: *Proceedings of the Machine Processing of Remotely Sensed Data Symposium*, Purdue University, West Lafayette, USA, 1976.
- Kouchi, K. and Yamazaki, F.: Characteristics of Tsunami-Affected Areas in Moderate-Resolution Satellite Images, *IEEE T. Geosci. Remote*, 45, 1650–1657, 2007.
- Laben, C. A. and Brower, B. V.: Process for enhancing the spatial resolution of multispectral imagery using pan-sharpening, *Eastman Kodak Company, Technical Report US Patent #6011875*, 2000.
- Lorena, R. B., Dos Santos, J. R., Shimabukoro, Y. E., Brown, I. F., and Kux, H. J. H.: A Change Vector Analysis technique to monitor land use/land cover in SW Brazilian Amazon: Acre State, in: *Proceedings of the International Society for Photogrammetry and Remote Sensing (ISPRS)*, Denver Co, USA, 8 pp., 10–14 November 2002.
- Lu, D., Mausel, P., Brondizio, E., and Moran, E.: Change detection techniques, *Int. J. Remote Sens.*, 25, 2365–2407, 2004.
- Malila, W. A.: Change Vector Analysis: an approach for detecting forest changes with Landsat, in: *Proceedings of the 6th Annual Symposium on Machine Processing of Remotely Sensed Data*, West Lafayette, USA, 10 pp., 1980.
- Mas, J.-F.: Monitoring land cover changes: a comparison of change detection techniques, *Int. J. Remote Sens.*, 20, 139–152, 1999.
- Obura, D. and Abdulla, A.: Assessment of tsunami impacts on the marine environment of the Seychelles, *International Union for the Conservation of Nature (IUCN) and United Nations Environment Programme (UNEP)*, 22 pp., 2005.
- Office of Natural Resources and Environmental Policy and Planning: 1 Year After Tsunami: Restoration of Thailand's Natural Resources and Environment, *Ministry of Natural Resources and Environment, Bangkok, Thailand*, 128 pp., 2005.
- Pajimans, K.: Part II Vegetation, in: *New Guinea Vegetation, CRISPO*, Canberra, Australia, 81 pp., 1976.
- Paphavasit, N., Aksornkoae, S., and De Silvia, J.: Tsunami Impact on Mangrove Ecosystem, *Thailand Environmental Institute, Nonthaburi, Thailand*, 211 pp., 2009.
- Phongsuwan, N., Yeemin, T., Worachananant, S., Duangsawasdi, M., Chotiyaputta, C., and Comley, J.: Post-tsunami status of coral reefs and other coastal ecosystems in the Andaman Sea coast of Thailand, in: *Status of coral reefs in tsunami-affected countries*, edited by: Wilkinson, C., Souter, D., and Goldberg, J., *Australian Institute of marine Science, Townville, Australia*, 63–78, 2006.
- Sirikulchayanon, P., Sun, W., and Oyana, T. J.: Assessing the impact of the 2004 tsunami on mangroves using remote sensing and GIS techniques, *Int. J. Remote Sens.*, 29, 3553–3576, 2008.
- Spanner, M. A., Pierce, L. L., Peterson, D. L., and Running, S. W.: Remote sensing of temperate coniferous forest leaf area index: the influence of canopy closure, understory vegetation and background reflectance, *Int. J. Remote Sens.*, 11(1), 95–111, 1990.
- Szczuczinski, W., Chaimanee, N., Niedzielski, P., Rachlewicz, G., Saisuttichai, D., Tepsuwan, T., Lorenc, S., and Siepak, J.: Environmental and Geological Impacts of the 26 December 2004 Tsunami in Coastal Zone of Thailand – Overview of Short and Long-Term Effects, *Pol. J. Environ. Stud.*, 15, 793–810, 2006.
- Tanaka, N., Sasaki, Y., Mowjood, M. I. M., Jimadasa, K. B. S. N., and Homchuen, S.: Coastal vegetation structures and their functions in tsunami protection: experience of the recent Indian Ocean tsunami, *Landsc. Ecol. Eng.*, 3, 33–45, 2007.
- Taylor, M.: IKONOS Planetary Reflectance and Mean Solar Exoatmospheric Irradiance, *GeoEye*, 2009.
- United Nations Environment Programme (UNEP): After the Tsunami, *Rapid Environmental Assessment*, Nairobi, Kenya, 140 pp., 2005.
- Vu, T. T., Matsuoka, M., and Yamazaki, F.: Dual-scale approach for detection of tsunami affected areas using optical satellite images, *Int. J. Remote Sens.*, 28, 2995–3011, 2007.
- Weissmiller, A., Kristofs, J., Scholz, K., Anutap, E., and Mommens, A.: Change detection in coastal zone environments, *Photogramm. Eng. Rem. S.*, 43, 1533–1539, 1977.
- Williams, M., Foryce, F., Pajitprapapon, A., and Charoenchaisri, P.: Arsenic contamination in surface drainage and groundwater in part of the southeast Asian tin belt, *Nakhon Si Thammarat Province, southern Thailand*, *Environ. Geol.*, 27, 16–33, 1996.
- Wong, P. P.: Coastal environment of southeast Asia, in *The Physical Geography of Southeast Asia*, edited by: Gupta, A., *Oxford University Press, Oxford, Great Britain*, 16 pp., 2005.
- Yanagisawa, H., Kushimura, S., Goto, K., Miyagi, T., Imamura, F., Ruangrassamee, A., and Tanavud, C.: The reduction effects of mangrove forest on a tsunami based on field surveys at Pakarang Cape, Thailand and numerical analysis, *Estuar. Coast Shelf S.*, 81, 27–37, 2009a.
- Yanagisawa, H., Kushimura, S., Goto, K., Miyagi, T., Imamura, F., Ruangrassamee, A., and Tanavud, C.: Damage to Mangrove Forest by 2004 Tsunami at Pakarang Cape and Namke, Thailand, *Pol. J. Environ. Stud.*, 18, 35–42, 2009b.

## Monitoring post-tsunami vegetation recovery in Phang-Nga province, Thailand – a remote sensing based approach

HANNES RÖMER\*†, JIRAPONG JEEWARONGKAKUL‡, GUNILLA KAISER†, RALF LUDWIG§ and HORST STERR†

† Department of Geography, Christian-Albrechts-Universität zu Kiel, Kiel, Germany

‡ Wetland International –Thailand office, Hat Yai, Thailand

§ Department of Geography, Ludwig-Maximilians-Universität München, Munich, Germany

### Abstract

The December 2004 tsunami strongly impacted coastal ecosystems along the Andaman Sea coast of Thailand. Since intact coastal ecosystems provide many important functions and services for human beings, their recovery is relevant for ecological and socio-ecological tsunami resilience of the coastal area. In this study field measurements and multi-date IKONOS imagery are used to estimate recovery processes of coastal vegetation at the Phang-Nga province coast including casuarina and mangrove forests, coconut plantations, grasslands and for the landscape level, three years after the tsunami. Two change detection algorithms were applied: the calculation of a recovery rate based on multi-temporal TNDVI-images (TNDVI-approach) and a combined approach of Change Vector Analysis (CVA). Although providing different types of information (quantitative for the TNDVI-approach, qualitative for the CVA), both change detection methods are comparable in terms of the results and accuracies. Results show that grasslands and coconut plantation could recover better than mangrove and casuarina forests. In comparison to the mangroves, recovery rates of casuarina forests are higher but the recovery area was found to be smaller. Furthermore the study discusses limitations of applying IKONOS imagery for assessing vegetation recovery on the local scale.

### 1. Introduction

The Indian Ocean Tsunami in 2004 was one of the most devastating natural disasters ever since. Besides the enormous number of fatalities and the massive destruction of settlements and infrastructure, coastal ecosystems were deteriorated or destroyed (e.g. Phongsuwan *et al.* 2006, Szczucinski *et al.* 2006). At the Andaman Sea coast of Thailand, the Phang-Nga province was one of the most severely affected regions. In total 386 ha of mangrove forests were impacted directly by the tsunami, other coastal forests were uprooted or washed away, coral reefs were affected in various ways, and beaches as well as tidal inlets were eroded (e.g. DMCR 2005, Paphavasit *et al.* 2009). Since intact ecosystems provide essential services, e.g. food, livelihood, tourist attractions, protection against shore erosion, natural buffer against tsunami impacts, nursery ground for animals, the knowledge about the recovery of these ecosystems is important to estimate ecological and socio-ecological tsunami vulnerability of the coastal area (Chang *et al.* 2006, Chatenoux and Peduzzi 2007, Danielsen *et al.* 2005, FAO-MOAC 2005, Paphavasit *et al.* 2009, UNEP-WCMC 2006).

In contrast to the numerous studies on short-term impact assessments of coastal vegetation in South-Thailand, there are only few studies focussing on the long-term effects and recovery processes. Field observations conducted in October and November 2005 at mangrove patches near Ban Nam Khem village (Phang-Nga province) and Bang Rong village (Phuket Province) revealed that mangrove forests are resilient to the tsunami since they have continued to serve as habitats, nursery and feeding grounds for numerous mangrove inhabitants (Paphavasit *et al.* 2009). Additionally a high recovery rate of mangroves was predicted. In contrast, other studies on mangroves such as FAO 2005a, FAO 2005b from Thailand and Wibisono and Suryadiputra (2006) from Indonesia reveal that regeneration rates are relatively slow, especially where tsunami-induced changes of habitat characteristics (e.g. sand accumulations on forest floors) have occurred. Fujioka *et al.* (2008) analysed stands and macrobenthic communities in mangrove swamps in Ranong province (Thailand) between September 26, 2003 and November 23, 2006. They concluded that population density and biomass of macrobenthic organism were not affected, but changes in community structure were observed. Regeneration rates of beach forests were reported to be slow (but even faster than for mangrove forests) and that *Casuarina equisetifolia* and *Derris*

\* Corresponding author. Email address: roemer@geographie.uni-kiel.de

Regeneration rates of beach forests were reported to be slow (but even faster than for mangrove forests) and that *Casuarina equisetifolia* and *Derris indica* could do well in competition with other tree species (Wibisono and Suryadiputra 2006, FAO 2005a, FAO 2005b). Hayasaka *et al.* (2009) pointed out that in spite of an invasion of forest floors by originally non-sandy beach species, sandy beach and maritime forests will recover their previous community composition. With regard to herbaceous vegetation, photos and field observations carried out on February 2006 in Phang-Nga and Phuket provinces indicate that most of the vascular plants reoccupied the previous areas (Szcucinski *et al.* 2006).

Remote sensing techniques are a widely used tool for monitoring recovery processes on a larger spatial scale, but there is still a lack of detailed studies referring to the 2004 Tsunami event. Common applications are post-fire recovery assessments, like Sriboonpong *et al.* (2001) using LANDSAT TM, GIS and field data in Mae Wong National park in Thailand or Mitri and Gitas (2010) applying object-oriented image analysis based on Earth Observing-1 (EO-1) Hyperion imagery. Post-earthquake vegetation recovery at the Jou-Jou Mountain landslide area in Taiwan was assessed by Lin *et al.* (2004) with NDVI derived from SPOT imagery. The analysis of the response of vegetation to climate changes or variations represents another field of applications of remotely sensed data, such as Washington-Allen *et al.* (2008) using mean-variance analysis and vegetation image differencing techniques based on LANDSAT imagery to assess vegetation dynamics during the severe 1982–1984 El Niño-induced drought in Bolivia. Studies based on NDVI temporal series from NOAA-AVHRR images (e.g. Simoniello *et al.* 2008, Vicente-Serrano *et al.* 2005) integrate a huge number of time steps allowing complex temporal analyses, but with limitations in the spatial resolution.

It can be concluded that there is still a lack of spatial information on the recovery processes of coastal vegetation formations for the tsunami impacted coastal areas in Phang-Nga province. In this study vegetation recovery will be estimated spatially for mangrove and casuarina forests, coconut plantations, grasslands and mixed vegetation cover and thus helps to understand the way coastal ecosystems could recover after the tsunami. Additionally the results contribute to the estimation of ecological tsunami resilience as well as the social-ecological dimension of tsunami vulnerability.

High-resolution satellite imagery based on IKONOS from the years 2003, 2005 and 2008 will be used for multi-temporal image analysis. By comparing two different change detection techniques this study also contributes to the general need for studies focussing on comparative evaluations of change detection studies (Mas 1999). The first change detection technique involves the calculation of the rate of recovery (%) from multi-date TNDVI images (Washington-Allen *et al.* 2008), the second method involves a modified change vector analysis (CVA) applied for the first two tasselled-cap components brightness and greenness (Horne 2003, Johnson 1994, Malila 1980). Ground truth measurements, conducted between January and March 2009, were used to compare, validate and interpret change detection results, as well as to identify the potentials and limitations in the remote sensing based approach.

## 2. Study area

The study area (figure 1) covers a 26 km long coastal strip in Phang-Nga province in Thailand from Ban Nam Khem in the north to Nang Thong city in the south. The area was strongly impacted by the 2004 tsunami with peak tsunami run-up heights of 12-14 m above sea level for Khao Lak and 8-9 m for Ban Nam Khem (Bell *et al.* 2004). The maximum horizontal penetration of the tsunami from the shoreline varied from 200 m around Ban Bang Sak beach to more than 1.5 km at Pakarang Cape (ZKI 2005, Szcucinski *et al.* 2006).

The northern part of the study area (8° 52' 10" N to 8° 46' 30" N) is dominated by agricultural land dominated by coconut plantations located near the shoreline as well as rubber and oil palm plantations further in the hinterland. Except the small fishing village of Ban Nam Khem, this area is sparsely populated. Khao Lak (between 8° 44' 30" N and 8° 37' 52" N) represents a young booming tourism resort with large hotel complexes scattered near the coast around the tourism villages Khuk Kak, Bang Niang and Nang Thong. The coastal low land between the villages is dominated by coconut plantations.

The study area is interspersed with smaller freshwater ponds resulting from tin mining activities from the last century (Williams *et al.* 1996, Szcucinski *et al.* 2006). The topography of the coastal area is relatively flat with elevations mostly below 20 m. Coasts are predominantly built-up by sand. A sequence of beach ridges occurs in many areas near the coasts. They are usually up to 2 m high and aligned parallel to the beach.



These ridges are often interspersed by linear swampy depressions termed swales. Rocky coasts occur only in the southern end of the study area (Pajimans 1976). Regarding the coastal vegetation characteristics, three types of coastal forests can be distinguished: mangrove forests, casuarina forests and coconut plantations. Mangrove forests can be found at four different sites throughout the study area with a size of 64 ha in total within the tsunami inundation area.

Whereas two patches (near Khuk Kak and near Krang Nui Cape) are located behind beach ridges systems of four meters in height, the others are located more exposed to the shore near river mouths (east of Ban Nam Khem and near Cape Pakarang). *Rhizophora apiculata*, *R. mucronata*, *Ceriops tagal* *Bruguiera* sp. are the dominant species (Yanagisawa *et al.* 2009, Phapavasit *et al.* 2009). Casuarina forests form a 40-50 m wide and 17 km long coastal stripe throughout the study area and are mostly pure stands of *Casuarina equisetifolia*. This species makes up the landward edge of the *pes-caprae* formation (named after *Ipomoea pes-caprae*) (Whitten *et al.* 1997) being a common pioneer in beach ridges and flat environment. The total forest area in the study area is 69 ha. Coconut plantations (*Cocos nucifera*) cover larger areas throughout the coastal plains with a total of 408 ha. Since being strongly influenced by human interventions, it cannot be considered as a natural forest. In natural environments *Cocos nucifera* belongs to the *Barringtonia* formation (named after *Barringtonia asiatica*) which usually occurs behind the *pes-caprae* formation (Whitten *et al.* 1997). Grasslands (mainly *Poaceae* family) occur in the entire area (463 ha) and according to Corlett (2008) are very likely the result of human impacts like clearance for agriculture or logging for timber. Additionally their occurrence is related to the former tin mining activities which negatively influenced soil conditions (Donner 1989, Szczucinski *et al.* 2006). In order to assess the landscape's response to the tsunami-driven impacts, a fifth vegetation class was introduced and termed as mixed vegetation cover. This class contains all types of vegetation occurring in the study area including all kinds of woodland (39%), grasslands (30%), tree plantations (26%) and scrublands and savannah (5%). Mixed vegetation cover also includes the other four vegetation formations as mentioned before. The total area is 17.3 km<sup>2</sup>.

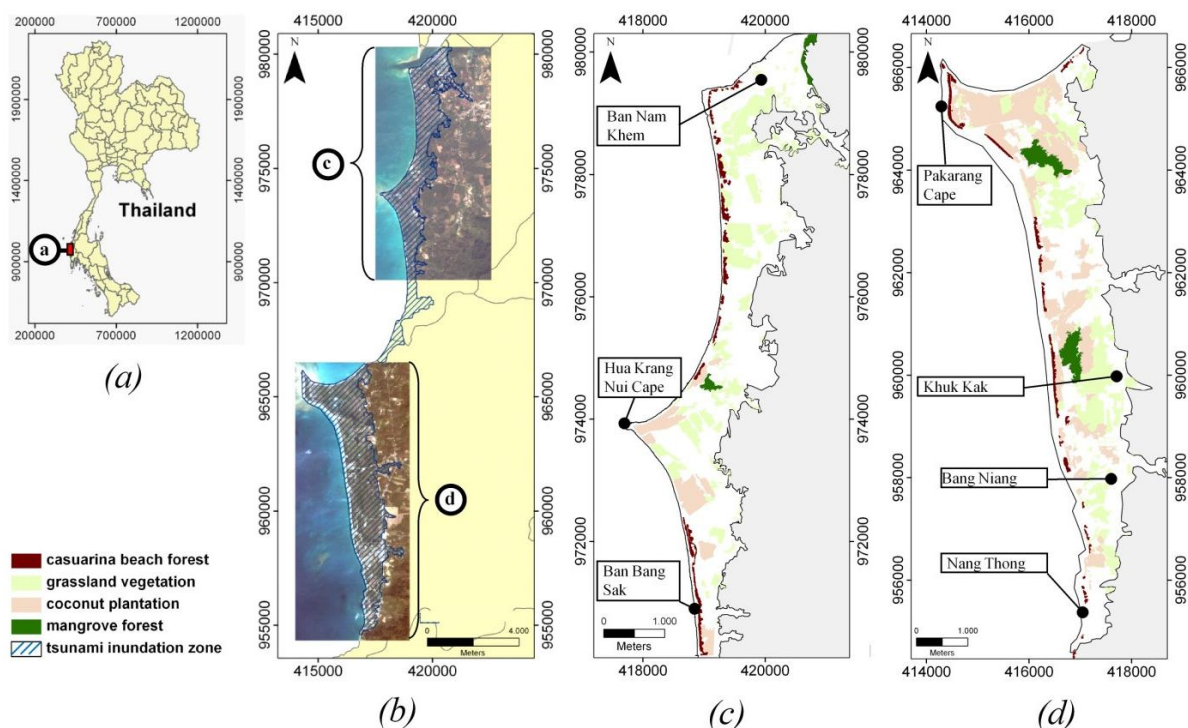


**Figure 1.** (a) the location of the study area in South Thailand, (b) the extents of IKONOS multispectral images (from January 2003), (c, d) the locations of the vegetation types (except mixed vegetation cover) examined in this study.

### 3. Methodology

#### 3.1 Remote sensing data and pre-processing

Three IKONOS scenes were selected to be used for this study, covering two coastal regions at the Andaman Sea coast of Thailand: a northern part (52 km<sup>2</sup>) between Ban Nam Khem and Ban Bang Sak and a southern part (59 km<sup>2</sup>) between Pakarang Cape and Nang Thong (figure 1). The three image dates are January 13, 2003, January 15, 2005 and February 20, 2008 covering dates before and after the tsunami.

IKONOS imagery was acquired from the Centre of Remote Sensing and Processing (CRISP) in Singapore and Spatial Dimension Solutions (SDS) in Bangkok (Thailand). In order to get a cartographic uniformity in all IKONOS scenes, geometric correction (co- registration) was carried out by using a set of ground control points from the pre-tsunami scene. The post-tsunami scenes were then warped to the base image. According to Taylor (2009), radiances at the sensor's aperture (W/m<sup>2</sup>/μm/sr) were obtained from IKONOS image products based on the band specific radiometric calibration coefficient and the bandwidth of the spectral band. The dark object subtraction, one of the simplest and most widely used image-based absolute atmospheric correction approaches, was used to minimize the noise due to atmospheric effects on satellite radiance and calibrate at-sensor radiance to scaled surface reflectance. Additionally, image pan-sharpening was applied using the Gram-Schmidt Spectral Sharpening approach (Laben and Brower 2000). Therewith, the low resolution multispectral data (4 m) were sharpened using the high spatial resolution panchromatic band (1 m). The resulting high-resolution multispectral dataset was used for visual image interpretation in order to locate appropriate study sites for the field campaign as well as to select test and training pixels for the digital change detection. After geometric, radiometric and atmospheric corrections, IKONOS scenes were masked out by the study area boundary in three steps: First, all non vegetated areas such as clouds, shadows, water and barren surfaces were masked out with an available land-use map which was created based on object-oriented image classification of the pre-tsunami IKONOS scene (Roemer *et al.* 2010). Second, only areas within the tsunami damage area were included in the study (ZKI 2005). The resulting number of pixels after masking was  $1.08 \cdot 10^6$  equating to the area of the mixed vegetation class (section 2).

#### 3.2 Digital change detection

##### 3.2.1 Calculation of the rate of recovery multi-temporal TNDVI images (TNDVI-approach)

The first change detection procedure is based on the calculation of three vegetation indices from 2003, 2005 and 2008 (here termed as TNDVI approach). The normalized difference vegetation index, which is a very common measure for describing spatial and temporal vegetation dynamics (Senay and Elliot 2000, Simoniello *et al.* 2008), was transformed as follows (Washington-Allen *et al.* 2008):

$$TNDVI = 50 \times (NDVI + 1) \quad (1)$$

where *TNDVI* is the transformed normalized vegetation index. Vegetation recovery was estimated based on the vegetation recovery rate, modified after Lin *et al.* (2004):

$$R = \frac{(TNDVI_{2008} - TNDVI_{2005})}{(TNDVI_{2003} - TNDVI_{2005})} \times 100 \quad (2)$$

where *R* is the vegetation recovery rate (%), *TNDVI*<sub>2008</sub>, *TNDVI*<sub>2005</sub> and *TNDVI*<sub>2003</sub> are the *TNDVI* values of the current (2008), post-tsunami (2005) and pre-tsunami (2003) scenes. In contrast to other possible recovery, e.g. the difference or ratio between *TNDVI*<sub>0</sub> and *TNDVI*<sub>*t*</sub>, this measure is robust against the scale of the vegetation index itself. Since *R* is strongly related with the impact (denominator), *R* would also be high, if the impact is negligible and approaches zero.



To overcome this problem complicating the interpretation of results, an impact threshold value distinguishing between impacted and non-impacted areas was selected. Different thresholds based on the standard deviation from the mean difference were tested and evaluated (compare Lu *et al.* 2004). For this, a set ( $N = 569$ ) of approved training pixels which were visually selected from the pan-sharpened IKONOS scenes of 2003 and 2005 were used. The threshold value selected was 62.2 corresponding to the 1.5 standard deviation from the mean difference of the training pixels (for more details please see Roemer *et al.* 2010). R was then calculated for areas exceeding this threshold ( $N = 724\,000$ ).

In order to compare the results and accuracies of both change detection methods, R was classified in two classes separating recovery from non-recovery pixels. The same threshold selection method as for the impact threshold was applied, but based on the later two images from 2005 and 2008. Only areas which were impacted first but did not recover (e.g. barren areas which still persist during both acquisition dates), were used for threshold definition. The recovery threshold of 41.2 (first standard deviation from mean) was defined based on 6573 training pixels.

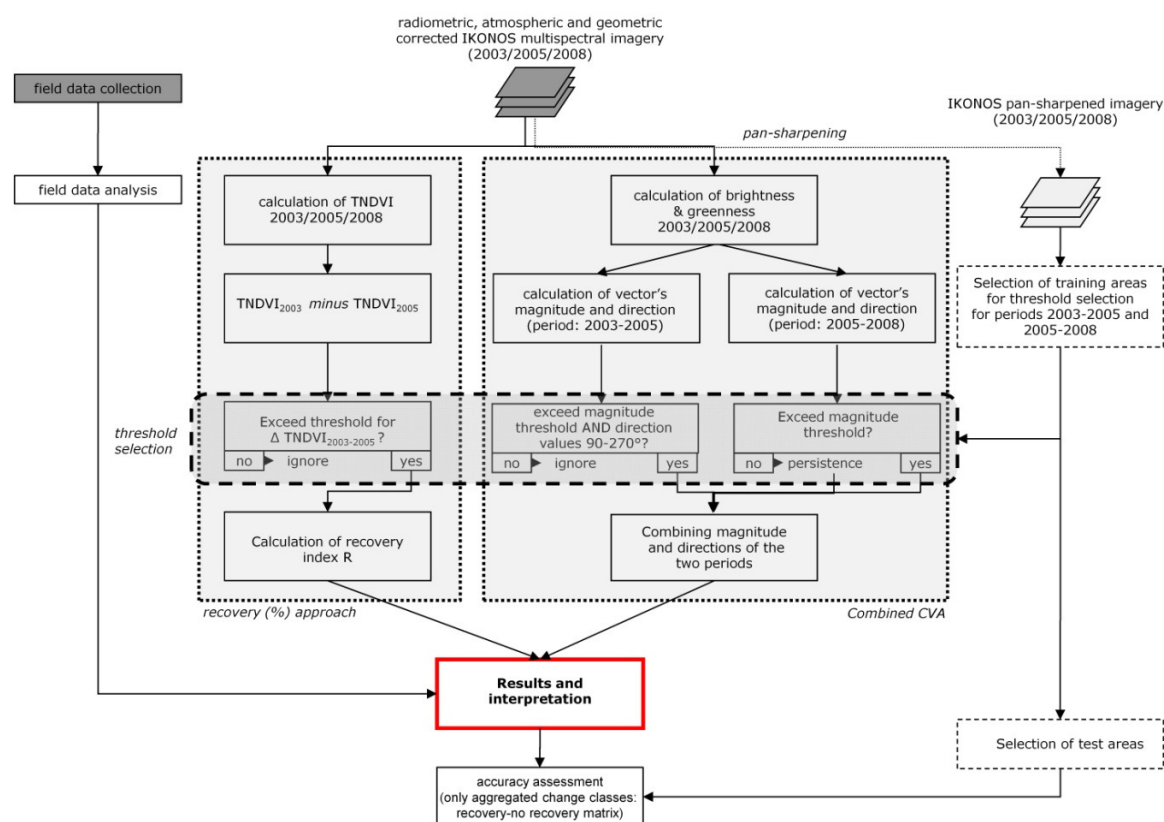


**Figure 2.** Flowchart illustrating the combined use of change detection and field data.

### 3.2.2 Change vector analysis (CVA)

CVA was applied using the tasselled cap components brightness (TC 1) and greenness (TC 2) as biophysical parameters (figure 2). The tasselled cap transformation rotates the IKONOS data such that according to Horne (2003) approximately 98% of the total variability is expressed in the first two components (TC 1 and TC 2), where TC 1 is correlated to variations of soil reflectance and the TC 2 is associated with amount and vitality of vegetation (Lorena *et al.* 2002). Tasselled cap components were calculated for the three multi-spectral data sets using the equations derived by Horne (2003).



The position variation of the same pixel during different data acquisitions within the two-dimensional space can be determined by the magnitude and direction of the spectral change vectors. Vector's magnitude and direction value were calculated twice in this study, first for the period between the first two acquisition dates (here termed as first period) and second for the period between the later two dates (here termed as second period). Magnitude is defined as the Euclidean distance between the positions of a pixel within the feature space of different data acquisitions, according to the Pythagorean theorem:

$$M = \sqrt{(ya - yb)^2 + (xa - xb)^2} \quad (3)$$

where  $M$  is the Euclidean distance,  $ya$  and  $xa$  are the greenness and brightness values of the earlier scene, respectively  $yb$  and  $xb$  for those of the later scene. Magnitude thresholds were determined for both magnitude images to separate change from no-change pixels. The first magnitude threshold (31.49) was defined based on the first standard deviation from the mean magnitude value, calculated for the same training areas as described in section 3.2.1 ( $N = 569$ ). The second magnitude threshold of 18.42 is based on the 0.5 standard deviation calculated for the same set of training pixels ( $N = 6\,573$ ) selected from the later two scenes (section 3.2.1).

The direction or angle of the change vector is determined by the type of the occurring change. Four change directions were extracted for each time period: quadrant I ( $0-90^\circ$ ) and quadrant III ( $180-270^\circ$ ) with an increase respectively a decrease in both components, quadrant II ( $90-180^\circ$ ) with an increase in brightness and a decrease in greenness and quadrant IV ( $270-360^\circ$ ) with a decrease in brightness and an increase in greenness. In order to estimate vegetation recovery, a combined examination of both direction and magnitude images was carried out (figure 2). Regarding the change vector derived from the first period, only pixels falling in the second and third quadrants and exceeding the magnitude threshold were masked out for further examinations. According to Roemer *et al.* (2010), direction values in the second and third quadrants are closely related to possible tsunami impacts, whereas angles between  $90$  and  $180^\circ$  are related to degradation of understory and woody vegetation and angles between  $180$  and  $270^\circ$  are associated to inundation processes resulting from intense erosion processes. Regarding the second period, areas not exceeding the magnitude threshold were classified as persistence (T). Cross-tabulating the two directions from the first with the five change classes (four quadrants and the persistence class) of the second period, a new change matrix was created containing ten possible change classes.

In order to relate these classes to real land use changes and recovery paths, pan-sharpened image trios from the three acquisition dates, as well as ground truth observations were analyzed and interpreted. Figure 3 illustrates the process of defining change classes, exemplified for the five most important classes, i.e. 92% of the entire area. Table 1 contains all change classes, including their frequency, calculated for the mixed vegetation cover class: The last two change classes (quadrant combinations II/III – T) were defined as persistence classes, since magnitude values for the second time period did not exceed the threshold (figure 2). Seldom quadrant combinations III – II and III-III (0.4% of the total area) could not clearly be related to specific land use changes and thus were ignored in this study. The most frequent combination II – IV (74.5% of the total area) was defined as *recovery* since degradation processes were followed by growth of vegetation (figure 3a). The quadrant combination II – I (figure 3b) represents areas of intense degradation processes (barren surfaces on the post-tsunami scene of 2005) followed by an increase in soil brightness which is often related with sedimentation of sandy sediments or erosion and clearing. This combination was termed as *persistence*. The quadrant combination III- I is related with accumulations of new sediments or vegetation growth in areas which were inundated in 2005 (figure 3c). Since an accumulation and recovery of sediments is a requirement for any further succession process of vegetation, this class was considered as *recovery*. Consequently, if degraded but terrestrial areas turned to water (or wet muddy soils) during the second period (combination II – III, figure 3d), this combination was termed as *degradation*. This applies also to the combination II – II, where degraded vegetation (e.g. remaining roots, defoliated trees) turned to barren areas during the second period (figure 3e). The combination III – IV is defined as persistence, but land-use changes show different patterns, for instance the transition of darker (muddy) to brighter soils or from darker to brighter (more cloudy or shallow) water. Finally, only diagonal quadrant pairs were considered as recovery paths, were the change vector rotates about  $180$  degrees in the two-dimensional feature space.

7 H. Roemer et al.: Monitoring post-tsunami vegetation recovery in Phang-Nga province, Thailand – a remote sensing based approach

**Table 1.** Definition of land use changes and recovery paths based on combined CVA.

Quadrant combination	Description	Class	Mixed vegetation cover	
			<i>N</i>	%
2003/2005 – 2005/2008				
II – I	<i>degradation of vegetation followed by:</i> - sand accumulation/increase of soil brightness - degradation - inundation/mud - growth	persistence degradation degradation recovery	50518	7.0
II – II			11781	1.6
II – III			31577	4.4
II – IV			534929	74.5
III – I	<i>first: inundation/mud, followed by:</i> - sediment accumulation or growth - unspecific (negligible) - inundation/mud (negligible) - no land-use changes, but unspecific	recovery ignore ignore persistence	32148	4.5
III – II			1454	0.2
III – III			1685	0.2
III – IV			9298	1.3
II – T* III – T*	<i>first: either vegetation to sand/barren or vegetation to mud/water, followed by:</i> persistence	persistence	44977	6.3

\* all four quadrants possible but magnitude values did not exceed magnitude threshold

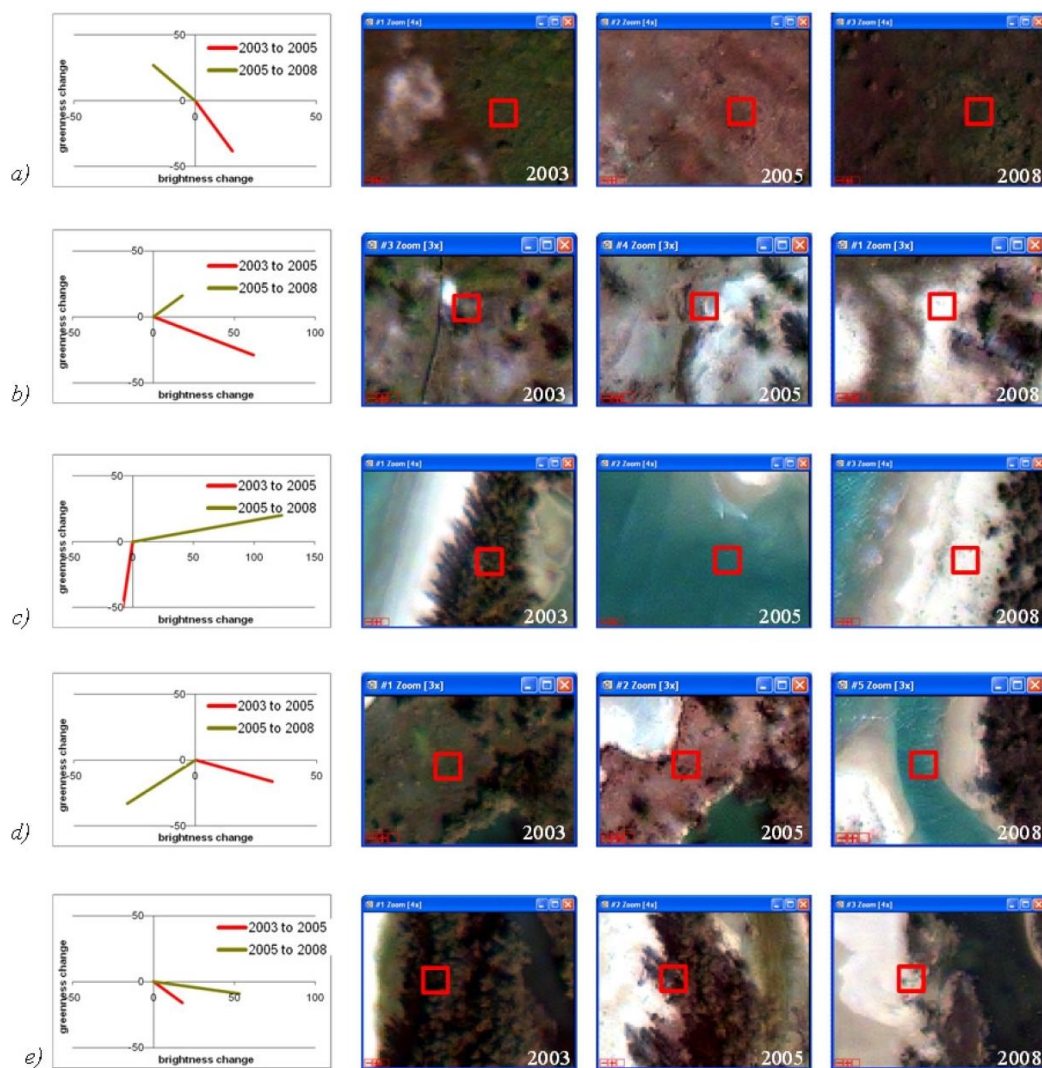


**Figure 3.** Change vectors calculated for both time periods (left) and land use changes detected from multi-date pan-sharpened image trios (right). (a) degradation followed by growth, (b) degradation followed by an increase of soil brightness, (c) inundation followed by sand accumulation, (d) degradation followed by inundation and (e) degradation followed by degradation (progressive degradation).



### 3.3 Field data collection and data analysis

Field data were collected between January and March 2009 in order to provide ground truth data for the change detection study. One aim of the field data collection was to provide quantitative measures of vegetation recovery which can be related directly to the change detection results and are thus used for validation purposes. Furthermore, qualitative aspects on the recovery processes were collected in order to better understand the processes of vegetation recovery and thus to better interpret the results of the change detection study.

The main approach of the field study was to observe the recovering vegetation after the tsunami. Here, high-resolution pan-sharpened IKONOS imagery of the three acquisition dates as well as hand GPS-devices were used in the field to locate areas that were intensively impacted by the tsunami. Thus, the observed succession processes could be traced back to the tsunami event. A nested sampling strategy was applied to each study site (15 x 15m) and plot (five plots per site at 5 x 5 m).

For the plot selection, the study site was divided into nine equal sized squares (5 x 5m) whereas only the centre-plot as well as the four corner-plots (NE, NW, SE, SW) were chosen. This pattern was applied in order to reduce the total area needed for the quantitative measurements and to allow a representative and even distribution of plots within the sites. From the 27 study sites which are covered by the IKONOS scenes, eleven sites were observed in former casuarina forests (termed as casuarina sites), ten in mangrove forests (mangrove sites) and six in coconut plantations (coconut sites). Except for the sites 10 and 25, where tsunami impacts were almost absent (reference sites), most of the former vegetation within the study sites were completely removed by the tsunami event. The recovery process was quantitatively assessed by analysing the seedlings and saplings occurring in a study site. At each plot, all individual seedlings/saplings were counted, identified by species and measured for diameter at knee height (DKH) and total height (H). Although the diameter at breast height (DBH) is the more common method for trunk measurements, the knee height at 0.5 m was used, since many saplings in mangrove forests did not exceed total tree heights of 1.0 meters (Otieno *et al.* 1991, Theron *et al.* 2004). With these parameters, vegetation stand properties were calculated for each study site, representing the recovery or successional rate of the respective forest type (compare Lu *et al.* 2003):

$$1. \text{ Average stand diameter (ADKH, cm): } ADKH = \frac{\sum_{i=1}^n SDKH}{N} \quad (4)$$

$$2. \text{ Average stand height (AH, m): } AH = \frac{\sum_{i=1}^n SH}{N} \quad (5)$$

$$3. \text{ Stand density (D; ha}^{-2}\text{): } D = \frac{n}{PA} \times 10000 \quad (6)$$

$$4. \text{ Basal area (BA; m}^2 \text{ ha}^{-1}\text{): } BA = \frac{\sum_{i=1}^n SBA}{PA} \quad \text{where} \quad SBA = \frac{\Pi}{4} \times SDKH^2 \quad (7)$$

$$5. \text{ Stand volume (V, m}^3 \text{ ha}^{-1}\text{): } V = \frac{\sum_{i=1}^n SV}{PA} \quad \text{where} \quad SV = 10^{-4} * \frac{\Pi}{4} \times SD^2 \times SH \quad (8)$$

In the above equations, *SDKH*, *SH*, *SBA* and *SV* are seedling/sapling DKH (in cm), height (in m), basal area (in cm<sup>2</sup>) and volume (in m<sup>3</sup>), *n* is the total number of seedlings/saplings in all plots, *PA* is the total plot area (in m<sup>2</sup>). Furthermore, vegetation recovery was assessed by the estimation of percentage ground cover of herbaceous vegetation (CH) as well as for seedlings/saplings (CS). Cover estimation was carried out in two ways: first, based on visual interpretation of percentage cover according to the Braun-Blanquet cover classes and second, on the basis of digital analysis of hemispherical photos that were taken at viewing angles of 180° vertical up and 0° vertical down in each plot (Rich 1990, Schroeder *et al.* 2007). Additionally, the canopy closure (CT, %) of mature plants which had survived the tsunami event was observed.

Except the assessment of species communities of seedlings/saplings, most of the general or qualitative data were assessed at the site level. These include information on tsunami impacts, human interventions, topography and soils. Soil texture of the first 20 cm of top soil was analysed in the field based on finger probe in order to distinguish between sandy beach environments (occurrence of dry and pure sands, without any noticeable organic matter) and mangrove environments with wet and muddier soils containing a higher proportion of silt and organic matter. A rough differentiation of the sand fraction into fine, medium and medium to coarse sand was carried out in the field (OSHA 2008, Wild 1993). Information on human impacts were collected at each site differencing between: cutting, clearing, burning activities, browsing damage (buffaloes), occurrence of garbage, reforestation activities.

## 4. Results

### 4.1 Findings from field data

Despite the fact that a limited number of study sites were observed, field data play an important role in this study: They provide a first picture on the recovery processes which occurred in the four years after the tsunami and they fill the gap of knowledge required to understand and interpret recovery information derived from multi-temporal image analysis. Regarding the community structure of seedlings/saplings, two major groups were distinguished in this study: mangrove species (termed as *M*) and species usually occurring in sandy beach environments, either belonging to the *Barringtonia* or *pes-caprae* formation (termed as *B*), compare FAO (2005a, 2005b), Sukardjo (2006) and Whitten *et al.* (1997). Regarding the casuarina sites, no change of community structure was observed: *Casuarina equisetifolia* is still the dominating species with an average of 95.8% of the recorded individuals in a site, followed by *Cocos nucifera* (1.6%) and *Terminalia catappa* (1.0%). In the mangrove sites (sites 12-21), community structure has changed at three sites indicated by higher abundances of non-mangrove species: The relation between community groups *B* and *M* was 1:45 (2.2%) at site 20, 4:21 (16.0%) at site 18 and 7:3 (70.0%) at site 12. At these sites, soils were found to be sandy with relatively low contents of organic matter which is likely to be an indicator of a transition from a mangrove habitat to a beach environment (compare Fujioka *et al.* 2008 or Wibisono and Suryadiputra (2006)). Observations from the coconut sites revealed that coconut plantations are man-made ecosystems which cannot naturally recover to their initial condition. Species composition equals to the casuarina sites with clear dominances of *Casuarina equisetifolia*. A shift of community structure towards higher abundances of mangrove species was not observed.

Quantitative measures collected at plot level (compare figure 4 and Appendix A) reveal that casuarina forests can recover faster than mangrove forests or coconut plantation (in terms of ADKH, AH, BA, V and CS). The maximum AH was 5.64 m measured at site 7, the maximum tree height (SH) and DKH were observed at site 8 with 11.4 m and 16.5 cm respectively. These values are impressingly high, especially when considering that these forests were not older than four years by the time of monitoring. But the growth rates relate well with other values described in the literature (Whistler and Elevith 2006). The six coconut sites observed are located in areas which are likely to be occupied by casuarina forests under natural conditions. This becomes apparent when analysing the species composition of the seedlings/saplings. Thus, coconut sites and casuarina sites are combined in figure 4. Regarding the distribution of the quantitative measures among the casuarina and coconut sites, two groups of sites can be distinguished: sites in which recovery processes occurred (sites 1, 2, 4-9 and 11) and sites with almost no recovery, like site 3 and all coconut sites. Recovery processes in most mangroves sites are present, indicated by a high number and density of seedlings/saplings. However, the rates of recovery respectively the growth rates are relatively low, indicated by low values of ADKH, AH, BA, V and CS.

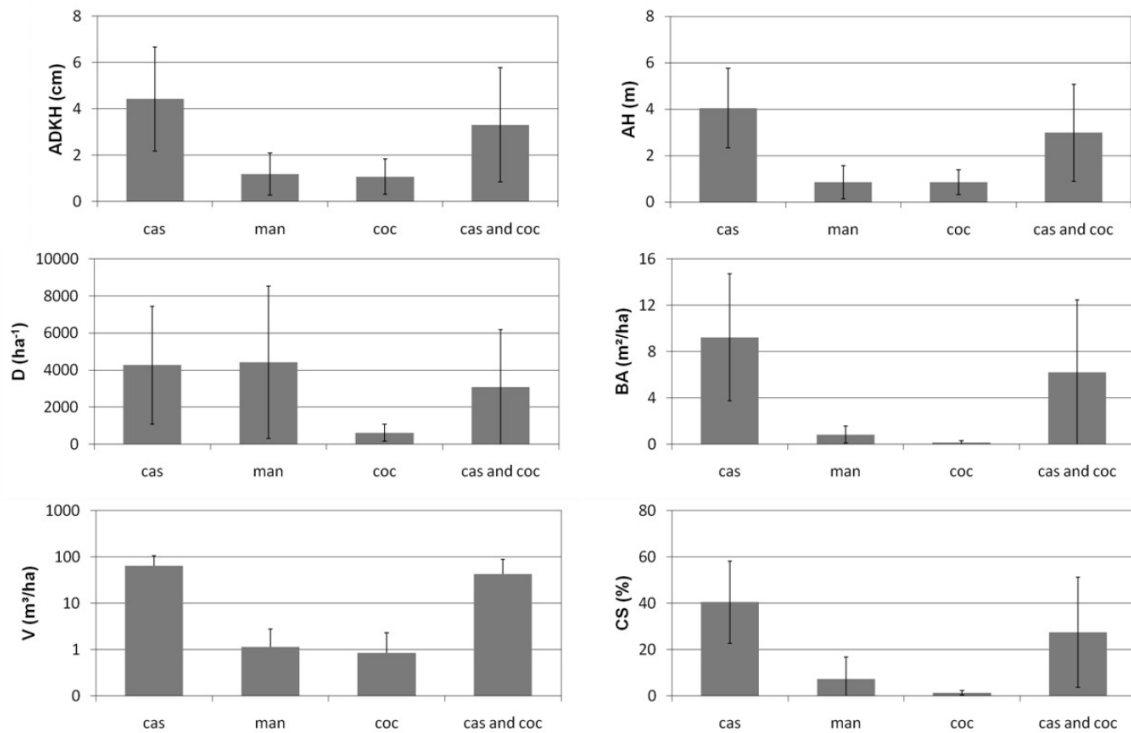


**Figure 4.** Quantitative measures derived from seedlings/saplings inventory: ADKH, AH, D, BA, V and C are the average diameter at knee height (ADKH, cm), average stand height (AH, m), stand density (D, ha<sup>-1</sup>), basal area (BA), stand volume (V; m<sup>3</sup>/ha) and the ground cover of seedlings/saplings (C, %) respectively. Cas, man and coc stand for casuarina sites, mangrove sites and coconut sites respectively.

#### 4.2 Results of recovery rates based on multi-temporal TNDVI images (TNDVI approach)

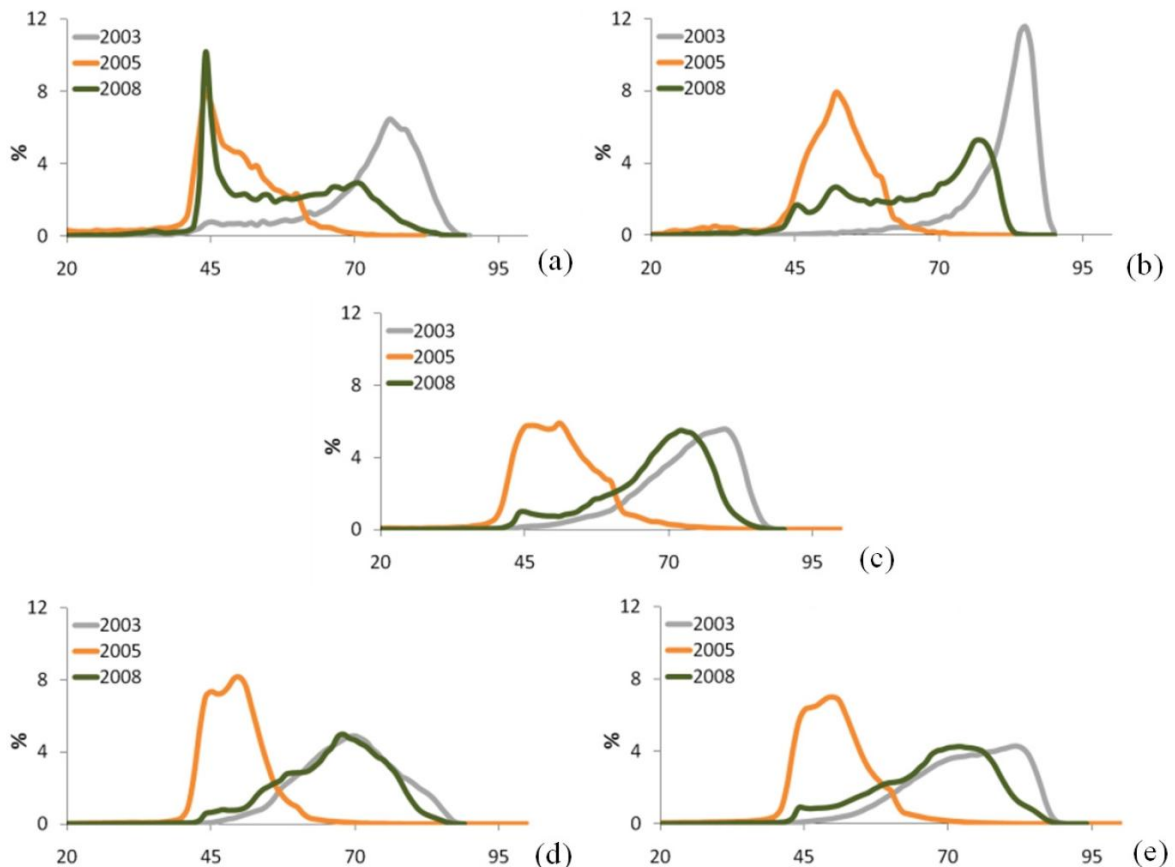
A correlation analysis was conducted in order to identify possible agreements between the field measurements and parameters derived from the IKONOS images. Here, the quantitative measures observed in the field (compare Appendix A) were correlated with the recovery rate  $R$  and the TNDVI of 2008 (Table 2). The results reveal that the single TNDVI of 2008 is well correlated with the vegetation parameters observed in the field whereas highest  $r$ -values occur at a ground cover of total vegetation (CT) and ground cover of seedlings/saplings (CS) with 0.75 and 0.51 respectively, followed by the basal area (BA) with 0.48. Correlation coefficients between field measurements and  $R$  are significantly lower. But this is not surprising, since field data represent vegetation states, whereas  $R$  includes multi-temporal information. Nevertheless expected positive correlation between  $R$  and field data can be detected.

**Table 2.** Correlation statistics between ground truth data and TNDVI values of 2008 and  $R$  (%).

stand properties	r-values		N
	TNDVI08	$R$ (%)	
ADKH (cm)	0.60	0.29	24
AH (cm)	0.67	0.46	24
D (ha <sup>-1</sup> )	0.19	0.11	25
BA (m <sup>2</sup> ha <sup>-1</sup> )	0.69	0.51	24
V (m <sup>3</sup> ha <sup>-1</sup> )	0.65	0.52	24
CS (%)	0.72	0.63	25
CH (%)	0.53	0.39	25
CT (%)	0.87	0.68	25

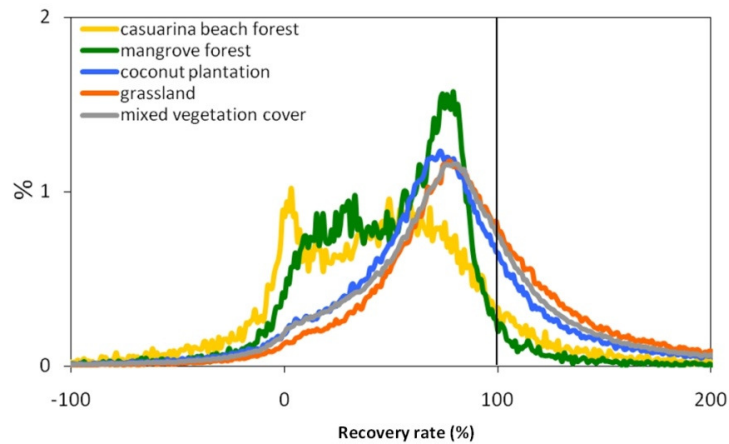


Figure 5 illustrates the changes of TNDVI values between the three image acquisition dates. The histograms show that there is a similar change pattern of the TNDVI values in all vegetation classes: first, a general decrease of the TNDVI values indicating a degradation of vegetation for the time between the first two IKONOS images followed by a general increase of the vegetation index indicating a recovery of vegetation. The more the green graph of 2008 equals the grey graph representing the previous state of vegetation, the more likely recovery has taken place. Thus, it can be concluded that that recovery of grassland vegetation, coconut and mixed vegetation cover is higher, than for mangrove or casuarinas forests. This observation can be confirmed by calculating the R-values (see also histograms in figure 6). The average recovery rate was estimated by the R-median value. Here, lowest recovery values occur for casuarina forests (46%), followed by mangrove forests (56%), coconut plantation (70%), mixed vegetation (75%) and grassland (79%). Regarding the shape of frequency distributions (figure 6), a clear bimodal distribution can be observed for casuarina forests with a first maximum at 0% indicating no recovery processes and a second maximum around 55% representing recovery processes. This also applies in an attenuated form to the mangrove forest having a second maximum at 25%. In contrast to this, recovery values exceeding 90% are more frequent for casuarina forests than for mangrove forests which is in agreement to the findings from the field measurements (section 4.1). Furthermore, the high recovery values of coconut plantations appear to disagree to the field data. This problem will be discussed in the section 5.2.1.



**Figure 5.** TNDVI statistics for the vegetation types. (a) casuarina forest, (b) mangrove forest, (c) coconut plantation, (d) grasslands and (e) mixed vegetation cover.





**Figure 6.** Histograms of the recovery rates (%) calculated for the five vegetation types.

Spatial patterns of vegetation recovery for all vegetation types (except for the mixed vegetation cover class) are provided in the change maps for selected subsets (figure 7). It becomes apparent that higher recovery rates occur in coconut plantations and grasslands whereas lower values are mostly in mangrove and casuarina forests. Furthermore, the maps show a great spatial variability of recovery patterns: Although recovery rates are mostly high for grasslands and coconut plantation, there is some area with relatively low values occurring either near the coasts in the west, such as for coconut plantation, or in the north east (grasslands). Some of these patterns can be explained by a landward shift of the coastline and coastal erosion and some of them by human interventions (compare section 5.2 and Bueno 2005, Szczucinski *et al.* 2006).

13 H. Roemer et al.: Monitoring post-tsunami vegetation recovery in Phang-Nga province, Thailand – a remote sensing based approach

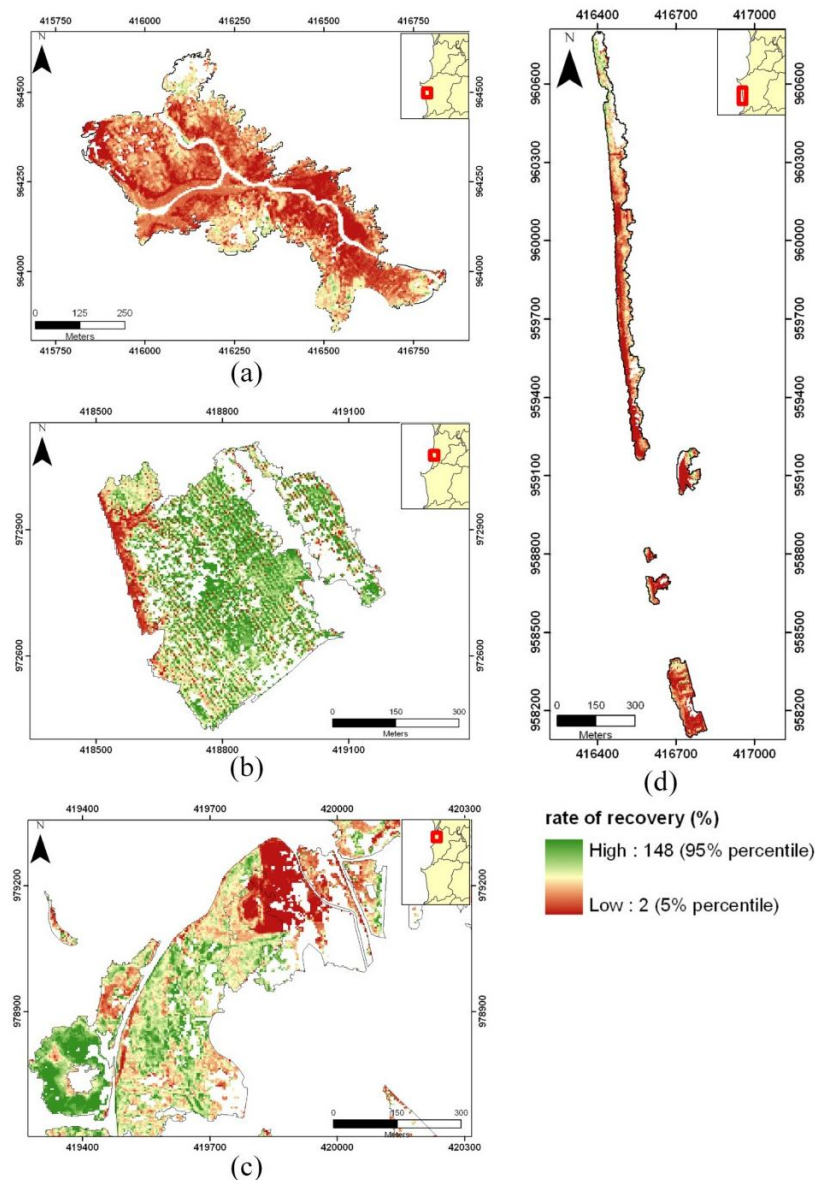


**Figure 7.** Change maps from the TNDVI-approach illustrating rates of recovery (%): (a) mangrove forests, (b) coconut plantation, (c) grasslands, (d) casuarina forests.

### 4.3 Results from CVA

The following figure 8 shows the frequency distributions of vector's directions for both time periods. It becomes apparent that for all vegetation types a maximum occurs in the second quadrant ( $90-180^\circ$ ) for the first period and another maximum in the fourth quadrant ( $270-360^\circ$ ) for the second period. This implies that the main characteristic of vegetation change can be described by a phase of degradation that is followed by a phase post-tsunami recovery or growth. Regarding the second period, recovery seems to be less pronounced for mangrove and casuarina forests, since bigger parts of the distribution are falling in the first and second quadrants. However, the figure does show direct transitions of direction values or quadrants between the both periods.

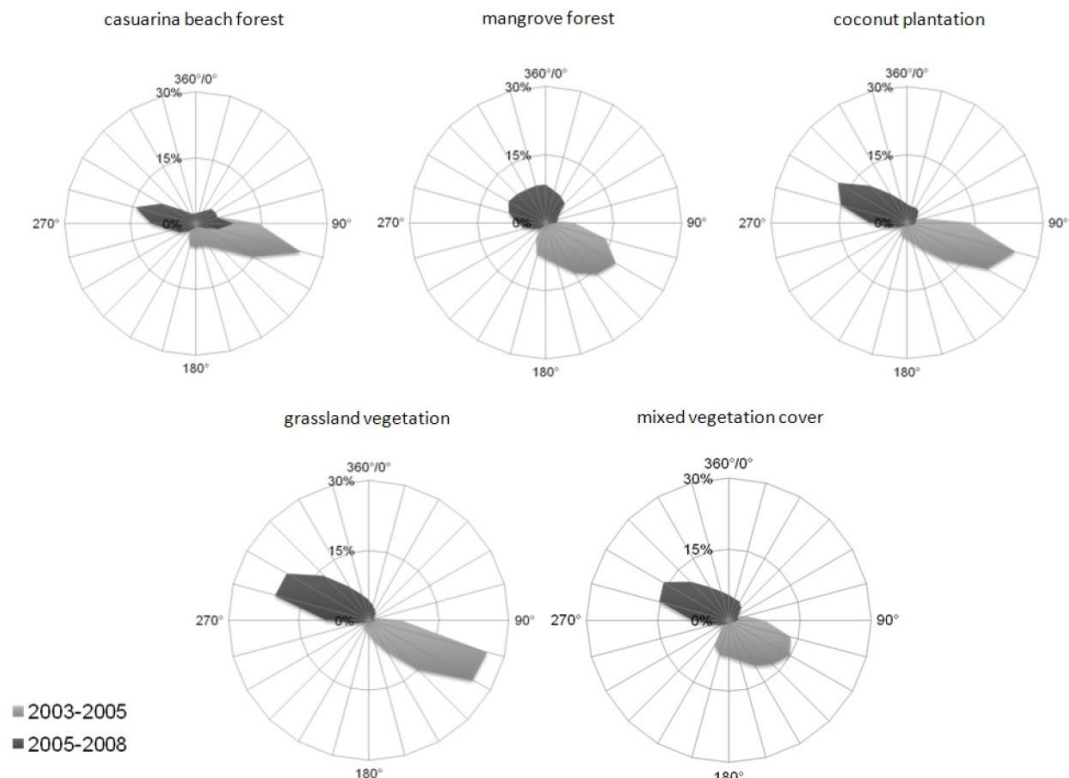


Figure 8. Frequency distributions of vector's directions for the two time periods for the five vegetation types.

Table 3 shows change class statistics for the examined vegetation formations, organized in aggregated classes (degradation, persistence and recovery) and sub-classes. These classes were created by the cross-tabulating process as described in section 3.2.2. The results reveal that recovery processes (mainly quadrant combination II-IV) are most frequent for grasslands (86.1%) followed by mixed vegetation cover (78.9%) and coconut plantation (78.1%). Relatively low values occur in mangrove and casuarina forests with 56.2% and 55.8% respectively. Persistence mainly occurs in mangrove forests with 35.7% followed by casuarina forests with 24.4%, whereas degradation paths are noticeable with a maximum for casuarina forests at 18.8%.

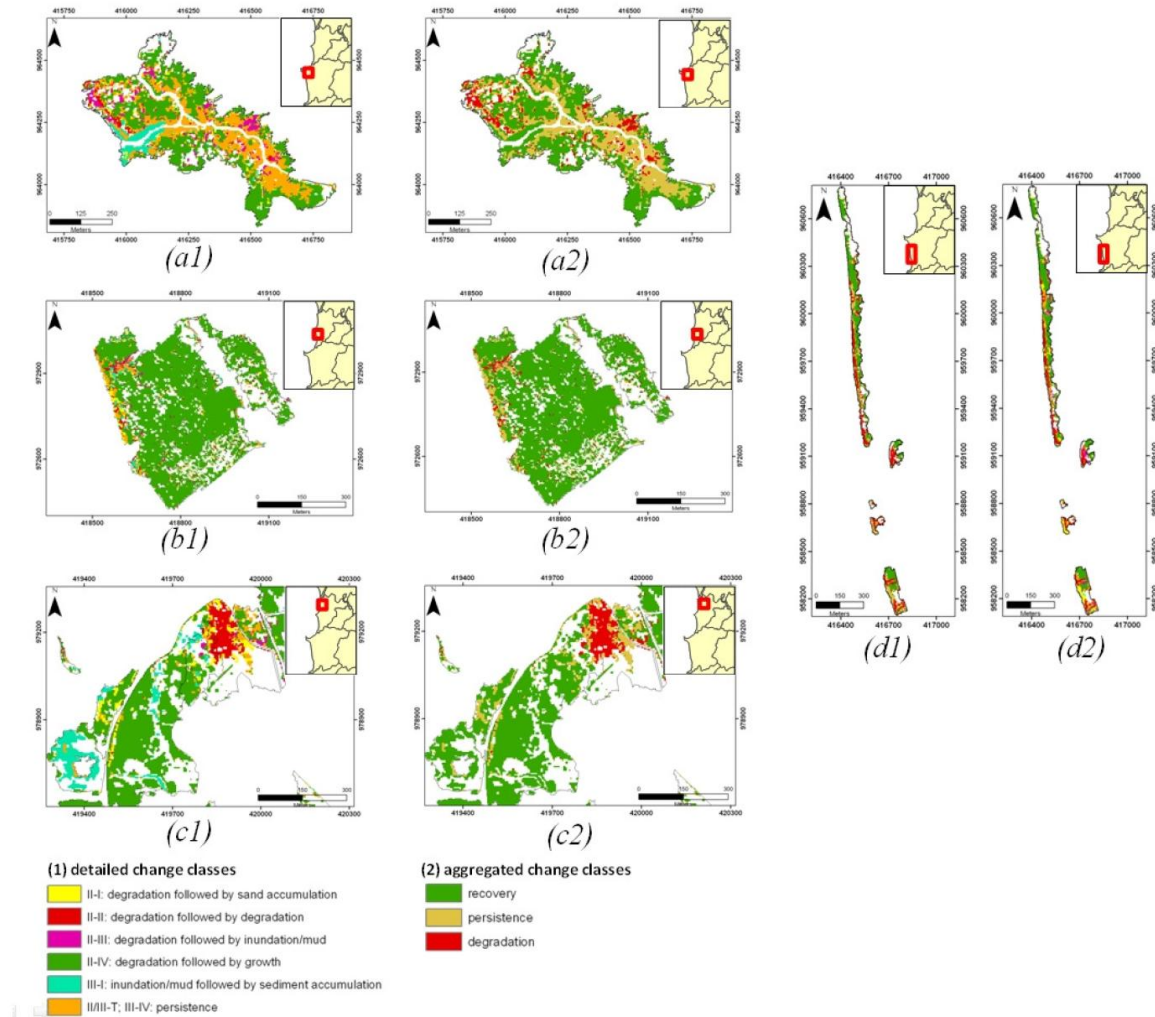
Magnitude values of the second time period are calculated for the two quadrant combinations that represent recovery processes, such as combination II-IV and III-I. Thus, they yield the information on the rates of recovery, similar to the first change detection method. Magnitude values are highest for casuarina forests with 64.0 for the combination II – IV and 70.4 for the combination III – I) and lowest for mangrove forests (37.1 respectively 49.0) which agrees to the results derived by the TNDVI-approach and the field measurements (compare sections 4.2 and 4.1 respectively). Magnitude values for the other vegetation types are comparably high for the combination II – IV (both values with 56.0) and relatively low (50.0 and 60.0) for the other combination III – I.

Table 3. Change class statistics based on CVA.

vegetation type	degradation classes			persistence classes				recovery classes		
	II-III	II-II	$\Sigma deg.$	III-IV	II/III-T	II-I	$\Sigma per.$	III-I	II-IV	$\Sigma rec.$
casuarina forest	8.1	10.8	18.8	0.6	10.5	13.3	24.4	7.2	48.5	55.8
mangrove forest	6.4	1.1	7.5	0.8	22.8	12.1	35.7	5.8	50.3	56.2
coconut plantation	6.8	2.3	9.0	0.8	5.2	6.6	12.5	2.5	75.6	78.1
grasslands	2.7	1.0	3.8	0.8	3.9	5.3	10.0	2.4	83.6	86.1
mixed vegetation cover	4.4	1.6	6.0	1.3	6.3	7.0	14.6	4.5	74.5	78.9



Aggregated and detailed change classes of the CVA are illustrated on the change maps (figure 9). In comparison to the change maps derived by the TNDVI-approach, these maps show qualitative change information. However, similar change patterns of recovery can be observed. The major underlying phenomena and processes causing these patterns will be further discussed in section 5.



**Figure 9.** Change maps of CVA. *a, b, c,* and *d* stand for mangrove forests, coconut plantation, grasslands and casuarina forests respectively, *1* and *2* indicate the applied classification system.

## 5. Discussion

This section is aimed at comparing and evaluating the change detection methods. Ground truth data plays a crucial role here, particularly for identifying the limitations and uncertainties when interpreting the change detection results.

### 5.1 Comparison of change detection methods and results

Both change detection methods applied in this study provide spatial information on recovery processes, but the type of information delivered by each method differs: Whereas in the TNDVI approach a single quantitative measure of recovery is provided, CVA provides more qualitative information. In order to compare both approaches in terms of accuracy and results, binary coded maps containing either “recovery” or “no recovery” were created for both methods. For the CVA, all change classes termed as “persistence” or “degradation” were aggregated into “no recovery”. Results provided in figure 10 indicate good agreement among both methods with difference values with less than 2% for all vegetation types, except for mangrove forests with 5.4%. The total number of pixels in both methods is not exactly the same (with a maximum relative difference for mangrove forests) resulting from the thresholding procedure as described in section 3.2. Nevertheless, in both methods recovery processes in mangrove and casuarina forests are significantly less frequent than in the other vegetation types with only 54.1 and 55.8% for casuarina forest and 61.6 and 56.2% for mangrove forests. This can also be proven by the calculation of effect size based on Cohen’s *d*, whereas recovery pixels were assigned with 1 and no recovery as 0 (Table 4). The results show that differences in mean recovery values (binary coded map) between coconut plantation and grasslands or casuarina beach and mangrove forest are relatively low (effect sizes < 0.3), whereas effect sizes for the other combinations are significantly higher. Accuracy assessment was carried out based on the binary coded change maps with a set of 3 151 pixels, visually detected from the pan-sharpened images. With an overall accuracy of 87.95 and 80.77% and kappa values of 0.77 and 0.65 (respectively for CVA and the TNDVI approach), both methods provide good results with some advantages for CVA.

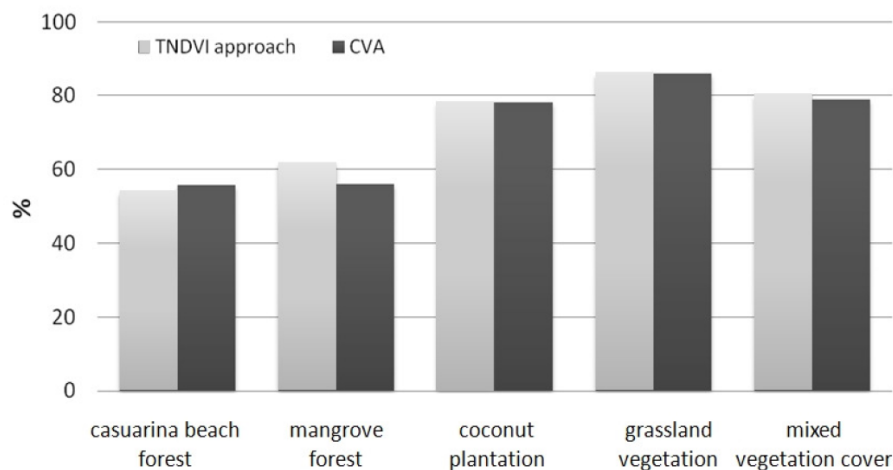


**Figure 10.** Comparison of areas representing vegetation recovery for both change detection techniques.

**Table 4.** Using effect size analysis based on Cohen’s *d* to compare mean difference values of recovery rates (%) for four vegetation types.

	mangrove forest		casuarina forest		coconut plantation	
	TNDVI approach	CVA	TNDVI approach	CVA	TNDVI approach	CVA
casuarina forest	0.19	0.05	-	-	-	-
coconut plantation	0.62	0.72	0.95	0.87	-	-
grasslands	0.94	1.10	1.26	1.21	0.20	0.22



## 5.2 Uncertainties and limitations in both change detection methods

### 5.2.1 Life cycle and human impacts

Both change detection techniques reveal that casuarina beach and mangrove forests recover slower and less frequent than coconut plantation and grasslands. These results are not surprising when comparing the different life cycles of each vegetation type with the time of recovery assessment. In contrast to woody plants such as casuarina or mangrove trees, non woody vegetation such as grasslands and herbaceous vegetation have a shorter life cycle and usually regenerate rapidly (i.e. within weeks or months) (Hayasaka *et al.* 2009, Szczucinski *et al.* 2006). Due to a low stand density (around 10 meters) and a low canopy closure, the spectral signature of a coconut plantation is composed of both, the coconut tree itself and the dense understory vegetation. Since the tsunami mainly affected the understory vegetation (Roemer *et al.* 2010), recovery rates analysed by change detection are comparably higher than those for grasslands. Thus, due to the long delay between impact and recovery assessment (3 years and 2 months after the tsunami) and the relatively short life cycle, recovery information derived for grasslands and coconut plantation cannot be automatically traced back to the recovery processes subsequently following the tsunami impact.

Since most of the grasslands and coconut plantations are in private ownerships, low recovery values can also be the result of human activities (burning, cutting, building activities) which may have taken place one or two years after the tsunami. The following figure 11 shows examples for human impacts detected on the latest IKONOS scene (February 2008).

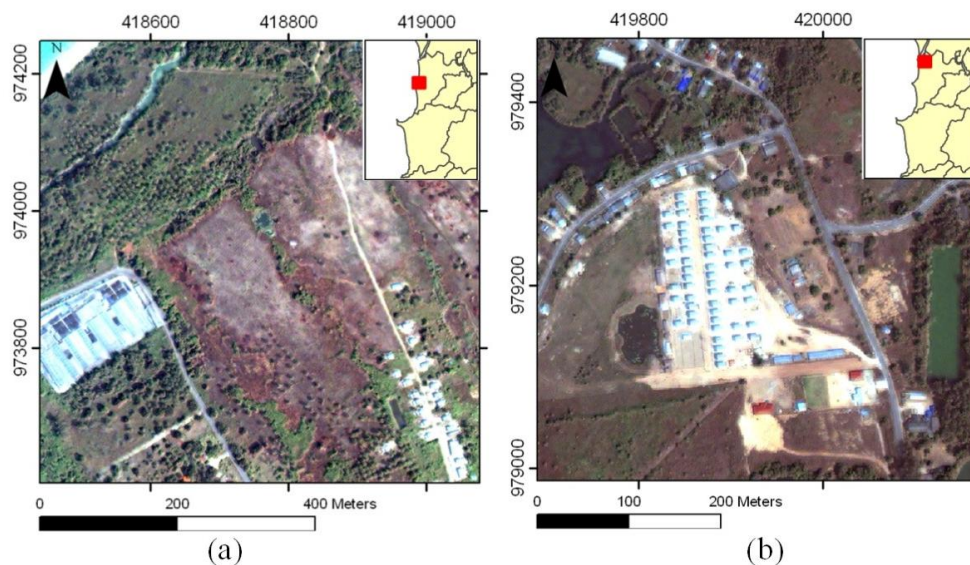


**Figure 11.** Human induced processes occurring in the study area and illustrated on the pan-sharpened IKONOS image of 2008. (a) burned areas and (b) new buildings near Ban Nam Khem.

### 5.2.2 Adaptive shift of coastal vegetation

Although casuarina trees can grow faster than mangrove trees (growth rates of *Casuarina equisetifolia* are 3 m in the first and 7-8 m after four years in contrast to less than one meter per year for *Rhizophora apiculata*), the change detection techniques reveal that the total recovery area is smaller and the area with progressive degradation even bigger than for the mangrove forests. This is surprising since the Casuarina tree can be regarded as a pioneer species, having a high invasive potential allowing them to colonize new places very quickly (Duke 2006, Whistler and Elevith 2006). In some places low or even no recovery of casuarina forests results from natural coastal erosion processes leading to a landward shift of the coastline and the coastal vegetation.



These processes, which only apply to the high dynamic narrow strips of casuarina forests, cannot be adequately represented in both change detection methods, because only the forest extents of the pre-tsunami scene (2003) were considered for recovery assessments. This phenomenon is illustrated in figure 12: The orange polygons (figure 12(c)) highlight patches of young casuarina forests which recovered after the tsunami. Due to a landward shift of forest patches, only the intersections between old and new casuarina patches (near the locations I and III on figure 12(d)) have high recovery values. Ignoring these processes of new colonization would underestimate the recovery and resilience of this forest type. Ground truth data which were collected near the locations I (site number 1) and III (site numbers 2 and 4) reveal that the new casuarina forest can rapidly recover with average stand heights ranging between 3.8 and 5.6 meters. In contrast to the area of recovery, ground truth measurements as well as both change detection methods reveal that recovery rates of casuarina forests are higher than those of mangrove forests (sections 4.2 and 4.3). Considering this adaptive shift as well as the high growth rates, casuarina forests turn out to be more resilient than mangrove forests.

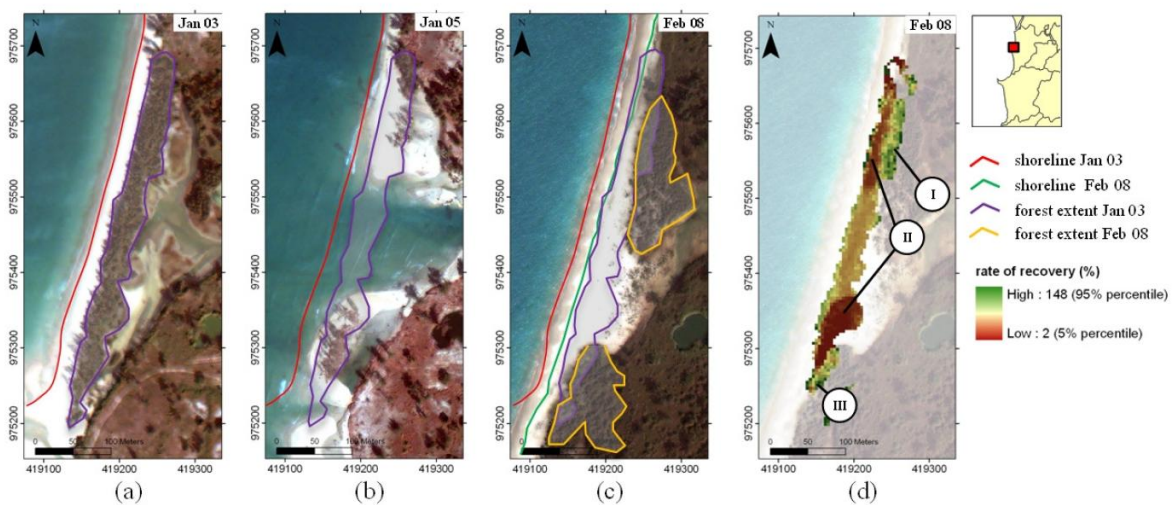


**Figure 12.** Landward shift of shoreline and casuarina forests. (a), (b) and (c) are the pan-sharpened IKONOS images from 2003, 2005 and 2008, (d) illustrates the rate of recovery (TNDVI approach). The locations I and III highlight high whereas II highlight low recovery rates.

### 5.2.3 Disturbance of the spectral signal due to high-water levels in mangrove fringes

Mangrove patches near Ban Nam Khem are directly bordering sheltered coastal waters (fringing mangroves). Field measurements from site number 16, 17, 19 and 20 reveal that recovery processes have taken place and can be connected to observed stand densities varying between 3440 and 10560 saplings per hectare (compare Appendix A). Especially in the outer fringes of the mangroves, forest floors can be inundated during mean high water levels. This affects spectral characteristics in these areas, since reflection values in the near-infrared spectrum as well as vegetation indices such as NDVI or the TC 2 will significantly be decreased. The figure 13 illustrates this phenomenon, exemplified for the site number 19: While the photo (compare figure 13(b)) indicates mangrove recovery (the average stand density is 10000 ha<sup>-1</sup> and average stand height 0.65 m), the corresponding spectral statistics (figure 13(c) and 13(d)) indicate a progressive degradation. This means, that for these areas, recovery processes will be underestimated by both change detection methods.

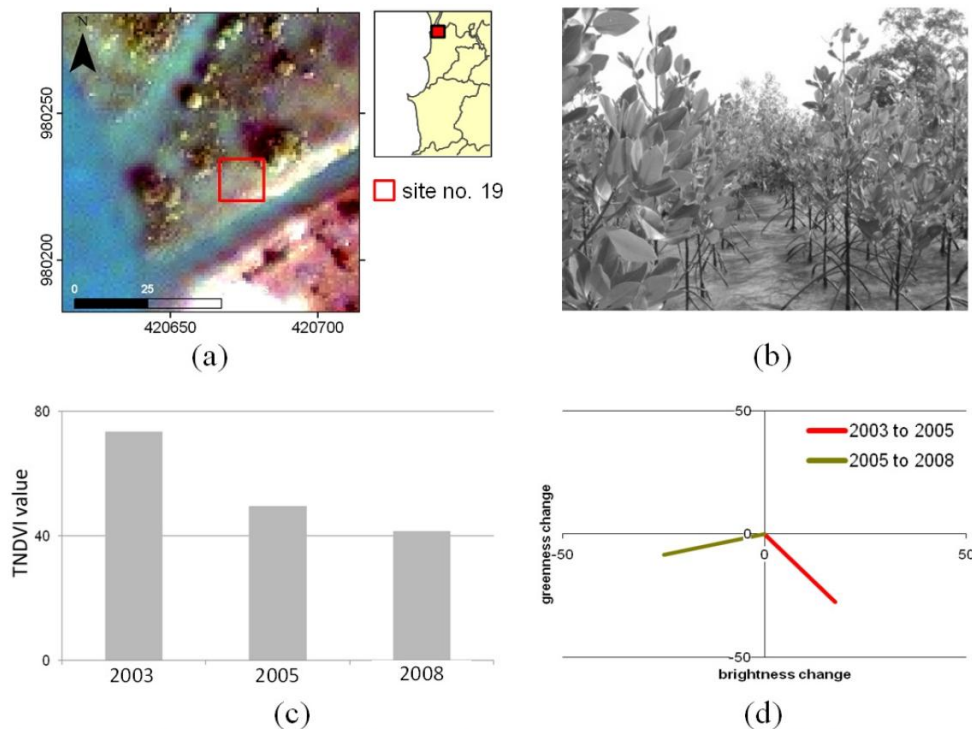


**Figure 13.** Change of spectral characteristics caused by inundation in mangrove fringes, exemplified for the study site number 19. (a) location of the study site, (b) photo of the study site, (c) TNDVI statistics and (d) quadrant combinations of combined CVA.

## 6. Conclusion

This paper presented a remote sensing based approach for estimating the vegetation recovery in the tsunami impacted coastal area of Phang-Nga province in Thailand. The results reveal that three years after the tsunami, most of the coastal vegetation has recovered to pre-tsunami conditions, but rates and percentage area of recovery vary spatially and in between vegetation types. Casuarina forests and mangroves recover slower than coconut plantations and grassland vegetation resulting from different life cycles, shoreline erosion or human impact (among other factors). Both change detection methods as well as the field data show that recovery rates of casuarina forests are higher than for mangrove forests. In contrast, a higher percentage area of recovery could be detected for mangrove forests.

The two change detection methods applied provide different types of information on the recovery processes, but yield comparable results and accuracies. The advantage of the TNDVI approach is its simplicity, making this method better transferable to similar applications. The combined CVA can provide more detailed information on land cover changes, but its application requires high technical and image interpretation skills.

Both methods have some limitations and inaccuracies in interpreting the results (short life cycle, human impacts), a lack of temporal resolution to better identify specific external driving forces, spectral inaccuracies at mangrove fringes and ecological processes that could not be adequately captured by pixel-based change detection (compare section 5). Another weak point in both change detection methods involves the definition of change thresholds which was realized by a mixture of a statistical approach and the visual interpretation of the high resolution pan-sharpened imagery. On the other hand ground truth data collected in 2009 provided additional valuable information, such as species composition or quantitative stand parameters. This information was used to describe and interpret the recovery process in more depth than by change detection alone. Its limitation results from the low spatial coverage of information, which means, that e.g. the total percentage area of recovery cannot be assessed by field work in a reasonable amount of time.

Finally, the study made clear that change detection results as well as field measurement data cannot replace each other and should be used complementary. Despite the aforementioned limitations, results from this study provide



new valuable information on the way and the degree to which different types of coastal vegetation has recovered after the tsunami.

Due to the use of ground truth data and high resolution pan-sharpened imagery, change detection results are closely tied to the underlying land-cover changes, making them more reliable and transparent for interpretation. As the approach provides spatial information, the recovery and resilience of the whole coastal area can be estimated. Additionally, if sufficient information on the regional ecosystem services is made available, this study can be used to assess changes of services in the coastal region and thus contribute to the estimation of social-ecological tsunami vulnerability in the region.

### Acknowledgment

Special acknowledgement and thanks go to the WWF-Team in Thailand for their support and assistance during the field campaigns. The team consisted of C.J. Dunbar, S. Chaksuin, S. Buanium and J. Jeewarongkakul. The research presented in this paper builds upon the project “Tsunami Risks, Vulnerability and Resilience in the Phang-Nga Province, Thailand” funded by the German Research Foundation.

### Appendix A. Quantitative measures of vegetation recovery.

site number	ground cover (%) <sup>*</sup>				stand parameters (seedlings/saplings)				
	CT	CH	CS	$C_{total}$	ADKH (cm)	AH (m)	D ( $ha^{-1}$ )	BA ( $m^2 ha^{-1}$ )	V ( $m^3 ha^{-1}$ )
1	0.00	2.50	51.51	54.01	3.65	3.77	3520	6.38	43.44
2	0.00	14.00	49.30	63.30	5.31	5.59	2720	11.28	102.40
3	0.00	9.50	1.25	10.75	0.53	0.81	640	0.04	0.10
4	23.60	36.75	44.76	100.00	3.44	3.89	4000	6.21	35.93
5	0.00	3.50	34.50	38.00	6.67	5.64	1040	4.65	33.27
6	0.00	75.75	20.40	96.15	1.38	1.55	11200	5.26	28.92
7	0.00	17.75	44.09	61.84	3.76	3.61	8240	12.58	68.48
8	0.00	27.25	62.84	90.09	6.87	5.54	3760	17.25	142.25
9	0.00	18.75	48.32	67.07	6.30	4.98	3680	13.72	90.61
10R	45.00	88.75	0.00	100.00	1.21	1.33	720	0.08	10.27
11	0.00	13.80	48.00	61.80	6.32	5.18	3900	15.00	95.00
12	0.00	25.13	28.63	53.75	2.91	2.35	640	1.42	4.20
13	0.00	0.75	1.00	1.75	1.17	0.89	320	0.18	0.19
14	0.00	0.00	0.00	0.00	0.00	0.00	0.00	0.00	0.00
15	0.00	4.25	2.00	6.25	0.87	0.52	5760	0.41	0.28
16	0.00	11.75	2.50	14.25	0.66	0.40	3440	0.20	0.14
17	0.00	1.75	5.00	6.75	1.18	0.60	10560	1.85	1.46
18	0.00	23.75	2.50	26.25	2.42	1.68	2000	1.63	3.59
19	0.00	0.00	19.75	19.75	0.81	0.65	10000	1.46	0.00
20	21.00	16.25	5.00	42.25	0.61	0.60	7040	0.37	0.39
21	4.90	1.01	6.67	12.58	no data	no data	5120	no data	no data
22	1.25	21.50	0.50	23.25	0.95	0.88	1040	0.01	0.01
23	0.00	40.50	2.00	42.50	1.74	1.49	960	0.25	0.44
24	0.00	0.75	0.00	0.75	0.00	0.00	0	0.00	3.38
25R	25.00	90.00	0.00	100.00	0	0.00	0	0.00	0
26	11.80	41.50	2.00	55.30	0.79	0.90	480	0.04	0.06
27	0.00	20.75	2.00	22.75	1.87	1.03	1040	0.38	0.36

\* CT is ground cover/canopy closure (%) of old trees which survived tsunami event; CH and CS stand for ground cover (%) of herbaceous vegetation and of seedlings/saplings respectively. R are reference sites with low or negligible tsunami induced damage

## References

- BELL, R., COWAN, H., DALZIELL, E., EVANS, N., O'LEARY, M., RUSH, B. and YULE, L., 2004, Survey of impacts on the Andaman Coast, Southern Thailand following the great Sumatra-Andaman earthquake and tsunami of December 26, 2004. *Bulletin of the New Zealand Society for Earthquake Engineering*, **38**, 123-148.
- BUENO, P., 2005, Impacts of Tsunami on Fisheries, Coastal Resources and Human Environment in Thailand. In *4th Regional Network of Local Governments Forum*, 27 April 2005, Bali, pp. 28.
- CENTER FOR SATELLITE BASED CRISIS INFORMATION (ZKI), 2005, *Thailand – Khao Lak region, map* (Wessling, Germany).
- CHANG, S.E., EERI, M., ADAMAS, B.J., ALDER, J., BERKE, P.R., CHUENPAGDEE, R., GHOSH, S. and WABNITZ, C., 2006, Coastal ecosystems and tsunami protection after the December 2004 Indian Ocean Tsunami. *Earthquake Spectra*, **22**, 863-25.
- CHATENOUX, B. and PEDUZZI, P., 2007, Impacts from the 2004 Indian Ocean Tsunami: analysing the potential protecting role of environmental features. *Natural Hazards*, **40**, 289-294.
- CORLETT, R.T., 2008, Vegetation. In *The Physical Geography of Southeast Asia*, A. Gupta (Ed.), pp. 105-119 (New York: Oxford University Press).
- DANIELSEN, F., SØRENSEN, M.K., OLWIG, M.F., SELVAM, V., PARISH, F., BURGESS, N.D., HIRAISHI, T., KARUNAGARAN, V.M., RASMUSSEN, M.S., HANSEN, L.B., QUARTO, A. and SURYADIPUTRA, N., 2005, The Asian tsunami: a protective role for coastal vegetation. *Science*, **310**, p. 643.
- DEPARTMENT OF MARINE AND COASTAL RESOURCES (DMCR), 2005, *Rapid Assessment of the Tsunami Impact on Marine Resources in the Andaman Sea, Thailand*, p. 76 (Bangkok: PMBC).
- DONNER, W., 1989, *Thailand - Räumliche Strukturen und Entwicklung von Wolf Donner*; p. 339 (Darmstadt: Wissenschaftliche Buchgesellschaft).
- DUKE, N.C., 2010, *Rhizophora apiculata*, *R. mucronata*, *R. stylosa*, *R. × annamalai*, *R. × lamarekii* (Indo-West Pacific stilt mangroves), ver. 2.1. In *Species Profiles for Pacific Island Agroforestry*, C.R. Elevitch (Ed.). Available online at: <http://www.traditionaltree.org>. (accessed 01 May 2010).
- FOOD AND AGRICULTURAL ORGANIZATION OF THE UNITED NATIONS (FAO), 2005a, *In-depth assessment of mangroves and other coastal forests affected by the tsunami in Southern Thailand*, THA/05/001, FAO Consultant Report by P. Saenger, International Consultant, November 2005, Bangkok.
- FOOD AND AGRICULTURAL ORGANIZATION OF THE UNITED NATIONS (FAO), 2005b, *In-depth assessment of mangroves and other coastal forests affected by the tsunami in Southern Thailand*, THA/05/001/01/12, Progress Report submitted to the Regional Office for Asia and the Pacific, Food and Agriculture Organization, Bangkok.
- FAO-MOAC. 2005, *Report of joint FAO/MOAC detailed technical damages and needs assessment mission in fisheries and agriculture sectors in tsunami affected six provinces in Thailand*, 11-24 January 2005. Available online at: [http://www.apfic.org/apfic\\_downloads/tsunami/FAO\\_MOAC\\_thai.pdf](http://www.apfic.org/apfic_downloads/tsunami/FAO_MOAC_thai.pdf). (accessed 05 July 2010).
- FUJIOKA, Y., TABUCHI, R., HIRATA, Y., YONEDA, R., PATANAPONPAIBOON, P., POUNGPARN, S., SHIBUNO, T. and OHBA, H., 2008, Disturbance and recovery of mangrove forests and macrobenthic communities in Andaman Sea, Thailand following the Indian Ocean Tsunami. In *Proceedings of the 11th International Coral Reef Symposium*, 7-11 July 2008, Ft. Lauderdale, Florida, pp. 825-829.
- HAYASAKA, D., FUJIWARA, K. and BOX, E.O., 2009, Recovery of sandy beach and maritime forest vegetation on Phuket Island (Thailand) after the major Indian Ocean tsunami of 2004. *Applied Vegetation Science*, **12**, 211-224.
- HORNE, J.H., 2003, A tasseled cap transformation for IKONOS images. In *Proceedings of the ASPRS Annual Conference 5-9 May 2003*, Anchorage, USA, p. 9.
- JOHNSON, R.D., 1994, Change Vector Analysis for disaster assessment: a case study of Hurricane Andrew. *Geocarto International*, **9**, 41-15.
- LABEN, C.A. and BROWER, B.V., 2000, Process for enhancing the spatial resolution of multispectral imagery using pan-sharpening. Eastman Kodak Company, Technical Report US Patent #6.011.875.
- LIN, C.Y., LO, H-M., CHOU, W-C. and LIN, W-T., 2004, Vegetation recovery assessment at the Jou-Jou Mountain landslide area caused by the 921 Earthquake in Central Taiwan. *Ecological Modelling*, **176**, 75-81.
- LORENA, R.B., DOS SANTOS, J.R., SHIMABUKORO, Y.E., BROWN, I.F. and KUX, H.J.H., 2002, A Change Vector Analysis technique to monitor land use/land cover in SW-Brazilian Amazon: Acre State. In *Proceedings of the International Society for Photogrammetry and Remote Sensing (ISPRS)*; 10-14 November 2002, Denver, Co., USA, p. 8.



- 22 H. Roemer et al.: Monitoring post-tsunami vegetation recovery in Phang-Nga province, Thailand – a remote sensing based approach
- LU, D., MAUSEL, P., BRONDÍZIO, E. and MORAN, E., 2003, Classification of successional forest stages in the Brazilian Amazon basin. *Forest Ecology and Management*, **181**, 301-311.
- LU, D., MAUSEL, P., BRONDÍZIO, E. and MORAN, E., 2004, Change detection techniques. *International Journal of Remote Sensing*, **25**, 2365-2407.
- MALILA, W.A., 1980, Change Vector Analysis: an approach for detecting forest changes with Landsat. In *Proceedings of the 6th Annual Symposium on Machine Processing of Remotely Sensed Data*; 1980, West Lafayette, USA, pp. 326-335.
- MAS, J.F., 1999, Monitoring land cover changes: a comparison of change detection techniques. *International Journal of Remote Sensing*, **48**, 139-152.
- MITRI, E.H. and GITAS, I.Z., 2010, Mapping Postfire Vegetation Recovery using EO-1 Hyperion Imagery. *IEEE Transactions on Geoscience and Remote Sensing*, **48**, 1613-1618.
- OTIENO, K., ONIM, J.F.M., BRYANT, M.J. AND DZOWELA, B.H., 1991, The relation between biomass yield and linear measures of growth in *Sesbania sesban* in western Kenya. *Agroforest Syst*, **13**, 131-141.
- PAJIMANS, K. (ed.), 1976, *New Guinea Vegetation*, p. 213 (Canberra: CRISPO).
- PAPHAVASIT, N., AKSORNKOAE, S. and DE SILVIA, J. (Eds.), 2009, *Tsunami Impact on Mangrove Ecosystem*, p. 211 (Nonthaburi, Thailand: Thailand Environmental Institute).
- PHONGSUWAN, N., YEEMIN, T., WORACHANANANT, S., DUANGSAWASDI, M., CHOTIYAPUTTA, C. and COMLEY, J., 2006, Post-tsunami status of coral reefs and other coastal ecosystems in the Andaman Sea coast of Thailand. In *Status of coral reefs in tsunami-affected countries*, C. Wilkinson, S. Souter and J. Goldberg (Eds.), pp. 63-78 (Townsville: S Australian Institute of Marine Science).
- RICH, P.M., 1990, Characterizing plant canopies with hemispherical photographs. *Remote Sensing Reviews*, **5**, 13-29.
- ROEMER, H., KAISER, G., STERR, H. and LUDWIG, R., 2010, Using remote sensing to assess tsunami-induced impacts on coastal forest ecosystems at the Andaman Sea coast of Thailand. *Natural Hazards and Earth System Sciences*, **10**, 729-746.
- SCHROEDER, T.S., WARREN, B.C. and YANG, Z., 2007, Patterns of forest regrowth following clear cutting in western Oregon as determined from a Landsat time-series. *Forest Ecology and Management*, **243**, 259-273.
- SENAY, G.B. and ELLIOTT, R.L., 2000, Combining AVHRR-NDVI and land use data to describe temporal and spatial dynamics of vegetation. *Forest Ecology and Management*, **128**, 83-91.
- SIMONIELLO, T., LANFREDI, M., LIBERTI, M., COPPOLA, R., and MACCHIATO, M., 2008, Estimation of vegetation cover resilience from satellite time series. *Hydrology and Earth System Sciences*, **5**, 511-545.
- SRIBOONPONG, S., HUSSIN, Y.A. and GIER, A.D., 2001, Assessment of forest recovery after fire using LANDSAT TM images and GIS techniques: A case study of Mae Wong National Park, Thailand. In *22nd Asian Conference on Remote Sensing*, 5-9 November 2001, Singapore, p. 6.
- SUKARDJO, S., 2006, Botanical Exploration in Small Islands: 1. Floristic Ecology and the Vegetation Types of Pari Island, West Java, Indonesia. *South Pacific Studies*, **26**, 73-87.
- SZCZUCINSKI, W., CHAIMANEE, N., NIEDZIELSKI, P., RACHLEWICZ, G., SAISUTTICHAJ, D., TEPSUWAN, T., LORENC, S. and SIEPAK, J., 2006, Environmental and Geological Impacts of the 26 December 2004 Tsunami in Coastal Zone of Thailand – Overview of Short and Long-Term Effects. *Polish Journal of Environmental Studies*, **15**, 793-810.
- TAYLOR, M., 2009, IKONOS Planetary Reflectance and Mean Solar Exoatmospheric Irradiance. GeoEye. Available online at: [http://www.geoeye.com/CorpSite/assets/docs/technical-papers/2009/IKONOS\\_Esun\\_Calculations.pdf](http://www.geoeye.com/CorpSite/assets/docs/technical-papers/2009/IKONOS_Esun_Calculations.pdf) (accessed 04 January 2009).
- THERON, J.M., VAN LAAR, A., KUNNEKE, A. and BREDEKAMP, B.V., 2004, A preliminary assessment of utilizable biomass in invading *Acacia* stands on the Cape coastal plains. *South African Journal of Science*, **100**, 123-125.
- UNEP-WORLD CONSERVATION MONITORING CENTRA (UNEP-WCMC), 2006, *In the front line: shoreline protection and other ecosystem services from mangroves and coral reefs*. UNEP-WCMC. Cambridge, p. 33.
- U.S. DEPARTMENT OF LABOR - OCCUPATIONAL SAFETY & HEALTH ADMINISTRATION (OSHA), 2008, *Field Method for Identification of Soil Texture*. Available online at: <http://www.osha.gov/doc/outreachtraining/htmlfiles/soiltex.html>. (accessed 05 July 2010).
- VICENTE-SERRANO, S.M., LASANTA, T. AND ROMO, A., 2004, Analysis of Spatial and Temporal Evolution of Vegetation Cover in the Spanish Central Pyrenees: Role of Human Management. *Environmental Management*, **34**, 802-818.
- WASHINGTON-ALLEN, R.A., RAMSEY, R.D., WEST, N.E. and NORTON, B.E., 2008, Quantification of the ecological resilience of drylands using digital remote sensing. *Ecology and Society*, **13**, p. 33.

## 6 Synthesis

The research presented in the two papers that form the core of this thesis reveals that multi-temporal IKONOS imagery and change detection techniques can be successfully applied to assess tsunami induced impacts and recovery processes in the examined ecosystems. Furthermore, the papers discuss which of the applied change detection techniques can be recommended to assess recovery processes and tsunami impacts on a local scale. But how can the methods and the results provided by this research be applied to estimate aspects of vulnerability? And furthermore, how can the potential of the applied remote sensing techniques generally be evaluated in a) contributing to the assessment of ecological vulnerability and b) supporting vulnerability and risk assessment as is aimed at in TRAIT? These questions are discussed and answered within this section. The chapter continues with a short summary of the key findings of the two articles with respect to both, the methodological findings and the results about impact and recovery in the examined coastal ecosystems.

### 6.1 Summary of key findings of the two articles

#### 6.1.1 Methodological aspects

The use of high resolution IKONOS imagery brought two main advantages for both studies: First, with regard to the classification, even small scaled exposure units, in particular the narrow stripes of casuarina beach forests (< 40 m wide) were successfully identified and extracted from the images. Furthermore, coconut plantations were identified by considering their characteristic single-tree-texture. Second, the high spatial variability of damage and recovery processes was adequately represented by the change detection techniques, which contributes to a better understanding of the underlying processes.

A zone based approach in both change detection studies was applied, introducing both advantages and some disadvantages. Due to the integration of accurate information (in terms of geometry and semantics) on the initial or pre-tsunami state of the specific ecosystem, the information content of the change detection results was significantly improved. A post-classification comparison was not used in this study. In this regard, Lu *et al.* (2004) stated that the time-consuming and difficult task of producing highly accurate classifications often leads to unsatisfactory change detection results, especially when high-quality training sample data are not available. Furthermore, the synergistic use of object-oriented image analysis and change detection turned out to be as very effect: As the forest zones were derived from image object, instead of pixels, they appeared very smooth and homogenously, which improved the cartographic quality of the change detection results (cp. Meinel *et al.* 2001; Römer 2007).

However, the zone-based change detection approach brought also some disadvantages: Growth and colonisation processes that occurred outside of the initial or pre-tsunami forest areas were not considered for the recovery analysis. Although this problem particularly appeared only in the dynamic casuarina beach forests (cp. Roemer *et al.* 2010b), it needs to be emphasized that growth processes in new areas must also be considered when estimating the recovery potential and the resilience of a specific ecosystem.

Although no ground truth for the tsunami induced impacts were available in this study, it can be concluded that damage processes can be easier detected by change detection applications than recovery processes. This is mainly due to the fact that only two time steps are needed for the investigation of tsunami impacts. In addition, impact processes are accompanied by obvious changes in land cover and can be easier identified and interpreted from multi-date images. In contrast, spectral changes are usually less pronounced in the case of recovery processes, which particularly applies for slow growing vegetation. Furthermore, as forest seedlings and saplings were mostly too small to be directly classified and mapped on an IKONOS image, change detection results provided only little qualitative information, i.e. on the type of the recovering vegetation. Thus, change detection techniques had to be complemented by a detailed field campaign in order to provide more comprehensive qualitative information on the recovery processes (cp. section 4.4).

However, both studies reveal that there are limitations in identifying the causal relationships between the observed processes: According to Roemer *et al.* (2010a), some difficulties occur in interpreting the tsunami impacts on coconut plantations, which is mainly due to the larger time gap between the pre-tsunami image and the tsunami (23 months). Regarding the recovery analysis, it cannot be clearly distinguished between natural recovery processes and human reforestation activities.

### 6.1.2 Ecological perspective

Considering the information provided by the change detection studies, the field measurements and also personal communication with local experts (here in particular with Jirapong Jeewarongkakul) led to the following conclusions about the ecological sensitivity and recovery of the examined coastal ecosystems.

#### Casuarina beach forests

The exposure analysis and the study on the tsunami induced impacts revealed that casuarina beach forests are very exposed and damage prone forests ecosystems. As these forests are located directly at the coastline, they were intensively impacted by the tsunami. Furthermore, due to the small width of forest patches and due to their occurrence on sandy substrates, they were sensitive to uprooting and erosion processes. According to the results derived from the direct multi-date classification (DMC), 38% of the initial forest area was directly damaged by the tsunami. Since this impact type can include a complete removal of the forest and the erosion of soils and sediments, this impact type can be considered as a proxy for a local loss of ecosystem functions, such as habitat functions or the capacity to stabilise sand dunes.

However, the field measurements and partly the change detection applications revealed that *Casuarina equisetifolia* as the dominating tree species, turn out to be a highly invasive species which rapidly occupies new habitats (Duke 2006; Whistler and Elevitch 2006). A high growth rate as well as a high stability in species composition is observed for this forest type. Furthermore, a high adaptive potential of this forest type is detected, e.g. in connection with natural coastal erosion processes which were increased in areas, where beach sediments were eroded by the tsunami. Beach forests stripes moved further inland as a consequence of a coastline retreat.

In contrast, change detection applications revealed that recovery processes have taken place in only 54 - 56% of the initial forest area. These low values can either be explained by a) the aforementioned adaptive shifts of forests, b) colonisation processes in new areas and c) by human activities that have taken place near the beach. In this regard, a high building activity in the beach area was observed during field studies, including the construction of walls, roads and houses or bungalows (cp. section 6.2.2.3). However, because of their invasive potential, rapid growth and the production of large quantities of easily dispersed seeds, casuarina beach forests can be considered a resilient coastal ecosystem (Duke 2006; Haysom and Murphy 2003; Whistler and Elevitch 2006).

### Mangrove forests

As most of the mangrove areas are located in sheltered areas (88.70%), this forest ecosystem is less exposed than the casuarina beach forests. Considering only the exposed areas, change detection results revealed that 55% of the forest area (respectively 6.2% of the entire forest area) was directly damaged by the tsunami which relates well with findings of Yanagisawa *et al.* (2009) for the mangroves near Pakarang Cape. Field investigations as well as change detection methods revealed that recovery processes took place in only 56 - 62% of the impacted forests area and that growth rates were found to be relatively low in comparison to the average growth rates (cp. Duke 2006; Roemer *et al.* 2010b). Furthermore, changes in community structure towards a transition to species that usually occur in beach environments (*Cocos nucifera*, *Casuarina equisetifolia*) are observed. These processes can be regarded as indicators for disturbed recovery and resilience.

When evaluating the sensitivity and resilience of mangrove forests, the forest patch sizes have to be taken into consideration. Small isolated forest patches, such as those near Pakarang Cape, near Khuk Khak and at Krang Nui Cape are likely more vulnerable than the bigger forest areas in the north (near Ban Nam Khem) and in the south (south of Tap Lamru). In this context, Kumpulainen (2006) argues that small and fragmented patches are more vulnerable, since they are likely to be totally destroyed if a hazard strikes. Adger *et al.* (2005) focuses more on the aspect of resilience and states that remnants of the former system become starting points for renewal and reorganisation such as mobile species and propagules that colonise and reorganise disturbed sites. Remnants are more likely available in the bigger forest areas, where the tsunami only impacted the outer mangrove fringes. Additionally, the southern mangroves are partly protected by national park status with its prohibition of human activities making them more resilient than the other patches occurring in the north (cp. Adger *et al.* 2004). The following photos on Figure 6-1 show two recovery situations observed in February 2009, one in an isolated mangrove area near Pakarang Cape (Figure 6-1a) and another from a larger patch near Ban Nam Khem (Figure 6-1b).





**Figure 6-1.** Recovery processes in mangrove forests observed in February 2009. (a) slow recovery processes in a small and isolated mangrove area near Pakarang Cape and (b) fast recovery processes in a larger mangrove area near Ban Nam Khem with high abundances of mature trees.

### Coconut plantation

Although being one of the most exposed ecosystems, with more than 90% of directly exposed plantation area, change detection results revealed that coconut plantation were less affected than casuarina or mangrove forests (28% of direct damage). Furthermore, as it was discussed in Roemer *et al.* (2010a), the total damage area was overestimated the change detection techniques, due to man made changes which very likely have occurred between the pre-tsunami IKONOS image and the tsunami event. Field investigations indicated that direct impacts such as tree breaking and uprooting of coconut palms have only occurred in close proximity to the shoreline (< 100 m), particularly near Ban Bang Sak or Pakarang Cape (cp. photo on Figure 6-2). Thus, it can be assumed that only 5-10% of the initial plantation area was actually affected by direct forest or tree damage. This observation is not surprising when taking the stand structure of coconut plantations into consideration: Coconut trees are characterised by their monopodial growth form and their highly flexible trunks and foliage. Furthermore due to the wide tree spacing, coconut trees provide very low drags to the tsunami making them to one of the most resistant coastline trees (Cochard *et al.* 2008).

Due to the fact that mostly just soils or understory vegetation were affected by the tsunami, recovery rates derived from change detection techniques assume very fast recovery processes. However, regarding the recovery of coconut trees, field measurements revealed a change in community structure indicated by the succession of tree species that usually occur in beach habitats with high abundances of *Casuarina equisetifolia* and *Barringtonia sp.*, cp. Table 4-4). Thus, from the ecological point of view, these ecosystems are indeed resistant to tsunamis but not resilient as they were not in an equilibrium state prior to the tsunami and need to be artificially preserved and cultivated.





**Figure 6-2.** Direct impacts on coconut plantations. The photo was taken in February 2009 and illustrates a swaley depression near Ban Bang Sak where sediments were eroded and coconut trees were completely removed by the tsunami backwash.

#### Mixed beach forests and melaleuca forests

These two forest ecosystems occur only in the southern part of the study area and are protected by a national park status. With a relative exposed area of 71% (mixed beach forests) and 94% (melaleuca forests), they can be considered as highly exposed ecosystems. However, damage patterns observed by digital change detection show that only 1.25% (mixed beach forests) and 1.22% (melaleuca forests) were directly affected. Indirect forest damages including defoliation, standing dead and yellowing of leaves were found to be the dominating impact with 53% for mixed beach forests respectively 21% for melaleuca forests being affected. Since indirect forest damages are not accompanied with a complete removal of soils and biomass, ecosystem functionality was only marginally affected by the tsunami. Field visits conducted in 2009 revealed that there were still some defoliated and dead adult trees present in the mixed beach forests (Figure 6-3) indicating a low tolerance or high sensitivity to soil salinity. However, concerning the main characteristics such as species and age composition, hardly any tsunami effects on either forest type were recorded in the field in 2009.



**Figure 6-3.** Defoliated and dead trees occurring in mixed beach forests. The photo was taken in March 2009.

### Conclusions

When comparing the five ecosystems, the author suggests that mangrove forests are most vulnerable to tsunamis, followed by the casuarina beach forests. Although casuarina beach forests are the most exposed ecosystems, there is a low chance that these forest systems will totally disappear in the coastal zone. In contrast, mangrove forests are highly specialised ecosystems which are adapted to specific environmental conditions. A low resilience results from their low adaptive capacity to changing environmental conditions (i.e. of soils, drainage) which can be also explained by their unique way of seedling reproduction (propagules). This makes them more vulnerable, as recovery processes always starts in the initial habitat area. It is difficult to evaluate the vulnerability of coconut plantation since they are not resilient in terms of natural regeneration. Nevertheless, due to their high resistance towards direct forest damages and their high tolerance against salinity, their vulnerability towards tsunami impacts can be regarded as low. Furthermore, a low tsunami vulnerability was also observed for mixed beach forests and melaleuca forests. However, these observations are mainly due to the fact that these two forest types are located in the south, where tsunami wave intensities were lower than in the north (cp. Ioualalen 2007). As several dead and defoliated trees were still present in 2009 (Figure 6-3), the author assumes a slightly increased system related vulnerability to tsunami impacts (cp. intrinsic vulnerability of Villa and McLeod 2002).

## 6.2 Assessment and analysis of the tsunami vulnerability

Although the methodological approach applied in this thesis is useful to provide information on the exposure, the tsunami induced impacts and the recovery, it needs to be investigated how these results can be applied to assess and analyse tsunami vulnerability in the examined ecosystems (cp. Figure 6-4): As the results provided in this thesis focus on the consequences of vulnerability or in general the impact (cp. Turner *et al.* 2003), they can be used to retrospectively assess the vulnerability (cp. section 6.2.1). However, a main problem encompasses the assessment of the vulnerability prior to a natural hazard, which requires knowledge about the factors (e.g. external or internal) that cause vulnerability (cp. Turner *et al.* 2003; Villa and McLeod 2002). Thus, section 6.2.2 focuses on the identification of causes or factors determining the tsunami vulnerability. In this regard, a statistical approach is presented, by which the change detection results are correlated and regressed against a set of independent or predictor variables.

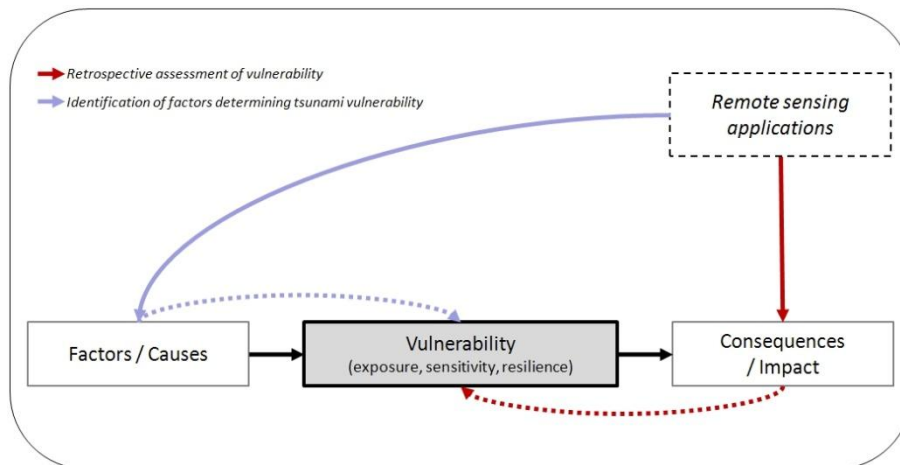


**Figure 6-4.** Two approaches for assessing and analysing tsunami vulnerability: Retrospective vulnerability assessment; Identification of factors determining tsunami vulnerability.

### 6.2.1 Retrospective analysis of tsunami vulnerability

As vulnerability is defined by the three components of exposure, sensitivity and resilience, it needs to be investigated how the results provided by the remote sensing studies (here the exposure analysis, the impacts analysis and the recovery analysis) can be used to retrospectively assess the vulnerability of the examined ecosystems.

Figure 6-5 illustrates a concept of how the remote sensing applications can be used for assessing the tsunami vulnerability, exemplified for a mangrove ecosystem. In order to better describe the vulnerability of a mangrove ecosystem in general, the spatial scale of the assessment was extended from the pixel-level to the patch level. A patch can be regarded as a functional unit of an ecosystem (cp. Burel and Baudry 2003).

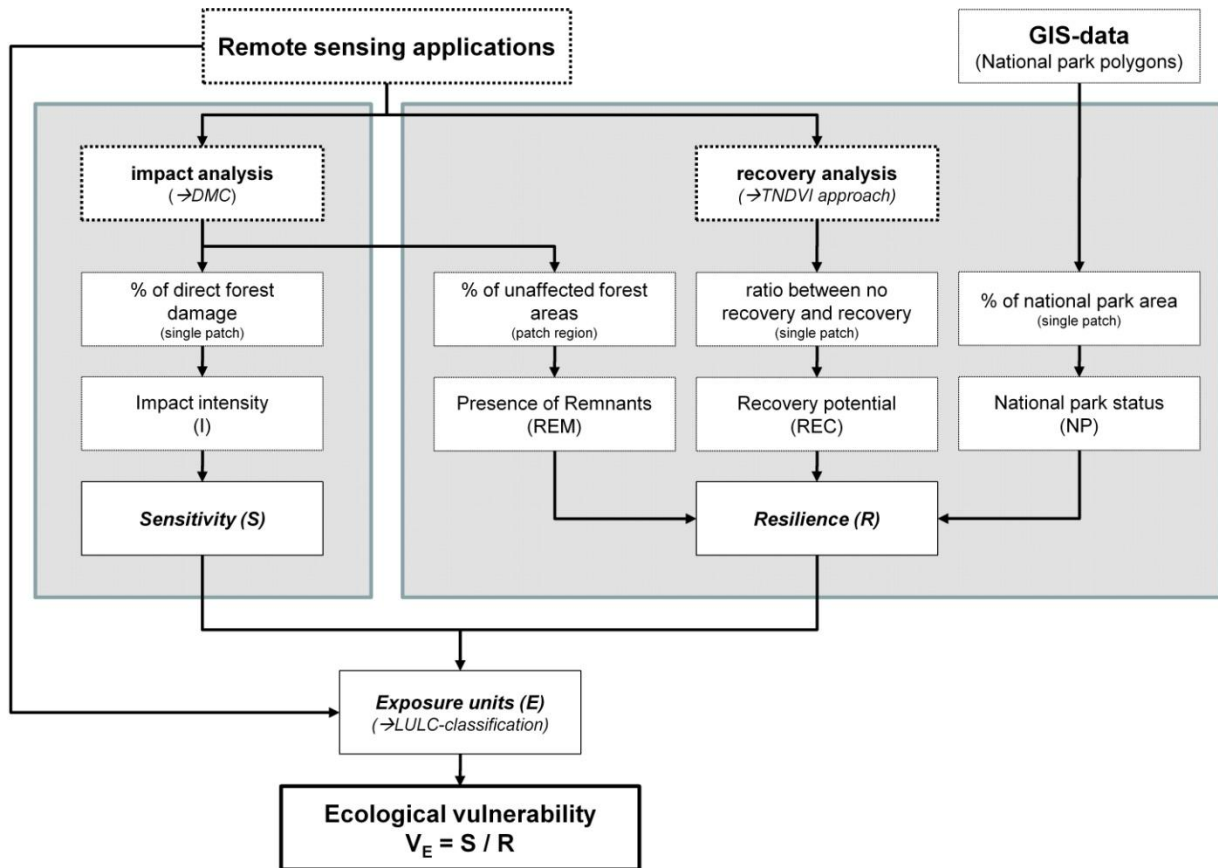


Figure 6-5. Retrospective assessment of the vulnerability of mangrove forests.

First, the ecological sensitivity ( $S$ ) of an exposed element can be indirectly determined by the tsunami impact intensity ( $I$ ) which can be expressed by the pixel ratio between the direct forest damage area and the total patch area. Here the change detection results are used, as provided by the direct multi-date classification (Roemer *et al.* 2010a).

$$\text{Sensitivity } (S) = \frac{\text{direct damage area}}{\text{patch area}} \quad (4)$$

The resilience can be estimated by the recovery potential ( $REC$ ), the presence of remnants ( $REM$ ) and the information on the national park status ( $NP$ ).  $REC$  is calculated for patches that were impacted by the tsunami, applying the pixel ratio between pixels indicating recovery and those indicating no recovery processes. Here, the binary coded change map derived from the TNDVI approach (cp. Roemer *et al.* 2010b) is applied. In order to focus more on the system understanding (Holling 1973), resilience is also assessed by considering the availability or presence of remnants (cp. Adger *et al.* 2005). Here, the spatial focus is changed from the single patch scale towards the patch region being composed of several connected mangrove patches (compare Burel and Baudry 2003). The idea is that propagules can easily be distributed and move in mangrove patches that are connected and thus belong to a mangrove patch region.

*REM* is quantified by the pixel ratio between the total of non-impacted mangrove area (derived from DMC, cp. Roemer *et al.* 2010a) and the total area of the respective mangrove patch region.

In the examined study area, five different mangrove patch regions can be distinguished (cp. Table 6-1): two larger connected mangrove regions with one being located in the northern part of the study area near Ban Nam Khem (93.55 ha) and the other being located in the south with an area of 830.48 ha, and three smaller isolated mangrove regions occurring between Krang Nui Cape and Khuk Kak with a total area of 57.78 ha comprising a total of four single forest patches. The national park status captures the information on the potential environmental stresses on the ecosystems and thus can be regarded as an indicator for ecological resilience (cp. Adger *et al.* 2004). *NP* was simply quantified by the ratio between the area under protective status and the respective patch area. The resilience term can be calculated by the arithmetic mean of the three described indicators and is scaled between 0 and 1:

$$\text{Resilience}(R) = \frac{1}{3} \times (\text{REC} + \text{REM} + \text{NP}), \text{ whereas} \quad (5)$$

$$\text{REC} = \frac{\text{recovery area}}{\text{no recovery area}}, \quad \text{REM} = \frac{\text{unaffected patch area}}{\text{area of patch region}}, \quad \text{NP} = \frac{\text{protected area}}{\text{patch area}} \quad (6)$$

\*in case of a non-impacted patch, the arithmetic mean of REM and NP was considered

The vulnerability of a specific exposure unit ( $V_E$ , *dimensionless*) is calculated by the ratio between sensitivity  $S$  and resilience  $R$  (cp. Villagrán De León 2006) and is scaled between 0 (no vulnerability) and 10 (high vulnerability) (e.g. in a case if  $S$  approaches 1 and  $R$  0.1, depending on the number of decimals used):

$$\text{Vulnerability}(V_E) = \frac{S}{R} = \frac{\frac{\text{direct damage area}}{\text{patch area}}}{\frac{1}{3} \left( \left( \frac{\text{recovery area}}{\text{no recovery area}} \right) + \left( \frac{\text{unaffected patch area}}{\text{area of patch region}} \right) + \left( \frac{\text{protected area}}{\text{patch area}} \right) \right)} \quad (7)$$

The results of the vulnerability analysis aggregated for the mangrove patch regions are illustrated in Table 6-1. It can be concluded that by trend the larger forest regions in the south (Tap Lamru estuary) and in the north around Ban Nam Khem are less sensitive, more resilient and thus less vulnerable to tsunamis than the three smaller patch regions. These results relate well with findings observed by Paphavasit *et al.* (2009) from the mangrove forests near Ban Nam Khem. They concluded from field observations conducted in November 2005 that the mangroves were resilient to the tsunami since they have continued to serve as habitats, nursery and feeding grounds for numerous mangrove species. The highest resilience can be observed for the southern areas near Thai Mueang due to the high availability of remnants within this area and due to fact that a main part (39%) is protected by national park status. Since no recovery assessment for these mangrove patches was made in this study, an estimated recovery value had to be accepted and was added for the tsunami impacted regions. The estimation was derived from the arithmetic mean of the recovery values calculated for the northern mangrove patches (0.63).



Even assuming a lower recovery potential, the resilience term would still be very high in comparison to the other mangrove areas. Highest vulnerability can be observed for the mangroves near Pakarang Cape, due to high tsunami sensitivity and low remnant quantity.

**Table 6-1.** Calculation of tsunami sensitivity, resilience and vulnerability for mangroves (patch region).

name of patch region	total area (ha)	N patches	REC	REM	NP	S	R	V
Ban Nam Khem	93.55	8	0.45	0.87	0.00	0.04	0.44	0.09
Krang Nui Cape	4.40	1	0.43	0.28	0.00	0.29	0.24	1.23
Pakarang Cape	25.61	1	0.36	0.24	0.00	0.75	0.20	3.75
Khuk Kak	27.77	2	0.91	0.46	0.00	0.30	0.46	0.65
Tap Lamru estuary	830.48	21	0.63	0.93	0.39	0.05	0.65*	0.08

\* an estimated REC- value calculated from the arithmetic mean REC-values of the change detection results provided for the other mangrove patches in the north.

The vulnerability can be roughly classified into “high vulnerable”, “medium vulnerable”, “low vulnerable” and “not vulnerable”. No vulnerability applies for those patches that were not affected by the tsunami ( $S$  is “0”). Low vulnerability applies when  $S$  is lower or equals the  $R$  value (Vulnerability: 0.01 - 1.00). A medium vulnerability occurs if  $R < S \leq 2R$  (1.01 – 2.00). A high vulnerability occurs if the term exceeds 2.00. Figure 6-6 shows the map of the vulnerability analysis of mangrove ecosystems using equation (7) and the described classification scheme. In general, most of the mangrove areas in the study area are either not or low vulnerable. However, medium and high vulnerabilities occur particularly for the smaller isolated patches near Krang Nui and Pakarang Cape, but also for some patches in the southern mangrove areas, in particular in the outer zone of the estuary near Tap Lamru.

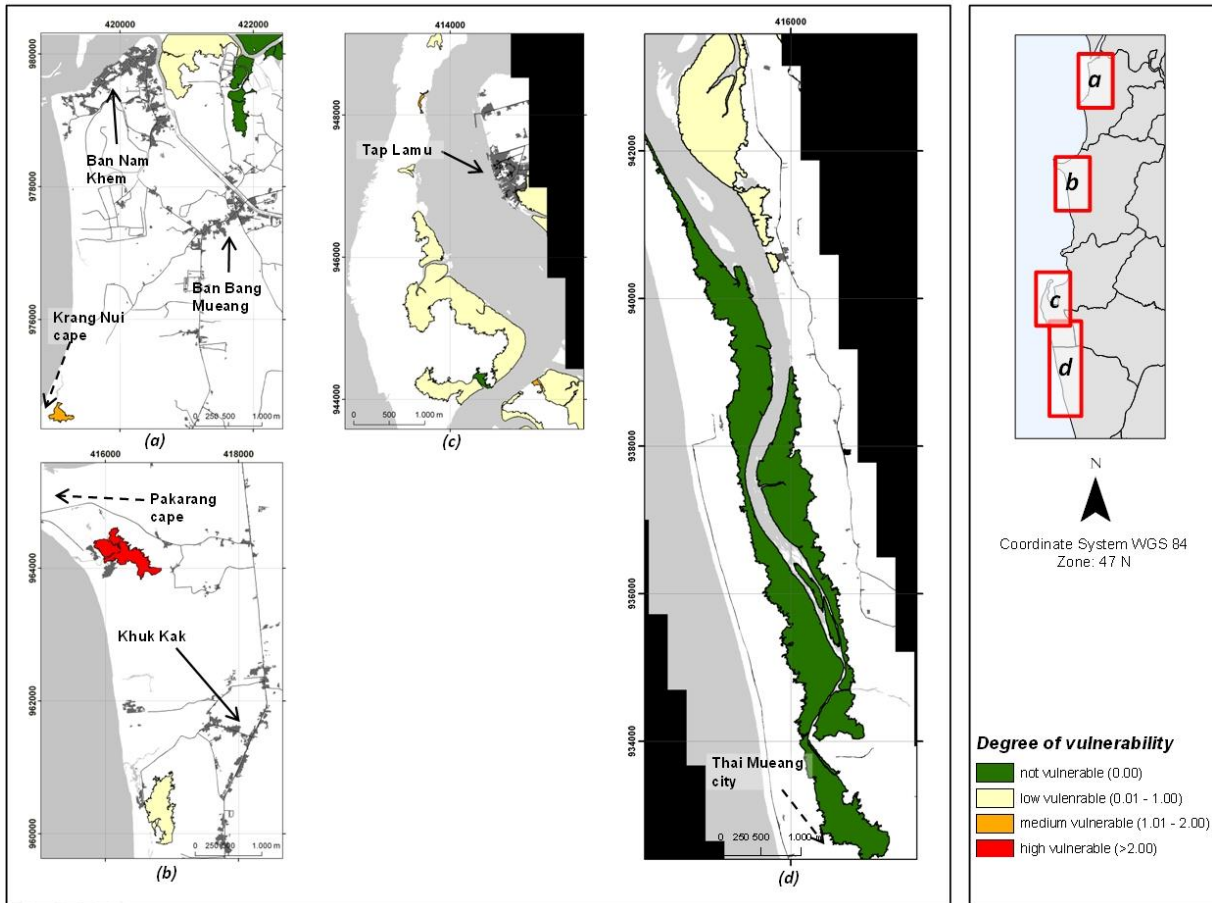


**Figure 6-6.** Retrospective analysis of tsunami vulnerability of mangrove areas (patch level). (a) the northern area with the patch region near Ban Nam Khem and the small are near Krang Nui cape, (b) the small patches at Pakarang cape and near Khuk Kak, (c) the outer part of the estuary near Tap Lamru and (d) the inner and sheltered part of the estuary north of Thai Mueang city.

It can be concluded that the presented approach is useful to retrospectively analyse and compare the tsunami vulnerability of a certain ecosystem for different coastal segments. The presented approach can also be extended and further developed: either by adding other vulnerability and resilience indicators or by incorporating more GIS-based vulnerability indicators focussing on the spatial patterns of forest patches (e.g. landscape metrics). Furthermore, the approach is in principle transferable to the other examined coastal ecosystems, but it needs to be mentioned that resilience indicators have to be carefully and specifically selected for each ecosystem. In this regard, the availability of remnants can be considered as relevant for mangrove forests, however, this indicator might be less important for other ecosystems, were seeds can be easily dispersed by wind.

### 6.2.2 Identification of factors determining the tsunami vulnerability

As spatially explicit information on the tsunami impacts and the recovery processes are derived within this study, a basic question remains whether the observed spatial variability can be explained or predicted by different underlying factors being related to physical impacts and vegetation recovery processes.

In order to provide a statistical evidence of these factors, a GIS-based approach is developed by which the two proxy indicators of vulnerability, recovery and impacts, are considered as dependent variables and are correlated and regressed against a set of predictor variables (or independent variables). The statistical approach is illustrated on Figure 6-7. For the regression, a multiple-linear regression approach was selected, which is a standard and widely used statistical method to model the relationships between multiple independent predictor variables and a single dependent variable (cp. FAO 1999; Rawlins *et al.* 2010). The model quality is estimated by the adjusted  $r^2$ , which is an appropriate measure when models with different numbers of independent variables need to be compared (Grimm and Yarnold 1994). Furthermore, standardised beta values ( $\beta$ -values) are calculated which provide information on the relative importance or weight of a predictor variable in the regression model. These values are described by the number of standard deviations that the outcome will change as a result of one standard deviation change in the predictor. Thus,  $\beta$ -values are measured in standard deviation units and are directly comparable. In order to better estimate the relative importance of a predictor variable, multicollinearity in the regression models had to be considered. Here, the Variance Inflation Factor (VIF) was calculated (for more details please see Grimm and Yarnold 1994).

All variables are aggregated to a uniform 30 x 30-meter grid. This allows the quantitative representation of even binary scaled input variables which is an important premise for the multiple linear regression approach. Besides the examined five coastal ecosystems, an additional ecosystem class (mixed vegetation cover) is added, including all kinds of vegetation classes distinguished in the LULC-classification (section 4.2.1). This class is considered to investigate both the tsunami impacts in the coastal area in general and the relationships between location and hazard variables (cp. section 6.2.2.2).

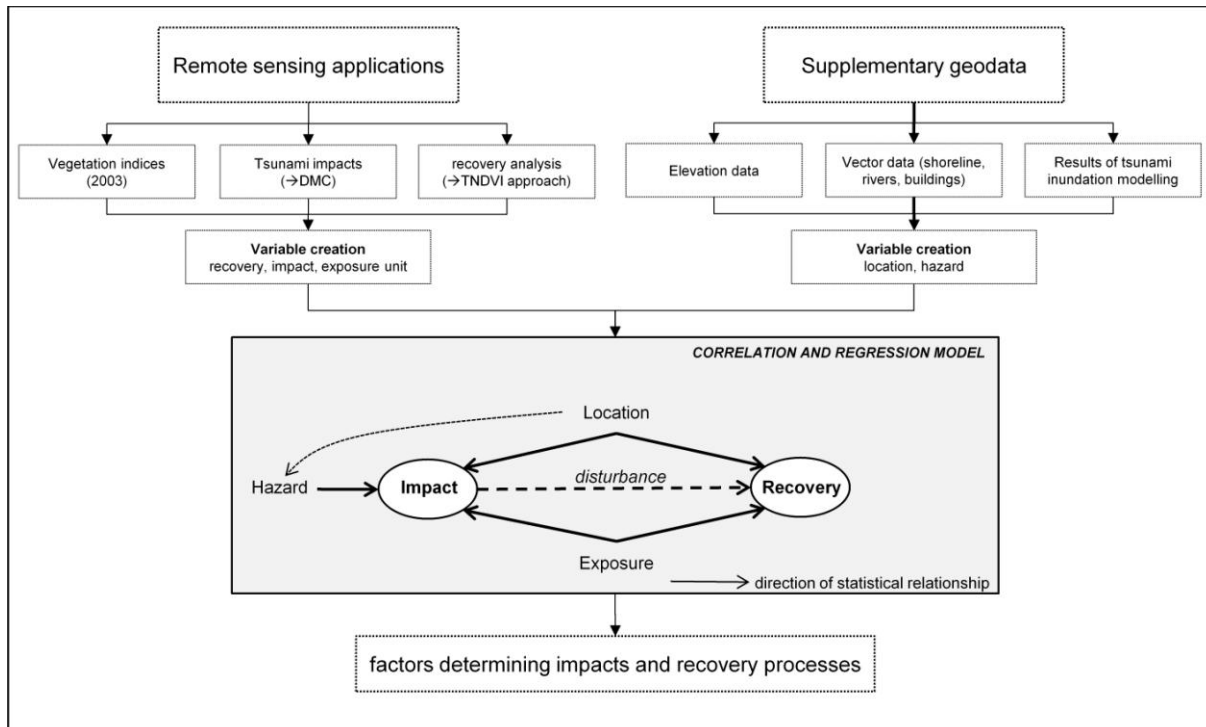


Figure 6-7. Concept of the statistical approach for the identification of factors determining tsunami sensitivity and recovery

#### 6.2.2.1 Dependent variables

The results of the impact and recovery analysis (cp. Roemer *et al.* 2010a/b) can be used to derive dependent variables. *Tsunami impact intensity* is represented by the variable  $I$  that is calculated as the pixel ratio between impacted and non-impacted pixels derived from the binary coded change map (DMC). Recovery is represented by two variables:  $R_1$  representing the *recovery potential*, and  $R_2$  being the *recovery rate*. Whereas  $R_1$  is calculated as the ratio between pixels indicating recovery and those indicating no recovery processes (TNDVI-approach),  $R_2$  is estimated from the mean value of the TNDVI-values of the post-tsunami scene of 2008. Due to the fact that recovery assessment was carried out for the northern part of the study area, mixed beach forests and melaleuca forests are not considered for the recovery analysis.

#### 6.2.2.2 Independent variables

Four types or groups of independent variables are considered in the statistical approach: a) *hazard variables* that refer to the physical intensity of the tsunami hazard itself, b) *location variables* that describe the characteristics of the location or the exposition of an exposed element (*location variables*), c) *exposure unit variables* that refer to the internal properties of the examined ecosystem and d) *the amount of disturbance* that characterises the intensity of tsunami induced impacts or damages on certain exposed ecosystem. The variable groups a), b) and c) are considered for the analysis of tsunami impacts, whereas b) and c) are considered for the recovery analysis.

### Exposure unit variables

Regarding the exposure unit variables, the literature review (cp. section 3.3) reveals that tsunami induced impacts on forests are determined by the tree species, respectively the type of forest and the forest age. Both attributes capture tree and stand characteristics, such as the properties of the roots and wood, the elasticity of stems and branches, the volume of tree crowns and the density of foliage (Cochard *et al.* 2008; FAO 2005b; Tanaka *et al.* 2007). Due to the lack of spatially explicit pre-tsunami information on these vegetation properties, proxy indicators need to be selected. In this approach the  $NDVI_{03}$  as well as the first tasselled cap component  $TC1_{03}$ , calculated from the pre-tsunami IKONOS image, are applied (Roemer *et al.* 2010a). According to Lu *et al.* (2004b) and Freitas *et al.* (2005), vegetation indices (e.g. the NDVI, Tasselled cap components) correlate well with forest stand parameters such as above ground biomass, basal area, average stand height or average stand diameter. Thus, the basic hypothesis was that forest impacts were more pronounced in forests with low stand densities, low average stem diameters and tree heights and therefore negatively correlates with the  $NDVI_{03}$  and respectively positively correlates with  $TC1_{03}$ . Due to the fact that coconut plantations, melaleuca forests and mixed beach forest were predominately not directly affected by the tsunami, exposure unit variables are not further considered for these ecosystems. Furthermore, the indices were tested and validated in dense forests and thus cannot be automatically transferred to open woodlands (Lu *et al.* 2004b).

Regarding the assessment of vegetation recovery, exposure unit variables encompass aspects such as ecosystem health or functionality and by the type of the ecosystem (ecological strategy). Due to a lack of detailed data on the pre- and post-tsunami functionality or system health, exposure unit variables could not be meaningfully represented as a spatially explicit variable. Thus, they are not further considered for this statistical analysis. However, regarding the comparison of recovery rates and recovery potentials between the examined ecosystems, a high relevance of exposure unit variables could be detected (cp. section 6.1.2 and Roemer *et al.* 2010b).

### Hazard variables

The *maximum total water depth above ground* ( $W, m$ ) and the *maximum current speed* ( $CS, ms^{-1}$ ) derived from inundation modelling (cp. section 4.5.2) are used as hazard variables. Accurate modelling results were only available for the northern areas between Khao Lak and Ban Nam Khem and thus cannot be considered for the southern area particularly containing melaleuca forests and mixed beach forests.

### Location variables

According to Cochard *et al.* (2008), the great variability in impacts at regional and local scales has not been sufficiently recognised by either managers or researchers. However, field measurements and the literature review reveals that tsunami damage intensities varied strongly by location. In order to consider these effects in the analysis of tsunami impacts and recovery processes, six variables are used and termed as location variables. The *distance to the shoreline* ( $D, m$ ) and the *distance to the river* ( $R, m$ ) taken from respective shape files (cp. Table 4-6).  $R$  is selected due to the observation that impacts on mangrove forests were more severe near the riverfront. The terrain effects are considered by two variables: *depth of topographic sinks* ( $S, m$ ) and *elevation asl.* ( $E, m$ ).  $S$  is calculated by using the fill-tool provided in ESRI's ArcGIS to fill all sinks in the MFC-DLSM (cp. Table 4-6). Then, the DLSM was subtracted from the fill-raster.



This variable is selected based on the hypothesis that degradation processes of vegetation are more pronounced in areas, where water has remained in pools or topographic depressions after the tsunami.  $E$  was used for the recovery analysis, since field observations suggested that recovery processes in low terrain are low. This applies particularly to the seafront area, where marine erosion processes have increased after beach sediments were massively eroded by the tsunami. Furthermore the *inclination of the coastline* ( $In$ , °) is considered for the impact analysis in order to investigate the effects resulting from different coastline expositions to the tsunami wave direction. As the modelling results reveal that the tsunami wave approached the coast from a western direction, the variable is calculated by the absolute value of the difference angle between the actual coastline orientation (°) and 270° (representing a west-exposed coast). Thus, lee- or eastbound coasts (e.g. north of Pakarang Cape) get higher values for  $I$  than west-exposed coasts. The sixth location variable ( $H$ , %) captures the effects from *human activities* occurring in a specific area and is only considered for the recovery or resilience assessment. The quantitative and geographical representation of the intensity of human impacts is a challenging scientific issue. Here, the change rate of building area (%) between 2003 and 2009 is derived from image analysis. The variable can be considered as an indicator of changes in population density or in tourism activity and is calculated by the change of building area (%) derived from the building polygons of 2003 (IKONOS) and those of 2009 (MFC-data, cp. section 4.5.1). As the change rates are calculated for bigger area (300 x 300 grid), the variable can be regarded as a rough proxy indicator for the degree of human activities that might have caused pressures (e.g. disposal of waste, construction of infrastructure) on surrounding ecosystems. It is assumed, that recovery processes are less pronounced in areas where human activities and developments were increased.

#### Amount of disturbance

Beside the variables that describe the local site conditions including the human pressure, resilience variables should also encompass the amount of disturbance in this case the tsunami impact. The *amount of disturbance* was represented by the variable  $AD$  calculated by the ratio between pixels classified as direct damages (forest → sand, forest → mud, forest → water) and those classified as other change classes such as indirect forest damage and no/low damages (Roemer *et al.* 2010a). It was assumed that recovery processes were less pronounced in areas that were highly impacted by the tsunami.

#### 6.2.2.3 Results of the statistical analysis

##### Relationship between hazard and location variables

Table 6-2a shows the correlation coefficients of location and hazard variables. The statistics are calculated for the northern part of the study area and the mixed vegetation cover class. The results show that both hazard variables strongly correlate with  $D$  and  $E$  (each with 0.66). Low correlations occur for the variables  $R$  and  $S$ , whereas moderate relationships can be observed for  $In$ . This implies that northern or southern exposed coasts obviously suffered from stronger tsunami impacts than west exposed coasts.

These results can causally be explained by the fact that most of the west-exposed coasts occur in bays such as between Hin Chang Cape and Pakarang Cape or between Krung Noi Cape and Ban Nam Khem where bathymetric slopes are generally lower than near the capes (cp. bathymetric map provided by Ministry of Defence, Table 4-6).

This implies an earlier breaking of tsunami waves in the bays and thus a lower wave energy reaching the coastal zones in these areas. A second reason can be seen in the wave refraction processes that predominately occurred near the capes and might also have caused higher wave energies in these areas. The results of the multiple regression model (Table 6-2d) using *CS* as dependent variable reveal that all locations variables together explain a main part of the variance of *CS* with an adjusted  $r^2$  of 0.56.

#### Relationship between impacts and hazard, variables, location and exposure

Table 6-2b illustrates the correlation coefficients between *I* and the predictor variables hazard, exposure unit and location. Table 6-2d shows the results of the regression analysis. Both tables reveal only low statistical relationships for coconut plantations. This is related to the fact that impact information derived from change detection applications a) cannot be traced back clearly to the tsunami event (cp. Roemer *et al.* 2010a) and b) are related to different damage processes such as damage to understory vegetation and direct damages to coconut trees. In general, hazard variables, and here particularly *CS*, correlates well for mangrove forests, casuarina beach forests and the mixed vegetation cover class (Table 6-2b). The corresponding multiple regression (Table 6-2d) reveals that 19%, 30% and 31% of the variance of *I* can be explained by using the hazard variables (for casuarina beach forests, mixed vegetation cover and mangrove forests respectively). In contrast, low statistical relationships between hazard variables and *I* can be observed for melaleuca and mixed beach forests and are likely the result of the lower accuracy in the input data used for this variable (cp. Table 6-2b/d).

Regarding the exposure unit variables, the  $NDVI_{03}$  show a medium (for mangrove forests) and a low (for casuarina beach forests) statistical relationship with *I* (Table 6-2b). The negative correlation with  $NDVI_{03}$  would confirm the hypothesis that tsunami impacts were more pronounced in forests with lower stand densities, trunk diameters and tree heights. However, correlation coefficients are significantly lower for  $TCI_{03}$ .

Referring to the location variables (Table 6-2b), *I* correlates best with *D* (max. *r*-value of 0.55). However, this does not apply for casuarina beach forests, as they are evenly arranged in stripes occurring on sand dunes at the seafront. In addition, high and medium correlations with *E* can be observed for mixed vegetation cover ( $r=0.50$ ), casuarina beach forests and melaleuca forests. In contrast, *E* is not strongly correlated with forest ecosystems that occur in low and flat areas, such as mangrove forests and mixed beach forests. *S* is usually low correlated with impacts and thus has a low explanatory power.

The distance to river (*R*) correlates moderately for mangrove forests (-0.22) and melaleuca forests (-0.38), which would generally confirm the above hypothesis. *In* refers to the orientation of the coastal zone, with highest correlation found for casuarina beach forests.

In the multiple regression models (Table 6-2d), location variables are aggregated and analysed as a group. The adjusted  $r^2$ -values ranges from 0.13 (casuarina beach forests) to 0.36 (melaleuca forests) indicating low respectively moderate statistical relationships. In the case of mangrove forests, the explanatory power of the model is significantly increased by adding the exposure unit variable  $NDVI_{03}$  to the model ( $r^2=0.33$ ). However, highest model quality is observed when hazard variables are combined with exposure unit variables, explaining 27% (casuarina beach forests) to 43% (mangrove forest) of the total variance of  $I$ .

#### Relationship between recovery, location and disturbance

The relationships between vegetation recovery, impact and location variables are illustrated in Table 6-2. The correlation statistics (Table 6-2c) reveal that  $R_1$  and  $R_2$  are mainly determined by the intensity of impacts and the elevation asl. (for casuarina beach forests mangroves). These findings relate well to observations from the literature (cp. section 3.2) and from the field surveys: casuarina beach forests recovered well particularly on the higher areas of the dunes.

In contrast, recovery in mangrove forests started from the inner, less impacted and slightly more elevated areas with higher abundances of mature trees acting as growth points for forest renewal (cp. Adger *et al.* 2005). A moderate positive correlation with  $R$  indicates that recovery processes in mangrove forests are less pronounced at the riverfront. This finding can be proved in several study sites, e.g. site number 14 (Roemer *et al.* 2010b). As tsunami impacts can include the erosion of soils and sediments or the deposition of marine sediments, it is plausible that recovery processes were less pronounced in intensively impacted areas. With regard to the mixed vegetation cover class and casuarina beach forests, human impacts tend to have a negative influence on recovery processes. This finding confirms the observations made during field visits. Particularly in higher populated areas such as near Ban Nam Khem and Khao Lak, many young and old casuarina trees were removed and replaced by houses or infrastructure. In contrast, the human influence on mangrove recovery cannot be clearly demonstrated by the statistical approach. However, the field studies and personal communication with Thai experts revealed that most of mangrove stands between Nang Thong and Ban Nam Khem have been strongly impacted by humans, e.g. the regulation and changes of the flow regimes or the construction of aquaculture in mangrove forests. Thus, one possible reason of the low positive correlation is related to the fact, that  $H$  does not adequately represent all types of human interventions occurring in the study area. Further, mangrove forests were replanted in some areas, which additionally complicates the interpretation of the observed recovery processes.

Due to the fact that recovery information derived for coconut plantation is related to the affected fast growing understory vegetation, correlation statistics for this ecosystem cannot be related to the succession and recovery processes following the tsunami and are thus not further considered (cp. discussion section in Roemer *et al.* 2010b). The problem in interpretation also applies in an attenuated form to the mixed vegetation cover class which is composed of fast growing grasslands and open landscapes. Regarding the regression statistics provided in Table 6-2d, the models can explain up to 50% and 44% of the total variance of  $R_2$  (for mangrove forests and casuarina beach forests, respectively). With regard to the mangrove forests,  $R_2$  is equally determined by location ( $r^2=0.29$ ) and impact variables ( $r^2=0.33$ ), while recovery of casuarina beach forests is particularly determined by the location variables only (0.35).

**Table 6-2.** Results of the correlation and regression analysis. (a)-(c) represent the correlation statistics between hazard and location (a) between impact, location, exposure and hazard (b) and between recovery, location and impact (c). (d) shows the results of the regression models (adjusted r<sup>2</sup>).

Variables <sup>d</sup> (N=59838)	W	CS
D	-0.66 <sup>b</sup>	-0.66 <sup>b</sup>
R	-0.12 <sup>b</sup>	-0.05 <sup>b</sup>
S	-0.00	-0.01
E	-0.66 <sup>b</sup>	-0.66 <sup>b</sup>
In	+0.21 <sup>b</sup>	+0.37 <sup>b</sup>

(a)

Variables <sup>d</sup>	variable group	Man N=10521	Cas N=986	Coc N=4152	MBF N=2026	Mel N=509	Mix N=59838
W	hazard	+0.35 <sup>b</sup>	+0.10 <sup>b</sup>	-0.06 <sup>b</sup>	+0.09 <sup>b</sup>	+0.33 <sup>b</sup>	+0.48 <sup>b</sup>
CS	hazard	+0.55 <sup>b</sup>	+0.44 <sup>b</sup>	-0.09 <sup>b</sup>	+0.21 <sup>b</sup>	+0.38 <sup>b</sup>	+0.54 <sup>b</sup>
NDVI <sub>03</sub>	exposure	-0.40 <sup>b</sup>	-0.12 <sup>b</sup>				
TC1 <sub>03</sub>	exposure	+0.17 <sup>b</sup>	+0.16 <sup>b</sup>				
D	location	-0.43 <sup>b</sup>	+0.03	+0.06 <sup>b</sup>	-0.55 <sup>b</sup>	-0.46 <sup>b</sup>	-0.48 <sup>b</sup>
R	location	-0.22 <sup>b</sup>	+0.04	+0.00	-0.04	-0.38 <sup>b</sup>	-0.01 <sup>b</sup>
S <sup>c</sup>	location	+0.18 <sup>b</sup>	+0.12 <sup>b</sup>	-0.10 <sup>b</sup>			-0.05 <sup>b</sup>
E	location	-0.11 <sup>b</sup>	-0.31 <sup>b</sup>	-0.14 <sup>b</sup>	-0.05 <sup>a</sup>	-0.23 <sup>b</sup>	-0.50 <sup>b</sup>
In	location	+0.20 <sup>b</sup>	+0.22 <sup>b</sup>	+0.13 <sup>b</sup>	-0.01	-0.01	+0.12 <sup>b</sup>

(b)

Variables <sup>d</sup>	Variable group	Man N=720		Cas N=845		Coc N=4105		Mix N=22425	
		R <sub>1</sub>	R <sub>2</sub>	R <sub>1</sub>	R <sub>2</sub>	R <sub>1</sub>	R <sub>2</sub>	R <sub>1</sub>	R <sub>2</sub>
AD	disturbance	-0.53 <sup>b</sup>	-0.57 <sup>b</sup>	-0.22 <sup>b</sup>	-0.41 <sup>b</sup>	+0.07 <sup>b</sup>	-0.10 <sup>b</sup>	-0.01	-0.15 <sup>b</sup>
D	location	-0.11 <sup>b</sup>	+0.11 <sup>b</sup>	+0.08 <sup>a</sup>	+0.22 <sup>b</sup>	+0.17 <sup>b</sup>	+0.09 <sup>b</sup>	+0.01	+0.17 <sup>b</sup>
R	location	+0.28 <sup>b</sup>	+0.20 <sup>b</sup>	+0.13 <sup>b</sup>	-0.01	+0.21 <sup>b</sup>	+0.20 <sup>b</sup>	+0.09 <sup>b</sup>	+0.04 <sup>b</sup>
E	location	+0.48 <sup>b</sup>	+0.27 <sup>b</sup>	+0.34 <sup>b</sup>	+0.57 <sup>b</sup>	+0.24 <sup>b</sup>	+0.32 <sup>b</sup>	+0.13 <sup>b</sup>	+0.27 <sup>b</sup>
S	location	-0.19 <sup>b</sup>	-0.30 <sup>b</sup>	+0.03	+0.00	-0.15 <sup>b</sup>	-0.12 <sup>b</sup>	-0.03 <sup>b</sup>	-0.01
H	location	+0.14 <sup>b</sup>	+0.13 <sup>b</sup>	-0.27 <sup>b</sup>	-0.17 <sup>b</sup>	-0.29 <sup>b</sup>	-0.29 <sup>b</sup>	-0.27 <sup>b</sup>	-0.24 <sup>b</sup>

(c)

Dep. Variables <sup>d</sup>	Independent variables		Model result (adjusted r <sup>2</sup> )					
	variable group	variables	Man	Cas	Coc	MBF	Mel	Mix
CS	location	D, R, E, S, In						(0.56)
I	exposure	NDVI <sub>03</sub>	0.19	0.03	-	-	-	-
I	location	D, R, E, In	0.25	0.13	0.05	0.34	0.36	0.30
I	hazard	W, CS	0.31	0.19	0.01	0.09	0.14	0.30
I	exposure, location	NDVI <sub>03</sub> , D, R, E, In	0.33	0.13	-	-	-	-
I	exposure, hazard	NDVI <sub>03</sub> , W, CS	0.43	0.22	-	-	-	-
R <sub>2</sub>	location	D, R, E, S, H	0.29	0.35	-	-	-	0.14
R <sub>2</sub>	disturb.	AD	0.33	0.17	-	-	-	0.02
R <sub>2</sub>	location, disturb.	D, R, E, S, H, AD	0.50	0.44	-	-	-	0.14

(d)

<sup>a</sup> correlation is significant at the 0.05 level (2-tailed)

<sup>b</sup> correlation is significant at the 0.01 level (2-tailed)

<sup>c</sup> Statistics were calculated only for the northern study area between Ban Nam Khem and Nang Thong

<sup>d</sup> variable abbreviations: **AD**=amount of disturbance (ratio); **CS**=max. current speed (ms<sup>-1</sup>); **D**=distance to shoreline (m); **E**=elevation asl. (m); **H**=human activities and population growth (%); **I**=tsunami impact intensity; **In**=Inclination of coastline (°); **NDVI<sub>03</sub>**=NDVI of pre-tsunami image; **R**=distance to river (m); **R<sub>1/2</sub>**=recovery potential (1) and rate (2); **S**=Depth of topographic sinks; **TC1<sub>03</sub>**=first tasseled cap component of the pre-tsunami image; **W**=max. total water depth above ground (m).

Man, Cas, Coc, MBF, Mel, Mix stand for mangrove forests, casuarina beach forests, coconut plantations, mixed beach forests, melaleuca forests and mixed vegetation cover, respectively.

### Standardised beta values – exemplified for mangrove forests

Standardised beta values can be used to estimate the relative effect or importance of a single independent variable in predicting the dependent variable. Low effects are indicated by values approaching zero, whereas values approaching either +1 or -1 indicate strong positive or negative effects. Standardised beta values are calculated for selected regression models and are illustrated in Appendix Q and in Figure 6-8 (here, exemplified for the mangrove ecosystem). As hazard and location variables are causally related, they are not combined in a regression model. Comparing the effects of hazard and exposure unit variables for mangroves, impacts are mostly determined by *CS* (+0.41) followed by the *NDVI<sub>03</sub>* (-0.36), cp. Figure 6-8a. In contrast, regarding the standardised beta values calculated for location and exposure unit variables (Figure 6-8b), mangrove impacts are mainly determined by *D* (-0.38), the *NDVI<sub>03</sub>* (-0.30) and *R* (0.08). Recovery processes of mangrove forests are predominantly determined by the amount of disturbance *AD* with -0.51 and the elevation *E* with 0.38, *H* (0.14) and *S* (0.11) (Figure 6-8c).

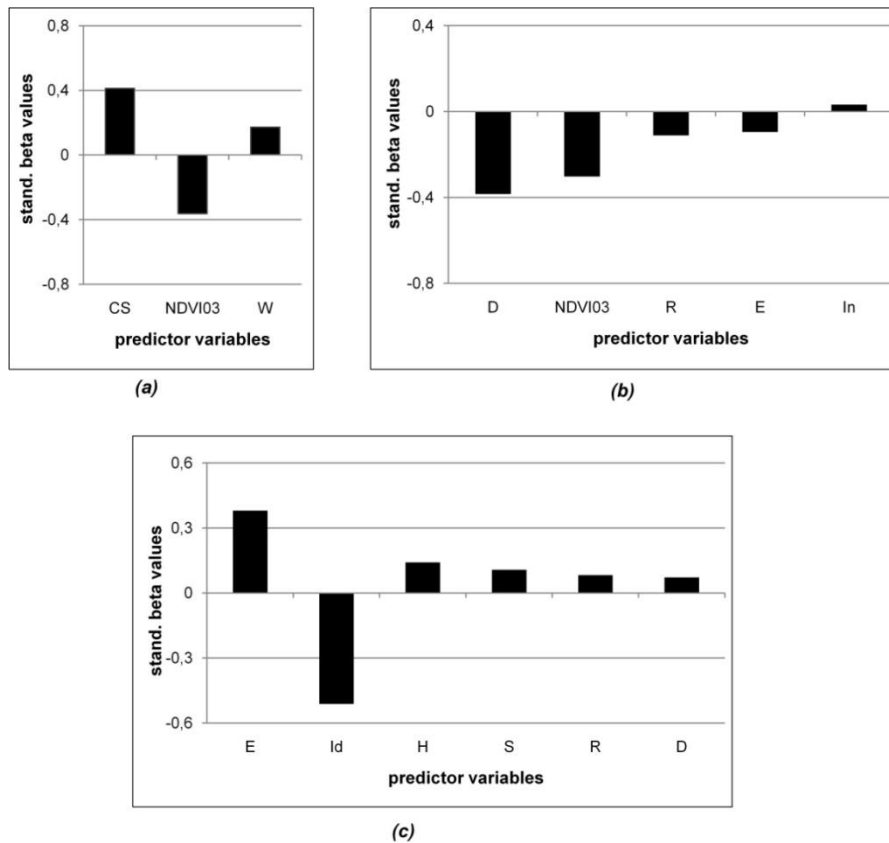


**Figure 6-8.** Standardised beta values calculated for selected regression models, exemplified for mangrove forest. The model (a) and (b) use *I* as dependent variables whereas model (c) uses  $R_2$  as dependent variable.

#### 6.2.2.4 Evaluation of the statistical approach

It can be concluded, that the correlation statistics and the regression models reveal only low or moderate statistical relationships for the following reasons: First, tsunami impacts and recovery processes are complex in ecosystems that are determined by a number of contributing factors.



Because of a lack of accurate spatially explicit pre- tsunami data that characterise the exposure units itself (e.g. type, density, age of vegetation), and due to a lack of pre-tsunami information on the health and functionality of the ecosystems in general, the statistical models cannot be regarded as complete. This is why the regression model cannot explain the total variance of the dependent variables. As the major part of the considered variables are related to the external system, including hazard and location variables and amount of disturbance, the main potential of this statistical approach is to analyse the extrinsic component of vulnerability (Villa and McLeod 2002). In contrast, the intrinsic or system-related vulnerability can only be partly considered in this approach (vegetation indices of the pre-tsunami situation or human impacts that are indirectly related to the ecosystem health).

The extent to which the regression models can be used to estimate and predict the tsunami vulnerability is exemplified for tsunami impacts on mangrove forests, as illustrated in Figure 6-9. In this example the observed impacts derived from change detection (Figure 6-9a) are compared to the modelled impacts (Figure 6-9b, c). Two models are used in this Figure: the first includes hazard and exposure unit variables with an adjusted  $r^2$  of 0.43 (cp. regression statistics in Appendix R and Figure 6-9b); the second model includes location and exposure unit variables with an adjusted  $r^2$  of 0.33 (Appendix S, Figure 6-9c). The corresponding linear regression equations are also added to this Figure. The maps confirm the assumption that the model with the higher  $r^2$ -value provides the more accurate results. However, even the model with lower  $r^2$  is capable to roughly predict tsunami induced impacts. Since location variables can be easier obtained (e.g. from remotely sensed data) than inundation modelling results, this model (Figure 6-9c) is more transferrable in this respect. However, as location variables are not related to the relevant physical processes, this model is only useful to predict impacts for this particular tsunami scenario.

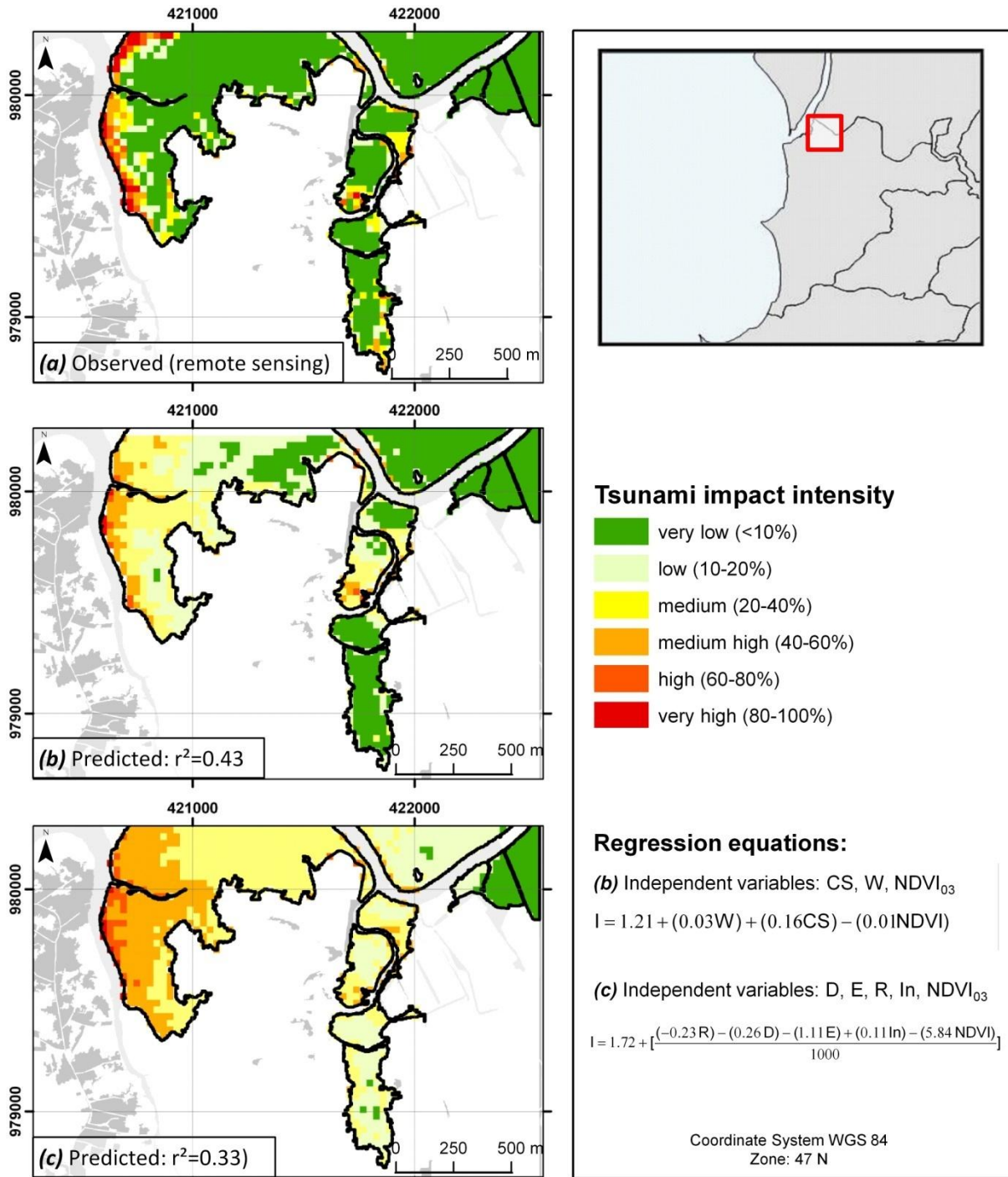


**Figure 6-9.** Observed and modelled tsunami induced impacts, exemplified for a mangrove area near Ban Nam Khem. (a) the observed impacts based on the change detection techniques (variable *I*), (b) and (c) are predicted (modelled) tsunami impacts based on linear regression models with (b) including hazard and location variables and (c) including location and exposure unit variables.

### 6.3 Evaluation of the potential and limitations of remote sensing techniques in ecological vulnerability analysis

Referring to the basic question asked in the introduction, it needs to be discussed to what extent remote sensing techniques can support the assessment of ecological vulnerability.

#### Potential

This thesis demonstrates that remote sensing techniques are useful to support the analysis and monitoring of ecological vulnerabilities on a local scale. The ability of providing spatially explicit information on the examined processes can be regarded as a main benefit of the methodological approach in this study. The results are useful to assess the short and long-term effects of the tsunami on coastal ecosystems for the entire coastline or to compare these effects between specific coastal segments. In contrast, field measurements need to be interpolated to get spatially explicit information which introduces some major inaccuracies. The information on the sensitivity and the recovery potential of ecosystems are valuable information that may be useful for foresters or local planners, i.e. to identify and locate vulnerable areas that need to be monitored and protected from human activities. Furthermore, maps on tsunami sensitivity and the recovery potential can be used to increase local awareness for the importance and fragility of the examined ecosystems. In this context the author experienced a general lack of knowledge among tourists and even locals, that there are unique and fragile ecosystems located in close proximity to the beaches and hotel complexes (e.g. mangrove forests near Pakarang Cape). In this case, sustainable management of these mangroves may encompass an adaptive form of tourism (e.g. guided tours on boardwalks for tourist groups) which increases local awareness, provides some local income and prevents the mangroves from amplified destruction. However, recent developments in 2008 (section 6.4) suggest that human induced degradation processes have continued after the tsunami.

As remotely sensed data (e.g. IKONOS) can be obtained for multiple acquisition dates, they can be used to monitor and analyse processes that have occurred over time. Thus, it was possible to retrospectively evaluate tsunami related processes such as impacts and recovery processes which could only partly be detected directly in the field in 2008 and 2009. Due to a general lack of spatially accurate information on the types of ecosystems (compare LULC-classification) and the tsunami impacts and recovery, new knowledge on the ecological vulnerability for this area is provided by this study. These data can be implemented in a coastal GIS application to support the assessment of the tsunami vulnerability in general which is required to estimate tsunami risk (section 1.1).

A main potential can be seen in the possibility to link the spatially explicit information provided in this study to data derived from other sources, such as expert interviews. This would allow a further in-depth analysis and understanding of the socio-ecological vulnerability: Just recently, a detailed database on the state and changes of ecosystem services and functions for major land use classes was created for the study area. The information was derived from expert interviews conducted in 2010 within the TRAIT project. As this information can be regionalised with the exposure and LULC-map and also with the damage and recovery information provided in this study, they can be used for the estimation of the regional losses and gains in ecosystem services.

The synergistic approach would help to estimate the social components of ecological vulnerability (Adger *et al.* 2005). For example, the information on tsunami impacts and recovery are useful to analyse the changes in the capacity of the landscape to buffer tsunami waves (Adger 2006; Dahdouh-Guebas *et al.* 2005; Renaud 2006).

Another advantage of spatially explicit information involves the ability to obtain information for areas that are not easily to access. Especially for the dense mixed beach forest in the national park area and also for the mangroves in the south (some were only accessibly by boat), remote sensing data are a valuable source of information. Furthermore, multi-temporal high-resolution images were very helpful for the preparation of the field campaign. Possible study sites were identified prior to the field investigation, which has considerably accelerated the field work.

Although the focus in this study was on the terrestrial ecosystems, it needs to be emphasized that IKONOS data can be used to provide information on other ecosystems, such as marine ecosystems (seagrass beds and corals in shallow water) or sandy beaches (cp. Choowong *et al.* 2009; Mishra *et al.* 2006; Klemas 2010; Vosberg 2010). This makes them to a flexible tool for the monitoring of tropical ecosystems in general and thus for the assessment of their vulnerability.

### Limitations

Regarding the limitations of remote sensing techniques in ecological vulnerability assessments, a main issue results from the fact, that information of a phenomenon occurring on the earth surface can only be derived indirectly. This implies that these phenomena or processes need to be associated with a distinguishable spectral signature or a temporal change in the spectral characteristics observed by a specific sensor. In the case of the applied IKONOS sensor, many processes occurring in the ground or in deep and turbid water or those being covered by dense tree canopies cannot be detected. Although there are some applications for optical and thermal imagers (working in the NIR and TIR range) as well as for microwave radiometer and imager to estimate phytoplankton concentrations, soil moisture, sea surface temperature, sea water salinity (Klemas 2010), their utilisation depends on the availability of detailed ground truth measurements. Furthermore, since thermal infrared sensors and, in particular, microwave imagers have lower resolutions (i.e. kilometres for passive microwave imagers), they are not useful for a local assessment such as carried out in TRAIT. Bio-physical and chemical characteristics of soils and water resources, such as the Marine Water Quality Index, needs to be comprehensively analysed in the laboratory based on soil or water samples (cp. DMCR 2005; Szczucinski *et al.* 2006; Tharnpoophasiam *et al.* 2006).

Remote sensing techniques can be used to analyse and regionalise vulnerability, but the causal relationships behind the observed results, here the identification of the factors determining vulnerability, could only partly be investigated by remote sensing. Indeed remotely sensed data can be potentially used to derive external factors such as tsunami impacts or location variables (e.g. elevation, distance to the shore), and thus can be used to analyse the extrinsic vulnerability, more detailed information derived from field surveys and laboratory analyses would be required to analyse the system-related or intrinsic vulnerability (cp. Nassel and Voigt 2006; Villa and McLeod 2002). As already mentioned there was lack on spatial explicit pre-tsunami information on some bio-physical properties of the examined ecosystems (age, species and stand characteristics, soil properties) in order to investigate tsunami sensitivity in a more detailed way.

A limitation in this study can be seen in the fact, that IKONOS images of only three different acquisition dates were used. A higher temporal resolution and as well as a longer observation period of the satellite images would have contributed to a) a reduction in uncertainty in the interpretation of the change detection results and b) to a better understanding of the pre-tsunami condition or health of the examined ecosystems: A time gap of 23 months between the pre-tsunami image and the tsunami event, respectively another gap of two weeks between the post-tsunami image and the tsunami had to be accepted. Thus, it had to be assumed that the state in the pre-tsunami image (13.01.2003) did not change until the tsunami event of 26.12.2004, which is, admittedly, not very likely for the human impacted coastal areas near Khao Lak and Ban Nam Khem. Thus, some tsunami-induced impacts observed on the post-images were likely not caused by the tsunami, but by human activities before the tsunami (cp. Roemer *et al.* 2010a). Regarding the assessment of recovery and resilience, some more time-steps between the last acquisition date from 2008 and the post-tsunami state from 2005 would have been useful to distinguish between fast growing vegetation, such as grasslands or herbaceous vegetation, and slow growing vegetation, such as wooden vegetation and scrubs. Furthermore, image data from a more current date (2009 and 2010) would be useful to investigate the long-term consequences of the tsunami on forest vegetation.

The limitation in the temporal resolution results from some problems in IKONOS imagery acquisition: IKONOS data are very expensive with a unit price of 44.00 US Dollars per square kilometre for a bundle product. This limits its application for studies at high spatial and/or temporal resolutions. Expectedly, a major problem encountered is the availability of a sufficient number of cloud free imagery of a study site. This problem particularly applies to study areas located in the humid tropical regions. Unfortunately, because of this problem, recovery analyses could only be conducted for the northern parts of the study area.

Furthermore, it can be assumed that the use of satellite images from older acquisition dates (e.g. 70s to 90s) acquired from other sensors (e.g. Landsat 1-3) might have been useful to investigate the pre-tsunami condition or the health status of the coastal ecosystems in general. According to Dahdouh-Guebas (2001), this is an important issue in understanding the ecological resilience. Unfortunately high-resolution imagery (e.g. IKONOS or Quickbird) are not available before 1999.

#### **6.4 Evaluation of the ecological vulnerability of the study area**

Regarding the findings derived within this thesis, including the remote sensing applications, the literature review on post-tsunami impact studies conducted in Thailand (section 3) as well as the results provided by Vosberg (2010), it can be concluded, that the ecological tsunami vulnerability in the study area was generally low to moderate. Most ecosystems and natural resources were only slightly affected by the tsunami, e.g. seagrass meadows, mangroves, coconut plantations or the seawater quality. Moderate impacts could be observed for coral reefs (13% of sites that were highly impacted), casuarina beach forests and groundwater and soils. However, most of the impacted natural resources and ecosystems did recover either within a few months (grassland vegetation, seagrass), or within one or two years (major impacted seagrass, soil and groundwater resources and sandy beaches), cp. section 3 and Roemer *et al.* 2010b. In contrast, recovery processes of impacted coastal forests and coral reefs will require more time, such as 10 years for coral reefs or about 10-15 years for mangrove forests (Duke 2006; Roemer *et al.* 2010b; UNEP 2005). Additionally, the study revealed that not all coastal areas and ecosystems were impacted with equal intensities.



This means that even though the general ecological tsunami vulnerability is mostly low, some areas are highly vulnerable to tsunamis (cp. section 6.2.1, Roemer *et al.* 2010a).

Even though the human related influences on the ecological vulnerability were not quantitatively detected on the local scale, it needs to be emphasised that the knowledge of the human related threats on the environment is crucial to estimate the ecological health, the ecological resilience and thus also the ecological tsunami vulnerability. For example, if humans continue to degrade mangrove areas, the potential area of remnants or growth points which is required for a forest renewal will decrease, making them less resilient and more vulnerable. The negative influence of human related impacts can be observed for coral reefs near Pakarang Cape (Phongsuwan *et al.* 2006; UNEP 2005). Due to off-shore tin mining activities in the last century, coral reefs have been degraded and were less resistant or more sensitive towards the tsunami. Furthermore, the degradation of one ecosystem could also negatively influence the vulnerability of another ecosystem: Due the capacity to filter silty substrates, a degradation of mangroves would also negatively affect the health and thus the tsunami resilience of coral reefs (Phongsuwan *et al.* 2006; UNEP 2005).

As the capacity of an ecosystem to provide a certain service is related to its ecological health status (e.g. Rosenberg *et al.* 1996; Shen *et al.* 2004), this knowledge is also crucial to understand the socio-ecological components of tsunami vulnerability. Renaud (2006), Adger (2006) and Dahdouh-Guebas *et al.* (2005) state that the pre-condition of mangrove stocks for example describe the buffering effect on the tsunami waves. Additionally, a decline in important ecosystem services will lead to a general reduction of the livelihood options available to local farming and fishing communities in the case of a tsunami (Adger *et al.* 2005).

In order to consider the human related pressures in the study area in general and thus to give a rough future estimation on the ecological health, resilience and tsunami vulnerability, an attempt is made to expand the spatial focus from the local to the regional scale. Here, four indicators that are related to human induced pressures are compared on a regional level for the following five Tambons: Ban Mueang, Khuek Kak, Laem Kaen, Thung Maphrao and Thai Mueang.

The following indicators were applied: a) the number of former tin mining areas ( $T$ ,  $n$ ), b) the population density ( $D$ , %), c) the agricultural area ( $A$ , %) and d) the population growth ( $G$ , %). Whereas  $T$  was derived from the analogue geological map provided by DMR (2001), the other three were created based on existing land cover classifications derived from ASTER data from March 2003 (variables  $D$  and  $A$ ) as well as from January 2006 and March 2003 for variable  $G$ , cp. section 4.5.3 and Table 4-6. For variable  $G$ , the aerial change of the land cover class "built-up area" between to image acquisition dates was applied. The applied indicators are appropriate to characterise the degree of human pressure on the environment in general: Whereas the indicators  $D$ ,  $G$  and  $A$  are taken from the literature (e.g. Noronha *et al.* 2001; OECD 1993),  $T$  is selected since it captures the long term negative threats resulting from open cast mining including possible arsenic and heavy metal contaminations of soils and sediments (cp. Donner 1989; Szczucinski *et al.* 2006). In order to compare the intensity of human pressure between in all four tambons, an average indicator value has to be defined. Thus, the four indicators are rescaled or standardised. This is carried out on the one hand by applying a ranking scale (with 1 representing the lowest and 5 the highest indicator value, respectively) and on the other hand by applying a linear scale between 0 (representing the lowest indicator value) and 1 (representing the highest indicator value), using the following equation:

$$I_{0...1} = \frac{I - \text{MIN}}{\text{MAX} - \text{MIN}} \quad (8)$$

where,  $I_{0...1}$  is the rescaled indicator value,  $I$  the indicator in the original scale,  $\text{MIN}$  and  $\text{MAX}$  are the minimum indicator value and the maximum indicator value in the group, respectively.

The results of this analysis are presented in detail in Table 6-3. Figure 6-10 shows the map of the four indicators in the original scale and the mean value, scaled between 0 and 1. The results reveal that human pressure is not evenly distributed in the study area. The southern tambons such as Thai Mueang, Thung Maphrao and Laem Kaen are less influenced by human activities and are likely more intact than the northern tambons. Ban Mueang has the highest pressure value resulting from a high density and growth of population (almost 4% growth occurring between 2003 and 2006) and the highest values of tin mining activity. Furthermore, the results reveal that ecosystems located in the northern tambons are more vulnerable to tsunamis than in the southern tambons. As most of the human related pressures (particularly the population density, tourism activity) will likely increase for the northern tambons, it can be assumed that the ecological tsunami vulnerability will also increase for these areas in the case of a future tsunami. Although this approach is only rough and can certainly be extended by more indicators in the future, such as the national park area, or density or growth of tourism industry, it can be assumed that the general spatial patterns would be remain similar.

**Table 6-3.** Comparison of human pressure indicators on tambon level.  $D$  (%) is the population density,  $G$  (%) the population growth,  $A$  (%) the area under agriculture and  $T$  (n) the number of tin mining areas.

Indicator	Bang Mueang			Khuek Kak			Laem Kaen			Thung Maphrao			Thai Mueang		
	value	rank* 1-5	scaled** 0...1	value	rank* 1-5	scaled** 0...1	value	rank* 1-5	scaled** 0...1	value	rank* 1-5	scaled** 0...1	value	rank* 1-5	scaled** 0...1
D (%)	1.39	5.00	1.00	0.84	2.00	0.55	0.99	3.00	0.67	0.18	1.00	0.00	1.07	4.00	0.73
G (%)	3.68	5.00	1.00	1.02	4.00	0.28	0.02	2.00	0.01	0.20	3.00	0.05	0.00	1.00	0.00
A (%)	38.13	4.00	0.56	46.07	5.00	1.00	35.30	3.00	0.40	28.07	1.00	0.00	32.60	2.00	0.25
T (n)	56.00	5.00	1.00	38.00	4.00	0.67	2.00	1.00	0.00	2.00	1.00	0.00	6.00	3.00	0.07
Mean	-	4.75	0.89	-	3.75	0.62	-	2.25	0.27	-	1.50	0.01	-	2.50	0.26

\*rank: "5" indicates highest pressure; "1" indicates lowest pressure

\*\* scaled values: "1" indicates highest pressure, "0" indicates lowest pressure

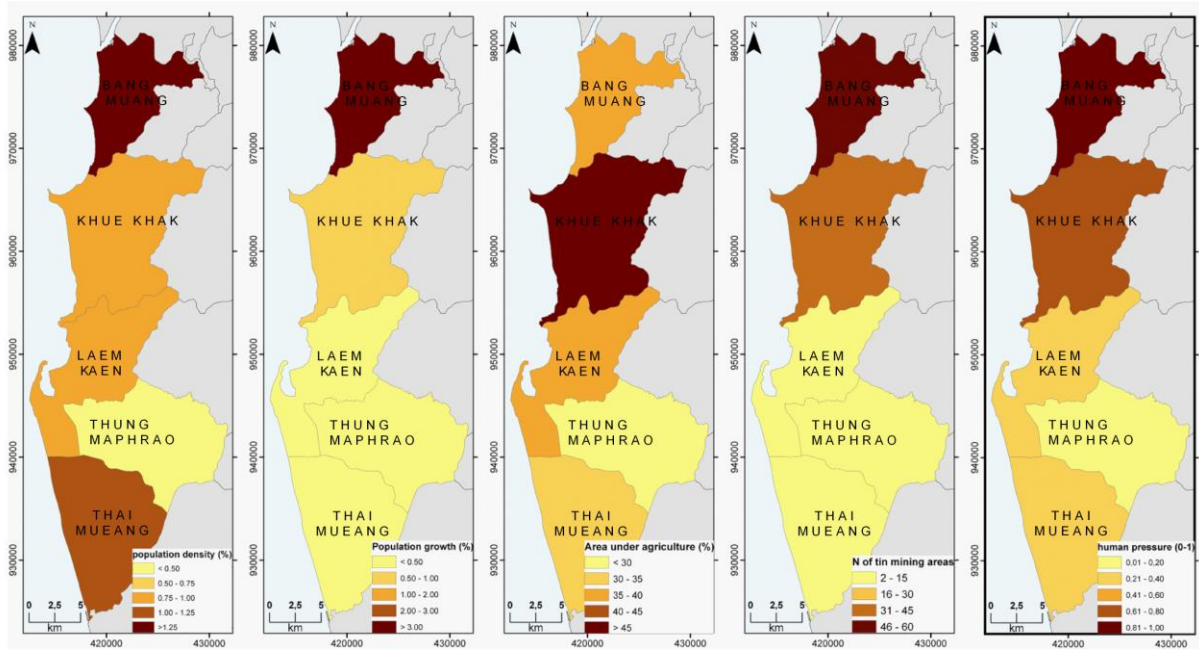
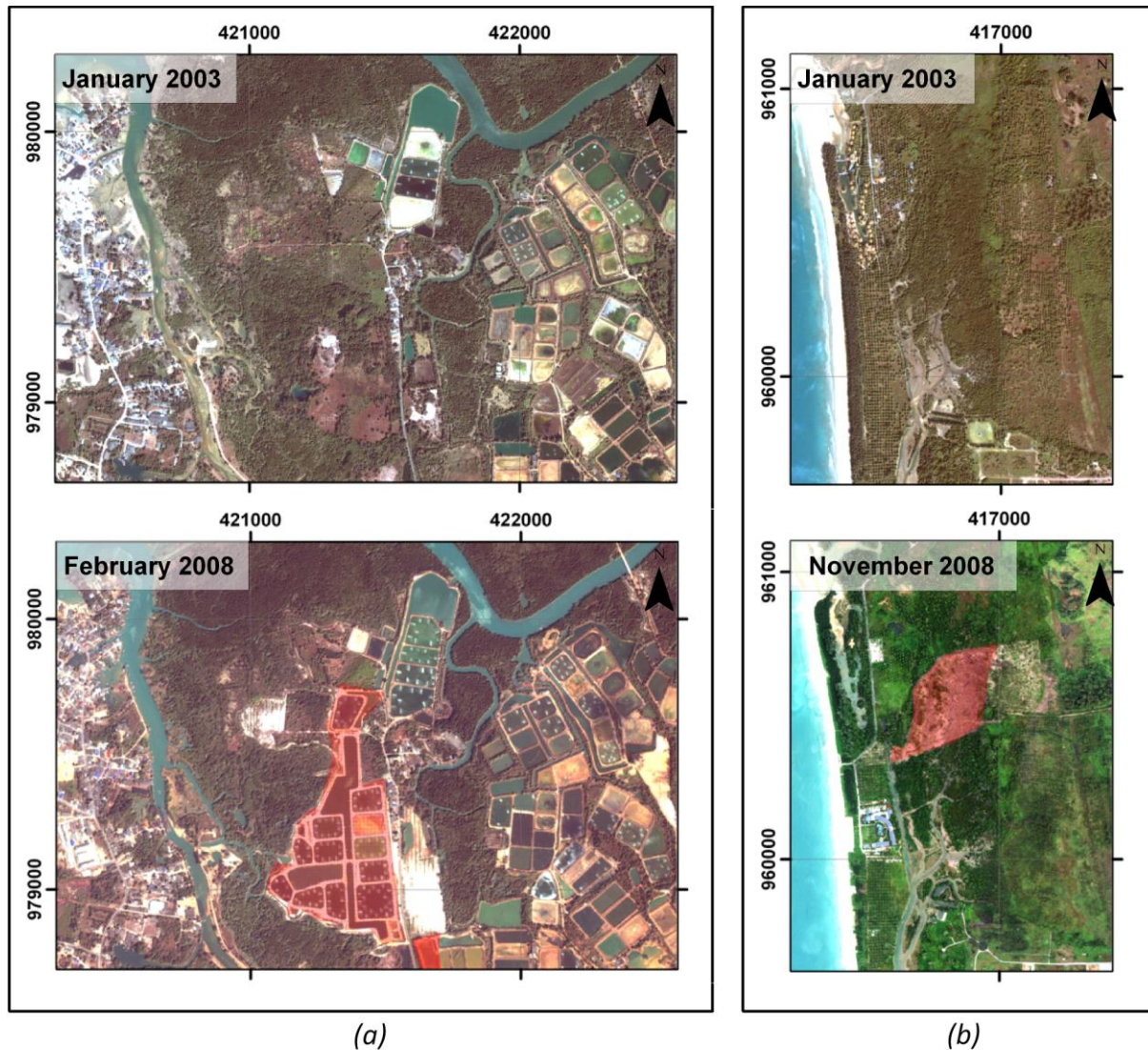


Figure 6-10. Human pressure on the environment on tambon level.

To verify that the results derived on the regional scale are also related to the local scale, Figure 6-11 illustrates two recent examples on human related impacts on the natural environment. One example shows the expansion of aquaculture industry in the area of Ban Nam Khem observed by the IKONOS images of 2003 and 2008 (Figure 6-11a). The second example (Figure 6-11b) indicates massive degradation processes near Khuk Kak that have occurred very recently end of 2008 (MFC-RGB images). In this particular case, Massmann (2010) concluded from field observations that new hotel complexes were planned to be built in the former mangrove area.



**Figure 6-11.** Human induced impacts on mangroves in the study area (cp. red polygons). (a) The expansion of shrimp farm industry near Ban Nam Khem and (b) intensive degradation processes of mangrove forests near Khuk Kak.

Finally, because of the complex interactive relationships between ecosystems and human activities that take place over time, the tsunami vulnerability of an ecosystem is both, a spatially and temporally variable condition.

Although this thesis focused on the vulnerability towards tsunami events, it can be concluded that the major threats to the ecosystems are not related to tsunami hazards, but to human activities (cp. section 1.4.2). This becomes clear when analyzing the historical databases on earthquakes and tsunami events that occurred in the Indian Ocean. In this regard, Løvholt *et al.* (2006) stated that another comparably strong M 9+ earthquake event in the Sumatra subduction zone with potential tsunami effects on Thailand is not likely to occur before at least 400 years after the 2004 megathrust earthquake. Thus, a low risk for tsunami induced impacts on ecosystems in the study area can be expected. Despite the rarity in mega tsunami occurrence, it needs to be emphasised that the ecological tsunami vulnerability is an essential element of the total coastal tsunami vulnerability and thus needs to be taken into account for a holistic tsunami risk management such as anticipated in TRAIT.



## 7 Conclusions and outlook

In this thesis, the tsunami vulnerability and resilience of coastal ecosystems at the Andaman Sea coast of Thailand was assessed using a remote sensing based approach. It is demonstrated that remote sensing techniques make a contribution to the spatial and retrospective analysis of tsunami vulnerability. A new geo-database on the spatial distribution on terrestrial ecosystems and their vulnerability for the study area was created, which can be implemented in a GIS-based vulnerability assessment approach of TRAIT. The use of high resolution IKONOS imagery, as well as the combined application of digital change detection techniques and object-oriented classification, turned out to be an effective way to map and analyse the tsunami induced impacts and recovery processes of the coastal ecosystems and thus to indirectly assess their tsunami vulnerability.

The results derived by the remote sensing applications reveal that tsunami vulnerability varied in space and in ecosystem type: Although casuarina beach forests prove to be the most impacted and sensitive forest ecosystem, its vulnerability is found to be relatively low as it recovered very quickly after the tsunami. In contrast, a high tsunami vulnerability is observed for some mangrove areas, particularly where forest patches are small and isolated. Coconut plantation prove to be the most resistant coastal ecosystem as it was affected by high wave intensities but suffered only low direct damages (cp. Ioualalen 2007; Kaiser *et al.* 2010b). However, field studies reveal that this (man-made) ecosystem is not resilient as it was not in an equilibrium or stable state prior to the tsunami and need to be artificially preserved and cultivated. As the other two examined forest ecosystems (mixed beach forests, melaleuca forests) were either low or not directly impacted by the tsunami, a low tsunami vulnerability was attested. However, these observations are mainly due to the fact that these ecosystems are located only in the southern part of the study where tsunami wave intensities were lower than in the north (cp. Ioualalen 2007).

It is proved by the statistical correlation and regression approach, that tsunami impacts and the recovery potential can be partly explained by external factors, such as those referring to a) the specific location of the exposed element, b) to the intensity of the hazard and c) to the amount of disturbance (here characterised by the severity of tsunami impacts). However, this approach also reveal that not all causal relationships can be quantitatively analysed and interpreted by means of remote sensing, particularly those that are related to the system-specific or intrinsic vulnerability.

It was emphasised that the tsunami vulnerability can not be assessed independently from human related threats on the environment. As this study area have been intensively impacted by human activities (expansion of agriculture and shrimp farm industry, off- and on-shore tin mining activities in the last century and just recently, the development of the tourism industry), an increased ecological tsunami vulnerability, particularly for the northern tambons was detected. Furthermore, it can be concluded that due to the rarity in mega tsunami occurrence in the study area, the major threats to the ecosystems at the Andaman Sea coast of Thailand are not related to tsunami hazards but to human activities.

The results of this study do not provide information on the values of ecosystems or the changes in ecosystem functions or services directly. However, such information would be necessary for a valuation or quantification of ecosystems and ecological vulnerability, which can be regarded as general future challenges in vulnerability research. The advantage of using a quantitative scale can be seen in the ability to compare and match the ecological vulnerability to other types of vulnerabilities (e.g. economic vulnerability) for conjoint methodological assessments (as in TRAIT).



But as the information on the values or ecosystem functions or services need to be derived from field studies, laboratory analyses or expert interviews (and thus are usually not spatially explicit), they can be spatially linked and regionalised by the geodata provided within this study (e.g. impact information, recovery information, ecosystem distribution). This would allow a spatial assessment of ecological vulnerability. Therefore, a main future potential and challenge for remote sensing applications can be seen in providing added value by means of synergistic use (Burkhard *et al.* 2006; Costanza *et al.* 1997).

The comprehensive assessment of the ecological resilience describes a further future challenge in remote sensing applications. It needs to be investigated which spatial and temporal resolution and furthermore, which observation period in the applied imagery is appropriate. A major challenge is to examine how internal system properties have changed over time to better estimate and predict the vulnerability of the respective ecosystem. In this case, a methodological challenge includes the combination of imagery from different sensors. However, the author recommends that remote sensing image acquisition and detailed field data analyses should be conducted in temporal coherence, in order to archive a best synergy between both spatial coverage and detailed knowledge on the processes to be examined.

The identification and quantification of the causes or factors of vulnerability based on (multi-date) remote sensing applications can be considered as a new and complex issue in vulnerability research. Thus, a further potential of remote sensing involves the spatial representation of vulnerability indicators on the regional or country scale and the combined use of remote sensing and landscape pattern analyses (cp. Zhang *et al.* 2009; Li *et al.* 2006; Jones *et al.* 2003). In this study, LULC-classification derived from ASTER imagery could be effectively applied to derive spatially explicit indicators on the regional or tambon level for a rough estimation of the ecological health status and ecological tsunami vulnerability. Additionally, it would be also possible to rank the land use classes or the examined ecosystems, derived from object oriented image analysis, by their vulnerability (e.g. the tolerance of a community to soil salinity, trunk diameters, average growth rates). This can also contribute to the assessment of tsunami vulnerability on the local scale (cp. De Lange *et al.* 2006 or Penghua *et al.* 2007).

## 8 References

- Adger, W.N., Brooks, N., Bentham, G., Agnew, M., Eriksen, S. (2004): New indicators of vulnerability and adaptive capacity. *Tyndall Centre for Climate Change Research Technical Report 7*, Norwich (UK), p. 128.
- Adger, W.N., Hughes, T.P., Folke, C., Carpenter, S.R., Rockström, J. (2005): Social-Ecological Resilience to Coastal Disasters. *Science*, **309**, 1036-1039.
- Adger, W.N. (2006): Vulnerability, *Global Environ Change*, **16**, 268–281.
- Adulyanukosol, K., Poovachiranon, S. (2008): Dugong (Dugong dugon) and seagrass in Thailand: present status and future challenges. *Proceedings of the Third International Symposium on SEASTAR2000 and Asian Bio-logging Science*, 13-14 December 2006, Bangkok, 41-50. Available online at: <http://chm-thai.onep.go.th/chm/MarineBio/Paper/Mammals/7thSEASTAR.41.pdf> (accessed at 08.10.2010).
- Alessa, L., Kliskey, A., Lammers, R., Arp, C., White, D., Hinzman, L., Busey, R. (2008): The Arctic Water Resource Vulnerability Index: an integrated assessment tool for community resilience and vulnerability with respect to freshwater. *Environ Manage*, **42**, 523–563.
- Altan, O., Toz, G., Kulur, S., Seker, D., Volz, S., Fritsch, D., Sester, M. (2001): Photogrammetry and geographic information systems for quick assessment, documentation and analysis of earthquakes. *Int Soc Photogramme*, **55**, 359–372.
- Arp, D. (2009): Estimating Hydrological Roughness in Coastal Habitats – A Case Study at the Andaman Coast of Thailand. *Diploma thesis*, Christian-Albrechts-Universität zu Kiel, Germany.
- Baatz, M.; Schäpe, A. (2000): Multiresolution Segmentation: an optimization approach for high quality multi-scale image segmentation. In: Strobl, J., Blaschke, T., Griesebner, G. (Eds.): *Angewandte Geographische Informations-Verarbeitung XII*, Karlsruhe, 12– 23.
- Bahugana, A., Nayak, S., Dam, R. (2008): Impact of the tsunami and earthquake of 26th December 2004 on the vital coastal ecosystems of the Andaman and Nicobar Islands assessed using RESOURCESAT AWiFS data, *Int J Appl Earth Obs*, **10**, 229-237.
- Bell, R., Cowan, H., Dalziell, E., Evans, N., O’Learly, M., Rush, B., Yule, L. (2004): Survey of impacts on the Andaman Coast, Southern Thailand following the great Sumatra-Andaman earthquake and tsunami of December 26, 2004. *Bulletin of the New Zealand Society for Earthquake Engineering*, **38**, 123-148.
- BIOTEC – National Center for Genetic Engineering and Biotechnology (2005): Thailand Marine Shrimp Culture Statistics. Available online at: <http://www.biotec.or.th/shrinfo/Others/> (accessed at 16.08.2007).
- Birkmann, J. (2005). Danger need not spell disaster - but how vulnerable are we? *Research Brief*, Number 1, United Nations University, Tokyo, p. 8.
- Birkmann, J., Wisner, B. (2006): Measuring the un-measurable – The challenge of vulnerability. *SOURCE*. No. 5/2006, Bonn, Germany, p. 64.
- Birkmann, J. (2007): Risk and vulnerability indicators at different scales: Applicability, usefulness and policy implications. *Environmental Hazards*, **7**, 20–31.
- Bogardi, J., Birkmann, J. (2004): Vulnerability assessment: the first step towards sustainable risk reduction. In: Malzahn, D., Plapp, T. (Eds.): *Disaster and Society—From Hazard Assessment to Risk Reduction*, 75–82.

- Bohle, H.-G. (2001): Vulnerability and Criticality: Perspectives from Social Geography. In: *IHDP Update 2/2001: Newsletter of the International Human Dimensions Programme on Global Environmental Change*, 1-7. Available online at: [http://www.ihdp.uni-bonn.de/html/publications/update/update01\\_02/IHDPUpdate01\\_02\\_bohle.html](http://www.ihdp.uni-bonn.de/html/publications/update/update01_02/IHDPUpdate01_02_bohle.html) (accessed at 10.10.2009).
- Börner, A., Hirschmüller, H., Scheibe, K., Suppa, M., Wohlfeil, J. (2008): MFC – A Modular Line Camera for 3D World Modelling. *Lect Notes in Compu Sc*, 4931, 319-326.
- Brooks, N., Adger, W.N., Kelly, P.M. (2005): The determinants of vulnerability and adaptive capacity at the national level and the implications for adaptation. *Global Environ Chang*, **15**, 151–163.
- Boughton, D.A., Smith, E.R., O'Neill, R.V. (1999): Regional vulnerability: a conceptual framework. *Ecosyst Health*, **5**, 312–333.
- Budicadi, Kaanzawa, Y., Ishii, H., Sabarudin, M. S., Suryanto, P. (2005): Productivity of kayu putih (*Melaleuca leucadendron* LINN) tree plantation managed in non-timber forest production systems in Java, Indonesia. *Agroforest Syst*, **64**, 143–155.
- Bueno, P. (2005): Impacts of Tsunami on Fisheries, Coastal Resources and Human Environment in Thailand. In *4th Regional Network of Local Governments Forum*, 27 April 2005, Bali, p. 28.
- Burkhard, B., Kroll, F., Müller, F., Windhorst, W. (2006): Provide ecosystem services – a concept for spatial modeling. *Landscape Online*, **15**, 1-22.
- Burel, F., Baudry, J. (2003): *Landscape ecology. Concepts, methods and Applications*. Science Publishers, INC. Enfield (USA).
- Cardona, O.D. (1999): Environmental Management and Disaster Prevention: Two Related Topics - A Holistic Risk Assessment and Management Approach. In: Ingleton, J. (Ed.): *Natural Disaster Management*, Tudor Rose. London.
- Cardona, O.D. (2001): Estimación Holística del Riesgo Sísmico utilizando Sistemas Dinámicos Complejos. Universidad Politecnica de Cataluna, Barcelona. Available online at: <http://www.desenredando.org/public/varios/2001/ehrisusd/index.html> (accessed at 12.10.2006).
- Cardona, O.D. (2004): The Need for Rethinking the Concepts of Vulnerability and Risk from a Holistic Perspective: A Necessary Review and Criticism for Effective Risk Management. In: Bankoff, G., Frerks, G., Hilhorst, D. (Eds.): *Mapping Vulnerability: Disasters, Development and People*, Earthscan Publishers, Londres.
- Carpenter, J.R. (1987): *Earth Science Source Book: Center for Science Education*, University of South Carolina, Columbia, South Carolina.
- Center for Satellite Based Crisis Information (ZKI) (2005): *Thailand – Khao Lak region, map* (Wessling, Germany).
- Chang, S.E., Eeri, M., Adams, B.J., Alder, J., Berke, P.R., Chuenpagdee, R., Ghosh, S., Wabnitz, C. (2006): Coastal ecosystems and Tsunami protection after the December 2004 Indian Ocean Tsunami. *Earthquake Spectra*, **22**, 863–887.
- Chatenoux, B., Peduzzi, P. (2005): Analysis on the role of bathymetry and other environmental parameters in the impacts from the 2004 Indian Ocean Tsunami. *A Scientific Report for the UNEP Asian Tsunami Disaster Task Force*. UNEP/GRID-Europe. Available online at: [http://www.grid.unep.ch/product/publication/download/environment\\_impacts\\_tsunami.pdf](http://www.grid.unep.ch/product/publication/download/environment_impacts_tsunami.pdf) (accessed at 01.09.2008).
- Chatenoux, B., Peduzzi, P. (2007): Impacts from the 2004 Indian Ocean Tsunami: analysing the potential protecting role of environmental features. *Nat Hazards*, **40**, 289–304.

- Chavez, P.S. (1988): An improved dark-object subtraction technique for atmospheric scattering correction of multispectral data. *Remote Sens Environ*, **24**, 459-479.
- Choowong, M., Phantuwongraj, S., Charoentitirat, T., Chutakosikanon, V., Yumuang, S. Charusiri, P. (2009): Beach recovery after 2004 Indian Ocean tsunami from Phang-nga, Thailand. *Geomorphology*, **104**, 134-142.
- Clark, W.C., Jager, J., Corell, R., Kaspersen, R., McCarthy, J.J., Cash, D., Cohen, S.J., Dickson, N., Epstein, P., Gutson, D.H., Jaeger, C., Leary, N., Levy, M.A., Luers, A., McCracken, M., Melillo, J., Moss, R., Parson, E.A., Ribot, J.C., Schellnhuber, H., Seielstad, G.A., Shea, E., Vogel, C., Wilbanks, T. J. (2000): Assessing vulnerability to global environmental risks. *Report of the Workshop on Vulnerability to Global Environmental Change: Challenges for Research, Assessment and Decision Making*, Warrenton, Virginia. Available online at: <http://ksgnotes1.harvard.edu/BCSIA/sust.nsf/pubs/pub1S> (accessed at 10.08.2010).
- Cochard, R., Ranamukhaarachchi, S.L., Shivakoti, G.P., Shipin, O.V., Edwards, P.J., Seeland, K.T. (2008): The 2004 tsunami in Aceh and Southern Thailand: A review on coastal ecosystems, wave hazards and vulnerability. *Perspect Plant Ecol*, **10**, 3-40.
- Coppin, P.R., Bauer, M.E. (1996): Digital change detection in forest ecosystems with remote sensing imagery. *Remote Sensing Reviews*, **13**, 207-234.
- Coppolillo, P., Gomez, H., Maisels, F., Wallace, R. (2004): Selection criteria for suites of landscape species as a basis for site-based conservation. *Biol Conserv*, **115**, 419-448.
- Corlett, R.T. (2008): Vegetation. In: Gupta, A. (Ed.): *The Physical Geography of Southeast Asia*, Oxford University Press, New York, 105-119.
- Costanza, R., d'Arge, R., De Groot, R., Farber, S., Grasso, M., Hannon, B., Limburg, K., Naeem, S., O'Neill, R., Paruelo, J., Raskin, R., Sutton, P. and Van den Belt, M. (1997): The value of the world's ecosystem services and natural capital. *Nature*, **387**, 253-260.
- Dahdouh-Guebas, F. (2001): Mangrove Vegetation Structure Dynamics and Regeneration, *Dissertation*, Vrije Universiteit Brussel, Brussels, Belgium, p. 317.
- Dahdouh-Guebas, F., Jayatissa, L.P., Di Nitto, D., Bosire, J.O., Io Seen, D., Koedam, N. (2005): How effective were mangroves as a defence against the recent tsunami? *Curr Biol*, **15**, 443-447.
- De Chazal, J., Quétier, F., Lavorel, S., Van Doorn, A. (2008): Including multiple differing stakeholder values into vulnerability assessments of socio-ecological systems. *Glob Environ Change*, **18**, 508-527.
- Definiens (2007): *Definiens Developer 7.0 Reference Book*. Definiens AG. München.
- De Lange, H. J., Sala, S., Vighi, M., Faber, J. H. (2009): Ecological vulnerability in risk assessment - a review and perspectives. *Sci Total Environ*. Article in press.
- De Lange, H. J., Van der Pol, J.J.C., Lahr, J., Faber, J.H. (2006): Ecological Vulnerability in Wildlife –A conceptual approach to assess impact of environmental stressors. *Alterra-rapport 1305*. Wageningen (NL), p. 113.
- Department of Groundwater Resources (DGR) (2006): *The Assessment of Groundwater Quality to Justify Remediation Approach of Groundwater Resources and Update Groundwater Map in Tsunami affected areas: Executive Summary*, Metrix Associates Co., Ltd., Bangkok.
- Department of Marine and Coastal Resources (DMCR) (n.d.): *GIS-data of coastal ecosystems in Phang-Nga province (pre-tsunami state)*. Bangkok.
- Department of Marine and Coastal Resources (DMCR) (2005): *Rapid Assessment of the Tsunami Impact on Marine Resources in the Andaman Sea*. Bangkok, Thailand, p. 76.

- Department of Mineral Resources (DMR) (2001): *Map of the Mineral Resources and mining activities in Thailand*. Bangkok. (in Thai).
- Department of National Parks, Wildlife and Plant Conservation (DNP) (2003): *Khao Lampi – Hat Thai Mueang Park*. Available online at: <http://www.dnp.go.th/parkreserve/asp/style1/default.asp?npid=43&lg=2> (accessed at 01.08.2010).
- DHI software (2009): *MIKE 21 FM Scientific documentation*.
- Donner, W. (1989): *Thailand - Räumliche Strukturen und Entwicklung von Wolf Donner*. Darmstadt, p. 339.
- Drude de Lacerda (Eds) (2002): *Mangrove ecosystems: function and management*. Springer, New York, p. 292.
- Duke, N.C. (2006). *Rhizophora apiculata*, *R. mucronata*, *R. stylosa*, *R. × annamalai*, *R. × lamarckii* (Indo–West Pacific stilt mangroves), ver. 2.1. In: Elevitch, C.R. (Ed.): *Species Profiles for Pacific Island Agroforestry*, Permanent Agriculture Resources (PAR), Hōlualoa, Hawai'i. Available online at: <http://www.traditionaltree.org> (accessed at 31.04.2009).
- Ebert, A., Kerle, N., Stein, A. (2007): Remote Sensing bases assessment of social vulnerability. *5th International Workshop on Remote Sensing Applications to Natural Hazards*, 10-11 September, 2007. Washington, D.C.
- Eichenberg-Suvarnatisha, D. (1991): Dezimierung und Deteriorierung natürlicher Ressourcen in Thailand unter besonderer Berücksichtigung der Entwaldung und von Gegensteuerungsmaßnahmen insbesondere mittels Schutzflächenausweisung. *Dissertation*, Johann-Wolfgang-Goethe-Universität zu Frankfurt am Main, Frankfurt.
- Ekstrand, S. (1994): Assessment of forest damage with Landsat TM: Correction for varying forest stand characteristics. *Remote Sens Environ*, **47**, 291–302.
- Food and Agriculture Organisation of the United Nations (FAO) (1999): Soil salinity assessment: methods and interpretation of electrical conductivity measurements. *FAO Irrigation and Drainage Paper*, **57**, p. 165.
- Food and Agriculture Organisation of the United Nations (FAO) (2005a): In-depth assessment of mangroves and other coastal forest affected by the tsunami in Southern Thailand. *THA/05/001/01/12. Progress Report submitted to the Regional Office for Asia and the Pacific, Food and Agriculture Organisation, Bangkok*. Kasetsart University, Bangkok.
- Food and Agriculture Organisation of the United Nations (FAO) (2005b): Back-to-office report: Backstopping support for the project: In-depth assessment of mangroves and other coastal forests affected by the tsunami in Southern Thailand. *THA/05/001. Reporting officer M. Kashio, Forest Resource Officer, November 2005*. FAO, Bangkok.
- Food and Agriculture Organisation of the United Nations (FAO) (2005c): In-depth assessment of mangroves and other coastal forests affected by the tsunami in Southern Thailand. *THA/05/001. Consultant Report by P. Saenger, International Consultant, November 2005*. FAO, Bangkok.
- Food and Agriculture Organisation of the United Nations (FAO) (2005d): *Report of the regional workshop on salt-affected soils from sea water intrusion: strategies for rehabilitation and management, 31 March-1 April 2005*, Bangkok, Thailand, p. 62.
- Food and Agriculture Organisation of the United Nations (FAO) and Ministry of Agriculture & Cooperatives (MOAC) (2005): *Report of Joint FAO/MOAC Detailed Technical Damages and Needs Assessment Mission in Fisheries and Agriculture Sectors in Tsunami Affected Six Provinces in Thailand 11-24 January 2005*. Available online at: [http://www.apfic.org/apfic\\_downloads/tsunami/FAO\\_MOAC\\_thai.pdf](http://www.apfic.org/apfic_downloads/tsunami/FAO_MOAC_thai.pdf) (accessed at 12.08.2010).



- Fernando, H.J.S., Mendis, S.G., McCulley, J.L., Perera, K. (2005): Coral poaching worsens tsunami destruction in Sri Lanka. *Eos T Am Geophys Un*, **86**, 301-304.
- Freitas, S.R., Mello, M.C.S., Cruz, C.B.M. (2005): Relationships between forest structure and vegetation indices in Atlantic Rainforest. *Forest Ecol Manag*, **218**, 353-362.
- Fujioka, Y., Tabuchi, R., Hirata, Y., Yoneda, R., Patanaponpaiboon, P., Pongparn, S., Shibuno, T., Ohba, H. (2008): Disturbance and recovery of mangrove forests and macrobenthic communities in Andaman Sea Thailand following the Indian Ocean Tsunami. *Proceedings of the 11th International Coral Reef Symposium*, 7-11 July 2008. Ft. Lauderdale, Florida, 825-829.
- GeoEye (2006): *IKONOS Imagery Products Guide Version 1.5*, p. 21. Available online at: [http://www.glcf.umd.edu/library/guide/IKONOS\\_Product\\_Guide\\_jan06.pdf](http://www.glcf.umd.edu/library/guide/IKONOS_Product_Guide_jan06.pdf) (accessed at 01.02.2008).
- Golden, N.H., Rattner, B.A. (2003): Ranking terrestrial vertebrate species for utility in biomonitoring and vulnerability to environmental contaminants. *Rev Environ Contam Toxicol*, **176**, 67-136.
- Green, E.P., Mumby, P.J., Edwards, A.J., Clark, C.D. (2000): *Remote Sensing Handbook for Tropical Coastal Management*. UNESCO publishing, Paris, p. 316.
- Green, K., Kempka, D., Lackey, L. (1994): Using remote sensing to detect and monitor land-cover and land-use change. *Photogr Eng Rem S*, **60**, 331-337.
- Grimm, L. G.; Yarnold, P. R. (1994): Reading and Understanding Multivariate Statistics. American Psychological Association, p. 373.
- Halpern B.S., Selkoe, K.A., Micheli, F., Kappel, C.V. (2007): Evaluating and ranking the vulnerability of global marine ecosystems to anthropogenic threats. *Conserv Biol*, **21**, 1301-1314.
- Haysom, K. A., Murphy, S. T. (2003): The status of invasiveness of forest tree species outside their natural habitat: a global review and discussion paper. *Working Paper FBS/3E*, FAO, Rome, Italy. Available online at: <ftp://ftp.fao.org/docrep/fao/006/J1583E/J1583E00.pdf> (accessed at 10.02.2010).
- Holling CS. (1973): Resilience and stability of ecological systems. *Ann Rev Ecol Syst*, **4**, 1-23.
- Horne, J.H. (2003): A tasseled cap transformation for IKONOS images. *Proceedings of the ASPRS Annual Conference*, 5-9 May 2003. Anchorage, USA, p. 9.
- Huh, O.K., Roberts, H.H., Rouse, L.J. (1991): Remote sensing of coastal environmental hazards. *Proceedings of SPIE*, **1492**: Earth and Atmospheric Remote Sensing, 378-386.
- Indonesian Agency for Agriculture Research and Development (IAARD) and New South Wales Department of Primary Industries (NSW DPI) (2008): *A practical guide to restoring agriculture after a tsunami*. 57p. Available online at: [http://www.dpi.nsw.gov.au/\\_\\_data/assets/pdf\\_file/0010/254863/A-practical-guide-to-restoring-agriculture-after-a-tsunami.pdf](http://www.dpi.nsw.gov.au/__data/assets/pdf_file/0010/254863/A-practical-guide-to-restoring-agriculture-after-a-tsunami.pdf) (accessed at 19.01.2010).
- Ioualalen, M., Asavanant, J., Kaewbanjak, N., Grilli, S.T., Kirby, J.T. Watts, P. (2007): Modelling the 26 December 2004 Indian Ocean tsunami: Case study of impact in Thailand. *J Geophys Res*, **112**, C07024, doi:10.1029/2006JC003850.
- Israngkura, A. (2005): Economic Impact of Tsunami on Thailand. *Natural Resources and Environment Program - Thailand Development Research Institute (TDRI)*. Bangkok, 27p. Available online at: <http://www.tdri.or.th/reports/published/n75.pdf> (accessed at 10.02.2010).
- Johnson, R.D. (1994): Change Vector Analysis for disaster assessment: a case study of Hurricane Andrew. *Geocarto International*, **9**, 41-15.

- Jones, K.B., Heggem, D.T., Wade, T.G., Neale, A.C., Ebert, D.W., Nash, M.S., Mehaffey, M.H., Hermann, K.A., Selle, A.R., Augustine, S. (2003): Indicator Development for Landscape-Level Aquatic Ecological Vulnerability Assessment in Western United States (Poster), *U.S. Environmental Protection Agency (EPA)*. Available online at: <http://www.epa.gov/esd/land-sci/pdf/285leba.pdf> (accessed at 30.08.2010).
- Kaiser, G.; Römer, H.; Arp, D.; Sterr, H.; Ludwig, R. (2010a): Use of high resolution geodata for inundation modeling as part of a tsunami risk assessment in Thailand. In: Schwarzer, K.; Schrottke, K.; Statteher, K. (Eds.): *From Brazil to Thailand – New results in coastal research*. Coastline Reports, 16, 25-34.
- Kaiser, G., Scheele, L., Kortenhaus, A., Römer, H., Leschka, S. (2010b): The influence of land cover roughness on high resolution tsunami inundation modelling. Submitted manuscript.
- King J.G., Sanger G.A. (1979): Oil vulnerability index for marine oriented birds. In: Bartonek J.C, Nettleship, D.N. (Eds.): *Conservation of Marine Birds of Northern North America: Wildlife Research Report 11*, Washington DC, 227–265.
- Klemas, V. (2010): Remote Sensing Techniques for Studying Coastal Ecosystems: An Overview. *J Coastal Res*, Article in press.
- Koshimura, S., Kayaba, S., Matsuoka, M. (2010): Integrated Approach to assess the impact of Tsunami Disaster in Safety, Reliability and Risk of Structures, Infrastructures and Engineering Systems. In: Furuta, H., Frangopol, D., Shinozuka, M. (Eds.): *Proceedings of the 10th International Conference on Structural Safety and Reliability, ICOSSAR*, 13-17 September 2009, Osaka, Japan, 2302-2307.
- Kumpulainen, S. (2006): Vulnerability concepts in hazard and risk management. In *Natural and technological hazards and risk affecting the spatial development of Europe regions*, Schmidt-Thomé, P. (Eds.): Geological Survey of Finland, Special Paper 42. Espoo (Finland), 65-74.
- Laben, C.A., Brower, B.V. (2000): *Process for enhancing the spatial resolution of multispectral imagery using pan-sharpening*. Eastman Kodak Company, Technical Report US Patent #6.011.875.
- Li, A., Wang, A., Liang, S., Zhou, W. (2006): Eco-environmental vulnerability evaluation in mountainous region using remote sensing and GIS—A case study in the upper reaches of Minjiang River, China. *Ecol Model*, **192**, 175–187.
- Lin, C.Y., Lo, H.-M., Chou, W.-C., Lin, W.-T. (2004): Vegetation recovery assessment at the Jou-Jou Mountain landslide area caused by the 921 Earthquake in Central Taiwan. *Ecol Model*, **176**, 75-81.
- Liverman, D.M. (1990): Vulnerability to global environmental change. In: Kasperson, R.E., Dow, K., Golding, D., Kasperson, J.X. (Eds.): *Understanding Global Environmental Change: The Contributions of Risk Analysis and Management*. Center for Technology, Environment and Development, Clark University, Worcester, MA, 27–44.
- Løvholt, F., Bungum, H., Harbitz, C.B., Glimsdal, S., Lindholm, C.D., Pedersen, G. (2006): Earthquake related tsunami hazard along the western coast of Thailand. *Nat Hazard Earth Sys*, **6**, 979-997.
- Lu, D., Mausel, P., Brondízio, E., Moran, E. (2003): Classification of successional forest stages in the Brazilian Amazon basin. *Forest Ecol Manag*, **181**, 301-311.
- Lu, D., Mausel, P., Bronidízio, E., Moran, E. (2004a): Change detection techniques. *Int J Remote Sens*, **25**, 2365-2407.
- Lu, D., Mausel, P., Bronidízio, E., Moran, E. (2004b): Relationships between forest stand parameters and Landsat TM spectral responses in the Brazilian Amazon Basin. *Forest Ecol Manag*, **198**, 149–167.
- Malila, W.A. (1980): Change Vector Analysis: an approach for detecting forest changes with Landsat. *Proceedings of the 6th Annual Symposium on Machine Processing of Remotely Sensed Data*, 1980, West Lafayette, USA, 326-335.

- Marris, E. (2005): Tsunami damage was enhanced by coral theft. *Nature*, **436**, 1071.
- Mas, J.-F. (1999): Monitoring land cover changes: a comparison of change detection techniques. *Int J Remote Sens*, **20**, 139-152.
- Massmann, F. (2010): Analyse der Vulnerabilität von Landwirtschaft und Fischerei an der Andamanküste Thailands im Kontext des Tsunami von 2004. *Diploma thesis*, Christian-Albrechts-Universität zu Kiel, Germany.
- McLaughlin, P., Dietz, T. (2008): Structure, agency and environment: Towards an integrated perspective on vulnerability. *Global Environ Chang*, **18**, 99-111.
- Meinel, G.; Neubert, M.; Reder, J. (2001): Pixelorientierte versus segmentorientierte Klassifikation von IKONOS-Satellitenbilddaten – ein Methodenvergleich. *Zeitschrift für Photogrammetrie, Fernerkundung und Geoinformation*, **3**, 157-170.
- Metzger, M., Schröter, D. (2006): Towards a spatially explicit and quantitative vulnerability assessment of environmental change in Europe. *Reg Environ Change*, **6**, 201–215.
- Millennium Ecosystem Assessment (2005a): *Current State & Trends. Chapter 19 Coastal Systems*. World Resources Institute, Washington, DC.
- Millennium Ecosystem Assessment (2005b): *Ecosystems and Human Well-being. Synthesis Report*. World Resources Institute, Washington, DC.
- Mishra, D.; Narumalani, S.; Rundquist, D., Lawson, M. (2006): Benthic habitat mapping in tropical marine environments using QuickBird multispectral data. *Photogramm Eng Rem S*, **72**, 1037–1048.
- Mittelbach, G., Turner, A., Hall, D., Rettig, J. (1995): Perturbation and resilience—a longterm, whole-lake study of predator extinction and reintroduction. *Ecology*, **76**, 2347-2406.
- Miura, H., Wijeyewickrema, A. C., Inoue, S. (2005): Evaluation of tsunami damage in the eastern part of Sri Lanka due to the 2004 Sumatra earthquake using IKONOS images. *Proceedings, First Bangladesh Earthquake Symposium*, 14-15 December 2005, Dhaka, p. 8.
- Mühr, B. (2006): *Klimadiagramme weltweit*. Available online at: <http://www.klimadiagramme.de/> (accessed at 09.07.2007).
- Nassel, M., Voigt, S. (2006): Vulnerability Assessment of the Built Environment. In: Birkmann *et al.* (Eds.): *Rapid and multidimensional vulnerability Assessment Sri Lanka*. UNU-EHS, Colombo, Bonn, 10-22.
- National Statistical Office (NSO) (2003): *Tambon statistical data*. Bangkok.
- Nicholls, R.J., Hoozemans, J. (2005): Global vulnerability analysis. In: Schwartz, M. (Ed.): *Encyclopedia of Coastal Science*. Kluwer Academic Publishers, Dordrecht, The Netherlands, 486–491.
- Noronha, L., Nairy, S., Sonak, S., Abraham, M. and Sreekesh, S. (2001): A framework of indicators of potential coastal vulnerability to development. *TERI working paper*, Gao, India, p. 34.
- Oesch, B. (2001): Fernerkundung und Naturgefahren – Methoden für Risk/Disaster Management und Humanitäre Einsätze. *Report for the Direktion für Entwicklung und Zusammenarbeit*. University of Bern, Switzerland, p. 88.
- Oliver-Smith, A. (1996): Anthropological research on hazards and disasters. *Annu Rev Anthropol*, **25**, 303–328.
- Oliver-Smith, A. (2009): Sea level rise and the vulnerability of coastal peoples – responding to the local challenge of global climate change in the 21st century. *Interdisciplinary Security Connections (InterSecTions)*, 7/2009, Bonn, Germany, p. 56.

- Olwig, M. F., Sørensen, M. K., Rasmussen, M. S., Danielsen, F., Selvam, V., Hansen, L. B., Nyborg, L., Vestergaard, K. B., Parish, F. and Karunagaran, V. M. (2007): Using remote sensing to assess the protective role of coastal woody vegetation against tsunami waves, *Int J Remote Sens*, **28**, 3153 – 3169.
- Organisation for Economic Co-operation and Development (OECD) (1993): *OECD core set of indicators for environmental performance reviews- a synthesis report by the Group on the State of the Environment*. OECD/GD(93)179, Paris, p. 39.
- Otieno, K., Onim, J.F.M., Bryant, M.J. and Dzwela, B.H. (1991): The relation between biomass yield and linear measures of growth in *Sesbania sesban* in western Kenya. *Agroforest Syst*, **13**, 131-141.
- Ott, W.R. (1978): *Environmental indices: Theory and Practice*. Ann Arbor Science Publishers, Inc., Michigan, p. 371.
- Pajimans, K. (1976): Part II Vegetation, In: Pajimans et al (Eds.): *New Guinea Vegetation*, CRISPO, Canberra, Australia, p. 81.
- Paphavasit, N., Aksornkoe, S., De Silvia, J. (2009): *Tsunami Impact on Mangrove Ecosystem*, Thailand Environmental Institute, Nonthaburi, Thailand, p. 211.
- Penghua, Q., Songjun, X., Genzong, X., Benan, T., Hua, B., Longshi, Y. (2007): Analysis of the ecological vulnerability of the western Hainan Island based on its landscape pattern and ecosystem sensitivity. *Acta Ecol Sin*, **27**, 1257–1320.
- Phongsuwan, N., Yeemin, T., Worachananant, S., Duangsawasdi, M., Chotiyaputta, C. and Comley, J. (2006): Post-tsunami status of coral reefs and other coastal ecosystems in the Andaman Sea coast of Thailand. In: Wilkinson, C., Souter, D. and Goldberg, J. (Eds.): *Status of coral reefs in tsunami-affected countries*, Australian Institute of Marine Science, Townville, Australia, 63–78.
- Phongsuwan, N., Brown, B. E. (2007): The influence of the Indian Ocean tsunami on coral reefs of Western Thailand, Andaman Sea, Indian Ocean. *The Atoll Research Bulletin (ARB)*, **544**, p. 14.
- Pimm, S.L. (1991): *The Balance of Nature?* Chicago: Univ. Chicago Press. 434 pp.
- Plathong, J., Sitthirach, N. (1997): *Traditional and current uses of mangrove forests in Southern Thailand*. Wetland International: Thailand Programme/PSU, Publication No. 3, Hat Yai (Thailand), p. 91.
- Polsky, C., Schröter, D., Patt, A., Gaffin, S., Martello, M.L., Neff, R., Pulsipher, A., Selin, H. (2003): Assessing Vulnerabilities to the Effects of Global Change: An Eight-Step Approach. *Belfer Center for Science and International Affairs Working Paper, Environment and Natural Resources Program*, John F. Kennedy School of Government, Harvard University, Cambridge, Massachusetts.
- Press, F., Siever, R. (2003): *Allgemeine Geologie*. Spektrum Akademischer Verlag Heidelberg. Berlin.
- Rachman, A., Fahmuddin, A., McLeod, M. and Slavich, P. (2008): Salt Leaching Processes in the Tsunami-Affected Areas of Aceh, Indonesia. *Paper presented at the 2nd International Salinity Forum*, 31.03 – 03.04 2008, Adelaide, Australia 31 March – 3 April 2008, p. 4.
- Wawilins, B. G.; Turner, G.; Mounteney, I.; Wildman, G. (2010): Estimating specific surface area of fine stream bed sediments from geochemistry. *Appl Geochem*, **25**, 1291-1300.
- Renaud, F. (2006): Environmental components of vulnerability. In: Birkmann, J. (Ed.): *Measuring Vulnerability to Natural Hazards—Towards Disaster-Resilient Societies*, UNU Press, Tokyo, New York.
- Rich, P.M. (1990): Characterizing plant canopies with hemispherical photographs. *Remote Sensing Reviews*, **5**, 13-29.

- Römer, H. (2007): Methoden der Fernerkundung als Grundlage zur Untersuchung von Tsunamivulnerabilität an der Andamanküste Thailands. *Diploma thesis*, Christian-Albrechts-Universität zu Kiel, Germany.
- Römer, H., Ludwig, R., Sterr, H. & G. Kaiser (2009): Potenziale der Fernerkundung zur Abschätzung von Tsunami-Vulnerabilität an der Andamanküste Südthailands. *Marburger Geographische Schriften*, **145**, 179 – 195.
- Roemer, H., Kaiser, G., Sterr, H. and Ludwig, R. (2010a): Using remote sensing to assess tsunami-induced impacts on coastal forest ecosystems at the Andaman Sea coast of Thailand. *Nat Hazard Earth Sys*, **10**, 729-746.
- Roemer, H., Jeewarongkakul, J., Kaiser, G., Ludwig, R., Sterr, H. (2010b): Monitoring post-tsunami vegetation recovery in Phang-Nga, Thailand – a remote sensing based approach. *Int J Remote Sens*, submitted manuscript.
- Rosenberg, R., Cato, I., Förlin, L., Grip, K., Rodhe, J. (1996): Marine environment quality assessment of the Skagerrak-Kattegat. *J Sea Res*, **35**, 1–8.
- San Miguel Ayanz, J., Vogt, J., De Roo, A., Schmuck, G. (2000): Natural hazards monitoring: forest fires, droughts and floods – The example of European pilot projects. *Surv Geophys*, **21**, 291–305.
- Scheele, L. (2010): Tsunami-Überflutungssimulationen unter Verwendung hochauflösender Geodaten: Dargestellt an Beispielen des ländlichen und urbanen Raumes in Südthailand. *Diploma thesis*, Christian-Albrechts-Universität zu Kiel, Germany.
- Schroeder, T.S., Warren, B.C., Yang, Z. (2007): Patterns of forest regrowth following clear cutting in western Oregon as determined from a Landsat time-series. *Forest Ecol Manag*, **243**, 259-273.
- Schultz, G.A. (1993): Hydrological modelling based on remote sensing information. *Adv Spac Res*, **13**, 149–166.
- Shen, W., Zhang, J.H., *et al.* (2004): Ecological environmental quality assessment of the three Gorges Reservoir areas based on remote sensing and GIS. *Resour Environ Yangtze Basin*, **23**, 159–162.
- Singh, A. (1989): Digital change detection techniques using remotely sensed data. *Int J Remote Sens*, **10**, 989–1003.
- Sirikulchayanon, P., Sun, W., Oyana, T.J. (2008): Assessing the impact of the 2004 tsunami on mangroves using remote sensing and GIS techniques. *Int J Remote Sens*, **29**, 3553-3576.
- Soltysik, J. (2010): Überflutungssimulation im Rahmen einer Tsunami gefährdungs- und Risikoanalyse für die Andamanküste Thailands. *Diploma thesis*, Christian-Albrechts-Universität zu Kiel, Germany.
- Spanner, M.A., Pierce, L.L., Peterson, D.L., Running, S.W. (1990): Remote sensing of temperate coniferous forest leaf area index: the influence of canopy closure, understory vegetation and background reflectance. *Int J Remote Sens*, **11**, 95-111.
- Sridhar, R., Thangaradjou, T., Kannan, L., Ramachandran, A., Jayakumar, S. (2006): Rapid Assessment in the Impact of Tsunami on Mangrove Vegetation of the Great Nicobar Island. *Journal of the Indian Society of Remote Sensing*, **34**, p. 5.
- Sterr, H. (2007): Tsunami Risks, Vulnerability and Resilience in the Phang-Nga Province, Thailand: Tsunami Risk and Information Tool = TRAIT. *Proposal for the Research Project TRAIT*. Department of Geography, Christian-Albrechts-University Kiel, Germany.
- Sukardjo, S. (2006): Botanical Exploration in Small Islands: 1. Floristic Ecology and the Vegetation Types of Pari Island, West Java, Indonesia. *South Pacific Studies*, **26**, 73-87.
- Szczucinski, W., Niedzielski, P., Rachlewicz, G., Subcynski, T., Ziola, A., Kowalski, S., orenc, S., Siepak, J. (2005): Contamination of tsunami sediments in a coastal zone inundated by the 26 December 2004 tsunami in Thailand. *Environ Geol*, **49**, 321-331.



- Szczucinski, W., Chaimanee, N., Niedzielski, P., Rachlewicz, G., Saisuttichai, D., Tepsuwan, T., Lorenc, S. and Siepak, J. (2006): Environmental and Geological Impacts of the 26 December 2004 Tsunami in Coastal Zone of Thailand – Overview of Short and Long-Term Effects. *Polish J of Environ Stud*, **15**, 793-810.
- Szczucinski, W., Niedzielski, P., Kozak, L., Frankowski, M., Ziola, A., Lorenc, S. (2007): Effects of rainy season on mobilisation of contaminants from tsunami deposits left in a coastal zone of Thailand by the 26 December 2004 tsunami. *Environ Geol*, **53**, 253-264.
- Tanaka, N., Sasaki, Y., Mowjood, M.I-M., Jinadasa, K.B.S.N., Homchuen, S. (2007): Coastal vegetation structures and their functions in tsunami protection: experience of the recent Indian Ocean tsunami. *Landscape Ecol Eng*, **3**, 33–45.
- Taubenböck, H. (2008): Vulnerabilitätsabschätzung der erdbebengefährdeten Megacity Istanbul mit Methoden der Fernerkundung. *Dissertation*, University of Würzburg, Germany, p. 174.
- Taubenböck, H., Post, J., Roth, A., Zosseder, K., Strunz, G. and Dech, S. (2008a): A conceptual vulnerability and risk framework as outline to identify capabilities of remote sensing. *Nat Hazard Earth Sys*, **8**, 409-420.
- Taubenböck, H., Post, J., Kiefl, R., Roth, A., Ismail, F., Strunz, G., Dech, S. (2008b): Risk and vulnerability assessment to tsunami hazard using very high resolution satellite data. *Proceedings of the EARSeL Joint Workshop: Remote Sensing: New Challenges of high resolution*. (Eds., Carsten Jürgens), Bochum, Germany, 77-86.
- Taubenböck, H., Wurm, M., Setiadi, N., Gebert, N., Roth, A., Strunz, G., Birkmann, J., Dech, S. (2009): Integrating Remote Sensing and Social Science: The correlation of urban morphology with socioeconomic parameters. *Urban Remote Sensing Joint Event*, Shanghai, China, p. 7.
- Taylor, M. (2009): *IKONOS Planetary Reflectance and Mean Solar Exoatmospheric Irradiance*, GeoEye. Available online at: [http://www.geoeye.com/CorpSite/assets/docs/technical-papers/2009/IKONOS\\_Esun\\_Calculations.pdf](http://www.geoeye.com/CorpSite/assets/docs/technical-papers/2009/IKONOS_Esun_Calculations.pdf) (accessed at 10.06.2009).
- Tegtmeier, J. (2009): Möglichkeiten der Gebäudekartierung mit hoch aufgelösten Fernerkundungsdaten. *Diploma thesis*, Ludwig-Maximilians-Universität München, Germany.
- Telford, J., Cosgrave, J. (2006): *Synthesis Report: Joint evaluation of the international response to the Indian Ocean tsunami*, Tsunami Evaluation Coaliton (TEC), July 2006, London, p. 176.
- Thailand Group, International Tsunami Survey Team of Indian Ocean Tsunami Disaster (Thailand Group) (2005): *The December 26, 2004 Sumatra Earthquake Tsunami, Thailand Field Survey around Phuket, Thailand*. Available online at: [http://www.drs.dpri.kyoto-u.ac.jp/sumatra/thailand/phuket\\_survey\\_e.html](http://www.drs.dpri.kyoto-u.ac.jp/sumatra/thailand/phuket_survey_e.html) (accessed at 07.09.2010).
- Tharnpoophasiam, P., Suthisarnsuntorn, U., Worakhunpiset, S., Charoenjai, P., Tunyong, W.; Phrom-in, S.; Chattanadee, S. (2006): Preliminary post-tsunami water quality survey in Phang-nga province, southern Thailand. *Southeast Asian J Trop Med Public Health*, **37**, 216-236.
- Theilen-Willige, B. (2006): Tsunami hazards in northern Venezuela. *Science of Tsunami Hazards*, **25**, p. 16.
- Theilen-Willige, B. (2010): Detection of local site conditions influencing earthquake shaking and secondary effects in Southwest-Haiti using remote sensing and GIS-methods. *Nat Hazard Earth Sys*, **10**, 1183-1196.
- Theron, J.M., Van Laar, A., Kunneke, A., Bredenkamp, B.V. (2004): A preliminary assessment of utilizable biomass in invading Acacia stands on the cape coastal plains. *South African Journal of Science*, **100**, 123-125.

- Tiffert, J. (2010): Erfassung der tsunami people exposure an der Andamanküste Thailands – Erstellung von Datengrundlagen zur bevölkerungs- und Touristenverteilung mit GIS & Fernerkundung. *Diploma thesis*, Christian-Albrechts-Universität zu Kiel, Germany.
- Tortell P. (1992): Coastal zone sensitivity mapping and its role in marine environmental management. *Mar Pollut Bull*, **25**, 88–93.
- Turner, B.L., Kasperson, R.E., Matson, P.A., McCarthy, J.J., Corell, R.W., Christensen, L., Eckley, N., Kasperson, J.X., Luers, A., Martello, M.L., Polsky, C., Pulsipher, A., Schiller, A. (2003): A framework for vulnerability analysis in sustainability science. *Proceedings of the National Academy of Sciences*, **100(14)**, 8074-8079.
- U.S. Geological Survey (USGS) (2004): *Shuttle Radar Topography Mission, 3 Arc Second scene*. Global Land Cover Facility, University of Maryland, College Park, Maryland, February 2000.
- United Nations Environment Programme (UNEP) (2002): *Global Environmental Outlook 3: Past, Present and Future Perspectives*. Earthscan, London.
- United Nations Environment Programme (UNEP) (2005): *After the Tsunami Rapid Environmental Assessment*. Available online at: [http://www.unep.org/tsunami/reports/TSUNAMI\\_report\\_complete.pdf](http://www.unep.org/tsunami/reports/TSUNAMI_report_complete.pdf) (accessed at 01.01.2009).
- United Nations Environment Programme - World Conservation Monitoring Centre (UNEP-WCMC) (2006): *In the front line: shoreline protection and other ecosystem services from mangroves and coral reefs*. UNEP-WCMC. Cambridge, p. 33.
- United Nations / International Strategy for Disaster Reduction (UN/ISDR) (2004): *Living with Risk, A global review of disaster reduction initiatives*. United Nations, Geneva. Available online at: [http://www.adrc.or.jp/publications/LWR/LWR\\_pdf/index.pdf#search=%22living%20with%20risk%20isdr%22](http://www.adrc.or.jp/publications/LWR/LWR_pdf/index.pdf#search=%22living%20with%20risk%20isdr%22) (accessed at 12.09.2008).
- United Nations Environment Programme (UNEP), Department of Marine and Coastal Resources (DMCR) (2007): *Post Tsunami impact on Marine and Coastal Resources in Thailand & Implementations for Future Work*. DMCR, Bangkok, p. 57.
- United Nations Inter-Agency Secretariat of the International Strategy for Disaster Reduction (UNISDR) (2005): *Tsunami Thailand One year later. National Response and Contribution of International Partners*. Bangkok, p. 122. Available online at: <http://www.unisdr.org/asiapacific/apublications/docs/un-tsunami-thailand-one-year-later.pdf> (accessed at 01.10.2010).
- Villa, F., McLeod, H. (2002): Environmental Vulnerability Indicators for Environmental Planning and Decision-Making: Guidelines and Applications. *Environ Manage*, **29**, 335–348.
- Villagrán De León, J.C. (2006): Vulnerability: A conceptual and methodological review. *SOURCE*. No. 4/2006, Bonn, Germany, p. 68.
- Vosberg (2010): Veränderung der Strandmorphologie an der thailändischen Andamanküste nach dem Tsunami von 2004. *Bachelor Thesis*, Christian-Albrechts-Universität zu Kiel, Germany.
- Vrabel, J. (1996): Multispectral Imagery Band Sharpening Study. *Photogr Eng Rem S*, **62**, 1075-1083.
- Wang, F., Xu, Y. J. (2009): Hurricane Katrina-induced forest damage in relation to ecological factors at landscape scale. *Environ Monit Assess*, **156**, 491–507.
- Wang, F., Xu, Y.J. (2010): Comparison of change detection techniques for assessing hurricane damage to forests. *Environ Monit Assess*, **162**, 311–326.
- Washington-Allen, R.A., Ramsey, R.D., West, N.E., Norton, B.E. (2008): Quantification of the ecological resilience of drylands using digital remote sensing. *Ecol Soc*, **13**, p. 33.

- Weidner, U.; Lemp, D. (2005): Objektorientierte Klassifizierung. In: Bähr, H.-P.; Vögtle, T. (Eds.): *Digitale Bildverarbeitung: Anwendungen in Photogrammetrie, Fernerkundung und GIS*, Heidelberg, 106-122.
- Weischet, W., Endlicher, W. (2000): *Regionale Klimatologie: Teil 2 Die Alte Welt: Europa, Afrika, Asien*. Stuttgart, Leipzig, p. 625.
- Weissmiller, A., Kristofs, J., Scholz, K., Anutap, E. Momens, A. (1977): Change detection in coastal zone environments. *Photogr Eng Rem S*, **43**, 1533-1539.
- Whistler, W.A., Elevitch, C.R. (2006): Casuarina equisetifolia (beach she-oak) and C. cunninghamiana (river she-oak), ver. 2.1. In Elevitch, C.R. (Ed.): *Species Profiles for Pacific Island Agroforestry*. Available online at: <http://www.traditionaltree.org> (accessed at 09.08.2010).
- Whitten, T., Damanik, S.J., Anwar, J., Hisyam, N. (1997): *The ecology of Sumatra*, Periplus Editions, Singapore, p. 583.
- Wibisono, I.T.C., Suryadiputra, I.N. (2006): Study of Lessons Learned from Mangrove/Coastal Ecosystem Restoration Efforts in Aceh since the Tsunami, *Wetlands International – Indonesia Programme*, Bogor, p. 86.
- Wilches-Chaux, G. (1993): La Vulnerabilidad Global. In: Maskrey, A. (Ed.): *Los Desastres no son Naturales*. La Red. Tercer Mundo Editores, Botoga.
- Williams, M., Foryce, F., Paijitprapapon, A., Charoenchaisri, P. (1996): Arsenic contamination in surface drainage and groundwater in part of the southeast Asian tin belt, Nakhon Si Thammarat Province, southern Thailand. *Environ Geol*, **27**, 16-33.
- Williams, L., Kaputska, L. (2000): Ecosystem vulnerability: A Complex interface with technical components. *Environ Toxicol Chem*, **19**, 1055–1058.
- Wisner, B. (2002): Who? What? Where? When? in an Emergency: Notes on Possible Indicators of Vulnerability and Resilience: By Phase of the Disaster Management Cycle and Social Actor. In: Plate, E. (Ed.): *Environment and Human Security*, Contributions to a workshop in Bonn, 23-25 October 2002, Germany, 12/7-12/14.
- Wisner, B.; Blaikie, P.; Cannon, T.; Davis, I. (2004): *At Risk: Natural hazards, People's Vulnerability and Disasters*. 2nd edn, Routledge, London. <<http://www.unisdr.org/eng/library/lib-select-literature.htm>>, 12 September 2006.
- Wolter, F., Clausnitzer, A., Akoglu, B., Stein, J. (2001): Piceatannol, a Natural Analog of Resveratrol, Inhibits Progression through the S Phase of the Cell Cycle in Colorectal Cancer Cell Lines. *American Society for Nutritional Sciences*, **131**, 2197-2203.
- Worldbank (2007): *Thailand Environment Monitor 2006*, Washington, USA), p. 42. Available online at: <http://siteresources.worldbank.org/INTTHAILAND/Resources/Environment-Monitor/2006term-forward.pdf> (accessed at 05.09.2010).
- Yanagisawa, H., Kushimura, S., Goto, K., Miyagi, T., Imamura, F., Ruangrassamee, A., and Tanavud, C. (2009): Damage to Mangrove Forest by 2004 Tsunami at Pakarang Cape and Namkem, Thailand. *Pol J Environ Stud*, **18**, 35–42.
- Zhang, H., Lin, X., Yu, G., Huang, X., Jing, G. (2009): Ecological vulnerability assessment in the middle and lower reaches of the Hanjiang river basin. *3<sup>rd</sup> International Conference on Bioinformatics and Biomedical Engineering (iCBBE 2009)*, 11-16 June 2009, Beijing, 1-4.

## 9 Appendix

### OVERVIEW

- A TRANSLATION OF THE LEGEND OF THE MAP ON THE MINERAL RESOURCES AND MINING ACTIVITIES.
- B PROCESS TREE DEVELOPED FOR THE NORTHERN AREA BETWEEN BAN NAM KHEM AND BAN BANG SAK.
- C CLASSES AND RULE SETS DEVELOPED FOR THE NORTHERN AREA BETWEEN BAN NAM KHEM AND BAN BANG SAK.
- D PROCESS TREE DEVELOPED FOR THE SOUTHERN AREA BETWEEN TAP LAMRU AND THAI MUEANG CITY.
- E CLASSES AND RULE SETS DEVELOPED FOR THE SOUTHERN AREA BETWEEN TAP LAMRU AND THAI MUEANG CITY.
- F-I LULC-CLASSIFICATION BASED ON OBJECT-ORIENTED IMAGE ANALYSIS.
- J ACCURACY ASSESSMENT OF THE LULC-MAP CREATED BY RULE-BASED OBJECT-ORIENTED CLASSIFICATION.
- K LULC-MAPPINGS: CLASS HIERARCHY.
- L FIELD PROTOCOL OF JANUARY 16, 2009.
- M-P EXPOSURE ANALYSIS.
- Q STANDARDISED BETA COEFFICIENTS.
- R REGRESSION STATISTICS ( $R^2=0.43$ ).
- S REGRESSION STATISTICS ( $R^2=0.33$ ).

**Appendix A. Translation of the legend of the map on the mineral resources and mining activities in the study area (original version).**



No.	English
1	Legend
2	Mineral Resource
3	dolomite
4	granite for construction industrial
5	limestone for cement industrial
6	limestone, dolomite limestone and dolomite
7	tin, tungsten and heavy mineral
8	Mineral Resource Potential Area
9	diamond
10	quartz (small quartz for making glass)
11	antimony
12	tin
13	tungsten
14	1,2,3.. mineral resource and potential mineral resource area
15	Mineral and Stone Abbreviation
16	aggregate
17	gold
18	diamond
19	dolomite
20	granite
21	ilmenite
22	leucocoxene
23	limestone
24	monazite
25	columbite
26	lead
27	rutile
28	antimony
29	quartz (small quatz for making glass)
30	samaraskite
31	tin
32	tantalite
33	tungsten
34	xenotime
35	zircon
36	mining patent permit, stone mining
37	cease-stone mining (finish operation)
38	mineral resource
39	bore hole-mineral resource exploration
40	founded mineral
41	stone mining industrial permit area
42	hot spring
43	slope differential level 100 m
44	Elevation point (m)
45	provincial boundary
46	province, district, district branch, village
47	road
48	railway
49	river, cannel, stream
50	lake, pond



## Appendix B. Process tree developed for the northern area between Ban Nam Khem and Ban Bang Sak.

at level a

- a) *classification of road*
  - multiresolution segmentation: 1000 [shape:0.1 compct.:0.5] creating 'Level a'
  - classification: classification of road
  - merge region: road at Level a: merge region
  - merge region: unclassified at Level a: merge region
  - multiresolution segmentation: unclassified at Level a: 500 [shape:0.1 compct.:0.5]
- b) *classification of ocean*
  - classification: unclassified at Level a: ocean
  - classification: unclassified at Level a: rest of ocean
  - merge region: rest of ocean at Level a: merge region
  - merge region: ocean at Level a: merge region
- c) *classification of streams, aquaculture, ponds*
  - multiresolution segmentation: rest of ocean at Level a: 250 [shape:0.1 compct.:0.5]
  - classification: rest of ocean at Level a: other water
  - merge region: other water at Level a: merge region
  - classification: other water at Level a: streams & canals
  - merge region: streams & canals at Level a: merge region
  - classification: at Level a: aquaculture: reservoirs
  - classification: other water at Level a: ponds
  - merge region: other water, rest of ocean at Level a: merge region
  - multiresolution segmentation: rest of ocean at Level a: 1000 [shape:0.5 compct.:0.7]
- d) *classification of beach, sand banks, rocks, intertidal areas*
  - chessboard segmentation: ocean at Level a: chess board: 40
  - classification: rest of ocean at Level a: sandy beaches\_a
  - merge region: sandy beaches\_a at Level a: merge region
  - classification: sandy beaches\_a at Level a: sandy beaches
  - merge region: rest of ocean, sandy beaches\_a at Level a: merge region
  - multiresolution segmentation: rest of ocean at Level a: 250 [shape:0.1 compct.:0.5]
  - classification: at Level a: rocks
  - classification: at Level a: intertidal areas
  - classification: rest of ocean at Level a: sand banks
- e) *classification of pool, casuarina shadows and forest, beach borders, pools*
  - merge region: sandy beaches at Level a: merge region
  - multiresolution segmentation: rest of ocean at Level a: 60 [shape:0.8 compct.:0.9]
  - chessboard segmentation: sandy beaches at Level a: chessboard: 10
  - classification: at Level a: pool
  - classification: at Level a: casuarina shadows
  - classification: at Level a: casuarina forests
  - merge region: casuarina forests at Level a: merge region
  - merge region: sandy beaches\_a at Level a: merge region
  - morphology: casuarina forests at Level a: closing: casuarina forests
  - merge region: sandy beaches at Level a: merge region
- f) *classification of aquaculture dry, riverbanks*
  - multiresolution segmentation: rest of ocean at Level a: 250 [shape:0.5 compct.:0.8]
  - classification: at Level a: aquaculture dry
  - assign class: aquaculture: reservoirs, aquaculture dry at Level a: aquaculture: reservoirs
  - merge region: aquaculture: reservoirs at Level a: merge region
  - chessboard segmentation: streams & canals at Level a: chessboard: 5
  - classification: rest of ocean at Level a: riverbank\_step1
  - multiresolution segmentation: riverbank\_step1 at Level a: 100 [shape:0.7 compct.:0.7]
  - classification: riverbank\_step1 at Level a: river mudflats
  - merge region: river mudflats at Level a: merge region
  - assign class: rest of ocean, riverbank\_step1 at Level a: rest of ocean
  - merge region: rest of ocean at Level a: merge region
  - merge region: streams & canals at Level a: merge region
- g) *classification of rainforest & mangroves*
  - multiresolution segmentation: rest of ocean at Level a: 550 [shape:0.5 compct.:1.0]
  - classification: at Level a: rainforest\_raw1
  - merge region: rainforest\_raw1 at Level a: merge region
  - classification: natural rainforest
  - assign class: rainforest\_raw1, rest of ocean at Level a: rest of ocean
  - merge region: rest of ocean at Level a: merge region
  - multiresolution segmentation: rest of ocean at Level a: 350 [shape:0.3 compct.:0.5]
  - classification: at Level a: mangrove forest
  - merge region: mangrove forest at Level a: merge region
  - merge region: rest of ocean at Level a: merge region
- h) *classification of sandy areas, road borders, mudflats*
  - multiresolution segmentation: rest of ocean at Level a: 135 [shape:0.5 compct.:1.0]
  - classification: at Level a: other sandy areas/bare soils
  - merge region: other sandy areas/bare soils at Level a: merge region
  - classification: at Level a: barren1 (road border)
  - assign class: barren1 (road border), road at Level a: road
  - merge region: road at Level a: merge region
  - classification: at Level a: mudflats

```

i) classification of plantation, secondary forests, woodlands, grasslands
  multiresolution segmentation: rest of ocean at Level a: 250 [shape:0.5 compct.:0.8]
  chessboard segmentation: sandy beaches at Level a: chess board: 10
  classification: rest of ocean at Level a: coconut
  classification: at Level a: oil palm
  merge region: coconut at Level a: merge region
  merge region: rest of ocean at Level a: merge region
  classification: rest of ocean at Level a: rubber
  merge region: rubber at Level a: merge region
  merge region: rest of ocean at Level a: merge region
  multiresolution segmentation: rest of ocean at Level a: 250 [shape:0.5 compct.:0.5]
  classification: at Level a: secondary forests_scale250
  classification: classification of savannah woodland
  classification: grassland
  classification: at Level a: sparse grassland
  assign class: grassland at Level a: dense grassland
  classification: at Level a: young plantation

j) classification of urban
  chessboard segmentation: road at Level a: chess board: 10
  classification: at Level a: built up low density
  merge region: built up low density at Level a: merge region
  classification: at Level a: built up high density
  classification: at Level a: urban at road
  classification: at Level a: shrimp farm industry

  merge region: road at Level a: merge region
  assign class: road, urban at road at Level a: road
  merge region: road at Level a: merge region
  assign class: rest of ocean, unclassified at Level a: rest of ocean
  merge region: rest of ocean at Level a: merge region

k) classification of bare soil, plantation and plantation buildings, grassland, forests scale 135
  multiresolution segmentation: rest of ocean at Level a: 135 [shape:0.6 compct.:1.0]
  classification: at Level a: bare soil
  merge region: bare soil at Level a: merge region
  classification: at Level a: prepared land
  classification: at Level a: sparsely covered by vegetation
  classification: at Level a: scrubland
  classification: at Level a: cashew nut
  classification: at Level a: other plantation
  classification: at Level a: plantation buildings

at level b
l) classification of buildings:
  multiresolution segmentation: rest of ocean at Level a: 25 [shape:0.8 compct.:0.8] creating 'level b'
  classification: at level b: building blue
  classification: at level b: building grey
  classification: at level b: building red
  classification: at level b: building bright
  merge region: with Existence of super objects rest of ocean (1) = 1 at level b: merge region

m) classification of trees and shadows
  classification: at level b: tree merge
  merge region: tree merge at level b: merge region
  multiresolution segmentation: unclassified at level b: 20 [shape:0.5 compct.:0.5]
  classification: unclassified at level b: trees
  classification: unclassified at level b: shadows
  classification: at level b: single scrub/tree
  classification: single trees at level b: small tree
  classification: single trees at level b: medium tree
  classification: medium tree at level b: medium round tree
  classification: shadows at level b: small shadow
  classification: shadows at level b: medium shadow
  classification: shadows at level b: medium round shadow

```

## Appendix C. Classes and rule sets developed for the northern area between Ban Nam Khem and Ban Bang Sak

Abbreviations:  
 ps: pan-sharpened  
 r/g/b/nir = mean value of red/green/blue/near-infrared band

classes created in level a

```

road
  and (min)
    Threshold: Length > 1000 m
    [5040-5050]: not X Center
    Threshold: Area < 290000 m²
    Threshold: Density <= 1.45

ocean
  or (max)
    and (min)
      [0.21-1.1]: Rel. border to ocean
      Threshold: Length/Width > 3
      Threshold: Brightness < 480
    Threshold: Area > 1500000 m²
  and (min)
    Threshold: Length/Width > 10
    Threshold: Rel. border to ocean = 1

```

```

other water
  and (min)
    Threshold: Mean ps nir < 275
    Threshold: Border to ocean < 500
    Threshold: Classified as rest of ocean = 1
    Threshold: Brightness <= 360
    Threshold: ndvi < 0.1
    Threshold: Rel. border to ocean < 0.2

streams & canals
  or (max)
    and (min)
      Threshold: Border to ocean < 100 m
      Threshold: Brightness < 600
      Threshold: Length/Width > 2.5
      Threshold: Distance to streams & canals < 250 m
      Threshold: ndvi < 0.2
      Threshold: Length > 200 m
      Threshold: Classified as rest of ocean = 1
      Threshold: Area < 1 ha
      Threshold: Length/Width < 8.8
    and (min)
      Threshold: Classified as other water = 1
      Threshold: Compactness > 5
    and (min)
      Threshold: Rel. border to ocean > 0
      Threshold: Classified as other water = 1
    and (min)
      Threshold: Distance to streams & canals < 360 m
      Threshold: Length/Width > 4.2
      Threshold: Length > 230 m
      Threshold: Classified as other water = 1
      Threshold: Distance to ocean > 0 m

aquaculture: reservoirs
  or (max)
    and (min)
      [1000-30000]: Area
      Threshold: Distance to aquaculture: reservoirs < 185 m
      Threshold: Rectangular Fit > 0.85
      Threshold: Mean nir < 300
    and (min)
      Threshold: Classified as other water = 1
    or (max)
      [4000-8500]: Area
      [10000-15600]: Area
      [1.5-1.6]: Compactness
      Threshold: Rectangular Fit >= 0.85

ponds
  and (min)
    Threshold: ndvi <= 0.02
    Threshold: Mean ps nir <= 235
    Threshold: Classified as other water = 1
    Threshold: X distance to image left border > 1000 m

sandy beaches a
  and (min)
    Threshold: Length/Width > 2.21
    Threshold: Border to aquaculture: reservoirs = 0
    Threshold: Brightness > 500
    Threshold: Distance to ocean <= 250 m
    Threshold: Classified as rest of ocean = 1

sandy beaches
  or (max)
    and (min)
      Threshold: Border to sandy beachesa > 100
      Threshold: Brightness > 450
      Threshold: Classified as rest of ocean = 1
      Threshold: Length/Width > 2
      Threshold: Border to ocean > 100
    and (min)
      Threshold: Classified as sandy beachesa = 1
      Threshold: Area > 35000

rocks
  and (min)
    not and (min)
      Threshold: Standard deviation b < 16
      Threshold: Area > 1 ha
      Threshold: Classified as rest of ocean = 1
    or (max)
      Threshold: Border to ocean > 100
      Threshold: Rel. border to ocean > 0.5
      [190-450]: Mean r
      [300-500]: Mean b
      [165-500]: Mean nir

intertidal areas
  or (max)
    and (min)
      Threshold: Brightness > 350
      Threshold: Classified as rest of ocean = 1
      Threshold: Distance to sandy beaches < 550 m
      [150-500]: Mean nir
      Threshold: Rel. border to streams & canals = 0
    and (min)
      Threshold: Border to intertidal areas > 100 m
      Threshold: Classified as rest of ocean = 1

```

```

sand banks
  and (min)
    Threshold: Rel. border to ocean = 1
    Threshold: Area > 1500
    Threshold: Brightness > 300

pool
  and (min)
    Threshold: Classified as rest of ocean = 1
    Threshold: Distance to sandy beaches <= 90 m
    Threshold: ndvi < -0.05

casuarina shadows
  or (max)
    and (min)
      Threshold: Brightness < 500
      Threshold: ndvi < 0.1
      Threshold: Classified as rest of ocean = 1
      Threshold: Rel. border to sandy beaches > 0.3
    and (min)
      Threshold: Classified as ponds = 1

casuarina forests
  or (max)
    and (min)
      or (max)
        Threshold: Brightness < 300
        and (min)
          [300-320]: Brightness
          Threshold: Rel. border to sandy beaches >= 0.1
        [0.22-0.49]: ndvi
        [180-246]: Mean r
        Threshold: Mean ps r < 215
        Threshold: Classified as rest of ocean = 1
        Threshold: Border to sandy beaches > 0 m
      and (min)
        Threshold: Classified as rest of ocean = 1
        Threshold: Distance to casuarina forests < 100 m
        Threshold: Rel. border to sandy beaches > 0.57
        Threshold: Border to sandy beaches > 100 m
    and (min)
      or (max)
        and (min)
          Threshold: Mean nir < 600
          Threshold: Distance to casuarina forests < 20 m
          Threshold: Border to road > 0
        and (min)
          Threshold: Border to casuarina forests > 0
          Threshold: Distance to sandy beaches < 24 m
      Threshold: Mean ps r < 208
      Threshold: ndvi < 0.52
      Threshold: Classified as rest of ocean = 1

aquaculture_dry
  and (min)
    Threshold: Classified as rest of ocean = 1
  or (max)
    and (min)
      [2350-17000]: Area
      [350-600]: Brightness
      Threshold: Compactness <= 1.71
      [150-200]: not Border to road
    and (min)
      Threshold: Distance to aquaculture: reservoirs <= 300 m
      Threshold: Classified as rest of ocean = 1
      [2000-13000]: Area
      [330-600]: Brightness
      Threshold: Distance to aquaculture_dry < 120 m
      Threshold: Compactness < 1.5

riverbank_step1
  and (min)
    Threshold: ndvi < 0.35
    Threshold: Distance to streams & canals <= 300 m
    Threshold: Classified as rest of ocean = 1

river_mudflats
  and (min)
    Threshold: Classified as riverbank basis = 1
    [-0.2-0.202]: ndvi
  or (max)
    and (min)
      Threshold: Rel. border to river mudflats > 0.5
    and (min)
      Threshold: Brightness <= 550
      Threshold: Border to river mudflats > 0
      Threshold: Border to sandy beaches < 40

rainforest_raw1
  or (max)
    and (min)
      Threshold: Classified as rest of ocean = 1
      Threshold: Rel. border to montaneous rainforest_raw1 > 0.8
      Threshold: Mean r < 150
    and (min)
      Threshold: Classified as rest of ocean = 1
      Threshold: ndvi > 0.45
      [174-200]: Standard deviation nir
      [100-194]: Mean r

```

```

natural rainforest
  or (max)
    and (min)
      Threshold: Area > 6 ha
      Threshold: Classified as montaneous rainforest_raw1 = 1
    and (min)
      Threshold: Rel. border to natural rainforest > 0.9

mangrove forest
  or (max)
    and (min)
      [85-130]: Standard deviation PAN
      [130-197]: Standard deviation nir
    or (max)
      Threshold: Border to streams & canals > 0
      Threshold: Distance to river mudflats < 200 m
    and (min)
      Threshold: Border to mangrove forest > 500 m
      [0.47-0.6]: ndvi
      [150-206]: Mean r
      [500-750]: Mean nir
      Threshold: Classified as rest of ocean = 1
      Threshold: Brightness <= 280
    and (min)
      [0.4-0.65]: ndvi
      Threshold: Brightness <= 282
      Threshold: Border to mangrove forest > 50 m
      Threshold: Mean r < 200
    and (min)
      Threshold: ndvi < 0.6
      Threshold: Rel. border to mangrove forest > 0.33
      Threshold: Border to mangrove forest > 600
      Threshold: Standard deviation PAN < 100
      Threshold: Mean r < 215

other sandy areas/bare soils
  and (min)
    Threshold: Classified as rest of ocean = 1
  or (max)
    Threshold: [Mean ps r]/[brightness ps] >= 1.1
  and (min)
    Threshold: [Mean g]/[Mean r] < 0.98
    Threshold: Brightness > 700
    [650-1000]: Brightness
  and (min)
    Threshold: Standard deviation nir < 160
    [-0.05-0.16]: ndvi
    Threshold: Classified as rest of ocean = 1
    Threshold: [Mean g]/[Mean r] < 0.92
    [430-800]: Brightness

barrenl (road border)
  and (min)
    Threshold: Rel. border to road > 0.45
    Threshold: Border to road > 50 m
    Threshold: Length/Width > 6
    Threshold: Classified as other sandy areas/bare soils = 1

mudflats
  or (max)
    and (min)
      Threshold: Distance to mudflats < 20
      Threshold: ndvi < 0.12
      Threshold: Standard deviation b < 50
    or (max)
      Threshold: Classified as rest of ocean = 1
      Threshold: Classified as sandy beaches = 1
    and (min)
      or (max)
        Threshold: Distance to sandy beaches < 200 m
        Threshold: Distance to streams & canals < 300
      or (max)
        Threshold: Classified as streams & canals = 1
        Threshold: Classified as sandy beaches = 1
        Threshold: Classified as rest of ocean = 1
      and (min)
        [400-700]: Brightness
        Threshold: ndvi <= 0.1
        Threshold: Standard deviation b < 30
    Threshold: Classified as river mudflats = 1

```



```

coconut
  and (min)
    [0.3-0.6]: ndvi
    Threshold: Classified as rest of ocean = 1
    Threshold: Area of sub-objects: mean (1) <= 65
  not and (min)
    Threshold: L/W-subobj. < 1.747
    Threshold: ndvi > 0.54
  or (max)
    and (min)
      Threshold: Distance to coconut < 100 m
      Threshold: Distance to sandy beaches < 300 m
      Threshold: Rel. area of sub objects medium tree (1) > 0.05
    and (min)
      Threshold: [Number of sub objects medium round shadow (1)]/[Number of sub-objects] >= 0.05
      Threshold: Number of sub objects medium round shadow (1) >= 30
      [500-1200]: Distance to sandy beaches
    and (min)
      Threshold: Area < 4.95 ha
      Threshold: Rel. border to coconut > 0.1
      Threshold: [Number of sub objects medium round shadow (1)]/[Number of sub-objects] > 0.04
      Threshold: Area of sub-objects: stddev (1) <= 40
    and (min)
      or (max)
        and (min)
          Threshold: Number of sub-objects > 250
          Threshold: [Number of sub objects medium round shadow (1)]/[Number of sub-objects] > 0.068
        and (min)
          Threshold: L/W-subobj. > 2
          Threshold: Number of sub-objects >= 300
          Threshold: Distance to coconut <= 60 m

oil palm
  [200-220]: Mean r
  Threshold: Classified as rest of ocean = 1
  or (max)
    and (min)
      Threshold: Rel. area of sub objects medium round tree (1) > 0.02
      Threshold: Border to oil palm > 0
      Threshold: Mean r > 195
    and (min)
      or (max)
        and (min)
          Threshold: Number of sub objects medium round shadow (1) >= 140
          Threshold: Number of sub objects medium round tree (1) > 50
          Threshold: Number of sub objects medium tree (1) > 100
        and (min)
          Threshold: L/W-subobj. < 2.2
          Threshold: Number of sub-objects > 200
          Threshold: Rel. area of sub objects medium round tree (1) > 0.03

rubber
  and (min)
    Threshold: Distance to sandy beaches > 150 m
    Threshold: Classified as rest of ocean = 1
  or (max)
    and (min)
      Threshold: Distance to sandy beaches > 770 m
      Threshold: Area > 1 ha
      Threshold: L/W-subobj. > 1.5
      Threshold: Rel. border to rubber > 0.1
      Threshold: Standard deviation nir < 110
    and (min)
      Threshold: Length/Width < 3.2
      Threshold: Border to rubber > 0
      Threshold: L/W-subobj. > 2.3
      Threshold: ndvi > 0.25
      Threshold: Area > 0.5 ha
    and (min)
      Threshold: Mean r <= 240
      [1.4-2.3]: l/w subobj.
      [90-160]: Standard deviation nir
      Threshold: [Mean g]/[Mean b] < 1.08
      [0.3-0.65]: ndvi
    and (min)
      Threshold: Mean r < 240
      Threshold: Border to rubber > 50 m
    or (max)
      Threshold: L/W-subobj. > 2.3
      Threshold: Standard deviation nir < 90
    and (min)
      Threshold: Standard deviation nir < 155
      Threshold: L/W-subobj. > 1.73

secondary forests_scale250
  and (min)
    Threshold: Mean ps nir < 175
    Threshold: L/W-subobj. < 2
    Threshold: Classified as rest of ocean = 1
    Threshold: ndvi > 0.5

savannah woodland (open woodland)
  and (min)
    [0.19-0.41]: ndvi
    Threshold: Brightness > 268
    Threshold: Classified as rest of ocean = 1
    Threshold: Rel. border to other sandy areas/bare soils < 0.8

```

```

grassland
  and (min)
    Threshold: Classified as rest of ocean = 1
  or (max)
    and (min)
      Threshold: Rel. border to grassland > 0.2
      Threshold: ndvi > 0.19
    and (min)
      Threshold: ndvi > 0.19
      Threshold: Area of sub-objects: mean (1) > 50
      Threshold: Standard deviation nir < 140
    and (min)
      [90-130]: Standard deviation nir
      Threshold: ndvi > 0.4
    and (min)
      Threshold: ndvi > 0.19
      Threshold: Standard deviation nir <= 100

sparse grassland
  and (min)
    Threshold: Classified as grassland = 1
    [0.19-0.41]: ndvi

young plantation
  and (min)
    not and (min)
      Threshold: Length/Width > 3
      Threshold: Border to road > 50 m
    or (max)
      and (min)
        [0.1-0.46]: ndvi
      or (max)
        and (min)
          Threshold: Border to young plantation > 0
          Threshold: Area > 0.48 ha
        or (max)
          and (min)
            Threshold: Border to rubber > 0
            Threshold: Border to young plantation > 0
            Threshold: Rel. border to rubber > 0.12
          and (min)
            Threshold: L/W-subobj. > 1.7
            Threshold: Brightness > 270
            Threshold: Rel. border to rubber > 0.2
      or (max)
        Threshold: Classified as rest of ocean = 1
        Threshold: Classified as sparse grassland = 1
        Threshold: Classified as dense grassland = 1
        Threshold: Classified as dense grassland (2) = 1
        Threshold: Classified as scrubland = 1

build up low density
  and (min)
    Threshold: Classified as rest of ocean = 1
    Threshold: Distance to road <= 200 m
  not and (min)
    Threshold: Area > 5000 m2
    Threshold: Standard deviation nir < 90
  or (max)
    and (min)
      Threshold: Max. pixel value psB > 800
    or (max)
      and (min)
        Threshold: Distance to road < 350 m
        Threshold: Rel. area of sub objects building red (1) >= 0.05
      and (min)
        Threshold: Distance to road < 100
        Threshold: Rel. area of sub objects building grey (1) > 0.05
      and (min)
        Threshold: Distance to road < 100 m
        Threshold: Rel. area of sub objects building bright buildings (1) > 0.05
        Threshold: Rel. area of sub objects building blue (1) > 0.05
    or (max)
      and (min)
        Threshold: Number of sub objects lb_bright buildings (1) >= 1
      and (min)
        Threshold: Rel. area of sub objects building blue (1) > 0.04
        Threshold: Number of sub objects building blue (1) >= 1
      and (min)
        Threshold: Distance to road < 20 m
        [1-9]: Number of sub objects grey building1 (1)
      and (min)
        Threshold: Classification value of building blue > 0.1

build up high density
  and (min)
    Threshold: Classified as build up low density = 1
    Threshold: ndvi < 0.2

urban at road
  and (min)
    Threshold: Rel. border to road > 0.45
    Threshold: Border to road > 50 m
    Threshold: Length/Width > 6
    Threshold: Classified as build up low density = 1

```

```

shrimp farm industry
  or (max)
    and (min)
      Threshold: Distance to aquaculture: reservoirs < 15 m
      Threshold: Distance to shrimp farm industry < 220 m
      Threshold: Classified as build up low density = 1
    and (min)
      Threshold: Classified as build up low density = 1
      Threshold: Brightness > 550
      Threshold: Area > 2 ha

bare soil
  and (min)
    Threshold: ndvi < 0.15
    Threshold: Classified as rest of ocean = 1

prepared land
  or (max)
    and (min)
      Threshold: Area > 1 ha
      Threshold: Classified as bare soil = 1
      Threshold: Distance to rubber < 30 m
      Threshold: L/W-subobj. > 1.5
    and (min)
      Threshold: Classified as rubber = 1
      Threshold: ndvi <= 0.15

sparsely covered by vegetation
  and (min)
    [0.15-0.2]: ndvi
    Threshold: Classified as rest of ocean = 1

scrubland
  and (min)
    Threshold: Classified as grassland = 1
  or (max)
    and (min)
      Threshold: [N small shadow]/[Area] > 0.7
      Threshold: Area < 1.6 ha
      Threshold: Number of sub objects small shadow (1) >= 18
      [0.3-0.5]: ndvi
    and (min)
      [40-65]: Area of sub-objects: mean (1)
      [250-290]: Brightness
      [0.4-0.5]: ndvi
      Threshold: Number of sub objects small shadow (1) > 15

cashew nut
  and (min)
    Threshold: Rel. area of sub objects unclassified (1) < 0.75
  or (max)
    Threshold: Classified as rest of ocean = 1
    Threshold: Classified as dense grassland = 1
    Threshold: ndvi > 0.45
  or (max)
    and (min)
      Threshold: Number of sub objects medium round tree (1) >= 12
      Threshold: Brightness >= 245
      Threshold: Rel. area of sub objects medium round tree (1) > 0.037
    and (min)
      Threshold: Rel. area of sub objects small and round tree (1) > 0.01
      Threshold: Number of sub objects small and round tree (1) >= 6

other plantation
  and (min)
    or (max)
      Threshold: Classified as rest of ocean = 1
      Threshold: Classified as sparse grassland = 1
    Threshold: Area > 3000 m²
  or (max)
    and (min)
      Threshold: Distance to other plantation < 200 m
    or (max)
      Threshold: N small shadow > 45
      Threshold: Rel. area of sub objects small shadow (1) >= 0.04
    and (min)
      Threshold: N small shadow > 80
    and (min)
      Threshold: Border to other plantation > 0
      Threshold: Number of sub objects small shadow (1) >= 25

plantation buildings
  and (min)
    or (max)
      Threshold: Rel. border to Young plantation > 0.9
    and (min)
      Threshold: Rel. border to oil palm > 0.4
      Threshold: Rel. border to Rubber > 0.4
      Threshold: Rel. border to Cashew Nut > 0.5
      Threshold: Rel. border to Coconut > 0.9
      Threshold: Rel. border to Rubber > 0.9
      Threshold: Rel. border to oil palm > 0.9
    Threshold: Classified as build up low density = 1

```

```

Classes created in level b

building blue
  and (min)
    Threshold: Mean nir > 250
    Threshold: ndvi ps < 0.2
    Threshold: Existence of super objects rest of ocean (1) = 1
    Threshold: [Mean psB]/[Mean psG] > 1.05
    Threshold: brightness ps >= 230

building grey
  and (min)
    Threshold: Rectangular Fit > 0.8
    Threshold: Mean nir > 260
    Threshold: Existence of super objects rest of ocean (1) = 1
    Threshold: ndvi ps < 0.15
    Threshold: [Mean ps r]/[Mean psB] < 0.9
    Threshold: Border to beach new lb = 0

building red
  and (min)
    Threshold: Length/Width < 3
    Threshold: Existence of super objects rest of ocean (1) = 1
    Threshold: Area < 500 m2
    Threshold: [Mean ps r]/[Mean psG] > 0.987
    [200-450]: brightness ps
    Threshold: Distance to barren_lb > 5 m

building bright
  and (min)
    Threshold: Existence of super objects rest of ocean (1) = 1
  or (max)
    and (min)
      Threshold: brightness ps > 600
      Threshold: [Mean ps r]/[Mean psB] < 1
    and (min)
      [0.9-1.25]: [Mean ps r]/[Mean psB]
      Threshold: brightness ps > 600
    Threshold: brightness ps > 800
    and (min)
      Threshold: brightness ps > 600
      Threshold: ndvi ps < -0.2

tree merge
  and (min)
    Threshold: Existence of super objects rest of ocean (1) = 1

trees
  and (min)
    Threshold: Mean diff. to brighter neighbors ps nir > 999
    Threshold: Existence of super objects rest of ocean (1) = 1
    Threshold: Classified as unclassified = 1

shadows
  and (min)
    Threshold: Classified as unclassified = 1
    Threshold: Existence of super objects rest of ocean (1) = 1
    Threshold: Mean diff. to darker neighbors ps nir > 99999

single scrub/tree
  and (min)
    Threshold: Existence of super objects rest of ocean (1) = 1
    Threshold: Classified as trees = 1
    [20-140]: Area

small tree
  and (min)
    [10-20]: Area
    Threshold: Classified as single scrub/tree = 1

medium tree
  and (min)
    [20-50]: Area
    Threshold: Classified as single scrub/tree = 1

Medium round tree
  and (min)
    Threshold: Classified as medium tree = 1
    [0.1-0.6]: Roundness

small shadow
  and (min)
    [10-20]: Area
    Threshold: Classified as shadows = 1

medium shadow
  and (min)
    [20-50]: Area
    Classified as shadows = 1

medium round shadow
  and (min)
    Threshold: Roundness <= 1
    Classified as Medium shadow = 1

```

## Appendix D. Process tree developed for the southern area between Tap Lamru and Thai Mueang city.

```
[...]
i) classification of plantation, secondary forests, woodlands, grasslands
multiresolution segmentation: rest of ocean at Level a: 250 [shape:0.5 compct.:0.8]
chessboard segmentation: sandy beaches at Level a: chess board: 10
  classification: rest of ocean at Level a: coconut
  classification: at Level a: oil palm
  merge region: coconut at Level a: merge region
  merge region: rest of ocean at Level a: merge region
  classification: rest of ocean at Level a: rubber
  merge region: rubber at Level a: merge region
  merge region: rest of ocean at Level a: merge region
multiresolution segmentation: rest of ocean at Level a: 250 [shape:0.5 compct.:0.5]
classification: at Level a: secondary forests scale250
classification: at Level a: peat swamp forest*
classification: at Level a: mixed beach forest
classification: at Level a: melaleuca savannah
classification: classification of savannah woodland
classification: grassland
classification: at Level a: sparse grassland
assign class: grassland at Level a: dense grassland
classification: at Level a: young plantation
[...]
```

## Appendix E. Classes and rule sets developed for the southern area between tap Lamru and Thai Mueang city.

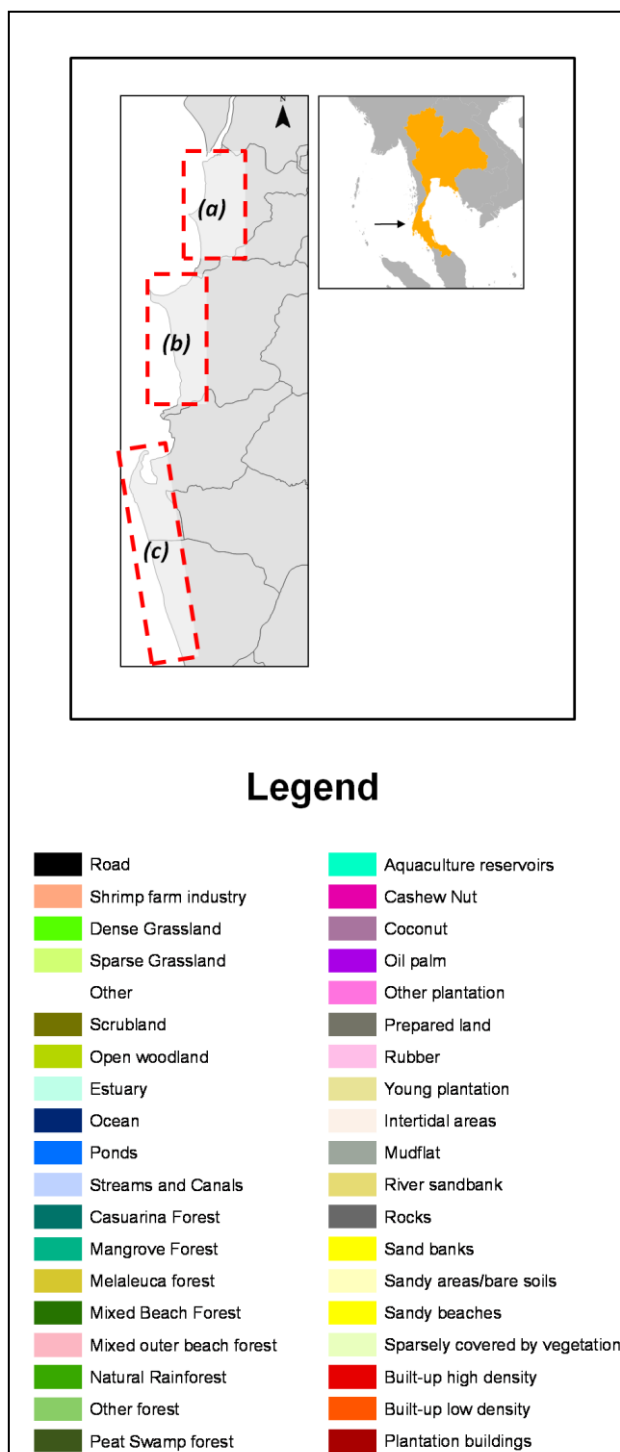
```
peat swamp forest
  and (min)
    [150-200]: Mean r
    [0.25-0.5]: ndvi
    Classified as rest of ocean = 1
  or (max)
    Threshold: Border to peat swamp forest > 0 m
    Threshold: Border to streams & canals > 0 m

mixed beach forest
  and (min)
    Threshold: Mean r > 210
    Threshold: ndvi > 0.5
    Classified as rest of ocean = 1
    Threshold: Distance to sandy beaches < 1000 m

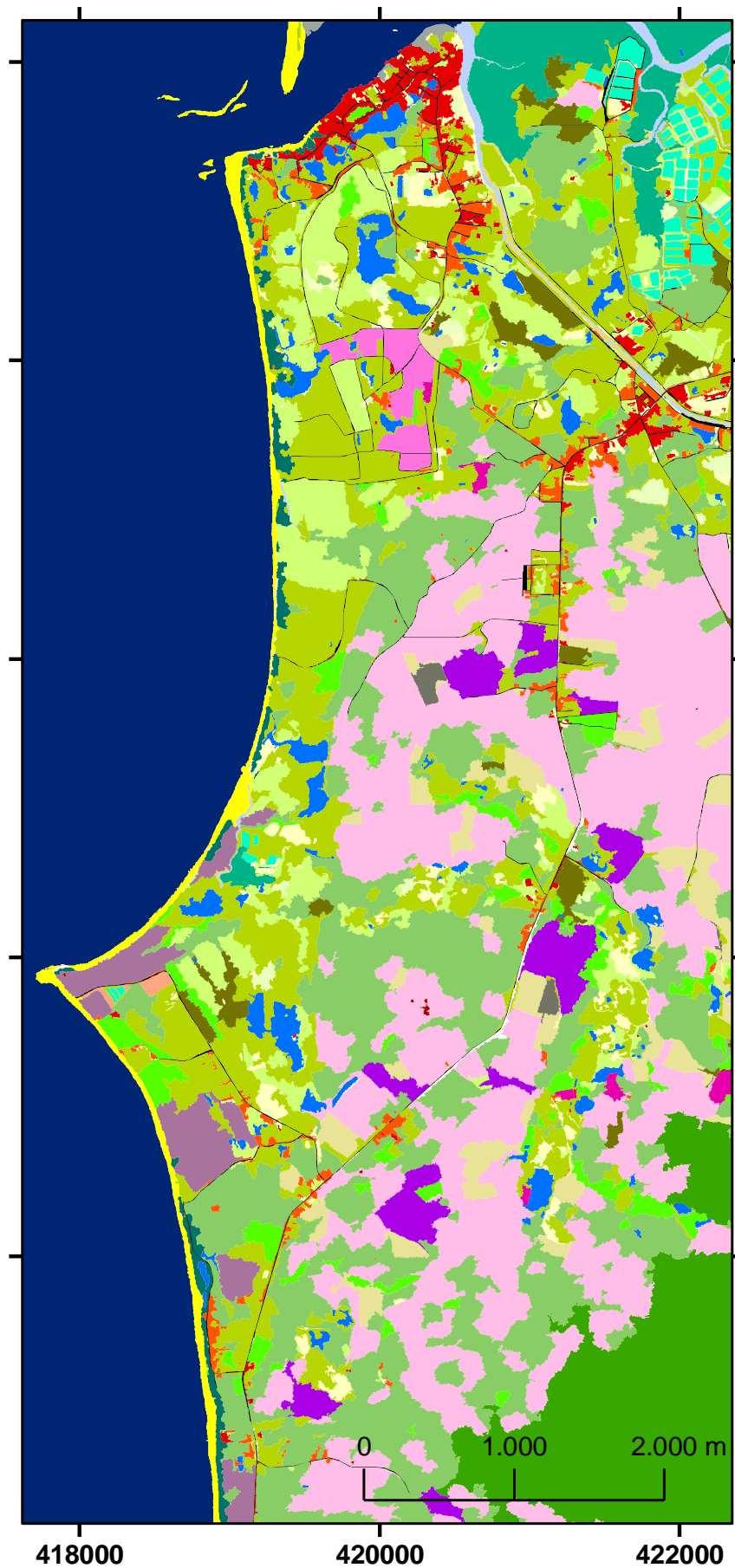
melaleuca savannah
  and (min)
    Threshold: Brightness < 335
    [220-325]: Mean r
    [0.2-0.36]: ndvi
    Classified as rest of ocean = 1
    Threshold: Distance to sandy beaches < 1000 m
    Threshold: Distance to mixed beach forests < 500 m
```



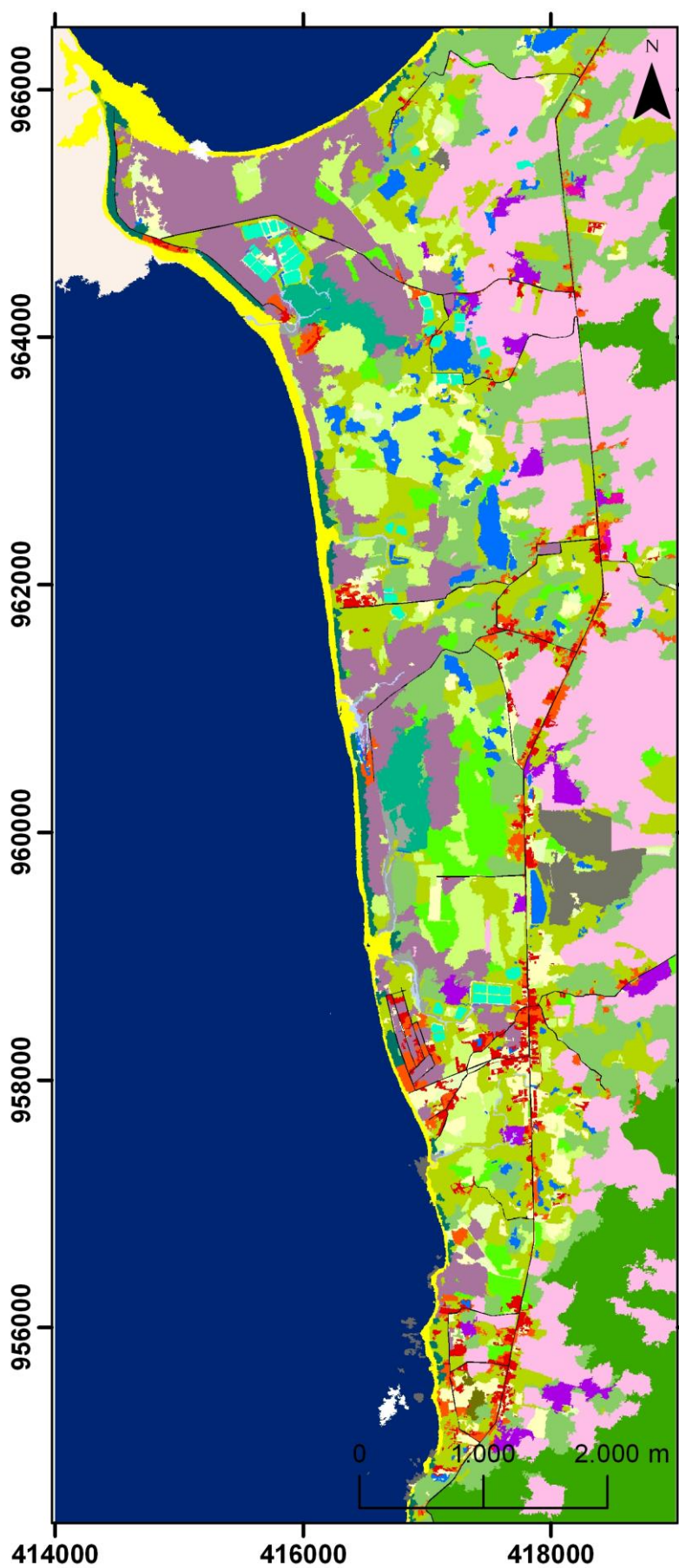
## Appendix F. LULC-classification based on object-oriented image analysis: legend.



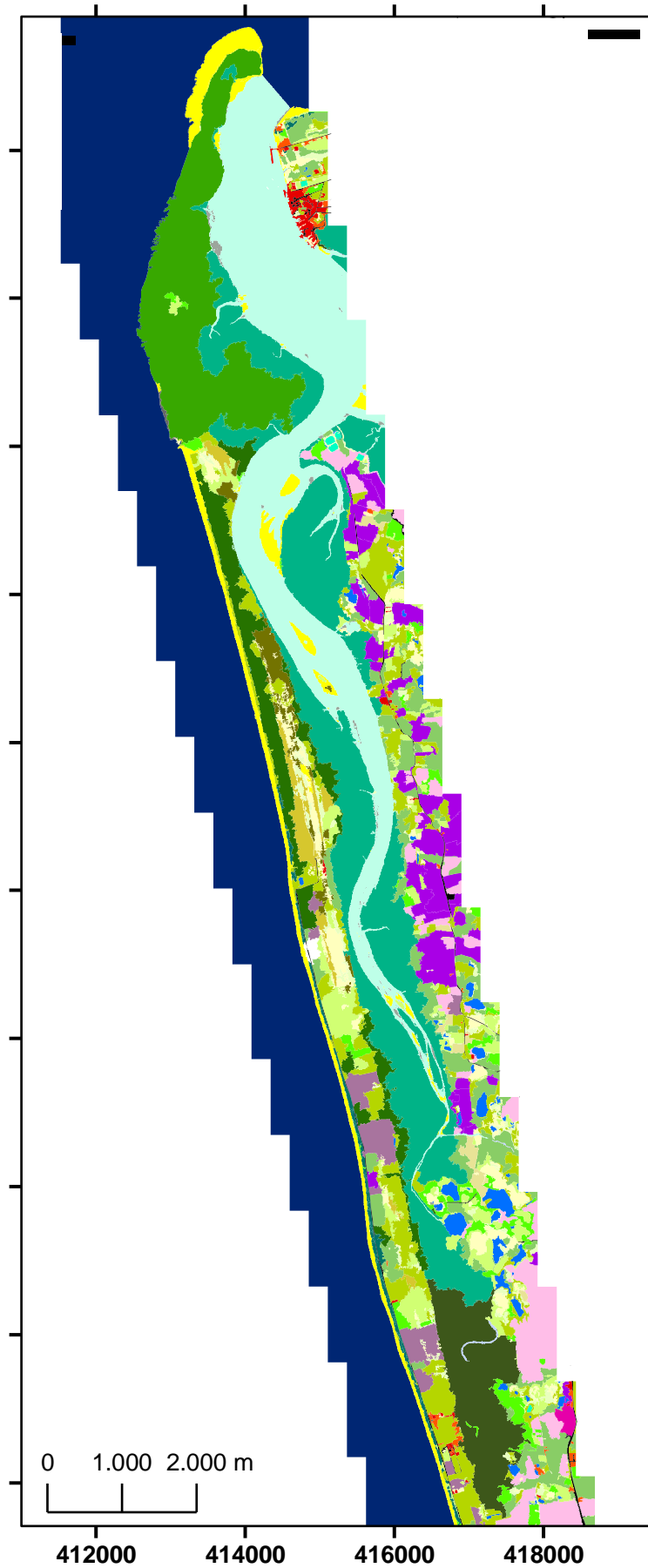
Appendix G. LULC-classification based on object-oriented image analysis: part (a).



## Appendix H. LULC-classification based on object-oriented image analysis: part (b).



Appendix I. LULC-classification based on object-oriented image analysis: part (c).







**Appendix K. LULC-mappings: class hierarchy**

Hierarchy level 1	Hierarchy level 2
1 Agriculture and aquaculture	<ul style="list-style-type: none"> <li>- Aquaculture reservoirs</li> <li>- Cashew Nut</li> <li>- Coconut</li> <li>- Mixed plantation</li> <li>- Oil palm</li> <li>- Orchards</li> <li>- Other plantation</li> <li>- Prepared land</li> <li>- Rubber</li> <li>- Young plantation</li> </ul>
2 Barren land	<ul style="list-style-type: none"> <li>- Rocks</li> <li>- Sand banks</li> <li>- Sandy areas/bare soils</li> <li>- Sandy beaches</li> </ul>
3 Built-up	<ul style="list-style-type: none"> <li>- Hotel complexes</li> <li>- Industrial area</li> <li>- Residential</li> <li>- Residential / Commercial</li> </ul>
4 Grassland and herbaceous	<ul style="list-style-type: none"> <li>- Grassland</li> <li>- Herbaceous</li> </ul>
5 Scrubland	<ul style="list-style-type: none"> <li>- Scrubland dense</li> <li>- Scrubland open</li> </ul>
6 Semi-open landscape	<ul style="list-style-type: none"> <li>- Open woodland</li> </ul>
7 Water	<ul style="list-style-type: none"> <li>- Canal</li> <li>- Pond</li> <li>- Stream</li> </ul>
8 Woodland	<ul style="list-style-type: none"> <li>- Casuarina forest</li> <li>- Mangrove forest</li> <li>- Melaleuca forest</li> <li>- Mixed beach forest</li> <li>- Mixed farm forest</li> <li>- Peat swamp forest</li> <li>- Secondary forest / Other forest</li> </ul>

## Appendix L. Field protocol of January 16, 2009.

Field Protocol – Ecological Resilience  
Site ID:

Page 1

TRAIT Project

## APPENDIX XY

## 1 General Information (study site scale)

Date/Time _____ / _____	Observer _____	Region: (a) B (b) K (c) T	Site ID _____			
Weather condition (a) sunny/fair (b) cloudy (c) overcast (d) rain (e) other: _____						
Study site coordinates & photo reference						
Point	X	Y	Z (m)	Photo ID	accuracy	View direction
1						
2						
3						
4						

<b>Study Site Area</b> (a) 225 m <sup>2</sup> (15x15m) (b) 900 m <sup>2</sup> (30x30m) (c) Other (exceptional case): _____
---

<b>Biotope (Pre-tsunami condition)</b> (a) Casuarina forest/Outer beach forest (b) Swamp Forest (c) Secondary Forest (d) Mangrove forest (e) Temporary Swamp Forest (f) Coconut Plantation (g) Rubber Plantation (h) Inner Beach forest (i) other: _____
<b>Initial Plant community / most frequent plant species (pre-tsunami)</b> 1 _____ 3 _____ 2 _____ 4 _____

<b>Local topography</b> (a) Hill top (b) Depression (c) Plain (d) Hillside (e) Other: _____ If "d", exposition (in °): _____
--

Remarks (obstacles, special features)

## 2 Impact Information (study site scale)

<b>Interview with land owners</b> name of interviewee: _____ age: _____ gender: _____ job: _____	
<b>Impact class</b> forest biotopes: (1) 80-100% of trees are dead / uprooted (2) 50-80% of trees are dead / uprooted (3) 20-50% of trees are dead / uprooted (4) >0-20% of trees are dead / uprooted (5) no damage	
<b>Type of impact</b> (a) Direct (b) Indirect (c) both (d) unknown/other: _____	
<b>Displacement of organic topsoil</b> (a) yes (b) no (c) unknown	<b>Sedimentation of marine (saline) sediments</b> (a) yes (b) no (c) fractional (d) unknown
<b>Land use history (3 decades):</b>	

Remarks/References:

**3 Qualitative Aspects of Recovery / Succession (study site scale)**

A) *Human Impacts*

**Intensity of human impacts since 26<sup>th</sup> of December 2004**  
 (a) strong      (b) low      (c) no impacts/not noticeable

**If “a” or “b”, what kind of impact:**  
 (a) Replanting/Seeding    (b) Levelling/clearing    (c) drainage    (d) Fertilization    (e) Other: \_\_\_\_\_

*Succession process*

**Most frequent new/recovered plant species**  
 1 \_\_\_\_\_      3 \_\_\_\_\_  
 2 \_\_\_\_\_      4 \_\_\_\_\_

**Changes in species composition** *(are there new/ recovered species being atypical for initial biotope conditions?)*  
 (a) Yes      (b) No (or inconsiderable)

**If “a”, which species?**  
 -      -  
 -      -  
 -      -

**Direction of Succession**  
 (a) Same biotope      (b) another biotope      (c) not yet predictable      (d) no succession process noticeable

**If “b” which biotope:** \_\_\_\_\_

Remarks/References

**4 Quantitative recovery measurements (plot & tree scale)**

**N of plots:**  
 (a) 5      (b) other: \_\_\_\_\_

**Area of plots**  
 (a) 25m<sup>2</sup> (b) 100m<sup>2</sup>: \_\_\_\_\_

**N trees (Pre-Tsunami):** \_\_\_\_\_

Remarks/References

**Sketch** *(corners of study site, grid, plot location and plot ID; North arrow)*

Table 1: Plot measurements:

	Photos ID		cover		Ground cover/Crown closure						Soil texture	
	1.3m above ground, vertical down	1.3m above ground, vertical up	All plants lower than 1.3m	Herbaceous vegetation	Species 1 (Sapling)	Species 2 (Sapling)	Species 3 (Sapling)	Species 4 (Sapling)	Species 5 (Sapling)	Species 6 (Sapling)	All Saplings	Centre plot
-NW												
-NE												
-SE												
-SW												
-C												

Table 2: Tree inventory

Individual	NW Plot				NE Plot				SE plot				SW-Plot				Centre-Plot			
	Species ID	DBH (50cm)	lr.	Height	Species ID	DBH (50cm)	Clr.	Height	Species ID	DBH (50cm)	Clr.	Height	Species ID	DBH (50cm)	Clr.	Height	Species ID	DBH (50cm)	Clr.	Height
1																				
2																				
3																				
4																				
5																				
6																				
7																				
8																				
9																				
10																				
11																				
12																				
13																				
14																				
15																				
16																				
17																				
18																				
19																				
20																				

Total Amount																				
Species ID: 1=	2=	3=	4=	5=	6=	9= other														

Remarks/References

Patterns (suitable for ground cover and crown closure estimation)

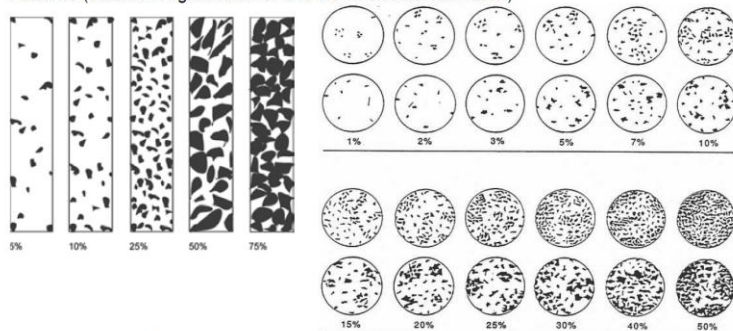


Table 1 BRAUN-BLANQUET scale

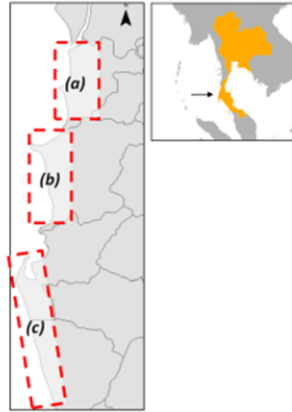
Braun-Blanquet scale	Range of cover (%)
5	75-100
4	50-75
3	25-50
2	5-25
1	<5; numerous individuals
+	<5; few individuals
0	No individuals, no coverage

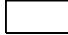





Table 1: BRAUN-BLANQUET scale

Table 2: Field Method for Identification of Soil Texture (<http://www.osha.gov/doc/outreachtraining/htmlfiles/soiltex.html>)

code	texture	Visual Detection of Particle Size and General Appearance of the Soil	Squeezed in hand and pressure released		Soil ribboned between thumb and finger when moist
			When air dry	when moist	
1	Stony/ gravel	grain size bigger than 2mm			
2	Sand	Soil has a granular appearance in which the individual grain sizes can be detected. It is free-flowing when in a dry condition.	Will not form a cast and will fall apart when pressure is released.	Forms a cast which will crumble when lightly touched.	Can not be ribboned.
3	Sandy loam	Essentially a granular soil with sufficient silt and clay to make it somewhat coherent. Sand characteristics predominate.	Forms a cast which readily falls apart when lightly touched.	Forms a cast which will bear careful handling without breaking.	Can not be ribboned.
4	Loam	A uniform mixture of sand, silt and clay. Grading of sand fraction quite uniform from coarse to fine. It is mellow, has somewhat gritty feel, yet is fairly smooth and slightly plastic.	Forms a cast which will bear careful handling without breaking.	Forms a cast which can be handled freely without breaking.	Can not be ribboned.
5	Silt loam	Contains a moderate amount of the finer grades of sand and only a small amount of clay. Over half of the particles are silt. When dry it may appear quite cloddy which readily can be broken and pulverized to a powder.	Forms a cast which can be freely handled. Pulverized it has a soft flourlike feel.	Forms a cast which can be freely handled. When wet, soil runs together and puddles.	It will not ribbon but it has a broken appearance, feels smooth and may be slightly plastic.
6	Silt	Contains over 80% of silt particles with very little fine sand and clay. When dry, it may be cloddy, readily pulverizes to powder with a soft flourlike feel.	Forms a cast which can be handled without breaking.	Forms a cast which can be freely be handled. When wet, it readily puddles.	It has a tendency to ribbon with a broken appearance, feels smooth.
7	Clay loam	Fine textured soil breaks into very hard lumps when dry. Contains more clay than silt loam. Resembles clay in a dry condition; identification is made on physical behavior of moist soil.	Forms a cast which can be freely handled without breaking.	Forms a cast which can be handled freely without breaking. It can be worked into a dense mass.	Forms a thin ribbon which readily breaks, barely sustaining its own weight.
8	Clay	Fine textured soil breaks into very hard lumps when dry. Difficult to pulverize into a soft flourlike powder when dry. Identification based on cohesive properties of the moist soil.	Forms a cast which can be freely handled without breaking.	Forms a cast which can be handled freely without breaking.	Forms long, thin flexible ribbons. Can be worked into a dense, compact mass. Considerable plasticity.
9	Other				

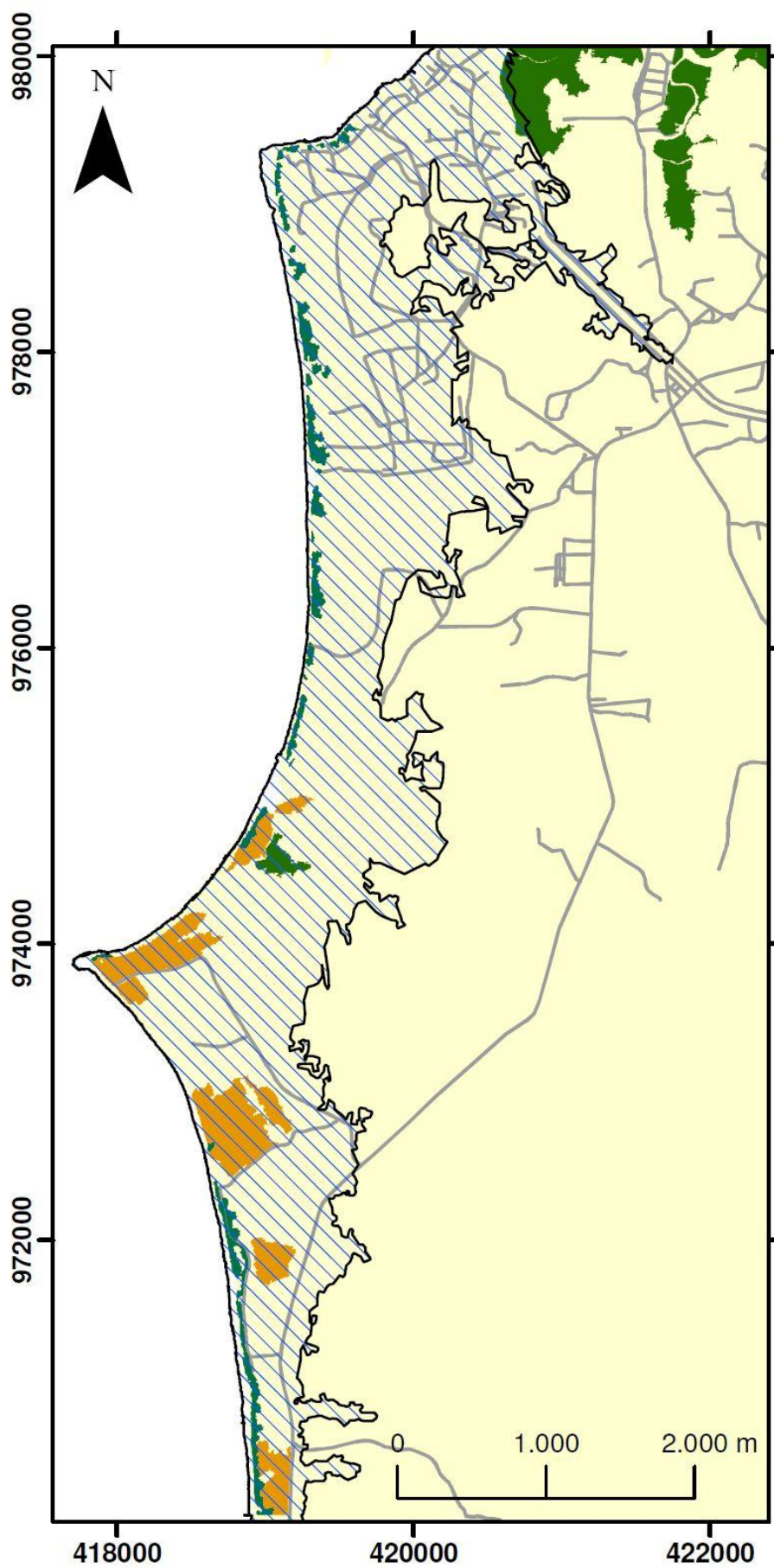
**Appendix M. Exposure analysis: legend.**



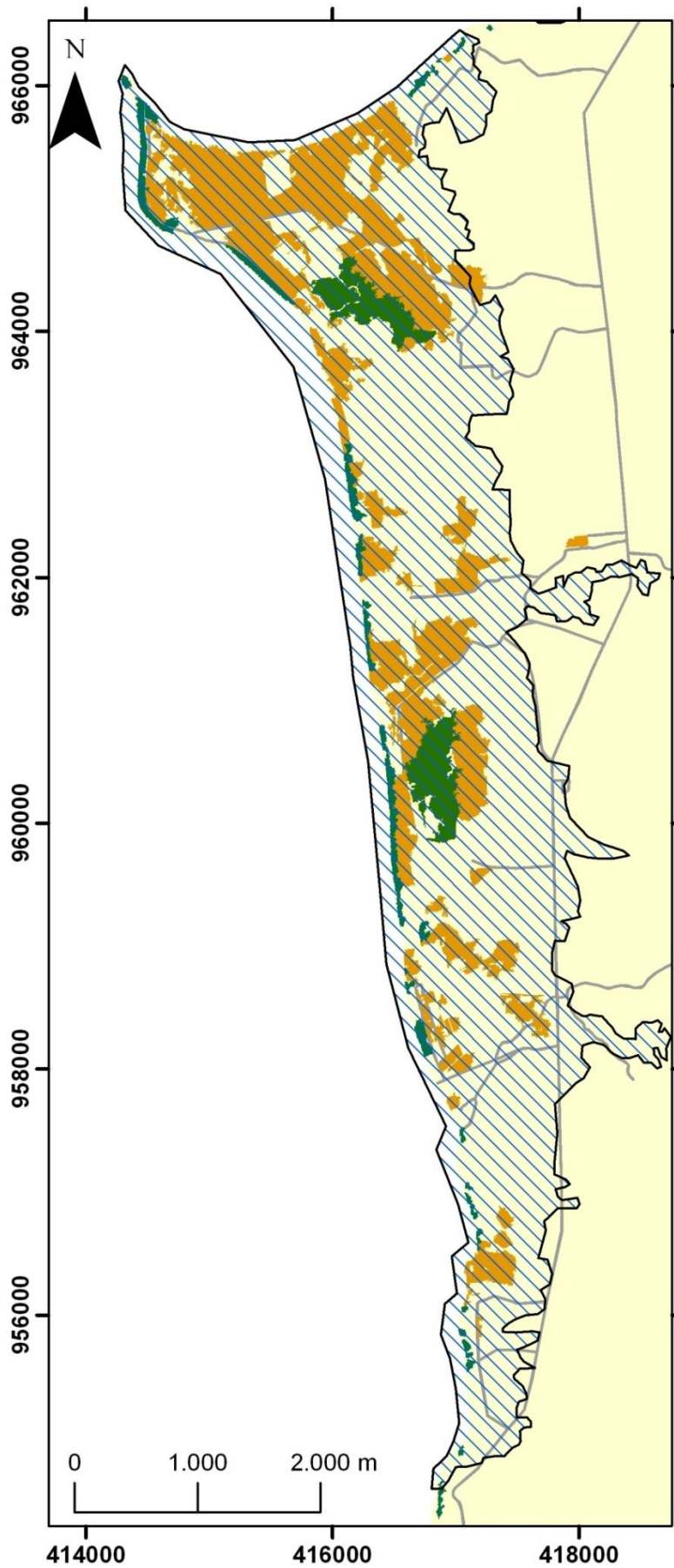
-  tsunami damage area
-  casuarina forest
-  coconut plantation
-  mangrove forest
-  melaleuca forest
-  mixed beach forest



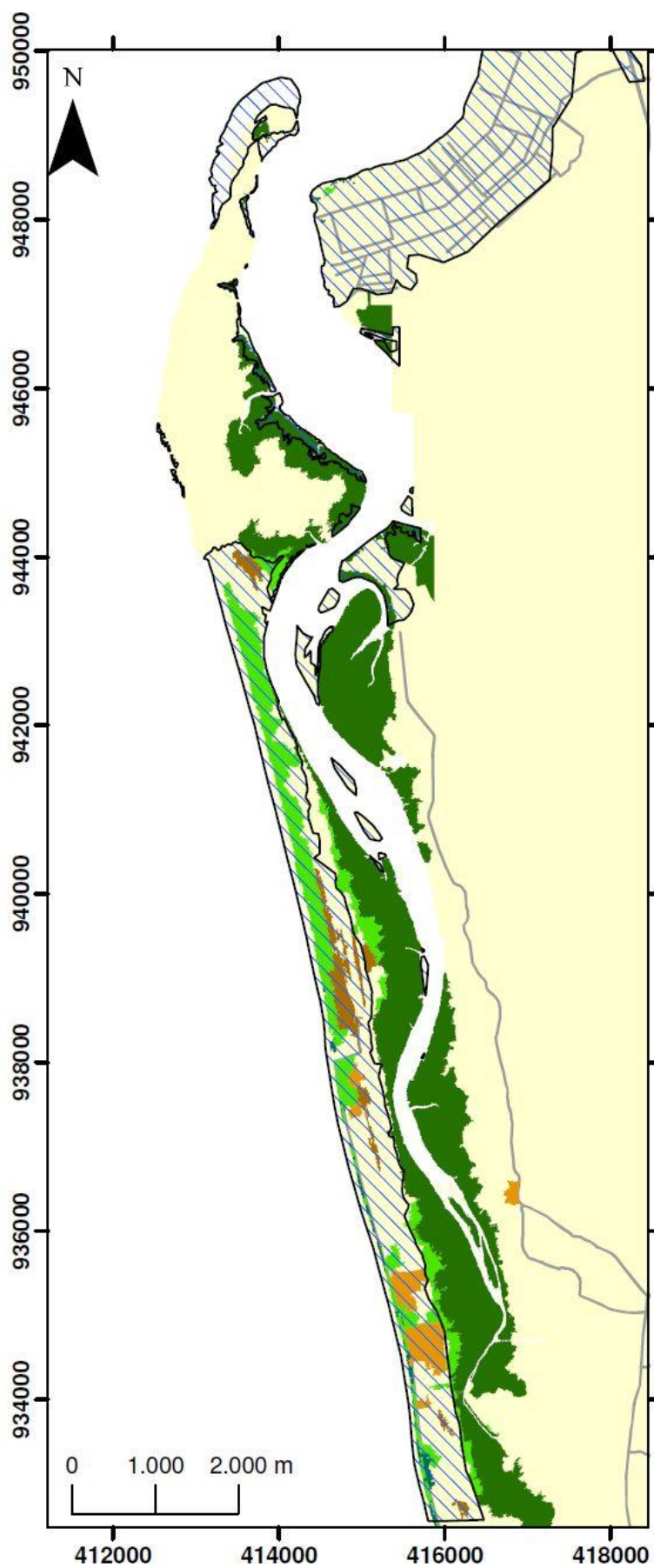
## Appendix N. Exposure analysis: part (a).



Appendix O. Exposure analysis: part (b).



## Appendix P. Exposure analysis: part (c).



**Appendix Q. Standardised beta coefficients.**a) Between impact (*I*), exposure unit and location variables

variable	Man (N=10521)	Cas (N=986)	Mbf (N=20269)	Mel (N=509)	Mix (N=59838)
D	-0.384	0.088	-0.593	-0.419	-0.286
NDVI <sub>03</sub>	-0.303	0.025			
R	-0.112	-0.113	-0.084	-0.359	0.092
E	-0.096	-0.288	-0.114	-0.139	-0.332
In	0.032	0.172	0.019	0.293	-0.037

## b) between impact, exposure unit and hazard variables

variable	Man (N=10521)	Cas (N=986)	Mbf (N=20269)	Mel (N=509)	Mix (N=59838)
CS	0.412	0.443	0.607	0.365	-0.07
NDVI03	-0.363	-0.074			
W	0.172	-0.04	-0.448	0.015	0.608

c) between recovery ( $R_2$ ), and location variables

variable	man (N=720)	cas (N=509)	mv (N=22425)
E	0.38	0.482	0.3
AD	-0.512	-0.321	-0.041
H	0.141	-0.266	-0.257
S	0.107	0.168	0.004
R	0.082	0.027	-0.015
D	0.072	0.16	-0.046

variable abbreviations: **AD**=amount of disturbance (ratio); **CS**=max. current speed ( $\text{ms}^{-1}$ ); **D**=distance to shoreline (m); **E**=elevation asl. (m); **H**=human activities and population growth (%); **I**=tsunami impact intensity; **In**=Inclination of coastline (°); **NDVI<sub>03</sub>**=NDVI of pre- tsunami image; **R**=distance to river (m); **R<sub>2</sub>**=recovery rate; **S**=Depth of topographic sinks (m); **W**=max. total water depth above ground (m).  
*Man, Cas, Coc, MBF, Mel, Mix* stand for mangrove forests, casuarina beach forests, coconut plantations, mixed beach forests, melaleuca forests and mixed vegetation cover, respectively.

**Appendix R. Regression statistics ( $r^2=0.43$ )****Variables Entered/Removed**

Model	Variables Entered	Variables Removed	Method
a	NDVI03, W, CS	.	Enter

a. All requested variables entered.

**Model Summary**

Model	R	R Square	Adjusted R Square	Std. Error of the Estimate
1	.657 <sup>a</sup>	.431	.430	.21105938707279

a. Predictors: (Constant), NDVI03, W, CS

ANOVA<sup>b</sup>

Model		Sum of Squares	df	Mean Square	F	Sig.
1	Regression	49.778	3	16.593	372.483	.000 <sup>a</sup>
	Residual	65.705	1475	.045		
	Total	115.483	1478			

a. Predictors: (Constant), NDVI03, W, CS

b. Dependent Variable: I

Coefficients<sup>a</sup>

Model		Unstandardised Coefficients		Standardised Coefficients	t	Sig.
		B	Std. Error	Beta		
1	(Constant)	1.206	.090		13.429	.000
	W	.032	.004	.172	7.206	.000
	CS	.160	.009	.412	17.216	.000
	TNDVI <sub>03</sub>	-.007	.000	-.363	-17.903	.000

a. Dependent Variable: I

## Appendix S. Regression statistics ( $r^2=0.33$ )

Variables Entered/Removed

Model	Variables Entered	Variables Removed	Method
1	TNDVI03, In, R, E, D <sup>a</sup>	.	Enter

a. All requested variables entered.

Model Summary

Model	R	R Square	Adjusted R Square	Std. Error of the Estimate
1	.577 <sup>a</sup>	.332	.332	.22843489149136

a. Predictors: (Constant), TNDVI03, In, R, E, D<sup>a</sup>ANOVA<sup>b</sup>

Model		Sum of Squares	df	Mean Square	F	Sig.
1	Regression	259.630	5	51.926	995.083	.000 <sup>a</sup>
	Residual	521.251	9989	.052		
	Total	780.881	9994			

a. Predictors: (Constant), TNDVI03, In, R, E, D<sup>a</sup>

b. Dependent Variable: I

Coefficients<sup>a</sup>

Model		Unstandardised Coefficients		Standardised Coefficients	t	Sig.
		B	Std. Error	Beta		
1	(Constant)	1.721	.036		47.333	.000
	D	-.00026	.000	-.384	-42.418	.000
	R	-.00023	.000	-.112	-13.083	.000
	E	-.00111	.000	-.096	-10.986	.000
	In	.00011	.000	.032	3.518	.000
	TNDVI <sub>03</sub>	-.00584	.000	-.303	-34.704	.000

a. Dependent Variable: I





# Lebenslauf

## 1 Persönliche Daten

Name: Hannes Römer (Dipl.-Geogr.)  
Anschrift: Adalbertstr. 19, 24106 Kiel  
Telefon: 0431 / 2599224  
E-Mail: [roemer@geographie.uni-kiel.de](mailto:roemer@geographie.uni-kiel.de)  
Geburtsdatum: 27.03.1982  
Geburtsort: Berlin Lichtenberg  
Familienstand: verheiratet, 2 Kinder, 1 und 3 Jahre



## 2 Schulische Ausbildung und Zivildienst

08/1988 – 07/1994 Besuch der Grundschule in Berlin Pankow  
08/1994 – 06/2001 Besuch des Gymnasiums (Wieland-Herzfelde Oberschule) in Berlin-Weißensee  
Abschluss: Allgemeine Hochschulreife, 21. 06. 2001  
07/2001 – 06/2002 Zivildienst am Verein Naturschutzstation Zippendorf e.V.

## 3 Studium und Promotion

10/2002 – 03/2005 Studium an der Ernst-Moritz-Arndt-Universität Greifswald  
Studiengang: Diplom-Geographie (Nebenfächer: Geologie, Ökologie)  
Abschluss: Vordiplom, 15. 09. 2004  
04/2005 – 12/2007 Studium an der Christian-Albrechts-Universität zu Kiel (CAU Kiel)  
Studiengang: Diplom-Geographie (Nebenfächer: Geologie und Wasserwirtschaft)  
Abschluss: Diplom, 14. 12. 2007  
Thema der Arbeit: Methoden der Fernerkundung als Grundlage zur Untersuchung von Tsunamivulnerabilität an der Andamanküste Thailands  
01/2008 – 12/2010 Wissenschaftlicher Mitarbeiter an der CAU Kiel, Sektion Geographie  
- Mitarbeit im DFG-Projekt TRAIT (Tsunami Risks, Vulnerability and Resilience at the Andaman Coast of Thailand)  
- Lehrveranstaltungen im Rahmen der Physischen Geographie (Seminare, Exkursionen)  
- Abgabe der Dissertation: 20.12.2010

## 4 Berufserfahrung und Praktika

10/2004 – 12/2004 Praktikum am Leibniz-Institut für Ostseeforschung Warnemünde (IOW),  
Abteilung Marine Geologie  
01/2005 – 02/2005 Praktikum am Helmholtz-Zentrum Potsdam Deutsches GeoForschungsZentrum (GFZ),  
Abteilung: Naturkatastrophen  
08/2005 – 09/2005 Praktikum an der Hannover Rückversicherung AG  
Abteilung: Underwriting and Actuarial Services / Modelling  
03/2006 – 04/2006 Praktikum am Landesamt für Natur und Umwelt des Landes Schleswig-Holstein  
Abteilung: Gewässer (Dz. 42: Hydrologie und Morphologie der Fließ- und Küstengewässer, GIS)  
seit 01/2011 Wissenschaftlicher Mitarbeiter am Deutschen Luft- und Raumfahrtzentrum (DLR),  
Deutsches Fernerkundungsdatenzentrum (DFD), Abteilung Zivile Kriseninformation  
und Georisiken